FOSSIL ENERGY

DOE/BC/14881-22
(DE97007192)

IMPROVING RESERVOIR CONFORMANCE USING GELLED POLYMER SYSTEMS

Final Report
September 25, 1992 to July 31, 1996

By
D. W. Green
G. Paul Willhite
C. Buller
S. McCool
S. Vossoughi
M. Michnick

October 1997

Performed Under Contract No. DE-AC22-92BC14881

The University of Kansas
Lawrence, KS

National Petroleum Technology Office
U. S. DEPARTMENT OF ENERGY
Tulsa, Oklahoma

DISCLAIMER

Portions of this document may be illegible in electronic image products. Images are produced from the best available original document.

DOE/BC/14881-22
Distribution Category UC-122

Improving Reservoir Conformance Using Gelled Polymer Systems

Final Report
September 25, 1992 to July 31, 1996

By
D. W. Green
G. Paul Willhite
C. Buller
S. McCool
S. Vossoughi
M. Michnick

October 1997

Work Performed Under Contract No. DE-AC22-92BC14881

Prepared for
BDM-Oklahoma/
U.S. Department of Energy
Assistant Secretary for Fossil Energy

Jerry Casteel, Project Manager
National Petroleum Technology Office
P.O. Box 3628
Tulsa, OK 74101

Prepared by:
The University of Kansas Center for Research, Inc
Energy Research Center
Lawrence, KS 66045-2223

Table of Contents

List of Figures

List of Tables

Abstract

The objectives of the research program were to (1) identify and develop polymer systems which have potential to improve reservoir conformance of fluid displacement processes, (2) determine the performance of these systems in bulk and in porous media, and (3) develop methods to predict their performance in field applications. The research focused on four types of gel systems — KUSP1 systems that contain an aqueous polysaccharide designated KUSP1, phenolic-aldehyde systems composed of resorcinol and formaldehyde, colloidal-dispersion systems composed of polyacrylamide and aluminum citrate, and a chromium-based system where polyacrylamide is crosslinked by chromium(III). Gelation behavior of the resorcinol-formaldehyde systems and the KUSP1-borate system was examined. Size distributions of aggregates that form in the polyacrylamide-aluminum colloidal-dispersion gel system were determined. Permeabilities to brine of several rock materials were significantly reduced by gel treatments using the KUSP1 polymer-ester (monoethyl phthalate) system, the KUSP1 polymer-boric acid system, and the sulfomethylated resorcinol-formaldehyde system. The KUSP1 polymer-ester system and the sulfomethylated resorcinol-formaldehyde system were also shown to significantly reduce the permeability to supercritical carbon dioxide. A mathematical model was developed to simulate the behavior of a chromium redox-polyacrylamide gel system that is injected through a wellbore into a multi-layer reservoir in which crossflow between layers is allowed. The model describes gelation kinetics and filtration of pre-gel aggregates in the reservoir. Studies using the model demonstrated the effect filtration of gel aggregates has on the placement of gel systems in layered reservoirs.

Executive Summary

OBJECTIVES

The general objectives of this research program were to (1) identify and develop gelled polymer systems which have potential to improve reservoir conformance of fluid displacement processes, (2) to determine the performance of these systems in bulk and in porous media, and (3) to develop methods to predict the capability of these systems to recover oil from petroleum reservoirs.

The research focused on four types of gel systems — KUSP1 systems that contain an aqueous polysaccharide designated KUSP1, phenolic-aldehyde systems composed of resorcinol and formaldehyde, colloidal-dispersion systems composed of polyacrylamide and aluminum citrate, and a chromium-based system where polyacrylamide is crosslinked by chromium (III).

The laboratory research was directed at the fundamental understanding of the physics and chemistry of the gelation process in bulk form and in porous media. This knowledge was used to develop conceptual and mathematical models of the gelation process. Mathematical models were then extended to predict the performance of gelled polymer treatments in oil reservoirs.

The project was divided into five major tasks. These were:

- Development and Selection of Gelled Polymer Systems
- Physical and Chemical Characterization of Gel Systems
- Flow and Gelation in Rock Materials
- Mathematical Modeling of Gel Systems
- Sponsor International Forums on Gelled Polymer Treatments

A summary of results for the program is described in the following sections.

SUMMARY OF PROGRESS

I. Development and Selection of Gelled Polymer Systems

Research activities were focused on development of the KUSP1 polysaccharide and derivatives and selection of an organic crosslinked system for further studies.

Development of KUSP1. KUSP1 is an unbranched (1®3)-D-glucan, which is produced by bacterial activity in a simple medium containing an excess of glucose as the carbon and energy source and is deposited as a capsule surrounding the bacterium. The polymer is separated from the capsule by dissolution in 1N NaOH. KUSP1 forms a gel when the pH is reduced to the vicinity of 10.8. The polymer is insoluble in water and organic solvents. The polymer is not toxic.

Research was conducted in three areas. A study was completed to enhance the properties of KUSP1 by modifying the extraction process or the polymer. Derivatives of KUSP1 were prepared

in an attempt to improve water solubility. Chemical modification of the KUSP1 polymer did not enhance the properties of the polymer for use in permeability modification treatments.

Standardized procedures were sought which yielded maximum amounts of the polymer. This was accomplished, first with small (500 ml) batch cultures and later with 1-liter tabletop fermentors. Results indicated that a 72-hr incubation period was optimum. Large-scale production of KUSP1 was investigated in cooperation with Abbott Laboratories, North Chicago, Illinois under the sponsorship of another DOE contract. Fermentation was carried out in a 40,000-liter fermentor vessel, which was operated at conditions very similar to those developed from the laboratory optimization study. A yield of 9.1-g (dry weight) of KUSP1 was produced per liter of culture. This was slightly better than the laboratory results. Large-scale production costs were estimated to be between 3.94 and 7.38 $/lb.

KUSP1-boric acid system. KUSP1 can be gelled using ortho boric acid. Boric acid gels are clear and appear much more resilient than the gels formed without boric acid which are white in color and tend to shatter. It is speculated that the borate crosslinks the polymer molecules to form gels. The gelation behavior of the KUSP1-boric acid system was characterized. Concentrations studied were 1.0% KUSP1, 0.1 to 0.5-M boric acid, 0 or 1.0% sodium chloride, and pH values between 9 and 13. The effect of temperature on gel times was investigated by conducting bottle tests at 25°C, 45°C and 65°C. Selection of the boric acid concentration or the pH of the gel solution can regulate gel times for the KUSP1-boric acid system from a few seconds to several days. At a given pH, a decrease in the boric acid concentration decreased the gel time. Gel times decreased and syneresis increased with increased temperature.

Other gel systems. An objective of the research program was to study an organic gel system. A database was developed containing 29 gel systems. Criteria for selection of an organic gel system were defined. Four criteria evolved from this process. They are: 1) environmental acceptance; 2) gel times on the order of several days to months; 3) wide temperature range with a minimum temperature of 25°C; 4) wide pH range that encompassed pH values between 6 and 8; and 5) cost. Because of environmental concerns associated with organic crosslinking systems, our search for gelling systems was expanded to consider low toxicity systems such as those which use aluminum ion as the crosslinker.

Resorcinol-formaldehyde/SMRF systems. Two phenolic-aldehyde systems were studied. One was composed of resorcinol and formaldehyde (designated the RF system) and the other composed of sulfomethylated-resorcinol and formaldehyde (designated the SMRF system). The resorcinol-formaldehyde (RF) system has limited applicability for use in gelled polymer treatments in the range of compositions that were studied in bottle tests (41 °C). At salt concentrations greater than 1%, the gel times are on the order of 10 hours or less. These relatively short gel times would only be applicable for near well-bore treatments in shallow wells. Additionally, the RF system did not gel at pH values less than approximately 7.5. The sulfomethylated resorcinol-formaldehyde (SMRF) system has improved gelling characteristics and wider field applicability as compared to the RF system. Bottle tests demonstrate that the SMRF system gels over longer time periods and over wider pH ranges (5-8) than the RF system.

Polyacrylamide-aluminum system. The polyacrylamide-aluminum colloidal-dispersion system is different from most gel systems in that a bulk gel is not formed. Instead, colloidal dispersions are claimed to develop in the solution. Colloidal dispersion gels are formulated with relatively low concentrations of polyacrylamide and aluminum. Size distributions for the polymer and/or aggregates were determined for the polymer solution without crosslinker and for gel samples that had reacted for up to 12 hours. The results showed little-to-no growth of aggregates in the gel samples. Significant development of aggregates and/or aggregate growth in the gel samples was not observed even though other measurements (TGU tests) indicated the development of structure.

II. Physical and Chemical Characterization of Gel Systems

Rheological studies. Rheological or kinetic studies were carried out on three gel systems. A study of the effect of shear rate on gelation was conducted using a polyacrylamide-Cr (III) gel.

The viscosity behavior of alkaline solutions of KUSP1 and polyacrylamide-aluminum citrate colloidal dispersion gels was characterized. Kinetic studies of the rate of hydrolysis of an ester system were done as a possible way to control pH and thus gel time for the KUSP1 gel system. For the third system, polyacrylamide-aluminum citrate, gelation behavior was examined using a screen-viscometer device. Results of these studies follow.

Methods to monitor gelation as a function of time using rheological measurements were developed. Experimental techniques were developed to determine the storage modulus as a function of time during gelation using oscillatory rheometry. Reproducibility was determined for a Cr (III)-polyacrylamide system under oscillatory shear. All measurements were made using a Weissenberg R-19 Rheogoniometer or a Bohlin Controlled Stress Rheometer.

The storage moduli of gels prepared at a specified frequency were a strong function of frequency of oscillation (from 0.01 Hz to 1.0 Hz) at all stages of the gelling process. Thus, the frequency of measurement must be considered in relating the storage modulus to gel structure. All gelation experiments showed an initial dependence of the rate of change of the storage modulus with frequency of oscillation. The maximum slope of the storage modulus-versus-time curve did not depend on the frequency of gelation. The gel time based on the equivalence of storage modulus and loss modulus increased as the frequency of oscillation increased. For the system studied, the gel did not attain an equilibrium value of the storage modulus even after 5 days of observation. Definition of gel point continues to be ambiguous in describing gel systems.

Steady shear experiments and parallel superposition experiments (simultaneous application of oscillatory shear and steady shear) were conducted. Shear rates examined ranged from 0.47 to 47 s^{-1}. The effect of shear on gelation was interpreted primarily from the time-dependent data of shear viscosity, storage modulus and loss modulus. Gelation time was measured by two methods, which correlated quite well. The first was the time at which the solution viscosity started to increase rapidly, while the second was the time at which the storage modulus and loss modulus curves crossed.

Several general observations resulted from the experiments. There is an induction period during which very small increases in shear viscosity and storage modulus occur. Apparently during this period aggregates formed by the gelation process are small and do not significantly affect the magnitude of the shear viscosity or storage modulus. Following this induction period there is an abrupt increase in the values of the parameters, indicating the onset of gelation. At low shear rates, less than 2.35 s^{-1}, the gel time is decreased as shear rate is increased. Gels formed at higher shear rates were weaker than those formed at low shear rates. No gelation occurred when shear rates were on the order of 40 s^{-1} or higher.

Effect of anions. During screening experiments, the gelation of polyacrylamide-Cr (III) systems was observed to vary with the anion present in the system as well as the concentration of the anion. A series of gelation experiments was completed in which the effects of nitrate, perchlorate, chloride, sulfate and acetate anions on the rate of gelation were determined using rheological measurements. A single polymer concentration (9,000-ppm) was used in these experiments with two Cr (III) concentrations. The time of gelation for the five systems studied is ordered as follows: $NO_3^- < ClO_4^- < Cl^- < SO_4^- < OAc^-$.

The dependence of gelation on anion concentration was examined by preparing solutions at salt concentrations ranging from 0.00 M to 1.0 M. Gelation time for the nitrate systems decreases with increase in salt concentration. The perchlorate system has a maximum gelation time between 0.1 M and 1.0 M salt concentration followed by a decrease in gelation time with a corresponding decrease in salt concentration. In the chloride system, gelation time increases with increasing salt concentration. Addition of acetate anion appears to inhibit gel formation in the pH range studied.

Kinetic studies (chromium oligomers). Chromium(III) is a commonly used crosslinking agent for polyacrylamide and polysaccharide. The chromium(III) used in some of these systems is present as monomeric Cr(III) when added to the polymer solution. The gelation process is sensitive to pH and it is known that oligomers of Cr(III) form as the pH increases. The gelation process is visualized as a two-step process. In the first step, the Cr(III) reacts with the polymer in what is termed the uptake reaction. This is followed by a gelation reaction where crosslinks are formed between polymer chains containing Cr(III).

A research program was completed to determine and compare the uptake and gelation rates of the Cr(III) monomer, dimer and trimer with partially hydrolyzed polyacrylamide. The three species of Cr(III) were separated by ion chromatography. Oligomer uptake was measured by separating unreacted chromium from the gel solution using a dialysis technique. Relative rates of gelation were determined from rheological measurements of the change of storage modulus with time.

Data were obtained for uptake and gelation in the pH range of 4 to 5, Cr(III) concentrations of 8-30 ppm and polymer concentrations of 4,000 - 20,000 ppm. Uptake and gelation rates increased with increasing oligomer size, oligomer concentration and pH. Uptake rate also increased with polymer concentration. In general, gelation reactions closely followed the uptake of oligomers by the polyacrylamide. Comparison of uptake results with other data indicated that the salt type and concentration affected the uptake rates.

A kinetic model was developed to describe the uptake rates for monomer at pH 4 and 5. The monomer data were well described by the model. The dimer data were less well described and the trimer data were not fit well at all by the model. A number of possibilities were examined to explain the lack of fit for the dimer and trimer.

Kinetic studies (gelation of KUSP1 by ester hydrolysis). The gelation of KUSP1 occurs when the pH of the alkaline solution is reduced from 13 to the vicinity of 10.8. Reduction of pH can be accomplished by adding an ester to the alkaline solution. Esters were examined to identify a candidate, which would be soluble in the alkaline solution containing KUSP1, and would hydrolyze at a slow enough rate to gel the polymer in a time period of several days. A commercially available ester that met these criteria was not found. The ester *ethylbenzoate-2-sulfonic acid* (EBSA) was easily prepared. Experimental data showed that the gelation of KUSP1 could be controlled by ester hydrolysis. Gel times on the order of days(at room temperature) were obtained. Gel times can be controlled by selection of the concentrations of the polymer and the ester.

The cost of *ethylbenzoate-2-sulfonic acid* appears to be prohibitive for use in field treatments. A less expensive ester was sought. After evaluating many esters, mono-ethyl phthalate (MEP) was found to be suitable for this application. Criteria used to evaluate the esters were cost, ease of preparation, solubility in water, rate of hydrolysis and toxicity. Experiments were conducted to examine the effects of MEP ester, sodium hydroxide and sodium chloride concentrations on the rate of pH reduction and viscosity increase in KUSP1 solutions. Additional runs in which KUSP1 concentration was varied were also conducted. Data were developed which allow gelation times to be set a priori by proper variation of the system concentrations. These data can be used for design of field implementation of the KUSP1 gel process. A kinetic model describes pH reduction in the absence of polymer, but does not satisfactorily describe the process when KUSP1 is present at concentrations required for gelation to occur.

Screen viscometer studies (polyacrylamide-aluminum system). TIORCO Inc., Englewood, CO developed the polyacrylamide-aluminum citrate system in the form of a colloidal dispersion gel. The formulation consists of low concentrations of a partially hydrolyzed polyacrylamide and a chelated aluminum citrate solution. Typical concentrations used in this system are 300-ppm polymer and 15 ppm Al^{3+}. These systems are reported to be slow forming which allows large volumes to be injected during field applications with the intent of altering flow patterns distant from the wellbore. It is speculated that polymer colloids, or gel aggregates, are formed which are then apparently filtered from solution by the rock, thereby reducing the permeability.

Different formulations of this system were analyzed using a screen viscometer type device (TGU apparatus) developed by TIORCO, Inc. Measurements on the device can be used as indicators of gelation time and gel strength. Data were obtained which were consistent with results reported in the literature. It was determined that very small concentrations of chlorine in the solution, on the order of 0.25 ppm, caused the polymer to degrade significantly and inhibited gel formation.

III. Flow and Gelation in Rock Materials

Gelation experiments in porous media were conducted with the sulfomethylated resorcinol-formaldehyde (SMRF) system, the KUSP1-boric acid system, the KUSP1-ester system and the polyacrylamide-aluminum citrate system. The capability of these systems to reduce the permeability of selected rock materials to subsequent brine flow (waterflooding) was assessed. Permeability reductions to supercritical carbon dioxide were determined for the SMRF system and the KUSP1-ester system. Experiments were also conducted to assess the importance of rock-fluid interactions on pH change.

SMRF system. The SMRF system was effective in reducing the permeability of limestone, dolomite and sandstone core plugs. Permeabilities to brine were reduced by factors greater than 9000.

pH change resulting from rock-fluid interactions. Since KUSP1 forms a gel when solution pH is lowered sufficiently, the effect of rock-fluid interactions on solution pH was examined. KUSP1 solutions were injected into several porous medium types, including unconsolidated sands, Berea core, and carbonate field cores. In all cases, the initial solution pH was high, at values where KUSP1 is soluble. The systems were allowed to set for long periods of time during which solution pH was periodically measured. In no case was there a significant change in pH which would affect the gelation of KUSP1.

KUSP1-boric acid system. Permeability reductions in sandpacks and Berea sandstone cores were determined for a selected gel system at 25 and 45 °C. Gel treatments significantly reduced the permeability. Permeabilities were reduced by factors that ranged from 50 to 3300 in sandpacks and Berea sandstone cores at 25 and 45 °C. Factors by which the permeabilities of brine were reduced were greater in the more permeable sandpacks and at the lower temperature.

In situ gelation of KUSP1 using ester hydrolysis. In situ gelation experiments with KUSP1 in unconsolidated sandpacks and Berea cores were carried out in which gelation resulted from lowering of pH through hydrolysis of MEP ester. The KUSP1-ester system significantly reduced the permeability of sandpacks, Berea sandstone cores and carbonate core-plugs. Permeabilities were reduced by factors greater than 200 in the absence of oil in the media. The presence of a residual oil saturation did not significantly alter the effectiveness of the treatment. Permeabilities were reduced uniformly along the length of the media. The gelled KUSP1-ester system was stable with time and throughput of brine. Little change in permeability was observed during the flow of many pore volumes of brine through the media over periods of many weeks.

In situ gelation of the polyacrylamide-aluminum citrate system. Experiments were conducted in unconsolidated sandpacks. The polymer solution and aluminum citrate solution were mixed in an in-line mixer located just ahead of the sandpack. Flow rates and the length of the pack were set such that there was sufficient residence time in the packs for gelation to occur based upon development of TGU values from batch experiments. The early experiments were plagued with the formation of gels on the sand retention screens, either at the entry or effluent ends of the packs. Gels did not form in the sandpack.

Gel solution propagated through a porous medium like a polymer solution when it was injected immediately after mixing in-line. Delaying the entry of the gel solution to allow time for the gel aggregates to develop resulted in retention of polymer at the inlet face. No in-depth development of resistance was observed in this study. Resistance developed at the porous media inlet only. When propagated through porous medic, the colloidal dispersion gel loses its gel-like properties. Effluent solutions obtained during both the polymer and gel displacement experiments had reduced viscosities and did not form any structure. Analysis of the effluent solution also indicated significant retention of aluminum. The colloidal dispersion gel does not appear to be capable of forming a gel-like network in a porous medium even after being shut-in for three weeks. No resistance was observed when brine was injected following the shut-in period.

In situ gelation of KUSP1 by CO_2. Gelation of alkaline solutions of KUSP1 in beakers can be accomplished by bubbling carbon dioxide gas into the solution. In this process, CO_2 dissolves in the aqueous solution and reacts with water to form an acidic species which lowers the pH. Gelation experiments were conducted in short sandpacks (30.2 cm). Two experiments were completed. In the first experiment CO_2 was injected continuously into a sandpack saturated by KUSP1 solution at a pH of 13.5. Initial permeability of the sandpack was 3,600 md. Uniform permeability reduction to an average permeability of 45 md was observed in this experiment. In the second experiment, alternate slugs of KUSP1 polymer solution and CO_2 were injected. Substantial permeability reduction was observed, but most of the reduction was limited to the front section of the sandpack.

Permeability reduction to supercritical carbon dioxide. Three systems were tested for their ability to reduce the permeability to supercritical carbon dioxide. In the first system, KUSP1 solutions were gelled in Berea sandstone cores by injecting carbon dioxide. The carbon dioxide reduced the in situ pH resulting in the gelation of the KUSP1. Permeabilities to brine and supercritical carbon dioxide were reduced by approximately 85%. Permeabilities to supercritical carbon dioxide were reduced by approximately 97% using the KUSP1-ester system. Both KUSP1 systems were stable to the injection of many pore volumes of supercritical carbon dioxide.

The sulfonated resorcinol-formaldehyde (SMRF) system was gelled in situ and was contacted with both brine and supercritical carbon dioxide. Permeabilities were reduced by about 99% with the SMRF system. The permeability reductions were maintained after the injection of many pore volumes of supercritical carbon dioxide and brine. The permeability reduction due to this system is significantly higher than for other systems studied.

IV. Mathematical Modeling of Gel Systems

Simulation of pH due to fluid-rock interaction. The gelation of many polymer systems is a strong function of solution pH. Fluid-rock interactions play an important role in determining the pH behavior of solutions injected into reservoirs. For example, in some porous rocks there may be sufficient fluid-rock interaction to cause gelation of an alkaline solution of KUSP1. Modeling efforts were focused on the important forms of fluid-rock interactions in reservoir sands with the objective of mathematically modeling their effects on the solution pH.

The initial steps in this project involved simulation of flooding experiments with high pH brine solutions using UTCHEM, a widely applied chemical-flooding simulator. Comparison with experimental data revealed that the kinetics of dissolution is important in many situations of practical interest. UTCHEM was developed by assuming equilibrium exists between all species and does not account for the kinetics of dissolution.

A kinetic model describing silica dissolution reaction was developed which is generally valid for all time frames. Based on sodium/hydrogen equilibria and silica dissolution kinetics, a new mathematical model was developed for describing core flood experiments. This model describes the effects of flow rate and core length in terms of the Damkohler Group. By varying the value of the Damkohler Group it is possible to scale the effects of silica dissolution from laboratory-scale conditions to field-scale conditions. A mathematical criterion was developed for checking the validity of the local equilibrium assumption.

The model was used to study sodium/hydrogen ion exchange in simulated core floods. Concentration profiles show formation of two distinct fronts which move through the porous medium, a salinity wave and an ion-exchange wave. Model calculations were compared to three independent core-flood experimental sets reported in the literature. In each case, the estimated values of the reaction parameters correspond to typical values suggested in the literature. In one series of calculations, a single set of parameters was used to simulate all concentration profiles in an experiment. These results establish the validity of the assumptions in the model and the underlying assumptions for silica dissolution and sodium/hydrogen ion exchange.

Simulation of crossflow during gelant injection. A mathematical model was developed to simulate the behavior of a chromium redox-polyacrylamide gel system that is injected through a wellbore into a multi-layer reservoir in which crossflow between layers is allowed. The model describes gelation kinetics and filtration of pre-gel aggregates in the reservoir.

The model was used to simulate the placement of a gel solution into a two-layer reservoir in which the ratio of permeabilities of the layers was varied between 10:1 and 100:1. For a given set of reservoir conditions, there is an optimal time for injection of the gelant to minimize gel penetration into the low permeability layer when both layers are open at the wellbore. Injection of gelant beyond this period results in diversion of gelant into the low-permeability layer without increasing the penetration of the gelant in the high-permeability layer. Viscous crossflow has a relatively small effect during typical near-wellbore treatments. Viscous crossflow may be more important in deeper treatments because the bulk of the crossflow occurs before the onset of filtration.

Gel-placement is most effective in reservoirs characterized with high-permeability contrast and low crossflow between layers. Permeability modification treatments are expected to be more effective in severe cases of water channeling . Isolation of the low-permeability layer results in a considerably more effective gel placement compared to conventional treatment where both layers

are open in the wellbore. Filtration of gel aggregates may aid in minimizing crossflow of gelant from the high-permeability regions into the low-permeability regions of the reservoir. Viscous crossflow is reduced when the viscosity of the gelant is reduced.

V. Sponsor International Forums on Gelled Polymer Treatments

The objective of this task was to conduct an international meeting, which would focus on conformance improvement through application of gelled polymer technology. Subsequent to funding of this proposal, the Society of Petroleum Engineers scheduled a forum on Improvements in Conformance Technology during the 1993 Forum Series under the leadership of Bob Sydansk, Marathon Oil Company. This forum which was held at Snowmass, CO, August 8-13, 1993. G. Paul Willhite was a member of the Planning Committee for this forum. Stan McCool also attended the forum and made a presentation. Response of the participants was quite favorable.

A one-day forum on permeability modification was held following the 1996 SPE/DOE Improved Oil Recovery Symposium and was attended by about 40 people.

Chapter 1

Introduction

The application of gelled polymer treatments to petroleum reservoirs can improve oil recoveries and reduce fluid-handling costs. This research program consists of laboratory investigation of chemical systems that are applicable for gelled polymer treatments and the development of mathematical models that describe gelled polymer treatments of oil reservoirs. Laboratory research focused on four types of systems - (1) KUSP1 biopolymer systems, (2) chromium-polyacrylamide systems (3) a polyacrylamide-aluminum citrate system, and (4) phenolic-aldehyde systems. Mathematical models were developed to estimate alkali interactions in sandstone reservoirs and to predict gel placement for a chromium-polyacrylamide system.

The development and application of KUSP1 polysaccharide for use in permeability modification treatments was investigated and results are presented in Chapter 2. Chapter 3 summarizes investigations on the effects of shear, anion types and the kinetics of chromium(III) uptake on the gelation of chromium-polyacrylamide gels.

Two studies of the polyacrylamide-aluminum citrate system were conducted and are reported in Chapter 4. Results of an investigation to determine the size of aggregates that form and grow in this system was completed. The performance of the polyacrylamide-aluminum citrate system in reducing permeability in sandpacks was studied. Chapter 5 presents gelation data for two phenolic-aldehyde systems. One was composed of resorcinol and formaldehyde (designated the RF system) and the other composed of sulfomethylated-resorcinol and formaldehyde (designated the SMRF system). The SMRF system was tested extensively in carbonate cores. The development of gel systems for application in carbon dioxide miscible displacement processes is summarized in Chapter 6.

A mathematical model was developed to simulate alkaline-sandstone interactions during flow processes in sandstones and is described in Chapter 7. A mathematical model was developed to simulate a gel treatment at reservoir scale using a polyacrylamide-chromium system. The model was used to study the placement of gelant in a layered radial system. Chapter 8 presents the results of this study.

Chapter 2

Development of KUSP1 Systems for Permeability-Reduction Treatments

Principal Investigators: G.P. Willhite, D.W. Green, C. Buller, S. Vossoughi and C.S. McCool
Graduate Research Assistants: P. Chen, M. Yougo, A. Fichadia, A. Shaw, S. Bhattacharya and A. Singh

The application of the KUSP1 polysaccharide for use in permeability-modification treatments was investigated. Initial research on the KUSP1 polysaccharide focused on the production process of the polymer and on the characterization and modification of the polymer molecule. The majority of the research was directed at the understanding of performance of KUSP1 in a treatment process. Rheological properties of KUSP1 solutions were determined. Investigations of methods to gel KUSP1 solutions were conducted. These methods utilized ester compounds, boric acid and rock-fluid interactions. Injectivity of KUSP1 solutions in porous media was assessed and improved. Finally, the permeability-reduction capabilities of several KUSP1 systems were evaluated.

This chapter assembles the results of research on the KUSP1 polymer that were presented in annual reports[1-3] and the results that have been obtained since. The results and details of the experimental procedures can be found in the annual reports as well as in other literature.[4-8]

Development and Production of KUSP1 and Derivatives

Growth *Cellulomonas flavigena* in excess glucose results in the production of a polysaccharide that is deposited around the bacteria as a capsule. Suspension of the encapsulated cells in 1 N NaOH solution results in the dissolution of the polysaccharide. Neutralization of the alkaline extract, with acid, or by dialysis, results in the formation of a polysaccharide hydrogel. The polysaccharide, which has been named KUSP1, is an unbranched (1→ 3)-β-D-glucan. KUSP1 is insoluble in water and organic solvents. It dissolves in alkali, concentrated formic acid and phosphoric acid, and in dimethylsulfoxide (DMSO).

The objectives for this segment of the research were to optimize the production process, to modify the polysaccharide in an attempt to improve its applicability for permeability-reduction treatments and to estimate costs of large-scale production.

Optimization of Production Process. Batch cultures and a 1-liter table-top fermentor were used to determine that 72 hours was an optimum incubation time. Longer incubation times sometimes resulted in slightly higher yields but also significantly increased the risk of development of hydrolytic enzymes. These enzymes can lower the degree of polymerization and, thus, the gelability of the polymer.

The effect of using 1 N NaOH solution to extract KUSP1 was investigated in order to determine if the NaOH reacted and modified the polymer. An alternate extraction process was developed using the solvent dimethylsulfoxide (DSMO). The degree of polymerization and gelling characteristics of the polymer extracted with DMSO were similar to that of polymer extracted with NaOH. It was concluded that the alkali-extraction process did not affect the properties of KUSP1.

Chemical Modification of KUSP1. Chemical derivatives of KUSP1 were prepared and tested for gelation characteristics. O-carboxymethyl-KUSP1, and methyl-, ethyl- and propyl-ethers of KUSP1 were synthesized. All of these derivatives were water soluble and did not gel as a function of pH. None of the derivatives were selected for additional testing.

Costs of Large-Scale Production of KUSP1. A large-scale run for the production of KUSP1 was conducted as part of another research project. Fermentation was conducted in a 40,000-liter vessel that was operated under conditions that were optimized as part of this project. A polymer yield of 9.1 gm/liter of culture was measured which is slightly better than yields obtained in lab-scale cultures. This was encouraging since a decrease in product yield usually accompanies simple scale-up to large-scale production.

The unit cost of KUSP1 in large-scale production was estimated using data from the 40,000-liter run and by consultations with engineers from The NutraSweet Kelco Company. Production costs were estimated using the following basis.

- Production costs of xanthan gum were used and adjusted to reflect the differences between the production processes of xanthan and KUSP1. Current variable and fixed costs for the NutraSweet Kelco biogum production facility in Okmulgee, OK were used.
- Polymer yields of the fermentation would be 9 g/L and 18 g/L.
- CM9 media would be used for fermentaion.

A breakdown of the costs for KUSP1 production is given in Table 2.1. The estimated total cost to produce KUSP1 at present yield is $7.38/lb. The cost is reduced to $3.94/lb if the yield can be increased by 100%. This magnitude of increased yield is reasonable for these processes through optimization of growth media and by improvements in the strain of the bacterium that produces KUSP1.

Viscosity and Bulk Gelation of KUSP1 Solutions

KUSP1 dissolves in alkali solution and forms a gel as the pH of the solution is lowered below a value of approximately 11. This change in physical state is the basis for use in permeability modification treatments. This section presents the results of a study of the viscosity of alkali KUSP1 solutions and of studies to develop and understand methods to gel KUSP1 solutions.

Viscosity of KUSP1 Solutions. Solutions of KUSP1 were prepared at selected concentrations of polymer and NaOH. Viscosity, pH and visual appearance were recorded over a ten-day period. Viscosity was measured as a function of shear stress using a controlled-stress rheometer.

The viscosity behavior of the KUSP1solutions as a function of pH (shear stress of 0.12 Pa and two-day old samples) is presented in Figure 2.1. The viscosity was less than 5 cp for all samples that had pH values greater than 13. Viscosity of the samples increased with a decrease in pH , particularly for the samples containing 1.0 and 2.0 % polymer. This indicated aggregation or structure build-up of the polymer with a decrease in pH. As, shown later, the aggregation appears to increase until a bulk gel is formed at a pH of 10.8. Aggregation could be important to the injection and transport of these solutions through porous media.

Table 2.1 : Cost breakdown for production of KUSP1 biopolymer per pound.

Yield of KUSP1	9 g/L	18 g/L
Polymer production/batch	2,800 lbs	5,6000 lbs
Variable Costs		
Fermentation		
raw materials	$ 2.00	$ 1.20
utilities	1.57	0.79
labor	0.39	0.20
Recovery		
raw materials	0.13	0.06
utilities	0.02	0.01
labor	0.21	0.11
Drying	1.00	0.50
Particle sizing	0.06	0.06
Fixed Costs		
maintenance	$0.76	$0.38
staff	0.27	0.14
culture lab	0.08	0.04
quality control	0.18	0.09
depreciation	0.71	0.36
TOTAL COSTS per lb KSUP1	$ 7.38	$ 3.94

Shear-thinning behavior was observed for the three samples that had viscosities greater than 20 cp as shown in Figure 2.1. Viscosity as a function of shear rate and time for a sample containing 2.0 % polymer and 0.12 % NaOH is presented in Figure 2.2. This sample exhibited power-law behavior and a moderate decrease in viscosity with time. All but one sample showed some decrease in viscosity with time. Samples with pH values greater than 12.8 changed color from white to yellow to brown over the ten-day period. The cause of the color change is unknown.

Bulk Gelation of KUSP1 by Ester Hydrolysis. KUSP1 forms a gel as the pH of the solution is lowered below 10.8. A method to reduce the pH of alkali KUSP1 solutions is to add a chemical that would react to form an acid. Of the several chemicals tested, two ester compounds exhibited the desired criteria of solubility in alkali KUSP1 solutions and slow reaction rates, i.e. gel times must be on the order of days for application of in-depth treatments. The esters were ethylbenzoate-2-sulfonic acid (EBSA) and monoethylphthalate (MEP). These compounds react with water to produce an acid and an alcohol. EBSA and MEP are not available commercially but are easily prepared by dissolving the respective anhydride in ethanol. Both EBSA and MEP donate two acid groups, one immediately upon mixing with an alkali solution and one by the ester hydrolysis reaction. Thus, the moles of ester required to produce time-delayed gelation is between 50 and 100% of the moles of NaOH in solution.

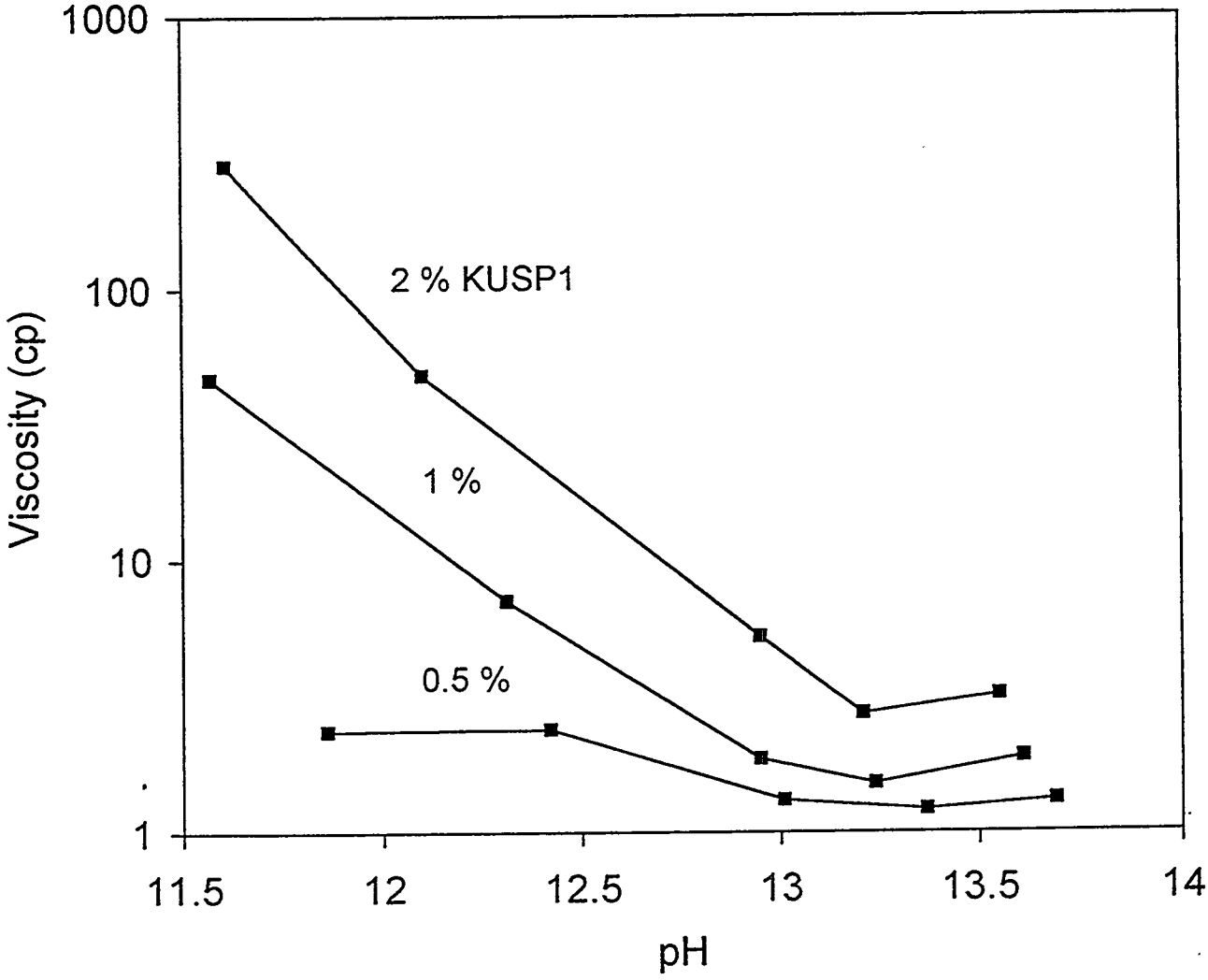

Figure 2.1 : Viscosity as a function of pH and KUSP1 concentration for solutions at an age of two days.

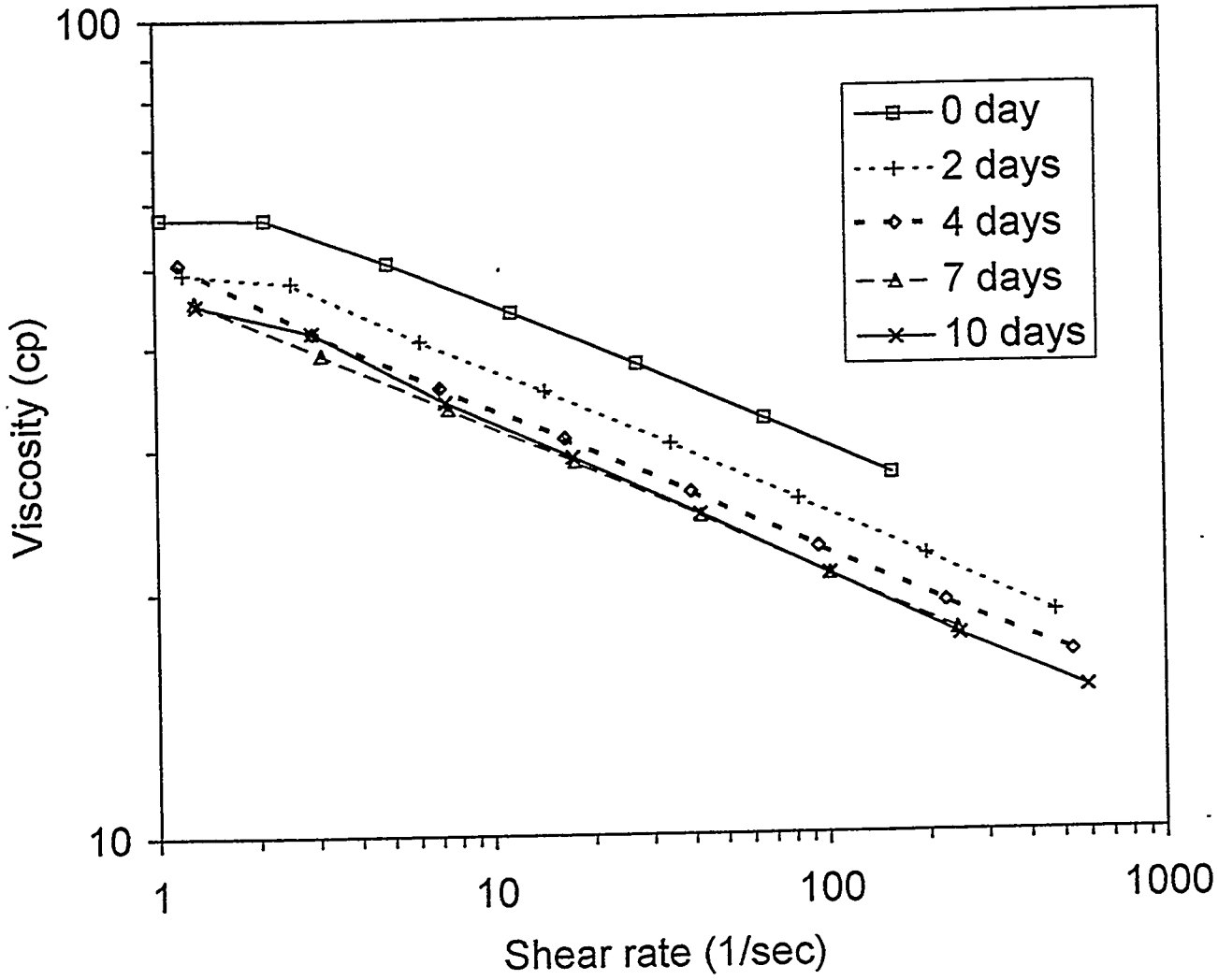

Figure 2.2 : Viscosity as a function of shear rate and time for solutions containing 2.0% KUSP1 and 0.12% NaOH.

Gelation of KUSP1 by the hydrolysis of EBSA was investigated by preparing samples at selected component concentrations and monitoring the pH and viscosity. Experiments were conducted at 25 °C. Time-delayed gelation between 2 and 11 days was observed for samples containing 1.0, 2.0 and 2.8 % KUSP1; 0.38 % NaOH; and EBSA-to NaOH mole ratios of 0.62 and 0.79.

pH-time data for different KUSP1 concentrations are shown in Figure 2.3. Gelation of the samples containing polymer occurred during the time period where the pH stabilized at a value of 10.8. A continuous drop in pH was observed for the sample that did not contain polymer. The data indicate that hydrogen ions are consumed during the gelation process.

Time-delayed gelation of KUSP1 was accomplished by the hydrolysis of EBSA. Gel times were on the order of days and can be controlled by the selection of component concentrations. The cost of the EBSA is probably prohibitive for use in field treatments. Detailed results of the gelation of the EBSA-KUSP1 system are presented in reference 1.

Monoethylphthalate ester (MEP) was identified as a low-cost alternative to EBSA. Experiments were conducted to determine the effect of NaOH and MEP concentrations on the rate of reaction of MEP without polymer. NaOH concentrations studied were 1.0, 0.32 and 0.10% with mole ratio of ester to NaOH of 0.50 and 0.75. The reaction between MEP and NaOH (after the initial pH drop) was modeled assuming that the rate of reaction was first order in both NaOH concentration and MEP concentration. The rate equation describing the kinetics was

$$\frac{dC_A}{dt} = -k * C_A * C_B$$

where C_A = concentration of NaOH (mol/L),
C_B = concentration of MEP ester (mol/L),
k = rate constant (L/mol/hr).

Stoichiometry of the reaction gives the following relationship.

$$C_{A0} - C_A = C_{B0} - C_B$$

Using the stoichiometric relationship, an analytical solution to the rate equation (when $C_{AO} \neq C_{B0}$) is

$$C_A = \frac{C_{A0} * (C_{B0} - C_{A0}) * \exp(-k * (C_{B0} - C_{A0}) * t)}{C_{B0} - C_{A0} * \exp(-k * (C_{B0} - C_{A0}) * t)}$$

This model represented the experimental pH-time data of the reaction between NaOH and MEP reasonably well with a reaction constant, k, of 5.0 liter/mole/hr.

Experiments were conducted to determine the gel times for the MEP-KUSP1 system. Gel times ranged from 8 to 118 hours for polymer concentrations of 1.0, 2.0 and 3.0%. NaOH concentrations studied were 1.0, 0.32 and 0.10% and the mole ratios of ester to NaOH were 0.50 and 0.75. Added NaCl to the samples had no significant effect on the rate of pH drop or the development of viscosity. The kinetic model did not

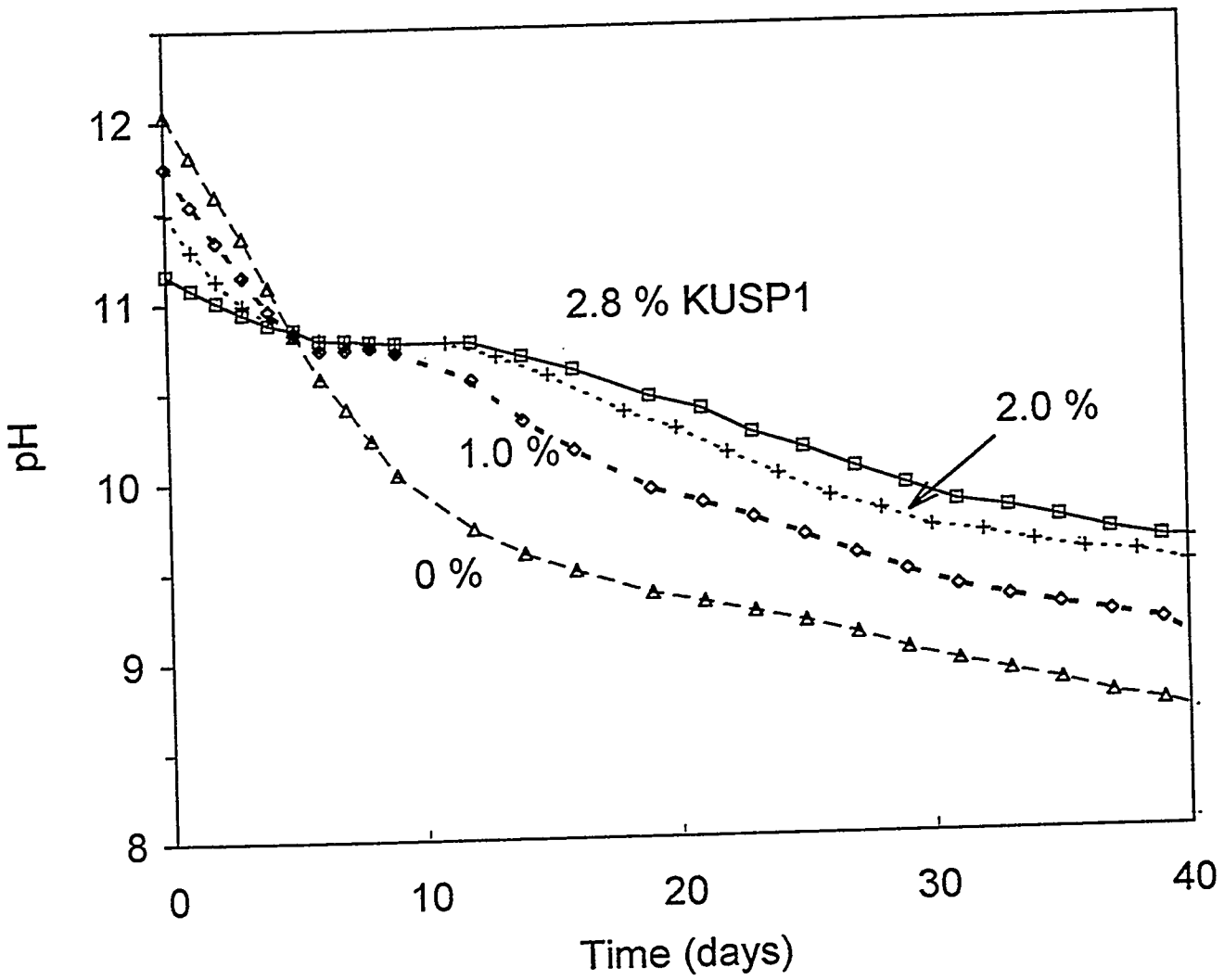

Figure 2.3 : pH as a function of time for KUSP1 solutions at a mole ratio of EBSA/NaOH between 0.78 and 0.80.

give satisfactory simulations of the pH-time data for solutions containing polymer in that a single rate constant did not match all sets of experimental data.

Bulk Gelation of KUSP1 using boric acid. The use of boric acid to trigger time-delayed gelation of alkali KUSP1 solutions was investigated. The physical nature of the KUSP1-boric acid gels was different from gels prepared by pH reduction without boric acid present. KUSP1 solutions without boric acid gel when the pH of the solution is dropped to a value of approximately 10.8 and the gel is white in color and has a tendency to shatter. Gels prepared at a boric acid concentration of 0.5 mole/kg solution were transparent and more resilient. As the boric acid concentration was decreased, the gels exhibited the same resiliency but they developed a white tinge.

Several series of samples were prepared and monitored to investigate the effect of boric acid concentration, initial pH and temperature on the gel time. Values of these parameters and the gel times are presented in Figures 2.4, 2.5 and 2.6. The results show that the gel time for 1.0% KUSP1 solutions can be regulated from instantaneous to several days by selection of boric acid concentration and initial pH.

Figures 2.4, 2.5 and 2.6 show that at constant initial pH, the gel time decreased with a decrease in boric acid concentration. This was contrary to the usual observation of shorter gel times with increased concentration. Gel times were also reduced as the temperature was increased. Syneresis of the gels increased with increased temperature and decreased pH. At 25 °C, syneresis (less than 10% solvent expulsion) was observed only at a pH of 10.0. At 45 °C, syneresis occurred at pH values of 11.0 and lower. Syneresis was observed at all pH values for samples maintained at 65 °C. Gels shrank to less than 25% of their original volume at 65 °C and at pH values less than 11.0

Alkaline KUSP1 solutions turned yellow and then brown over a period of many days when stored at room temperature. The rate at which the solutions changed color increased with temperature. Gel time was not affected by the color change for polymer solutions stored at 25 °C up to 7 days. Longer storage periods resulted in the solutions developing a dark brown color and a diminished gelling ability. Storage of 1.0% KUSP1 solutions with 0.2 M boric acid and at a pH of approximately 13 resulted in no color change and no gelation for several weeks at 25 °C. Samples prepared with a polymer solution stored under these conditions did not affect the gelation behavior. The shelf life of KUSP1 solutions may be extended by this technique.

Injectivity and Permeability Reduction in Porous Media

Flow experiments were conducted to investigate the capability of KUSP1 systems to reduce the permeability of various rock media. Three methods to trigger the gelation of KUSP1 were investigated. Interactions of alkali KUSP1 solutions with the rock media were studied to determine if those interactions were sufficient to reduce the pH to values where KUSP1 gelled. Permeability reduction by the in situ gelation of the KUSP1-ester system and the KUSP1-boric acid system was assessed.

Initial experiments revealed a problem with the injectivity of KUSP1 solutions in porous media. The research program was expanded to identify the cause of the problem and to develop a procedure to improve the injectivity of KUSP1 solutions.

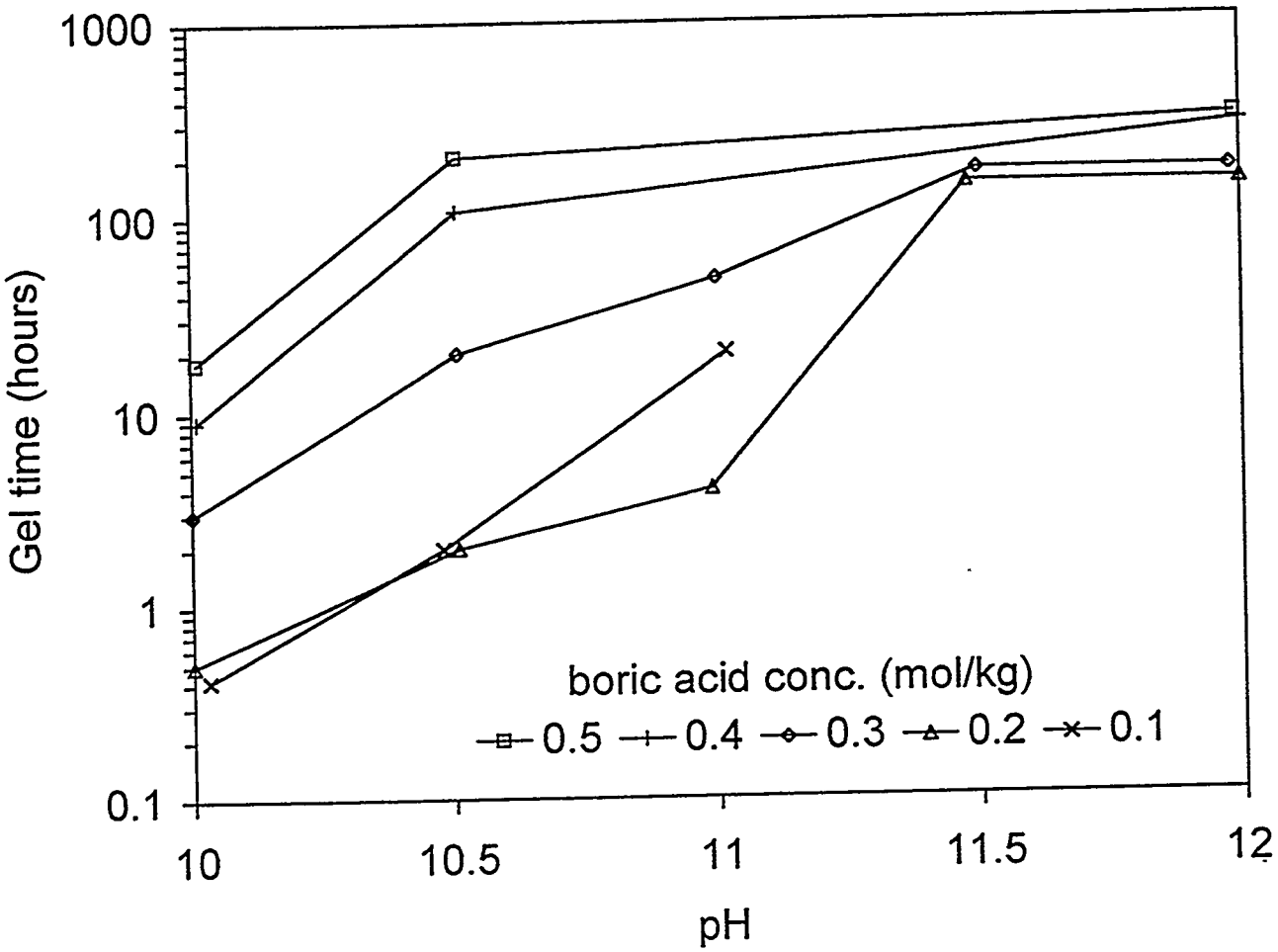

Figure 2.4 : Gel time as a function of pH and boric acid concentration for the KUSP1-boric acid gel system at 25 °C.

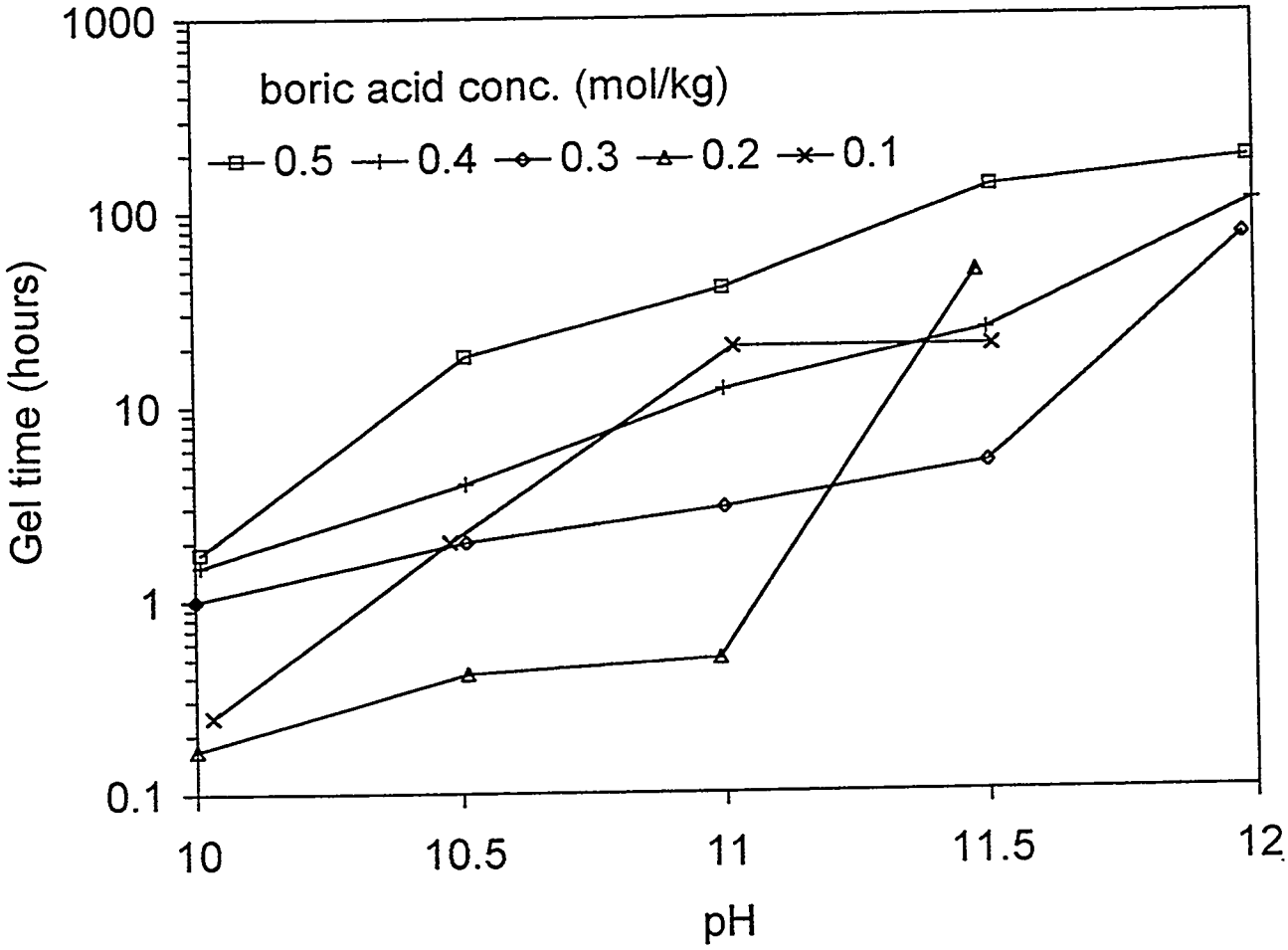

Figure 2.5 : Gel time as a function of pH and boric acid concentration for the KUSP1-boric acid gel system; 1.0% KUSP1, 45 °C.

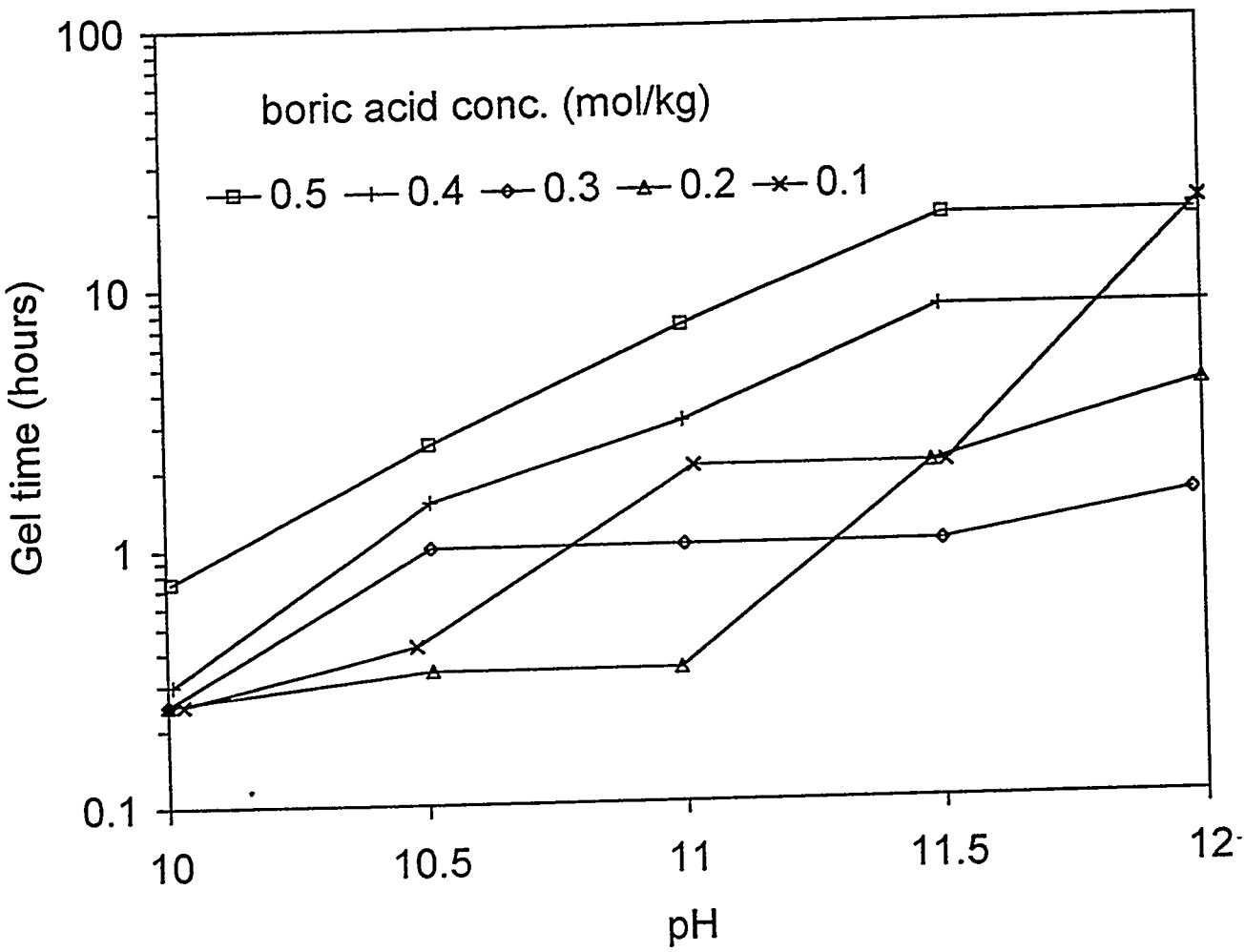

Figure 2.6 : Gel time as a function of pH and boric acid concentration for the KUSP1-boric acid gel system at 65 °C.

Injectivity of KUSP1 solutions. A continuous increase in flow resistance in the entrance section of Berea sandstone cores was observed during the injection of alkali KUSP1 solutions. Filtration of the polymer solution through a 5-μm filter did not eliminate front-end loading. Filtration tests revealed that the problem was due to accumulation of a small amount of debris that was present in KUSP1 solutions. NaCl added to the solution enhanced the formation of the insoluble component and decreased injectivity.

Elimination of front-end loading during the injection of KUSP1 solutions was achieved by using carbon black and filter aid during filtration through a 5-micron filter. Tests revealed that the particulate material in the solutions was sensitive to the pH and NaCl content of the polymer solutions. It was determined that a minimum of 0.1 M NaOH must be used in KUSP1 solutions that contain 1% NaCl to eliminate front-end loading.

Gelation triggered by fluid-rock interactions. Experiments were conducted to determine if interactions between alkaline KUSP1 solutions and selected rock media were sufficient to reduce the pH of the solution to levels required for gelation. Silica sandpacks and small cores of Berea sandstone, Baker dolomite and J-Alpha grainstone (Lansing-Kansas City formation) were saturated with solutions containing 1.0% KUSP1, 1.0% NaCl and either 1.0 M or 0.1 M NaOH. The saturated media were maintained at 25°C for selected periods of shut-in times. Small volumes of KUSP1 solution were then injected into each core and the effluent was collected. The viscosity, pH and polymer content of the effluent were determined. Pressure drops measured during injection were analyzed.

No significant change in flow resistance or effluent viscosity was observed for any of the cores after shut-in periods that ranged from 6 to 60 days. The lowest pH measured was 11.54 after a 55-day shut-in period. This was measured in the effluent of a Berea sandstone core that was saturated with KUSP1 solution containing 0.1M NaOH. A pH value of approximately 10.8 must be achieved to trigger gelation. The results indicate that fluid-rock interactions are not sufficient to cause gelation of KUSP1 solutions in oil reservoirs.

In-Situ Gelation of the KUSP1-Ester System. The primary objective of this work was to determine the magnitude of permeability reduction produced by the gelation of the KUSP1-ester system in selected rock samples. The ester used was monoethylphthalate (MEP). Experiments were conducted in sandpacks, in Berea sandstone cores and in carbonate field cores (J-Alpha Grainstone of the Lansing-Kansas City formation). The long-term stability of the treatments and the effect of residual oil saturation were also determined.

Rock media were injected with approximately two pore volumes of gelant over a period of about an hour. The gelant contained 2.0% KUSP1, 0.1 N NaOH and 0.06 M MEP ester and had a bulk gel time between 30 and 35 hours. The media were shut-in for three to four days at 25 °C. Brine was then injected to determine the post-treatment permeabilities. Tracer tests were conducted on the media before and after the treatment. Permeabilities measured over a period of many weeks was used to determine the long-term stability of the treatments.

Permeabilities of the media were significantly reduced by the treatments as shown in Table 2.2. Pressure measurements across sections of the cores showed that the permeability reduction was uniform along the length of the cores. Residual oil saturations did not significantly alter the effect of the treatment process.

Table 2.2 : Porous Media Properties and Results of Flow Experiments for the KUSP1-ester system.

Experiment Code	Porous Medium Type	Dimensions length x diameter (cm x cm)	Overall Permeability (mD)		Residual Resistance Factor	Post-Treatment Pore Volume (% of orig. PV)
			Before Treatment	After Treatment		
SP1	Sandpack	30.5 x 3.81	7750	34	230	0.97
SP2	Sandpack	30.5 x 3.81	9470	2.1	4500	0.85
SP3	Sandpack	30.5 x 3.81	7340	4.3	1700	0.90
BC1	Berea SS	30.5 x 5.1 x 5.1*	157	0.54	290	0.96
BC2	Berea SS at residual oil saturation (S_{or})	30.5 x 3.81	45 (at S_{or})	0.59	76	0.67 at S_{or}, 0.66 after treatment
BC3	Berea SS	30.5 x 3.81	600	1.3	460	0.98
JAG1	Limestone	6.5 x 2.6	115	0.18	640	0.86
JAG2	Limestone at residual oil saturation (S_{or})	5 x 2.4	14.3 (at S_{or})	0.04	360	0.74 at S_{or}, 0.62 after treatment
JAG3	Limestone	5 x 2.4	145	0.41	350	0.92

* square cross-section.

Tracer tests were conducted to determine the pore volume contacted by the injected brine after the treatment. Tracers contacted 85 to 99 % of the pore volume during post-treatment tests which indicated that the gel was permeable to brine.

Stability of the permeability-reduction treatments was assessed in six of the cores. No significant increase in permeability was observed even after the injection of many pore volumes of brine over a period of up to six months.

In-Situ Gelation of the KUSP1-Boric Acid System. The performance of the KUSP1-boric acid system was determined in sandpacks and Berea sandstone cores at 25 and 45 °C. The gelant was composed of 1.0% KUSP1, 0.5 mole of orthoboric acid (H_3BO_3) per kg of gelant and 1.0% NaCl. A gel time of 24 hours was controlled by adjusting the pH of the gelant to 9.9 at 25 °C and to 10.5 at 45 °C. Two-to-three pore volumes of gelant were injected into the media over a time period of about an hour. The media were then shut-in for approximately 30 hours before post-treatment brine injection.

During the injection of gelant, flow resistance in the media did not exceed that due to the viscosity of the gelant which indicated no problems with the injectivity of the gelant. Atypical behavior was observed during post-treatment brine injection in that several pore volumes of brine were injected before pressure drops stabilized. Pressure drops declined at a given flow rate demonstrating an increase in permeability with volume of brine injected. Post-treatment permeabilities were determined after more than 400 hours of injection which corresponded to more than four pore volumes of brine injected. Pre- and post-gelation permeabilities are given in Table 2.3. The residual resistance factors, which is the ratio of these permeabilities, show that the permeabilities were reduced by factors greater than 50. Permeabilities were reduced less at 45 °C than at 25 °C, possibly due to more syneresis occurring at the higher temperature. At a given temperature, permeabilities were reduced by larger factors in sandpacks than in Berea sandstone cores.

Data from tracer tests conducted before and after the gel treatment were used to determine the fraction of pore volume that was contacted by the displacing tracer. Values of the fraction of pore volume contacted by the tracer during the post-treatment tracer test are given in Table 2.3. The results show that the gel reduced the volume contacted by the tracer. Similar experiments conducted with the KUSP1-ester system showed that most of the pore volume was contacted by tracer. These results indicate the differences between the two KUSP1 system in how the gel reduces the permeability of porous media.

Table 2.3: Results for treatments in porous media using the KUSP1- boric acid system.

Exp. Code	Porous Media Type	Temp. (°C)	Initial Permeability (md)	Post-Treatment Permeability (md)	Residual Resistance Factor	Post-Treatment Pore Volume (% of orig. PV)
SP1	sandpack	25	6700	2	3300	-
SP2	sandpack	25	6800	2.6	2600	-
SP3	sandpack	45	7000	112	62	20
BC1	Berea sandstone	25	560	1.2	470	44
BC2	Berea sandstone	45	610	12.5	50	22
BC4	Berea sandstone	45	460	4.7	98	9
BC5	Berea sandstone	45	510	2.0	250	19
BC6	Berea sandstone	45	470	18	26	13

Summary

1. The growth conditions for the production of KUSP1 biopolymer were optimized.
2. Chemical modifications of the KSUP1 biopolymer did not enhanced the properties of the polymer for use in permeability modification treatments.
3. Large-scale production costs were estimated to be between 3.94 and 7.38 $/lb.
4. The viscosity behavior of alkaline solutions of KUSP1 was characterized.
5. Two esters, ethylbenzoate-2-sulfoic acid and monoethylphthalate, were identified that would trigger gelation of KUSP1 solutions. Gel times for the KUSP1-ester systems ranged up to 11 days at 25 C. Monoethylphthalate is inexpensive and attractive for use in field treatments.
6. Boric acid added to KUSP1 solutions triggered time-delayed gelation. Gel times for the KSUP1-boric acid system ranged up to several days. Syneresis of this gel system increased with temperature.
7. Interactions between KUSP1 solutions and several types of rocks were not sufficient to reduce the pH of the solution and trigger gelation.
8. The KUSP1-monoethylphythalate ester system significantly reduced the permeability of several types of rock media. The gel treatments were stable for time periods up to six months.
9. Permeabilities of sandpacks and Berea sandstone cores were significantly reduced by treatments with the KUSP1-boric acid system.

References

1. Green, D.W. and Willhite, G.P., "Improving Reservoir Conformance Using Gelled Polymer Systems - Annual Report - September 25, 1992 to September 24, 1993," U.S. Department of Energy report number DOE/BC/14881-5.
2. Green, D.W. and Willhite, G.P., "Improving Reservoir Conformance Using Gelled Polymer Systems - Annual Report - September 25, 1993 to September 24, 1994," U.S. Department of Energy report number DOE/BC/14881-12.
3. Green, D.W. and Willhite, G.P., "Improving Reservoir Conformance Using Gelled Polymer Systems - Annual Report - September 25, 1994 to September 24, 1995," U.S. Department of Energy report number DOE/BC/14881-18.
4. Shaw, A.K., "An Experimental Study of Permeability Modification by In Situ Gelation of KUSP1 Biopolymer-monoethyl Phthalate Ester System in Porous Media," M.S. Thesis, University of Kansas (1995).
5. Fichadia, A., "Survey of Gelation Systems and a Study of the Gelation of KUSP1 by Hydrolysis of Mono-ethyl Phthalate," M.S. Thesis, University of Kansas (1995).
6. Yougo, M., "An Experimental Study of the Bulk Gelation of a Microbial Polysaccharide (KUSP1) by hydrolysis of the ester 'acid ethyl o-sufphonbenzoate' and Modeling of the Ester Hydrolysis Process," M.S. Thesis, University of Kansas (1994).
7. Bhattacharyia, S., "Fluid-Rock Interaction and Injectivity Studies of KUSP1 in Porous Media," M.S. Thesis, University of Kansas (1996).
8. Singh, A., M.S. Thesis, University of Kansas (in progress).

Chapter 3

Investigations on the Gelation of Polyacrylamide-Chromium(III) Systems

Principal Investigators: G.P. Willhite, D.W. Green, M.J. Michnick and C.S. McCool
Graduate Research Assistants: Mark McGuire, Carol Dona, Prashant Khanna and Ajay Kumar

Introduction

Polyacrylamide-chromium(III) systems are currently popular for use in field treatments. This chapter summarizes investigations on three aspects of the gelation of polyacrylamide-chromium(III) gelants. Gelants are subjected to shear deformation as they are pumped through a wellbore and into a reservoir. The effect of shear on the gelation of a polyacrylamide-chromium(III) gelant was investigated using rheometers. Polyacrylamide-chromium(III) systems contain anions that are introduced as the counter ion to Cr(III) and as added salts. The effect of anion types and concentrations on the gelation of polyacrylamide-chromium(III) gelants was studied. Chromium(III) can react with itself to form oligomers (dimers, trimers, etc.) at the conditions that gelants are prepared. A kinetic study of the reactions of chromium(III) monomer, dimer and trimer with partially-hydrolyzed polyacrylamide to form gels was conducted.

Effect of Shear on the Gelation of a Polyacrylamide-Chromium(III) System

This investigation is summarized here. Detailed results and experimental procedures are given in annual reports[1,2] and other literature.[3,4]

The effect of shear deformation on the gelation of the polyacrylamide-chromium(III) system was investigated using rotational rheometers that subjected gelant samples to steady shear and/or oscillatory shear deformations. The measurements yielded the viscosity, storage modulus and loss modulus of the gelant as a function time. Storage and loss moduli were obtained from the oscillatory experiments and are measurements of the elastic and viscous nature of the sample, respectively.

Experimental techniques were developed for the rheological measurements. The collection of reproducible data during the gelation of samples on rheometers required a precise technique for preparation of the sample (including the age of stock solutions) and the control of evaporation of the sample while on the rheometer platens.

Accurate rheological data was dependent on the selection of measurement parameters used on the rheometer. Data was analyzed to assure the measurements satisfied the underlying theory. For oscillatory measurements, the data conformed to linear viscoelastic theory and the gap loading condition was satisfied.

The effect of the frequency of oscillation on the development of storage modulus and the storage-loss moduli crossover was investigated. Initially, the loss modulus is greater than the storage modulus as shown in Figure 3.1 for a typical experiment. As gelation precedes, the storage modulus of the sample increases to values greater than the loss modulus. The time at which the loss and storage moduli are equal is the crossover. The crossover has been used as a measurement

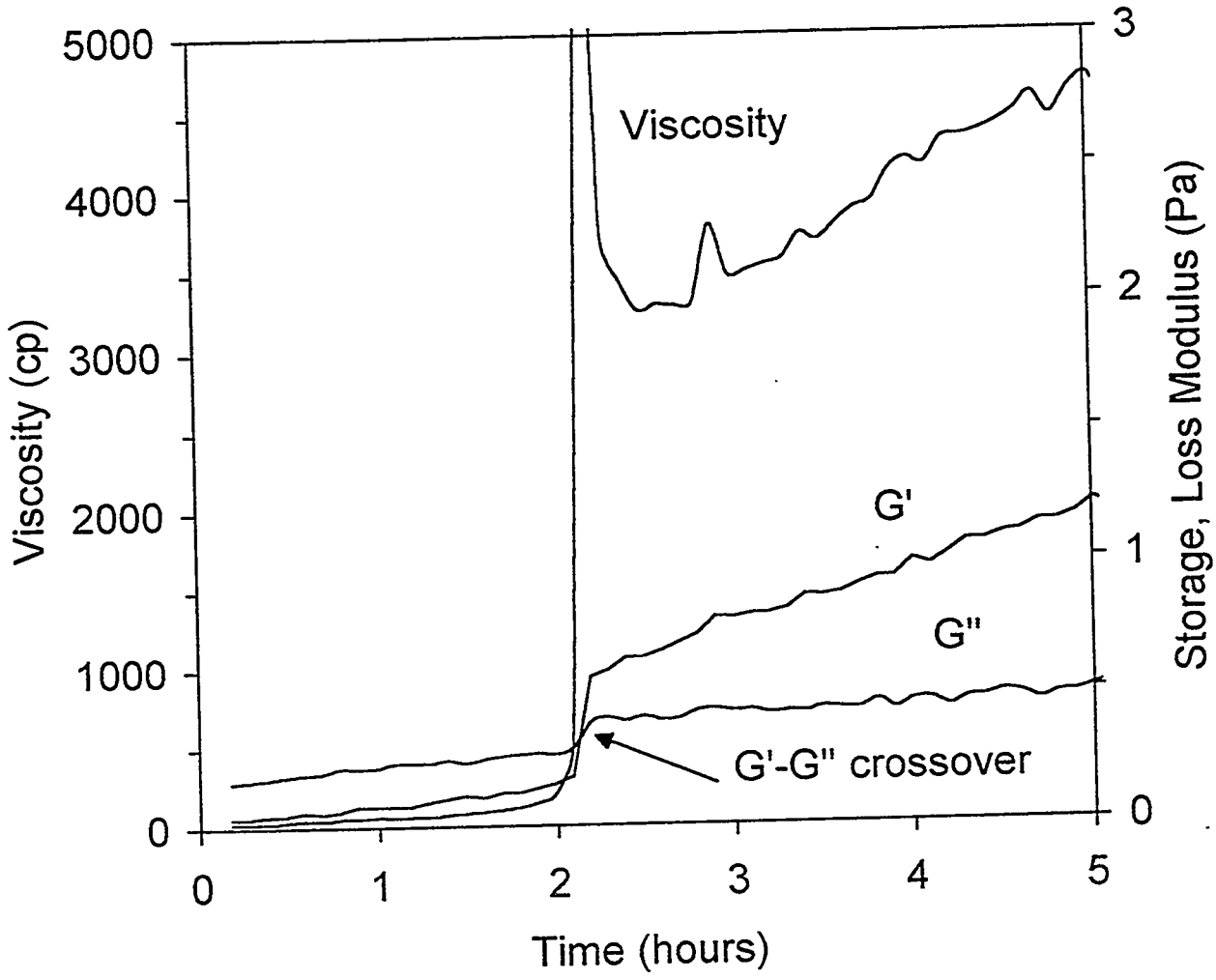

Figure 3.1 : Determination of gel times from rheological data. Sample subjected to oscillatory shear at 1.0 Hz and to a steady shear rate of 0.74 s^{-1}.

of the gel time of the sample. Results showed that the development of the storage modulus with time and the crossover times were functions of the oscillation frequency. For the particular sample studied, the crossover time at a frequency of 1.0 Hz was 40 % higher than the crossover time measured at 0.01 Hz. When comparing rheological data and when relating these data to gel structure, the oscillation frequency must be considered.

Steady shear experiments and experiments with the application of steady and oscillatory shear were conducted to determine the effect of shear on the gelation of a polyacrylamide-chromium(III) gelant. The viscosity behavior was consistent between these two type of experiments. That is, oscillatory shear superimposed on the steady shear did not alter the viscosity behavior. Viscosity as a function of time at selected shear rates are shown in Figure 3.2 and in Figure 3.3 for the early time period. The data show an induction period where the viscosity increased slowly for an hour or two. For shear rates less than 14.8 s^{-1}, an abrupt increase in viscosity was observed after the induction period. Using the abrupt rise in viscosity as a measure of gel time, gelation was accelerated by increasing shear rates up to a rate of 2.35 s^{-1} and retarded for higher shear rates.

The development of storage modulus for selected shear rates are shown in Figure 3.4 and in Figure 3.5 for the early time period. An induction period was followed by an abrupt rise in storage modulus was observed. The storage modulus showed the same general trends with shear rate as did the viscosity.

Gel times were defined two ways - (1) the time of the abrupt rise in viscosity and (2) the time of the storage-loss moduli crossover. Examples of these occurrences are shown in Figure 3.1 for a typical experiment. The results showed that the these gel times were approximately the same and that the gel times indicated significant growth of structure in the sample.

Effect of Anions of the Gelation of Polyacrylamide-Chromium(III) Systems

This section presents a summary of an investigation that was conducted to determine the effects of anion type and concentration on the gelation of polyacrylamide-chromium(III) gels. Details of this work are given elswhere.[1,5]

The anions studied were nitrate, perchlorate, chloride, sulfate and acetate. The concentration of anions in solution ranged up to 1.0 molal. Gelants were prepared and maintained at 25 C. Samples of the gelants were monitored by a rheometer using oscillatory shear. The results of these measurements were displayed in terms of the storage modulus and the loss modulus. Gel time for a sample was defined as the time when the loss modulus was equal to the storage modulus as shown. An example of these data for the perchlorate system is shown in Figure 3.6.

All gelants contained 9,000 ppm polyacrylamide and 100 ppm chromium(III). Chromium salts and sodium salts for the particular anion was used. The initial pH of gelants were adjusted to 5.0.

Gel times for the systems studied varied greatly as shown in Figure 3.7. Gelants containing nitrate gelled the fastest and the gel times did not vary much with concentration. Gelants prepared with chloride and perchlorate had similar gel times. Added sulfate delayed gelation. Samples containing 1.0 m sulfate did not gel within 90 days. Acetate significantly retarded gelation. Gelation was not observed in samples containing 0.1 and 1.0 m acetate.

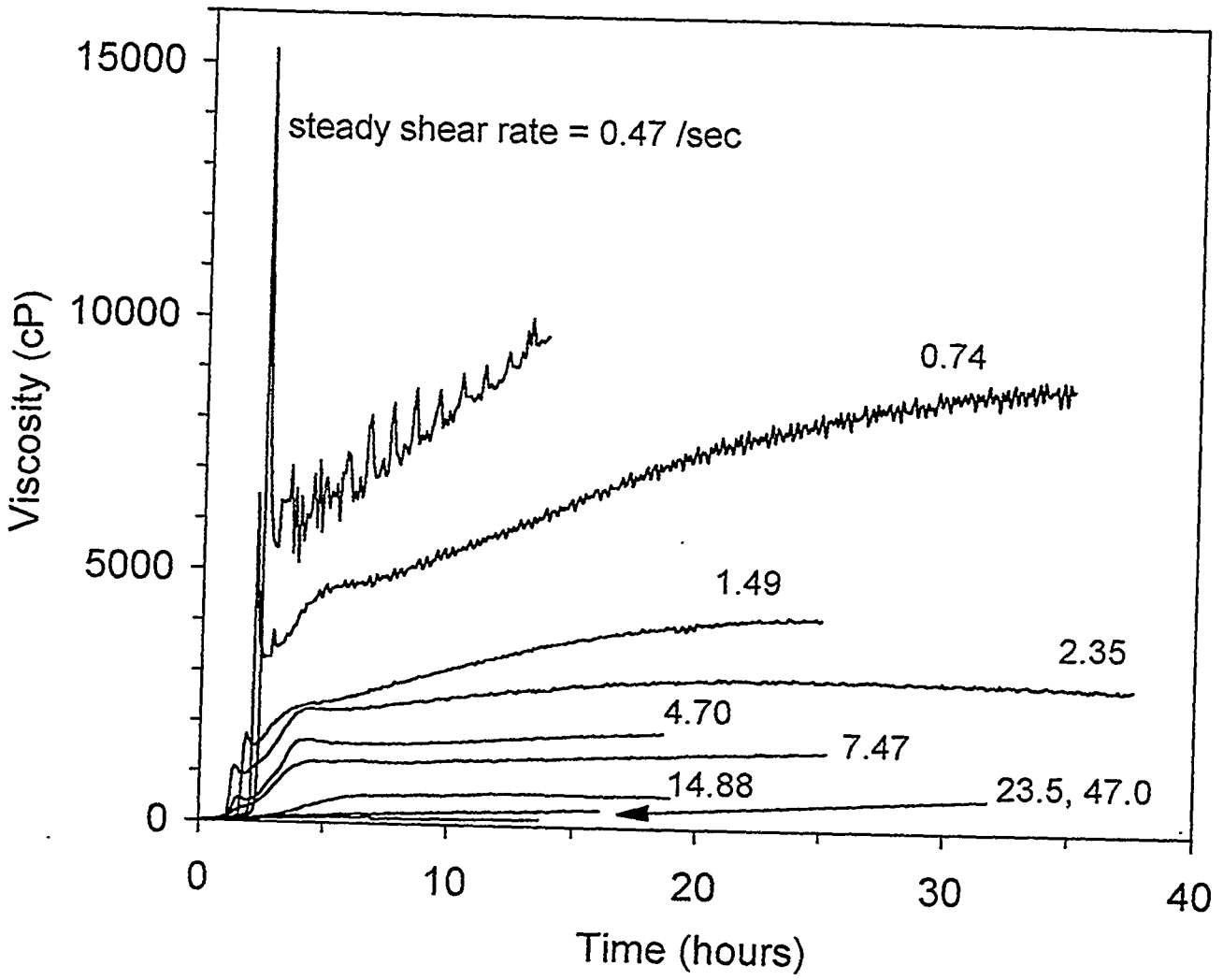

Figure 3.2 : Viscosity behavior during gelation under shear.

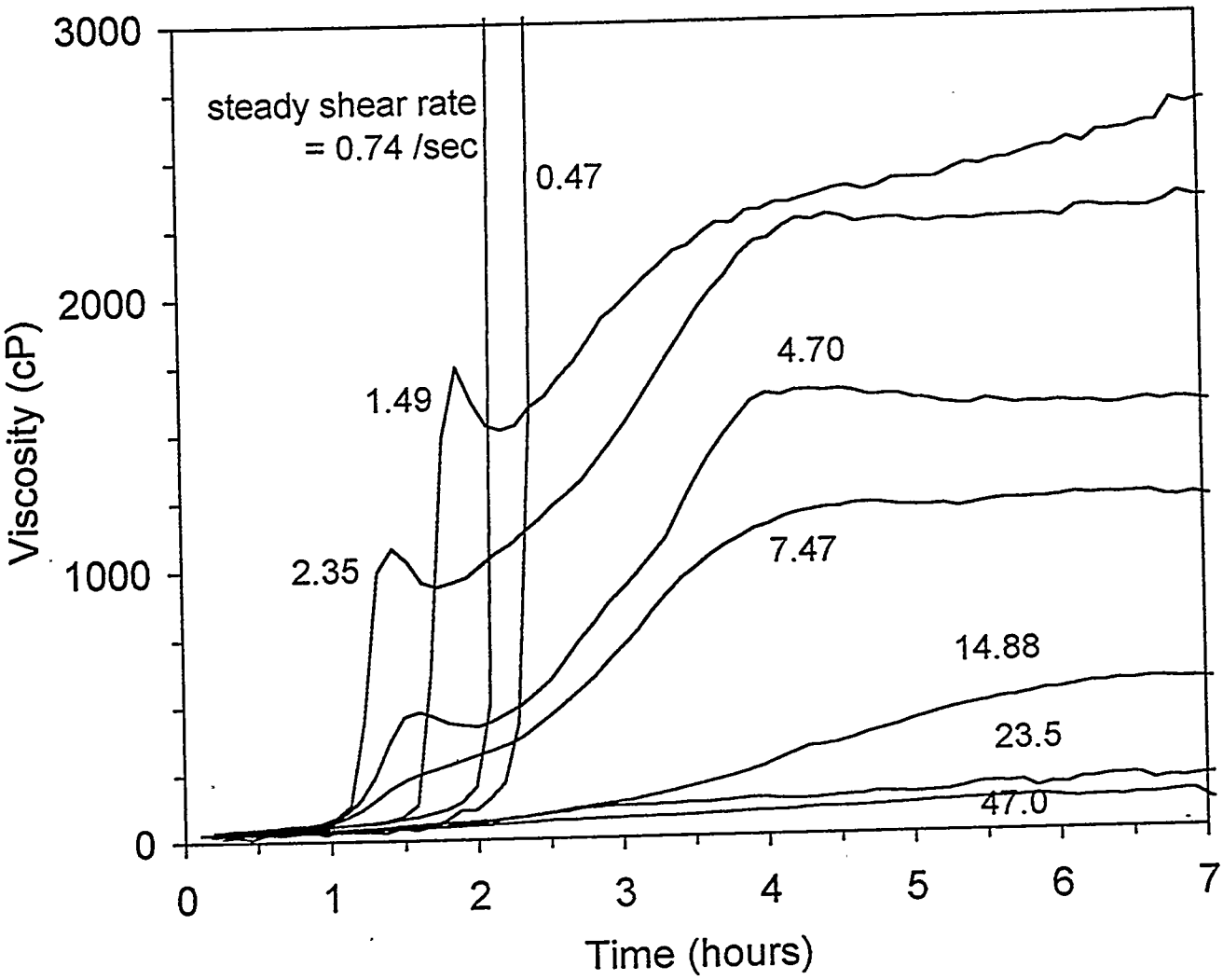

Figure 3.3 : Viscosity behavior during gelation under shear - early time period.

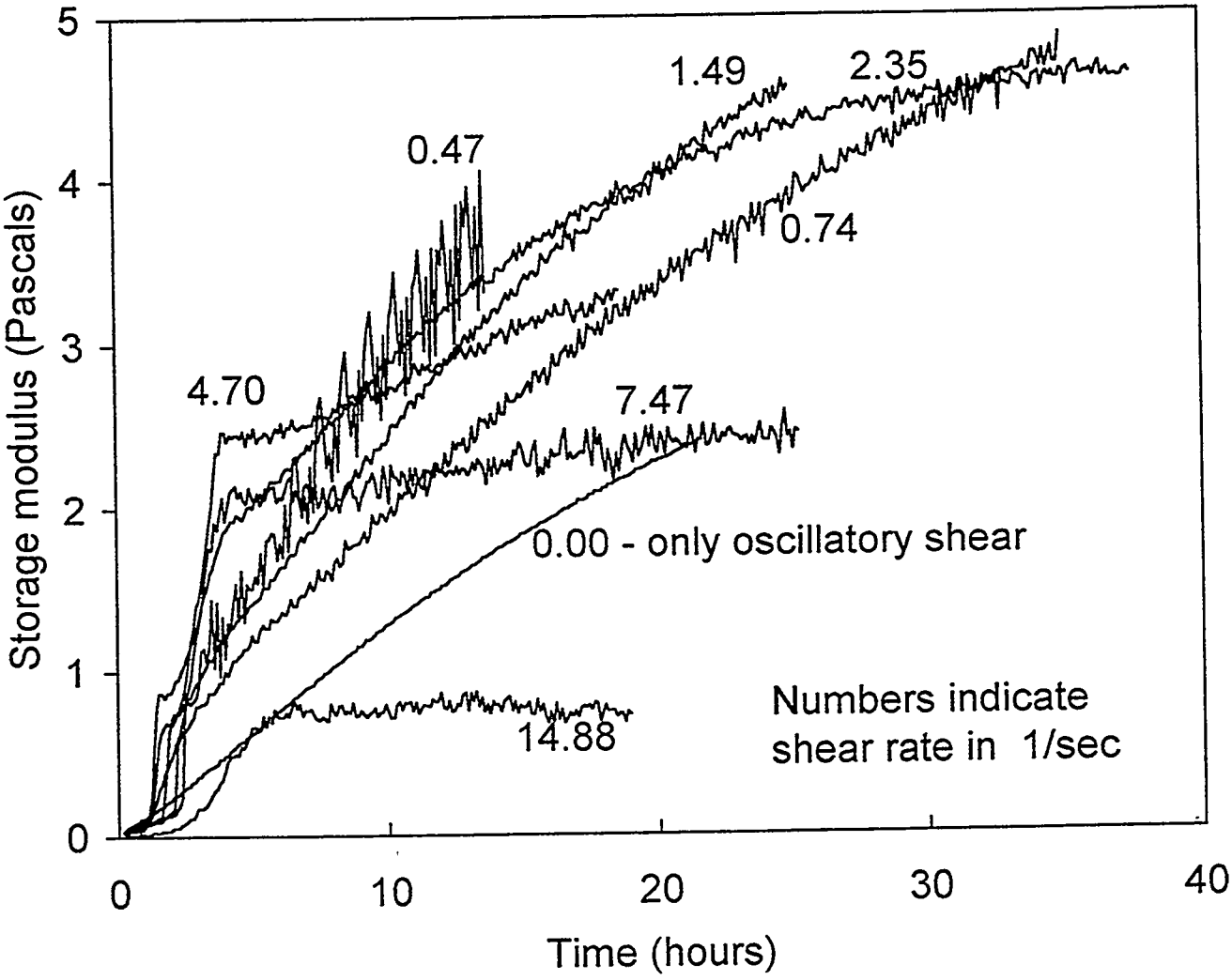

Figure 3.4 : Development of storage modulus during gelation under shear.

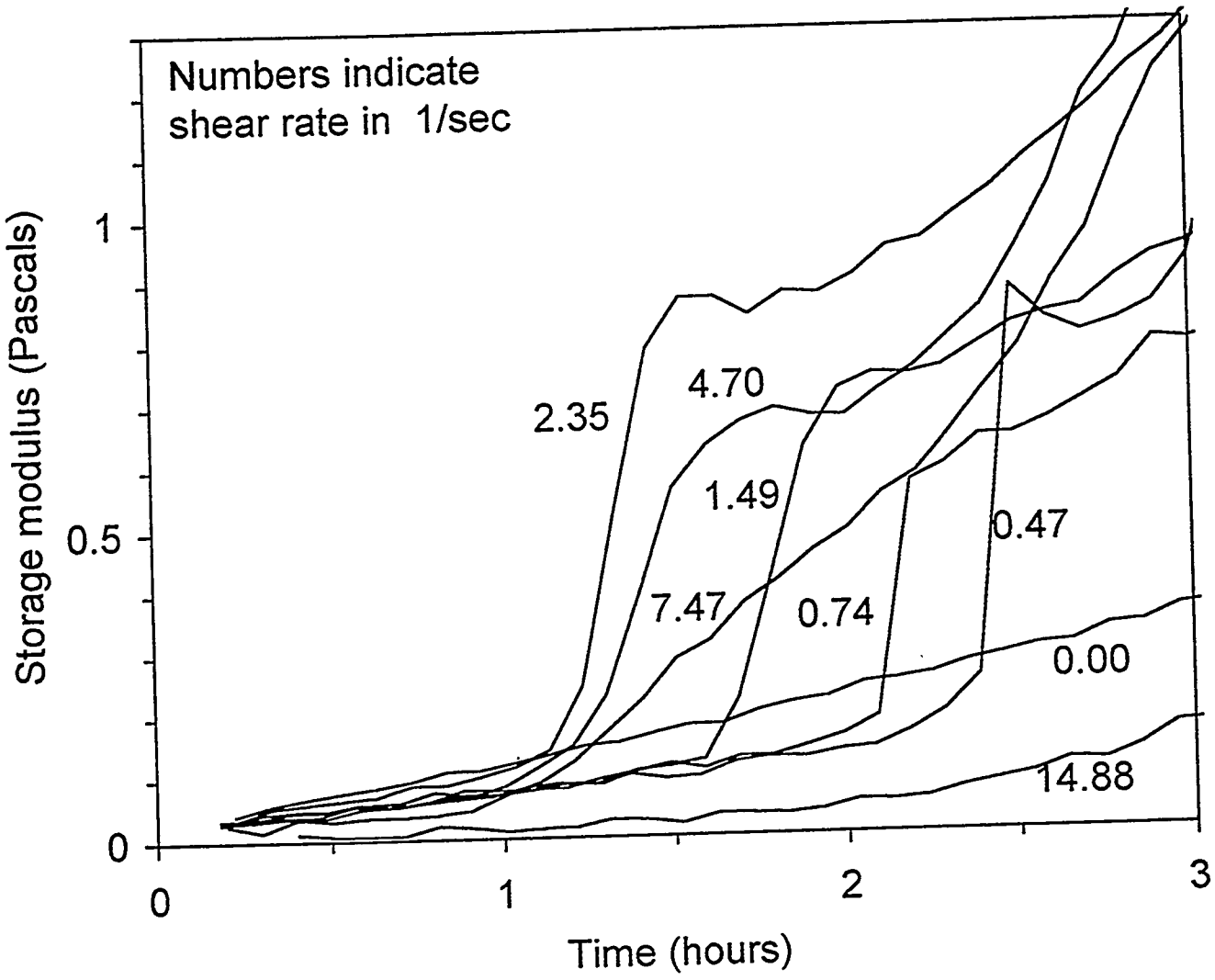

Figure 3.5 : Development of storage modulus during gelation under shear - early time period.

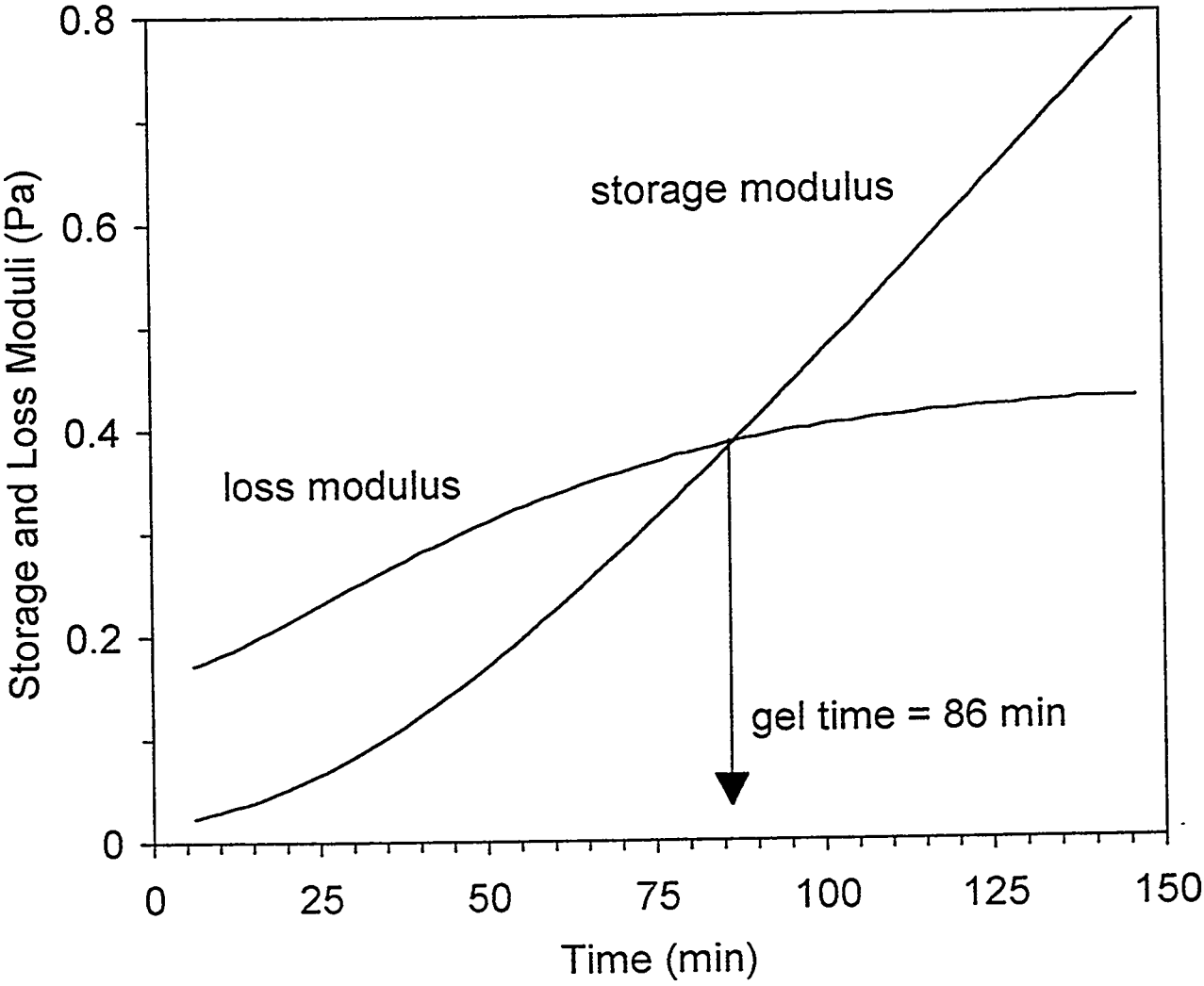

Figure 3.6 : Determination of gel time from the development of storage and loss modulus during gelation for the perchlorate system.

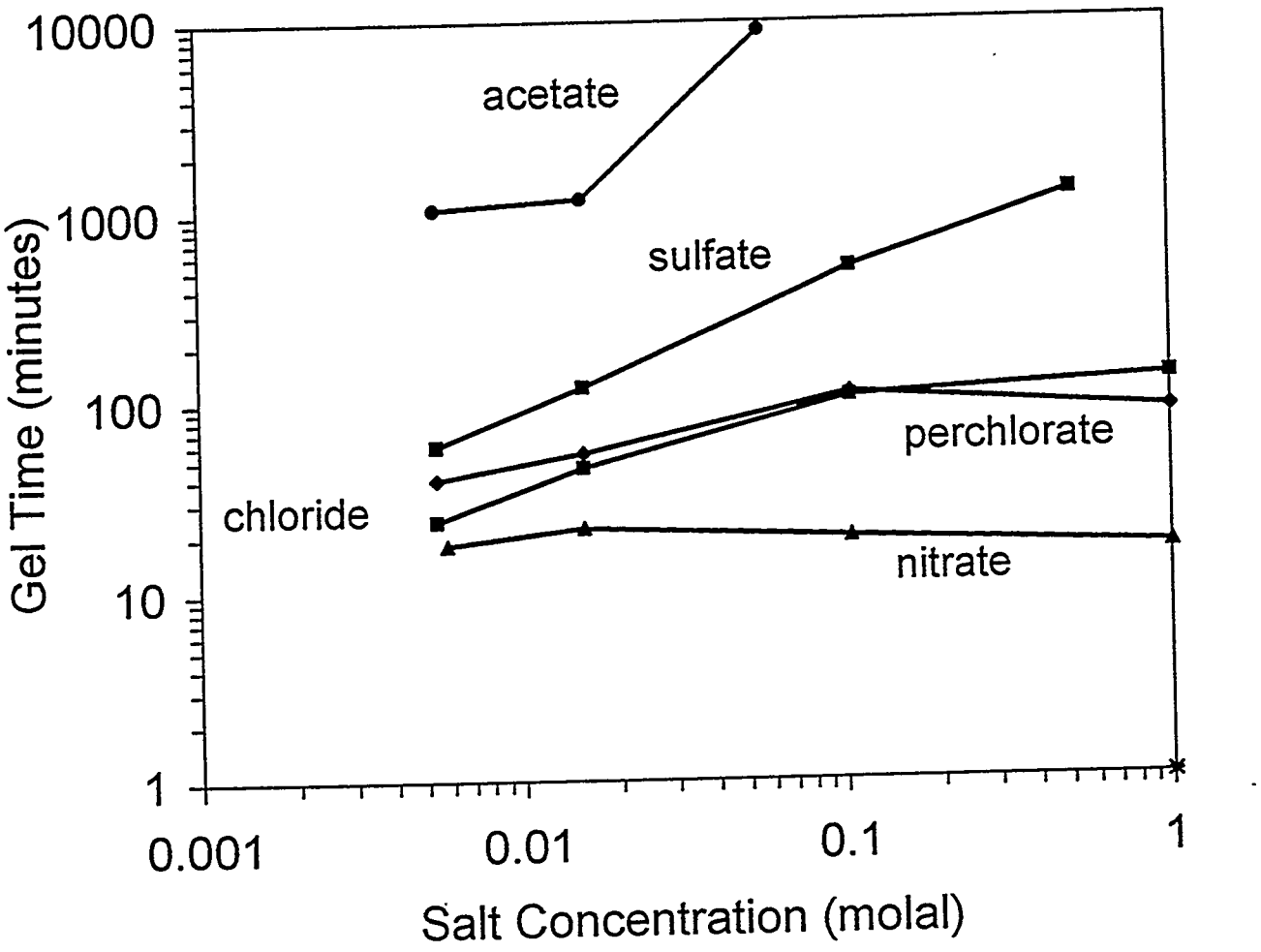

Figure 3.7 : Effect of anion type and concentration on the gel time.

Kinetics of the Reactions Between Chromium(III) Oligomers and Polyacrylamide

This section summarizes the investigation on the reaction rates between chromium(III) oligomers and polyacrylamide. Details of the experimental work can be obtained elsewhere.[1,6]

Chromium(III) in aqueous solution reacts to form dimers, trimers and higher order oligomers depending on conditions. The reactions between chromium(III) monomer, dimer and trimer with polyacrylamide were followed to assess the effects of oligomer type, oligomer concentration, pH and polyacrylamide concentration.

Two types of experiments were performed. The first type followed the reaction of free-solution chromium(III) with polyacrylamide, termed here the uptake reaction. Samples that had reacted for specified times where quenched and dialyzed. Concentrations of chromium(III) on both sides of the dialysis were measured which allowed the calculation of the amount of chromium(III) that had reacted with the polyacrylamide.

Relative rates of the gelation reaction (crosslinking between polymer molecules) were monitored with rheological measurements. Samples were subjected to oscillatory shear and the results were displayed as the storage modulus and the loss modulus. Two relative measures of the gelation rate were used. The first was the initial slope of the storage modulus-time data. In the second method, a gelation time was defined as the time when the storage modulus had increased to the value of the loss modulus, the G'-G" crossover time.

Two general sets of experimental conditions were used. The first set used approximately 25 ppm chromium(III), polymer concentration between 4400 and 19,800 ppm, 1M $NaClO_4$, and an initial pH value of 4. The second set use approximately 10 ppm chromium(III), approximately 15,000 ppm polymer, 1M NaClO4, and an initial pH of 5.

Uptake Reaction. Example data showing the effect of oligomer type on the rate of oligomer uptake by the polyacrylamide is shown in Figures 3.8 and 3.9. The results show that the uptake rates are fastest for the trimer and slowest for the monomer. Rates for the dimer and trimer are greater than those extrapolated from the monomer data and assuming equal molar rates of reaction. This suggests that the dimer and trimer are more reactive on a molecular level with the polymer than the monomer. The trimer exhibited particularly high reactivity.

The effect of polyacrylamide concentration on oligomer uptake is shown in Figure 3.10. An increase in uptake rate with polymer concentration was observed. The effect of pH on trimer uptake is shown in Figure 3.11. The rate of timer uptake increased with pH. Trimer uptake was particularly rapid at pH 5, where 90% of the trimer had reacted with the polymer within five minutes when the first sample was taken.

Gelation Reaction. Gelation rates were examined by following the storage (G') and loss (G") moduli as functions of time. The data are presented as the increase in G' above the initial G' value at zero time due to the sensitivity of the initial G' value to polymer concentration. The effect of oligomer type on the increase-in-storage modulus is shown in Figure 3.12. The initial slopes for these curves were 0.008, 0.024 and 0.299 Pa/hour for the monomer, dimer and trimer, respectively.

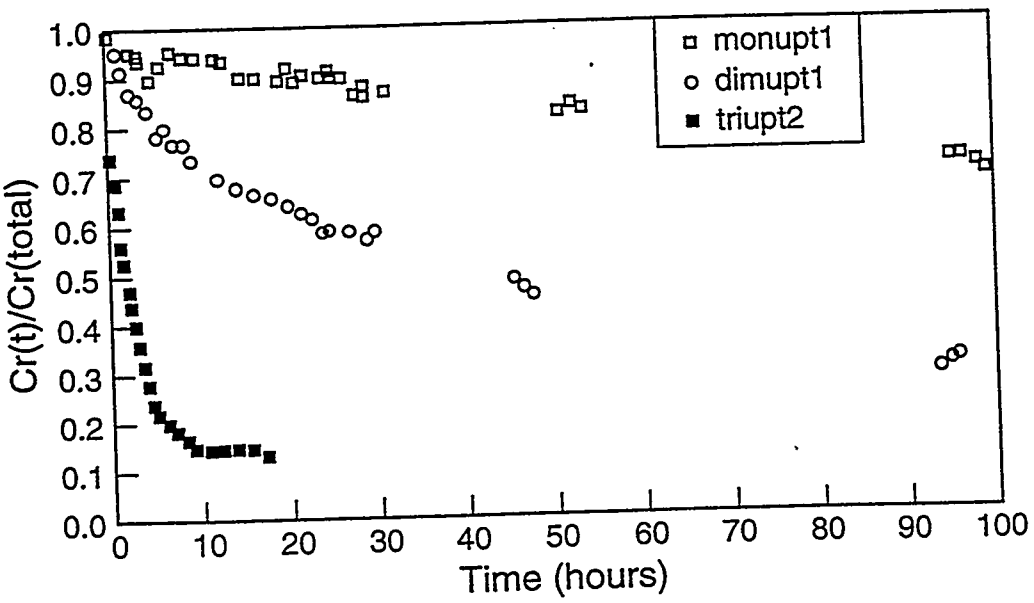

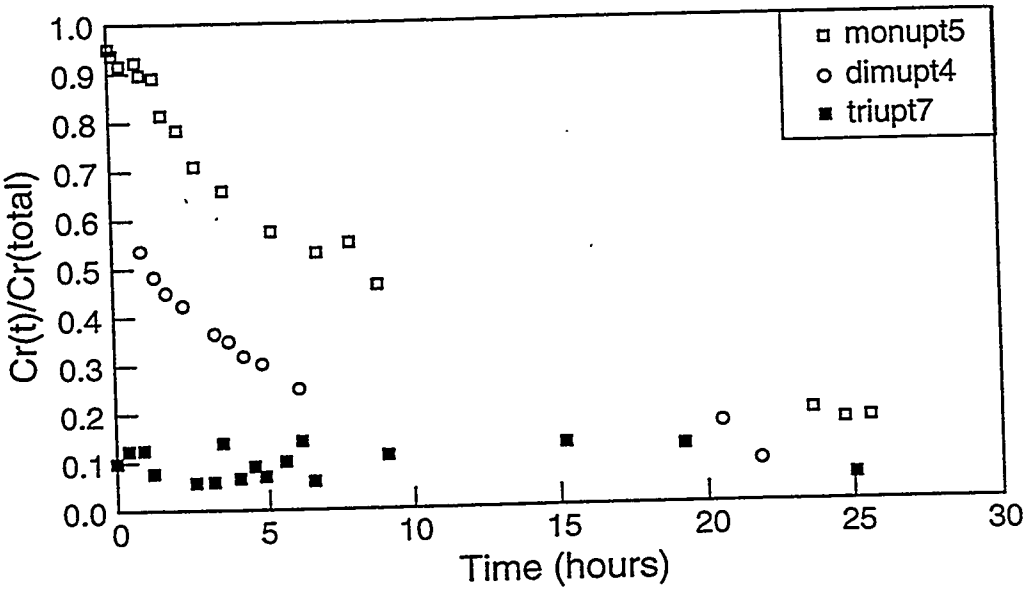

Figure 3.9 : The effect of oligomer type on chromium uptake; pH = 5, 8 - 11 ppm Cr(III), 14,000 - 15,000 ppm polyacrylamide; ■-trimer, O-dimer, □-monomer.

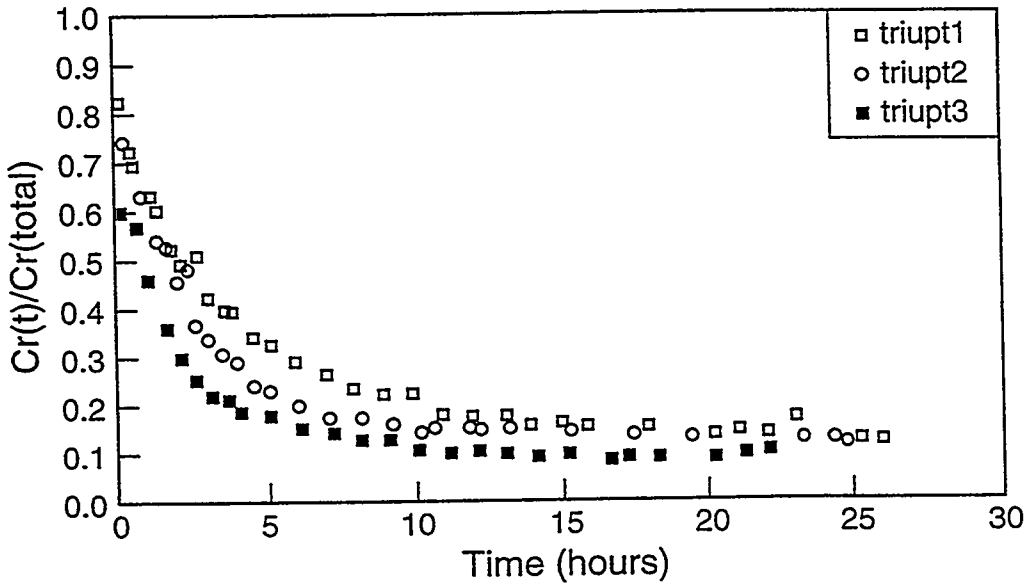

Figure 3.10 : The effect of polymer concentration on chromium uptake; pH = 4, 23 - 25 ppm Cr(III); ■-13,200ppm polymer, O-8,630ppm, □-4,430ppm.

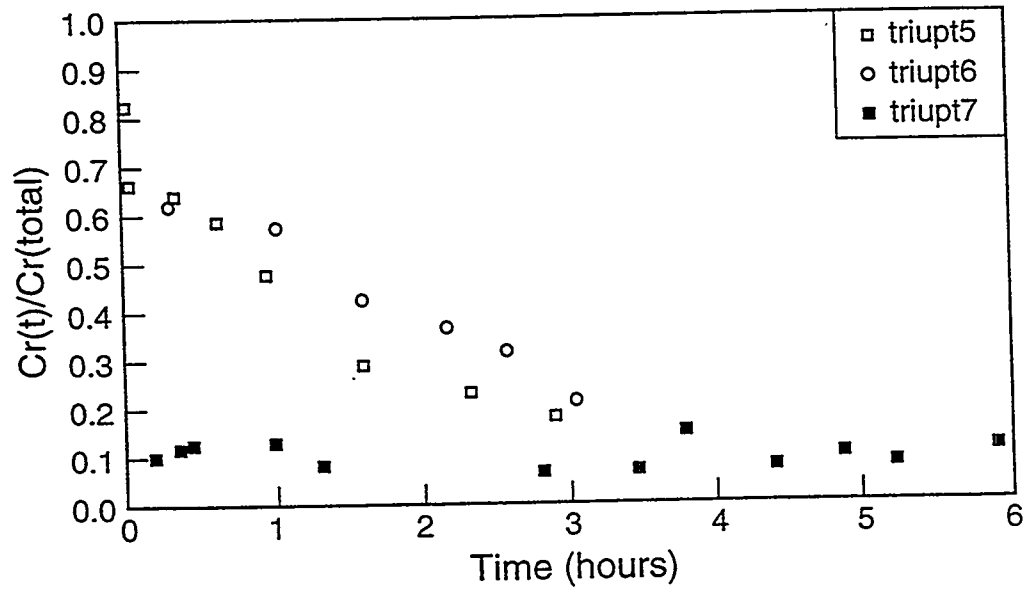

Figure 3.11 : The effect of pH on chromium uptake; 7.1 - 11 ppm Cr(III), 14,000 - 14,900 ppm polyacrylamide; ■-pH=5, O-pH=4, □-pH=4.

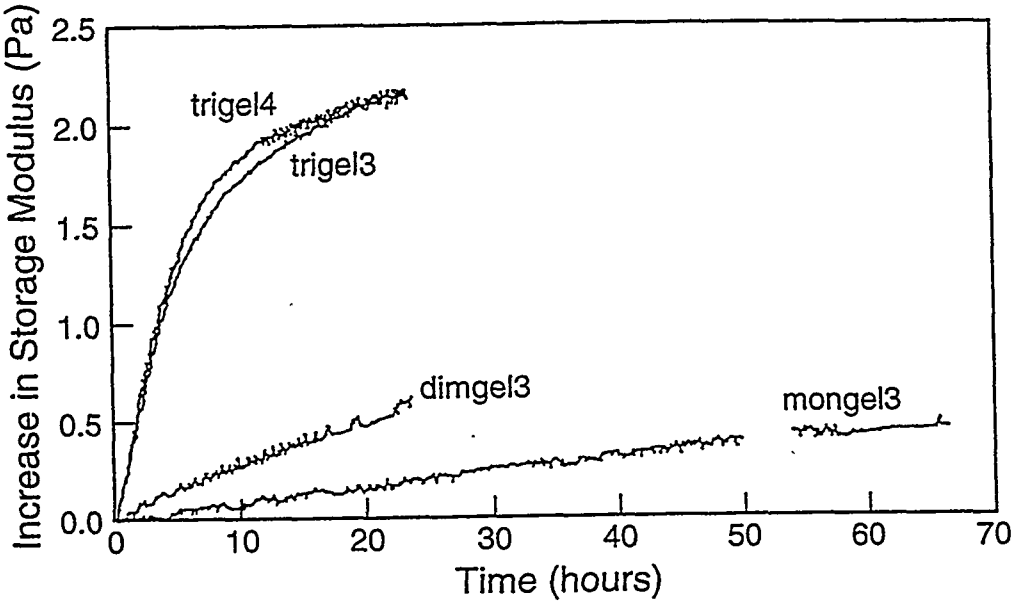

Figure 3.12 : The effect of oligomer type on the increase in G'; pH = 4, 7.4 - 11.7 ppm Cr(III), 14,700 - 15,000 ppm polyacrylamide.

These data show the rates of gelation increase with oligomer size. The increase in gelation rate is even more dramatic with oligomer size when comparing on a molar concentration basis.

The effect of chromium concentration on the gelation rate is shown in Figure 3.13 for the dimer. Comparisons of the initial slopes of the G'-increase - time curves with the initial chromium concentrations indicated that the gelation rates increased above that expected from a linear dependence of the gelation rate on oligomer concentration.

The effect of pH on the gelation rate for the monomer is shown in Figure 3.14. The gelation rate, as indicated by the initial slopes, increased 24 times with a pH change from 4 to 5. The gelation rate for the dimer and trimer increased 7.9 and 3.7 times, respectively, for the same pH change.

The rates of uptake and gelation were compared by plotting the fractional chromium(III) reacted and the increase-in-G' as functions of time. The increase-in-G' curves approximately paralleled the increase in oligomer uptake, especially during the early time periods. For the trimer runs, the G' value continued to increase slowly after most of the trimer uptake had occurred.

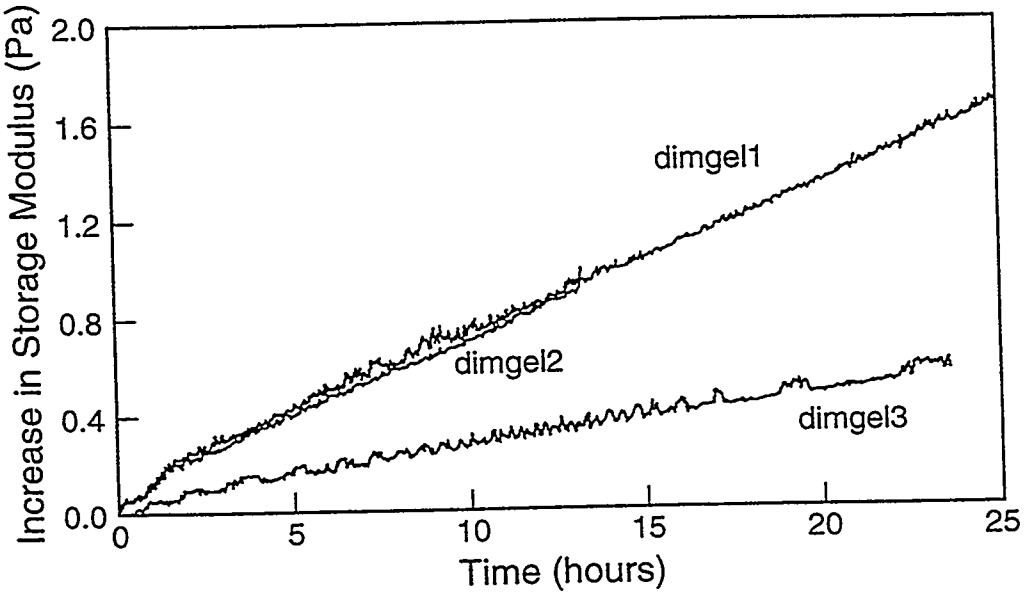

Figure 3.13: The effect of Cr(III) dimer concentration on the increase in G'; dimgel1 and dimgel2 - 21 ppm Cr(III), dimgel3 - 10.9 ppm Cr(III); pH=4, 14,800 - 15,000 ppm polymer.

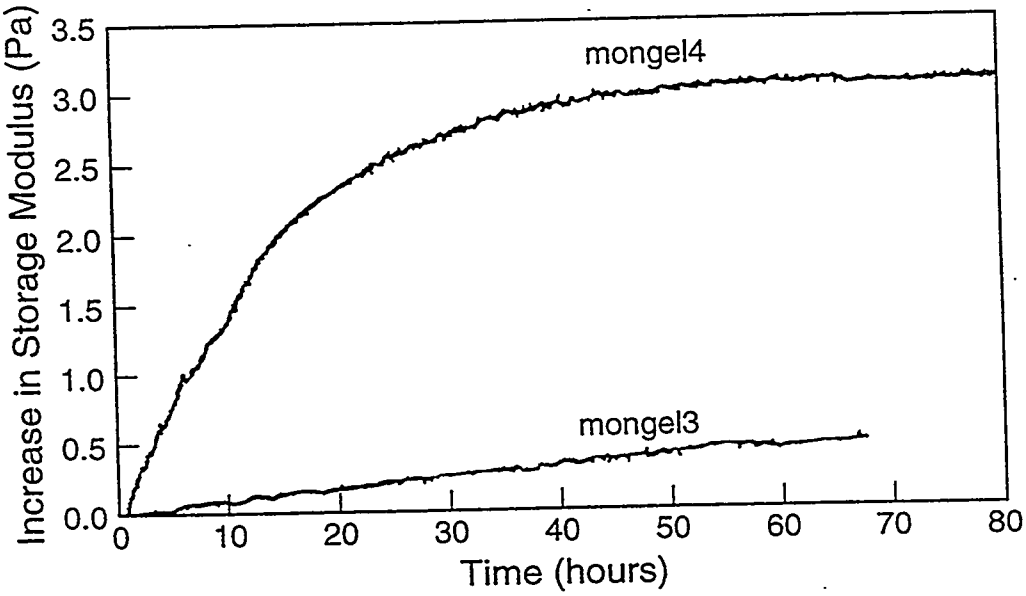

Figure 3.14: The effect of pH on the increase in G'; pH=5 for mongel4, pH=4 for mongel3; 10.9 - 11.7 ppm Cr(III); 15,000 ppm polymer.

Modeling of the Uptake Data. The rate for the uptake reaction was described by eqn (1).

$$\frac{d[Cr\,]}{dt} = -k\frac{[Cr\,][carboxyl]}{[H^+]} \qquad \text{(eqn - 1)}$$

Integration of equation (1), with [Cr] equal to [Cr(initial)] at time equal to zero and at constant pH and constant polymer concentration, gives equation (2).

$$\ln\left(\frac{[Cr\,(t)]}{[Cr\,(initial)]}\right) = -k't \qquad \text{(eqn - 2)}$$

with

$$k' = \frac{k[carbxyl]}{[H^+]} \qquad \text{(eqn - 3)}$$

Many of the experiments showed a rapid, initial uptake of chromium and [Cr(initial)] was less than the total chromium in the system, [Cr(total)].

Data from the uptake experiments were regressed to determine the rate constant, k', as shown in Figure 3.15 for monomer uptake experiments at a pH of 4 and at three different polymer concentrations. The values of k' were then regressed against polymer concentration according to eqn (3) to give a value of k equal to 1.07 10^{-4} $hour^{-1}$. Deviations were observed between the model and data for the uptake reaction of dimer and trimer.

Summary

Effect of Shear. Several characteristic responses were observed when a chromium(III)-polyacrylamide gel system was subjected to continuous steady shear during gelation. An induction period was observed where small increases in shear viscosity and storage modulus occur. After the induction period, and abrupt increase in shear viscosity and storage modulus was observed for shear rates less than 15 sec^{-1}. Gelation was accelerated by increased shear rate, reaching a maximum at 2.35 sec^{-1}, and was retarded for higher shear rates. No gelation occurred when shear rates were on the order of 40 sec^{-1} and higher.

Effect of anions. Anion type and concentration significantly affected the gel time of a chromium(III)-polyacrylamide gel system. Gelants containing nitrate gelled the fastest and the times did not vary much with concentration. Gelants prepared with chloride and perchlorate had similar gel times. Added sulfate delayed gelation even more. Acetate significantly retarded gelation. Gel times of the chloride, perchlorate, sulfate and acetate increased with concentration.

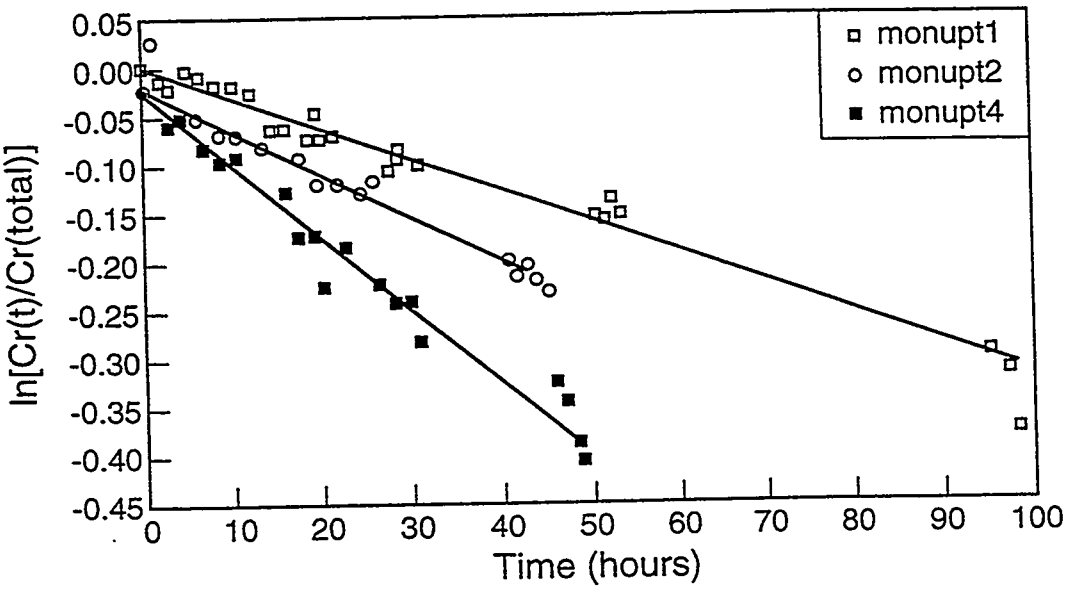

Figure 3.15 : Regressions to determine rate constants for uptake data of Cr(III) monomer; pH=4, 25.4 - 27.3 ppm Cr(III); ■-19,900ppm polymer, O-13,400ppm, □-8,800ppm.

Kinetics of Uptake and Gelation Reactions. The rates of the uptake and gelation reactions increased with the size of the chormium oligomer, oligomer concentration and pH. The gelation reaction, as indicated by rheological data, closely followed in time the uptake of oligomers by the polymer. A kinetic model was developed that reasonably matched the uptake data for the chromium monomer.

References

1. Green, D.W. and Willhite, G.P., "Improving Reservoir Conformance Using Gelled Polymer Systems - Annual Report - September 25, 1992 to September 24, 1993," U.S. Department of Energy report number DOE/BC/14881-5.
2. Green, D.W. and Willhite, G.P., "Improving Reservoir Conformance Using Gelled Polymer Systems - Annual Report - September 25, 1993 to September 24, 1994," U.S. Department of Energy report number DOE/BC/14881-12.
3. Khanna, P., "A Study of Rheological Method to Monitor Gelation of Polyacrylamide-Chromium(III) Gels," MS thesis, University of Kansas (1994).
4. Kumar, A., "A Rheological Study of the Effects of Shear Rate on Gelation of Polyacrylamide-Chormium(III) System," MS thesis, University of Kansas (1994).
5. McGuire, M., MS thesis in progress, University of Kansas.
6. Dona, C., "An Experimental Study of the Uptake and Gelation Reactions of Cr(III) Oligomers with Polyacrylamide," PhD dissertation, University of Kansas (1993).

Chapter 4

Study of the Gelation and Permeability Reduction of the Polyacrylamide-Aluminum Citrate System

Principal Investigators: D.W. Green, C.S. McCool and G.P. Willhite
Graduate Research Assistants: Raja Ranganathan

Introduction

The polyacrylamide-aluminum citrate colloidal dispersion gel system developed by TIORCO Inc., Englewood, Colorado is claimed to penetrate deep into reservoirs.[1,2] This gel system consists of low concentrations of HiVis® 350, a partially hydrolyzed polyacrylamide, and TIORCO 677, a chelated aluminum citrate solution. Typical concentrations used in this system are 300 ppm polymer and 15 ppm Al^{3+}. This system is reported to be slow forming, thus allowing for in-depth permeability treatment of oil reservoirs. It is hypothesized that polymer colloids, or gel aggregates, are formed which are then apparently filtered from solution by the porous media, thereby reducing the permeability. These claims are based on interpretation of field performance in which large volumes of HiVis® 350 have been injected into petroleum reservoirs. There is little laboratory work which supports either the hypothesis of gel formation or the interpretation of the field data.

This chapter summarizes our research to investigate the process by which this polymer-metal ion system reduces permeability. Our research program had three objectives. These were to determine: (1) the rheological properties of the system, (2) the size and rate of aggregate formation, and (3) how the system propagates and reduces permeability in porous media. The entire study is presented by Ranganathan et al.[3]

Rheological Measurements

Fluid Structure. The principal measure of fluid structure for the HiVis® 350 polymer is a parameter termed the transition pressure which was developed by TIORCO, Inc. using a modified screen viscometer.[4] The modified screen viscometer(termed the TGU apparatus) is a polyethylene tube(diameter) with a screen pack (five 100-mesh stainless-steel screens) attached to one end with a Swagelok or comparable fitting. The tube is is mounted vertically and is connected to an air source which maintains the pressure constant at the inlet end of the tube. A test is performed by loading a specified volume of solution (polymer or gel) into the tube and applying pressure to force the solution through the screen pack. The ratio of the time required for the gel solution to flow through the screen packs to that required by the polymer solution is defined as a TGU quantity.

When HiVis® 350 solutions containing aluminum citrate are displaced through the TGU apparatus, the flow characteristics of the solution change with time and applied pressure drop. At low pressure drops(if reaction time is sufficient), a blob of gel-like material collects on the end of the screen viscometer restricting the flow rate. The size and characteristics of this blob depends upon the age of the solution. At low pressure(low flow rates), the solutions "ooze" from the TGU apparatus while at high pressures(high flow rates), the polymer solution flows freely through the screen pack.

The transition from restricted flow to free flow in the TGU apparatus can be described by plotting both the polymer flow rate (ml/sec) and the TGU values as functions of test pressures as done in Figure 4.1. The point at which these curves cross is designed as the transition pressure. At the transition pressure, it has been hypothesized that these gels undergo a transformation from a squeeze flow to a free fluid-like flow through the screen pack. Additionally, the transition pressure is a measure of gel strength in that higher transition pressures denote stronger gels.

Our initial work on the TIORCO system consisted of testing the gel and polymer solutions using a TGU apparatus that was constructed in our laboratory. The testing was conducted to confirm consistent formulation of solutions with those reported in the literature.

Typical TGU and flow-rate curves are shown in Figure 4.1 for two times after mixing for a polymer concentration of 900 ppm (in 0.5wt% KCL) and polymer-to-aluminum ratio of 20:1. The intersection of the TGU and the flow rate curve denotes the transition pressure which was 18 psi for a sample that was 8 hours old. Development of structure was indicated by the increase in transition pressure with time. Transition pressures determined for samples containing 600, 900 and 1200 ppm polymer were consistent with values reported in the literature.[4]

Transition pressure data for a 300 ppm polymer, 15 ppm aluminum gel system are presented as the top curve in Figure 4.2. The data indicated that *fluid structure* developed within the first 12 to 24 hours. Gelation was in the form of aggregation with little visible structure as the sample did not indicate strong gel-like behavior. After 24 hours, the transition pressure increased marginally. The transition pressure obtained for this gel formulation was consistent with published data (Smith, 1989).

Initial tests on solutions at a polymer concentration of 300 ppm exhibited anomalous behavior. As can be seen from Figure 4.2, the transition pressure increased initially to 8 psi at 24 hr and thereafter, declined with time. Visual observation of the gel indicated it to be water-like in appearance which indicated degradation of the gel. Flow rate of the polymer solutions of 300 ppm concentration also indicated similar degradation. The viscosity also declined with time. The cause was determined to be trace levels of chlorine (1/4 ppm) in the laboratory water.

Formulations consisting of polymer concentrations of 300, 600, 900, and 1200 ppm and polymer to aluminum ratios of 20:1 and 40:1 were studied.

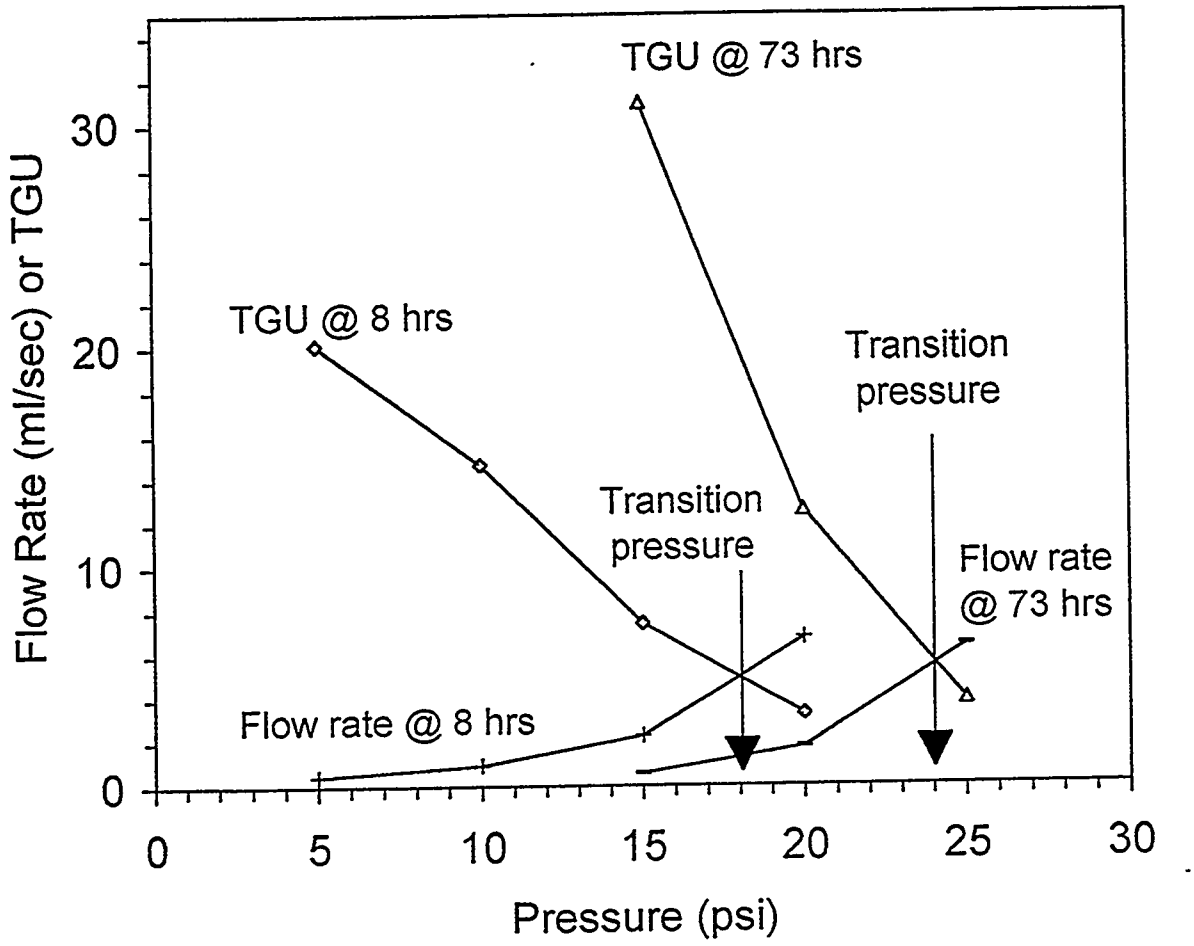

Figure 4.1 : Transition pressures determined from TGU and flow-rate curves
- Gelant composition: 900 ppm polymer, 45 ppm Al(III) and 0.5% KCl.

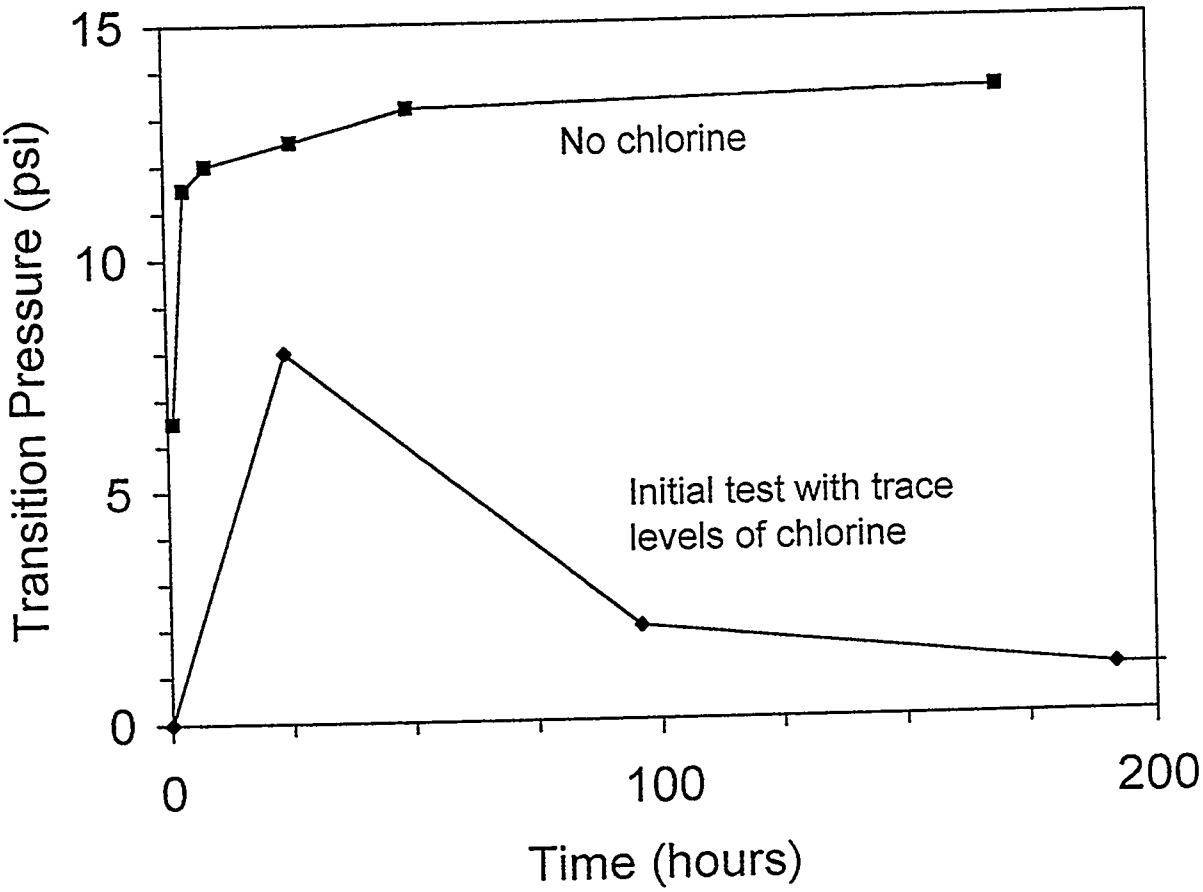

Figure 4.2 : Development of transition pressure with time
Gelant composition: 300 ppm polymer, 15 ppm Al(III) and 0.5% KCl.

Viscosity of HiVis® 350 Solutions. The viscosity of the HiVis® 350 polymer solution as a function of concentration and shear rate was determined[5] to characterize the polymer. Viscosity of HiVis® 350 gel-systems was determined as a function of polymer concentration, shear rate and time. Polymer concentrations studied were 300 ,900, 1500 and 3000 ppm in 0.5 wt. % KCl.

The viscosity data for the solutions containing 900 ppm are presented in Figure 4.3. The polymer is shear thinning . However, there was a decrease in viscosity with time in the first three weeks, suggesting either a change in the structure of the polymer in solution or a deterioration of the polymer with time.

The viscosity data for solutions with an age of 1 day were correlated as a function of polymer concentration and shear rate with Eq. 3.1. The correlation represented the viscosity data well except for the 300 ppm polymer solutions.

$$\mu = K\gamma^{n-1} \qquad (4.1)$$

where

μ	=	viscosity, (cP)
γ	=	shear rate, (sec^{-1})
K	=	$1.739 * 10^{-4}\ C^{1.903}$
1/n	=	$0.2916\ C^{0.2676}$
C	=	polymer concentration, (ppm)

Aggregate Growth in the Polyacrylamide-Aluminum Citrate System. It was hypothesized that HiVis® 350-aluminum citrate solutions react to form aggregates at relatively low concentrations of polyacrylamide and aluminum. The objective of this work was to measure the size of the gel aggregates as they form and grow in the polyacrylamide-aluminum citrate system. The information derived from this study will then be used to determine the mechanisms by which the system affects fluid flow in porous media.

The size of aggregates was studied using by quenching a HiVis® 350-aluminum citrate solution by dilution and using membrane dialysis to determine the size distribution of the aggregates that formed.[6] In this technique, the quenched gel solution is placed on one side of a dialysis cell, separated from the other side by a membrane of a specific hole size. Sufficient time is allowed for the concentrations to reach equilibrium on both sides of the membrane. Both sides are analyzed for polymer concentration to determine the amount of polymer in the diffusate for a given membrane size. An overall material balance is also made to evaluate internal consistency of the experiment.

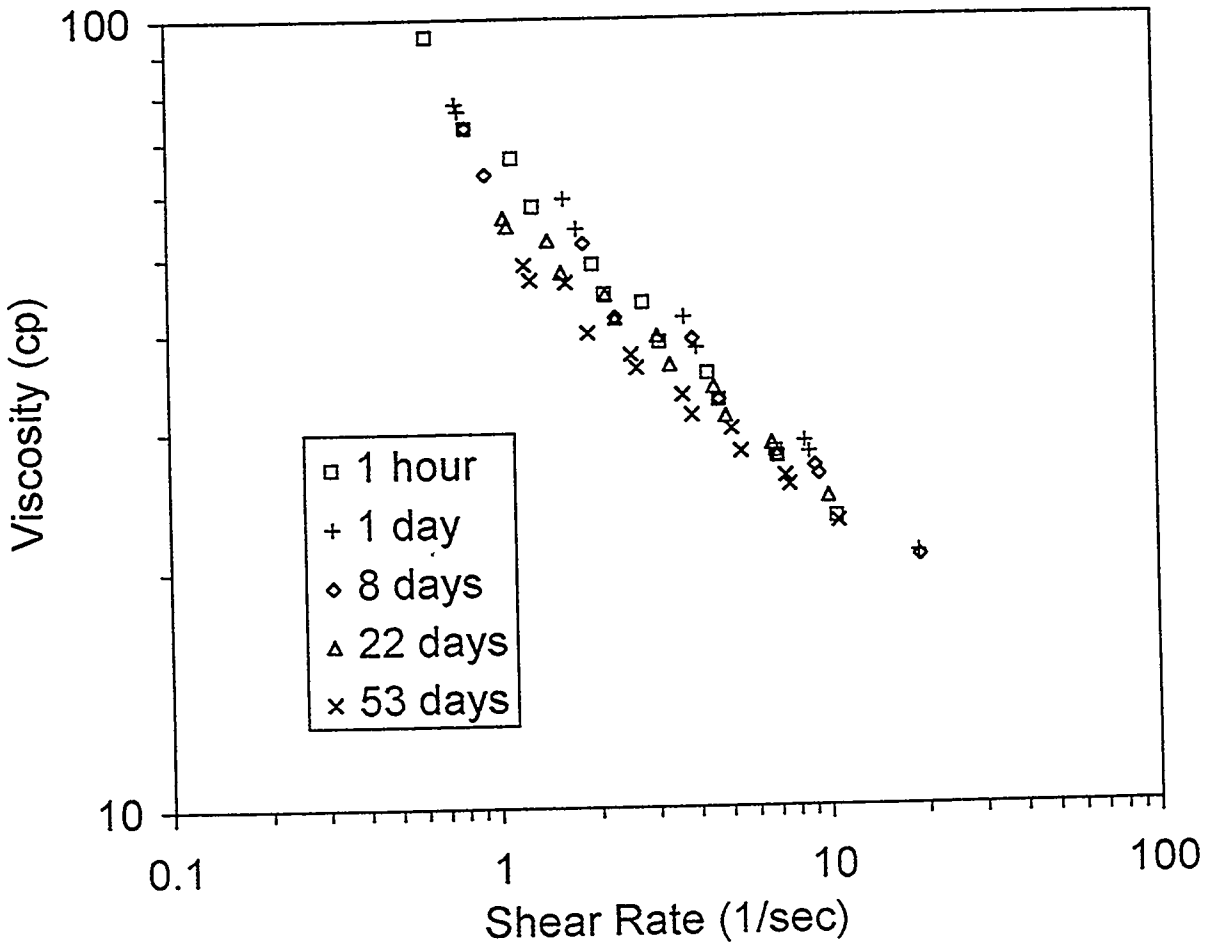

Figure 4.3 : Viscosity as a function of shear rate and age
Composition: 900 ppm polymer and 0.5% KCl.

Size measurements of aggregates were conducted on a sample of the polymer solution to determine the time required to attain equilibrium as well as the approximate size distribution of HiVis® 350. Experiments were conducted for selected membrane-dialysis time periods and with several different membrane pore diameters. The results showed that transfer of polymer across the membrane was essentially complete by five weeks of dialysis time. Material balances were calculated as the percentage of polymer measured with respect to the amount charged to each cell. The balances in most cases were within a few percent of the amount charged.

One gel formulation containing 300 ppm polyacrylamide, 15 ppm aluminum and 0.5 wt. % KCl was studied. Experiments were conducted on two different samples aged for 8 hours. The polymer material balance data for the retentate and diffusate half-cells is included in reference 6.

The size distributions for the polymer and gel are presented in Figure 4.4. The distributions are presented as the cumulative mass of polymer that is smaller than the indicated diameter. Significant development of aggregates and/or aggregate growth in was not observed in the gel samples aged for 4 and 8 hours even though TGU measurements indicated the development of structure.[6] Experiments were conducted with gel samples aged longer than 12 hours but the polymer analyses of these samples were not consistent.

Permeability Modification by In Situ Gelation

The objective of this work was to investigate and identify the mechanisms governing the propagation and in situ gelation behavior of the TIORCO colloidal dispersion gel in porous media. Several experiments were conducted in which the gelant was displaced through unconsolidated sandpacks which were 4 ft in length and 1.5" in diameter. Pressure differentials were measured across eight sections along the sandpacks in order to determine the permeability. In one run, polymer and aluminum concentrations in the effluent fractions were analyzed to aid in interpretation of the gel behavior. Polymer and aluminum concentrations in the gels were 300 ppm and 15 ppm, respectively in 0.5 wt. % KCl. The experimental procedure was described elsewhere.[3,5,7] One experiment was conducted in a 5.08 cm x 5.08 cm Berea core which was 30.48 cm in length. A slot was cut half the length of the core to simulate a fracture.

In most runs, aluminum citrate and polymer solutions were mixed inline and injected into the sandpack at a displacement rate of about 2 ft/day. During the first displacement experiment ,a large mass of gel material gradually formed on the inlet screen causing the injection pressure to increase. The inlet screen plugged after approximately 53 hours of injection (PV). No reduction in permeability was observed in the sandpack prior to the inlet screen plugging even though structure development in a bulk gel was nearly complete within 25 hours. The plugged screen was removed and polymer solution was injected to displace the resident gel solution in the sandpack. Two hours after the gel solution was detected in the effluent, the downstream side of the outlet

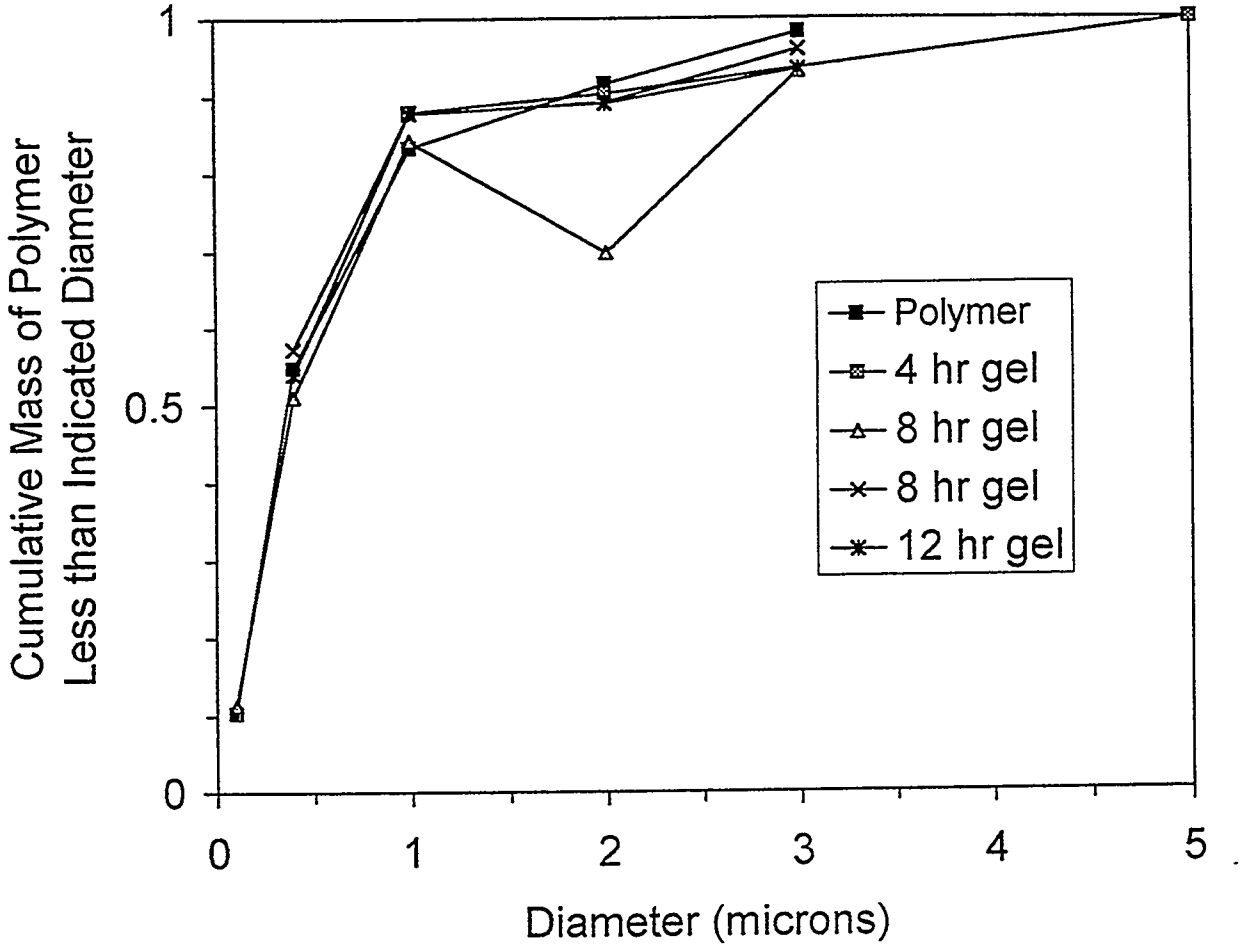

Figure 4.4 : Size distributions for polymer and gel aggregates as a function of reaction time.

screen was plugged by another large mass of gel material.[5] This behavior was observed in other displacement runs.[5]

Results from three key displacement experiments (SP5, SP6 and SP7) are summarized in this section. A polymer solution displacement experiment was conducted in sandpack SP5 to provide the basis for analyzing and interpreting the results of the gel solution displacement experiments in sandpacks SP6 and SP7. In Runs SP7 and SP8, the gel solution was mixed in-line and injected immediately into the sandpack while in Run SP6, a two hour delay time was introduced between mixing and injection into the sandpack by flowing the gelant through coiled tubing. In all runs, coarse sand and larger mesh screens were used at inlet and outlet sections in an attempt to eliminate filtration of gel aggregates on screens which was observed in the initial experiments. Three additional displacement experiments (SP8, SP9 and SP11) were conducted to verify behavior observed in these runs.

Run SP5. In Run SP5, the average permeability prior to polymer injection was 3445 md. Six pore volumes of polymer solution were injected into the sandpack followed by 0.5% KCl brine. The permeability of the sand pack was reduced by factors ranging from 2.55 to 4.0 from the retention of polymer with an average value of 2.83. We observed no buildup of flow resistance on either inlet or outlet screens. Effluent polymer samples were less viscous than the injected solution even after the pressures stabilized. This indicates that the effluent polymer concentration did not reach the injected concentration and polymer retention was still occurring or the polymer solution was degraded as it flowed through the sandpack. Effluent polymer concentrations were not measured. Data for this run are presented elsewhere.[5]

Run SP7. In Run SP7, the gelant was injected immediately after in-line mixing. Flow behavior during injection of the first 1.2 pore volumes of gelant was identical to that observed in Run SP5 where polymer was injected. However, after about 1.2 PV of injection, the apparent viscosity in the inlet section of the sandpack began to rise rapidly. Injection was discontinued in order to check and clean the pressure ports in this section. Upon resumption of injection, the pressure drop across in the first section increased rapidly, exceeding the pressure limit of the transducer and injection was stopped after an additional 0.11PV of gelant was injected.

A disk of filter cake was found at the interface between the coarse sand and the regular sand which reduced the permeability to essential zero. Examination of the sand beneath this disk revealed no cohesive gel structure or rigidity. There was no evidence of in-situ gelation at any other location in the sandpack.

The regular sand was removed to a depth of about 2 cm below the original coarse sand/sand interface and replaced with coarse sand. Injection of gelant was resumed at the same rate. However, a similar sharp increase in pressure was observed across this section within 0.2 pore volumes of gelant injection and injection was stopped. The sandpack was shutin for three weeks in an attempt to promote in-situ gelation. Then 0.5% KCl brine was injected to displace mobile gelant. We observed no increase of flow resistance above what would have been obtained from

the polymer solution alone. Reduction of permeability caused by in-situ gelation or filtration of gel aggregates did not occur at any location other than at the interface between the coarse sand and the regular sand.

Rapid buildup of flow resistance is believed to be the result of filtration of gel aggregates at the interface between the coarse and regular sands. This behavior is analogous to front end loading which was observed in other polyacrylamide-aluminum citrate systems and documented in earlier studies by Parmeswar and Willhite,[8] and Rocha et al.[9] In this gelant system, extremely high flow resistance develops at the inlet section with little resistance in downstream sections. Results are consistent with experiments of Seright[10] who found that the colloidal dispersion gel could not be continuously propagated through a 707 md Berea core.

The interpretation of pressure and flow resistance data is supported by polymer and aluminum concentrations in the effluent fractions. Data from Run SP7 are presented in Figure 4.5. Aluminum concentrations in the effluent averaged 5 ppm between arrival of aluminum in the effluent and 1.5 pore volumes injected. By 2.1 PV, the aluminum concentration was still about 2/3 of the injected concentration. Aluminum was continuously retained throughout the displacement experiment. In contrast, the amount of polymer retained appeared to be relatively small. Physical appearance of the effluent fractions was unlike those seen with the gels in beaker tests. The effluent fractions were thinner and less viscous. Effluent samples did not develop a gel structure.

Run SP6. Run SP6 was designed to simulate the residence time that a gelant solution would have in flowing through injection tubing from the point of mixing to the formation sandface. Details of this run are described in reference 3. A ¼ inch tubing loop was inserted between the in-line mixer and the sandpack inlet to delay entry of gel solution by two hours.

Gelant was injected continuously at a superficial velocity of 1.81 ft/d. After 10 hours of injection, the pressure drop across the inlet section began to increase continuously. At 40 hours of injection(1.5 PV), pressure port 1 at the inlet end appeared to be plugged and injection was stopped temporarily to clean the port. Injection continued until about 3.2 pore volumes of gelant injected when the apparent viscosity at the inlet sections had increased to 2000 cP, indicating buildup of a region of high flow resistance at the inlet of the sandpack. During this time, apparent viscosities in downstream sections decreased continuously, indicating stripping of the polymer from the gelant solution in the inlet sections.

When the inlet end was opened at 3.2 PV, a filter cake disc was found similar to those described earlier. This disc consisted of the inlet face screen, 50 mesh coarse sand and gelatinous material. The disc was 0.5 cm thick and was easily separated from the remainer of the sandbody. A similar gelatinous material filled the space between the sandpack and the sandpack holder depicted in Figure 4.6 to a depth of 2 to 3 cm. The inlet end was cleaned to enable resumption of gel injection. The sand underneath the filter cake disk was clean and loose with no evidence of gel structure.

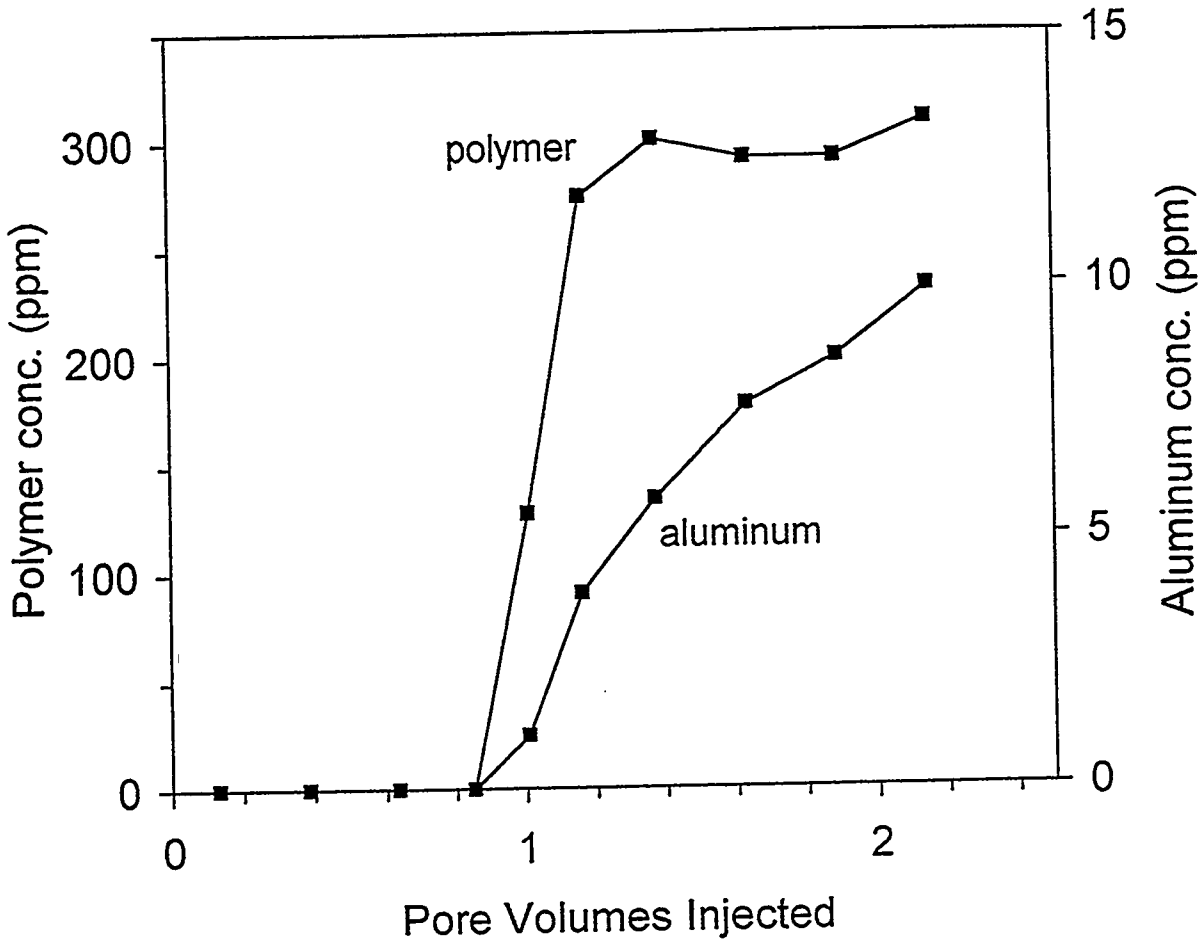

Figure 4.5 : Polymer and aluminum concentrations in the effluent from SP7.

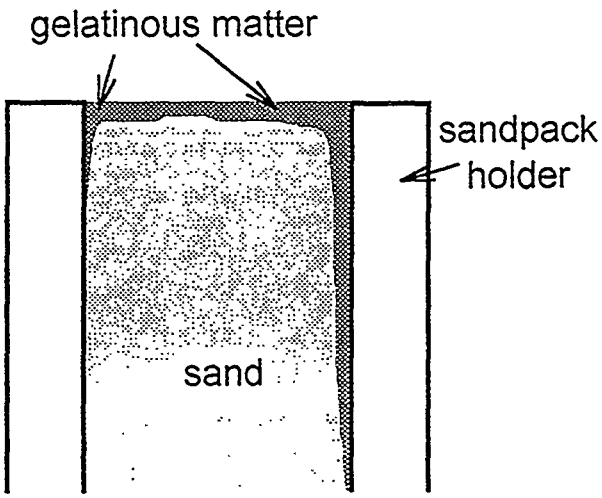

Figure 4.6 : Diagram of gelantinous matter that developed at inlet of SP6.

Gel displacement in Run SP6 was resumed at the same injection rate but pressure ports in the eight sections became plugged and did not sense pressure. Injection was stopped several times to clean the pressure ports with hypodermic needles and reestablish hydraulic connection to the transducers. Screens placed in the pressure ports to hold sand in place also became plugged. By the time 5.5 pore volumes of gelant had been injected, nearly all of the pressure ports had become plugged. We also observed that a gelatinous structure developed on the upper side of the sandpack holder, filling a small gap that had developed between the sand and the sandpack holder due to gravity settling of the sand while the apparatus was positioned horizontally. Unfortunately, the pressure ports were on the top of the coreholder which contributed to the plugging that we observed.

The inlet end was opened and a filter cake was found as described previously. The inlet section was cleaned and replaced with clean sand. Pressure ports were opened and cleaned thoroughly. During cleaning, we observed that gelatinous matter had formed a strand-like structure under each port. The shape and position of the strands indicated that they formed along needle holes in the sand body which were made during gel displacement runs to establish communication through the pressure ports.

The sandpack was shut in for two weeks and then the mobile gelant solution was displaced with 0.5wt% KCl brine. Permeability reduction was comparable to values observed when polymer was injected into a sandpack at the same rate. Thus, there was no gelation within the sandpack.

At the end of this experiment, the sand was carefully displaced out of the sandpack to examine the thin layer of gel-like material that had formed in the small gap between the top of the sand and the the sandpack holder. A schematic diagram of this material is shown in Figure 4.7. Physical examination of this material showed that it consisted of sand grains and gelled polymer and was elastic. The structure is believed to be made of gel aggregates that filtered out of the solution in the gap between the sand and the sandholder.

Effluent samples collected during injection of gelant were analyzed for both aluminum and polymer. Polymer and aluminum concentrations are shown in Figure 4.8. Eighty percent of the injected aluminum was retained in the sandpack. Polymer retention was not significant until about 1.25 PV when the polymer concentration in the effluent leveled off and declined to an average value of about 60 ppm by 2.5 PV of injection and remained there for the duration of the injection period. The loss of polymer and aluminum in the effluent after 2.5 PV of injection is 240 ppm and 12 ppm respectively. This is the same ratio at which the gelant was prepared and injected, i.e. 20:1 polymer to aluminum. We interpret these results to indicate that gel aggregates formed in the delay loop and were filtered out at the inlet face, in the gel-like material found in the space between the top of the sand and the sandpack holder and in holes created when cleaning the pressure ports. The effluent fractions did not develop a gel like structure.

Run SP8. An important observation with the previous gel displacement experiments was that the effluent solution was less viscous than the injected solution. The effluent in the polymer solution displacement experiment was also less viscous than the injected HPAM solution. Analysis of effluent

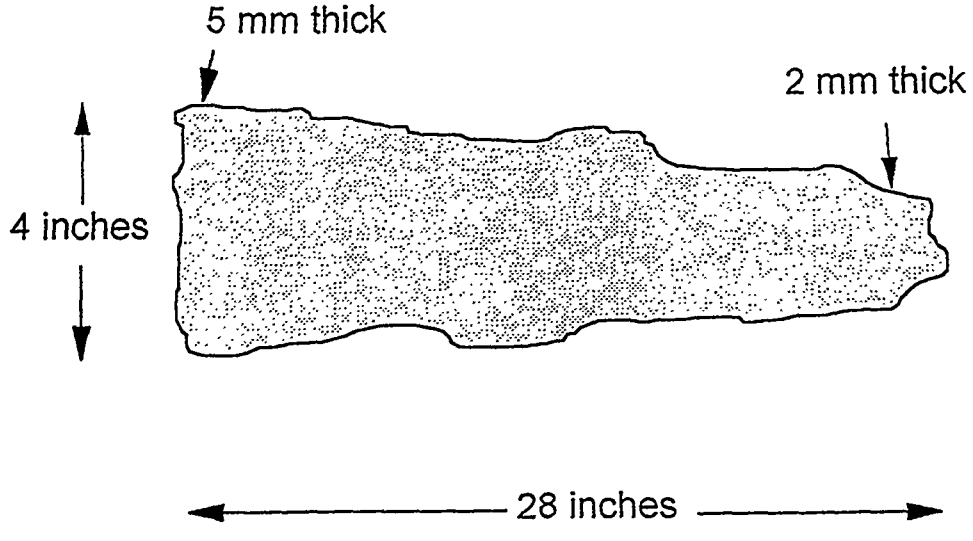

Figure 4.7 : Diagram of gelantinous structure that developed along gap between sand and holder in SP6.

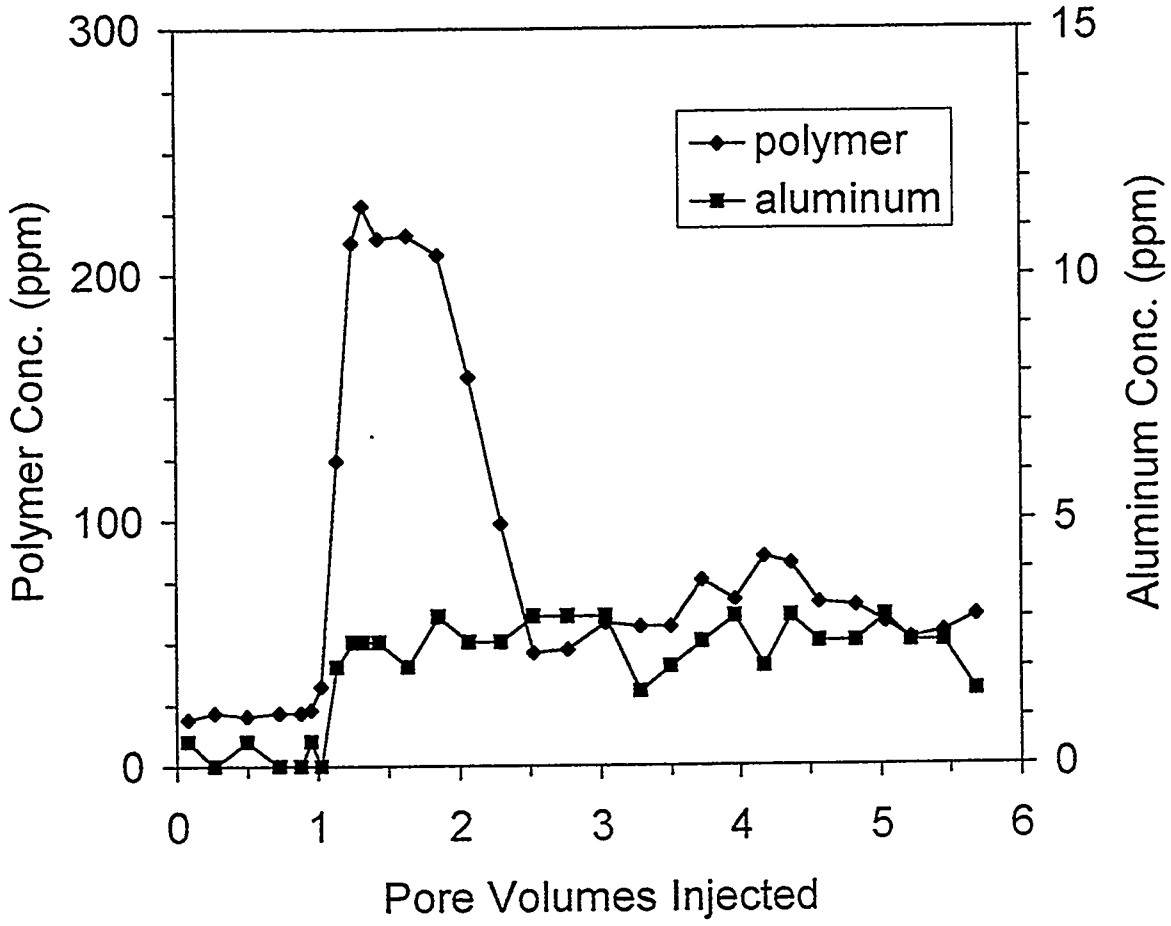

Figure 4.8 : Concentrations of polymer and aluminum in effluent of SP6.

solutions collected after one pore volume was injected had revealed that they contained about 300 ppm polyacrylamide, close to the concentration of the injected solution. The analytical technique for polymer concentration is not sensitive to the molecular weight of the polymer. This difference in solution viscosity could be explained by either or both of the following reasons:

- HiVis 350 is a partially hydrolyzed polyacrylamide, with a viscosity averaged molecular weight of around twenty-seven million. The polymer would mostly consist of long-backbone chains to attain this high molecular weight, and be extremely fragile when exposed to shear environment. The passage of these polyacrylamide molecules through the porous media exposes the polymer to a shear environment and may cause shear degradation and hence shorter-backbone molecules. This could explain the presence of polymer at injected concentrations in the effluent but with a lower viscosity.

- The high viscosity averaged molecular weight could be due to the presence of a small concentration of large polyacrylamide chains. When the polyacrylamide solution flows through the porous media, these huge molecules could be retained and the filtered solution would have a lower average molecular weight and hence viscosity.

We investigated changes in the properties of the polymer solution caused by flow through porous media by injecting uncrosslinked polymer solution under conditions identical to the previous experiments and monitoring the effluent viscosity and polymer concentration. The pore volume of the sandpack was determined by a dispersion test and was found to be 483 ml which gives a porosity of 32.8%. Permeability to brine for the individual sections and total sandpack was determined and the data is presented in Table 4.1.

Three-hundred ppm HiVis 350 HPAM solution was prepared in deionized water for injection into the sandpack SP8. Viscosity of the polymer solution was determined using Bohlin Rheometer before and after displacement for comparison with the viscosities of the effluent fractions. The displacement rate was maintained at 10 mL/hr which gives a frontal velocity of 2 ft/day. Injection was continued till about five pore volumes of the polymer solution had been injected through the sandpack.

Apparent viscosities for the sections A through H and the total sandpack SP8 during polymer displacement are presented in Figures 4.9. Effluent analysis are presented in Figure 4.10. The sandpack was shut in for three weeks. Then, 5000 ppm potassium chloride brine was injected to displace the polymer solution. After the polymer solution was displaced, pressure differentials were then measured at three different flow rates. Residual resistance factors were determined and are presented in Table 4.1 with the permeability to brine measured at the beginning of the displacement experiment. The resistance factors are similar to those obtained with the previous experiments.

Table 4.1: Permeability to brine and the residual resistance factors for sections A through H and total sandpack length - SP8.

Section	Total	A	B	C	D	E	F	G	H
Permeability, md	3400	3030	3500	3400	4100	3400	3350	3330	2270
RRF	1.8	1.3	1.8	1.9	2.1	1.8	1.7	1.7	1.1

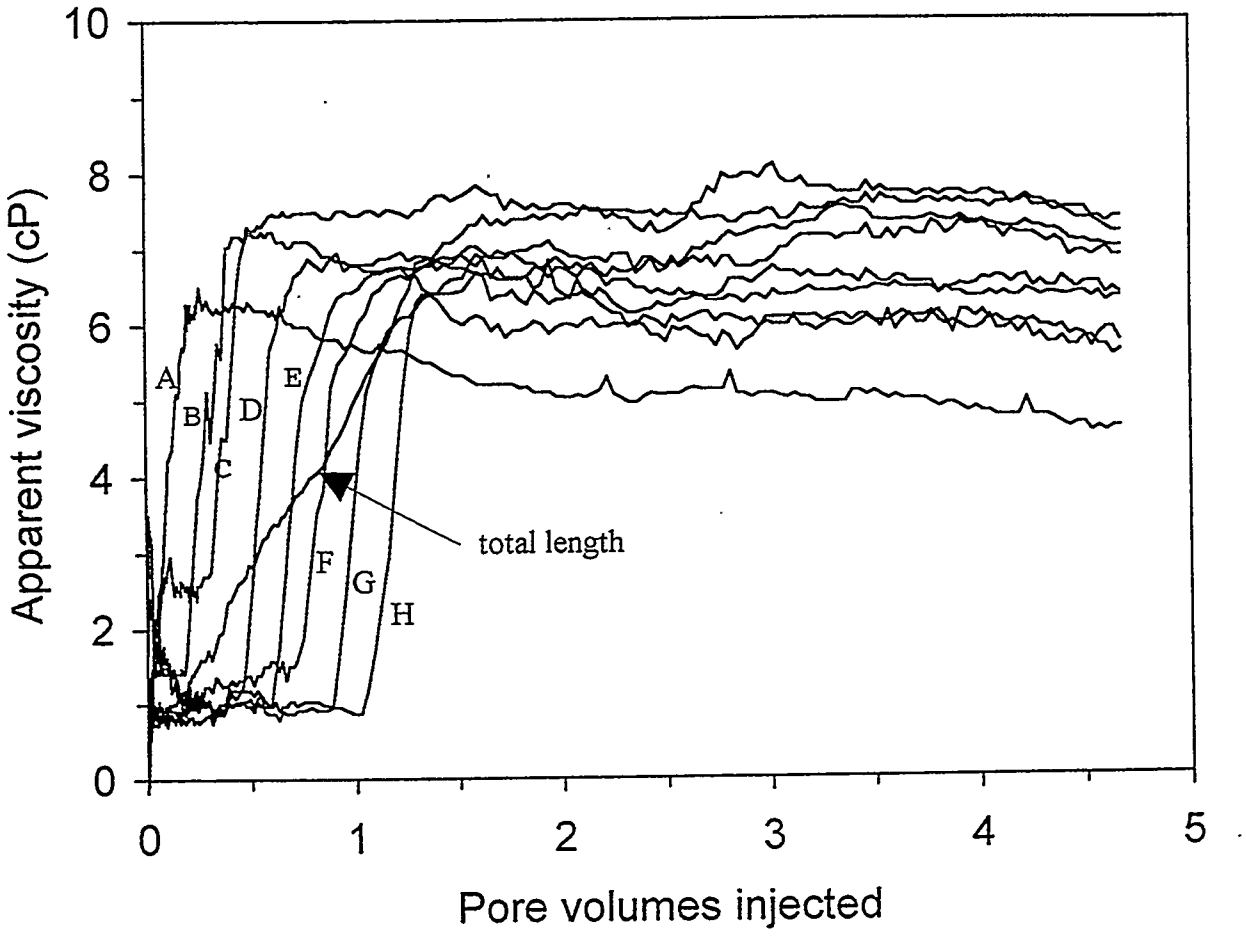

Figure 4.9 : Flow resistance of sections and total sandpack - SP8.

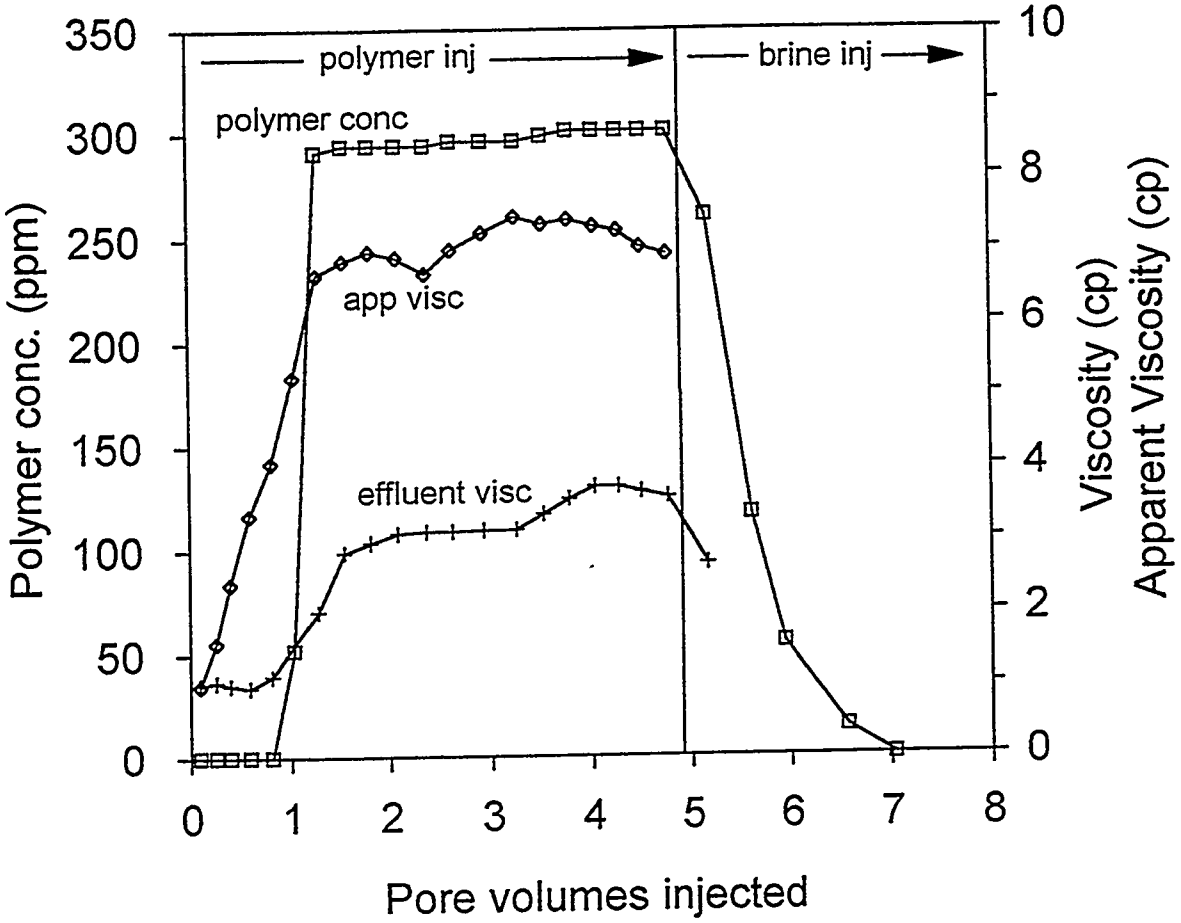

Figure 4.10 : Polymer concentration and viscosity of effluent and apparent viscosity for SP8.

The results of Run SP8 are summarized as follows.

1. The results are comparable to the previous experiments in which polymer was injected.
2. There is a loss in solution viscosity due to flow of HiVis 350 through sandpacks even when the effluent concentration is equal to the injection concentration. This is consistent with the hypotheses that either the long-backbone chains of the polyacrylamide are breaking down or some large polyacrylamide molecules are retained, resulting in loss of viscosity. A combination of the two could also be a possibility.

Run SP9. The displacement experiment in sandpack SP9 was designed to explore the effect of interfaces in the flow path of the gel solution. In previous experiments we observed that the gel solution forms a filter cake across that interface and plugs further flow if an interface of coarse sand/regular sand is present at the inlet end. In this experiment it was decided to examine the effect of flowing gel solution through the sandpack with interfaces some distance from the inlet end.

The sandpack (Figure 4.11) was designed to have two interfaces in the middle of the sand pack where there were abrupt changes in permeability. This section was obtained by using two different sand grain sizes. Acid-washed Wedron silica sand was separated using sieves into :

- a regular sand between 70 and 240 mesh sieve sizes, and
- a coarse sand between 50 and 70 mesh sieve sizes.

It was decided to mount the sandpack vertically and inject into the top end so that it would not be necessary to use a screen or coarse sand at the inlet of the sandpack to retain the sand. Packing was achieved in three stages. After placing a coarse screen (40 mesh) and a layer of coarse sand (< 50 mesh sieve size) was placed at the bottom of the sandpack. Regular sand was packed into the sandpack to the second interface point shown in Figure 4.11 at Section F. After achieving reasonable compacting of the regular sand, the coarse sand was packed into the sandpack to the first interface point. This layer was compacted and then the rest of the sandpack was packed with the regular sand. Compacting during the different packing stages was achieved by injecting brine into the sandpack and applying a back pressure at the outlet of the sandpack. The sandpack was tapped from outside to aid in the settling process. Average permeability for the sandpack SP9 and its sections are presented in Table 4.2.

Table 4.2 : Permeability to brine for the sections A through H and total sandpack length - SP9.

Section	Total	A	B	C	D	E	F	G	H
Permeability, md	4510	2900	3720	3610	5740	15900	7810	3590	3800

A sharp permeability contrast (nearly 4:1) was obtained across the interfaces I and II. The pore volume was determined through a dispersion test and found to be 501.98 mL. The dispersion coefficient of $5.96*10^{-3}$ ft^2/hr was comparable to the coefficients obtained for the sandpacks in previous experiments.

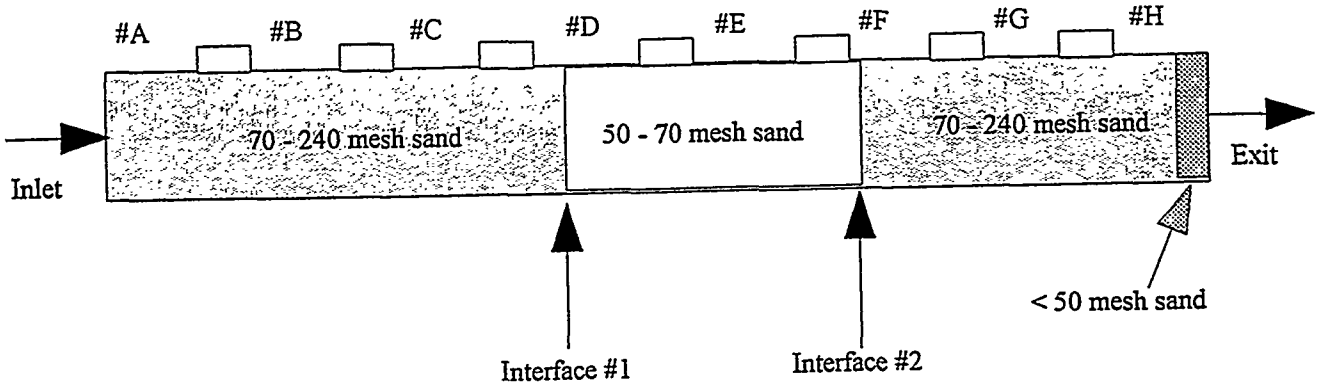

Figure 4.11 : Diagram of sandpack SP9.

The displacement setup used for this experiment was identical to the previous experiments where gel solution was mixed in-line and injected immediately into the sandpack. Viscosities for the the polymer solution, in-line mixed gel and the reference bulk gel solutions are presented in Figure 4.12. The injection rate was maintained at 10 mL/hr, equivalent to a frontal velocity of 2 ft/day. Effluent solutions were collected continuously in sample bottles, and were monitored for flow rate, viscosity, polymer and aluminum concentrations. The injection pressure increased rapidly to about 100 psi after 121 hours of injection time (2.45 pore volumes injected). This pressure increase was unexpected and since it occurred at midnight when the experiment was unattended, the sandpack was subjected to a high pressure(about 100 psi) for about 8 hours before pumping was discontinued and pressures released. High pressures developed across the overall sandpack and across the Section H, the effluent end section.

The apparent viscosities for the total sandpack and sections A through H are presented in Figure 4.13. The profiles are identical to those obtained with the earlier gel solution displacement experiments. The gel solution propagated through the sandpack like a polymer solution. The apparent viscosities ranged from 8-12 cP and are consistent with the earlier experimental results. An average injection rate of 9.73 mL/hr was achieved at a superficial velocity of 1.95 ft/day which was reasonably close to the planned rate of 2 ft/day.

The apparent viscosity for the inlet section increased with time as observed in earlier experiments. No resistance developed across interfaces I and II during the displacement process. This, coupled with the development of resistance at the inlet face, indicates that retention of polyacrylamide and aluminum at the inlet face could be a significant factor in the development of filter cake across the interface in the previous gel solution displacement experiments.

When the sandpack was opened, a gel blob was found across the effluent screen (both upstream and downstream) at the effluent port. This behavior was identical to that observed in previous experiments, where the gel solution would flow through the remainder of the sandpack like a polymer solution but would form a filter cake(gel blob) and develop resistance across effluent end screen. Most of the pressure ports were plugged by gel. A gel blob was found across the screen installed in the fitting to prevent sand from entering the pressure tap. It is hypothesized that the gel solution tried to extrude through these pressure ports and developed gel blobs when the sandpack was left subjected to high pressures for a period of 8 hours. The inlet and outlet ends were cleaned to remove gel material as well as the pressure ports in preparation for resumption of injection of gel solution.

Injection was resumed but pressure differentials across the overall sandpack and Section F, where interface II was located started increasing sharply. The apparent viscosities are presented as a function of volume injected in Figure 4.14. The low volume of fluid injected (2.6 ml) indicates the the pressures increased almost immediatedly after resumption of injection. The displacement was discontinued. Pressure ports and pressure transducers were examined and were found to be functioning properly. However, when injection was resumed a similar trend was observed (Figure 4.15). The sandpack was disconnected from the experimental setup and the sand was displaced from the sandpack to examine the interface II in section F. A filter cake of gelatinous matter similar to those observed in the earlier experiments had developed across interface II.

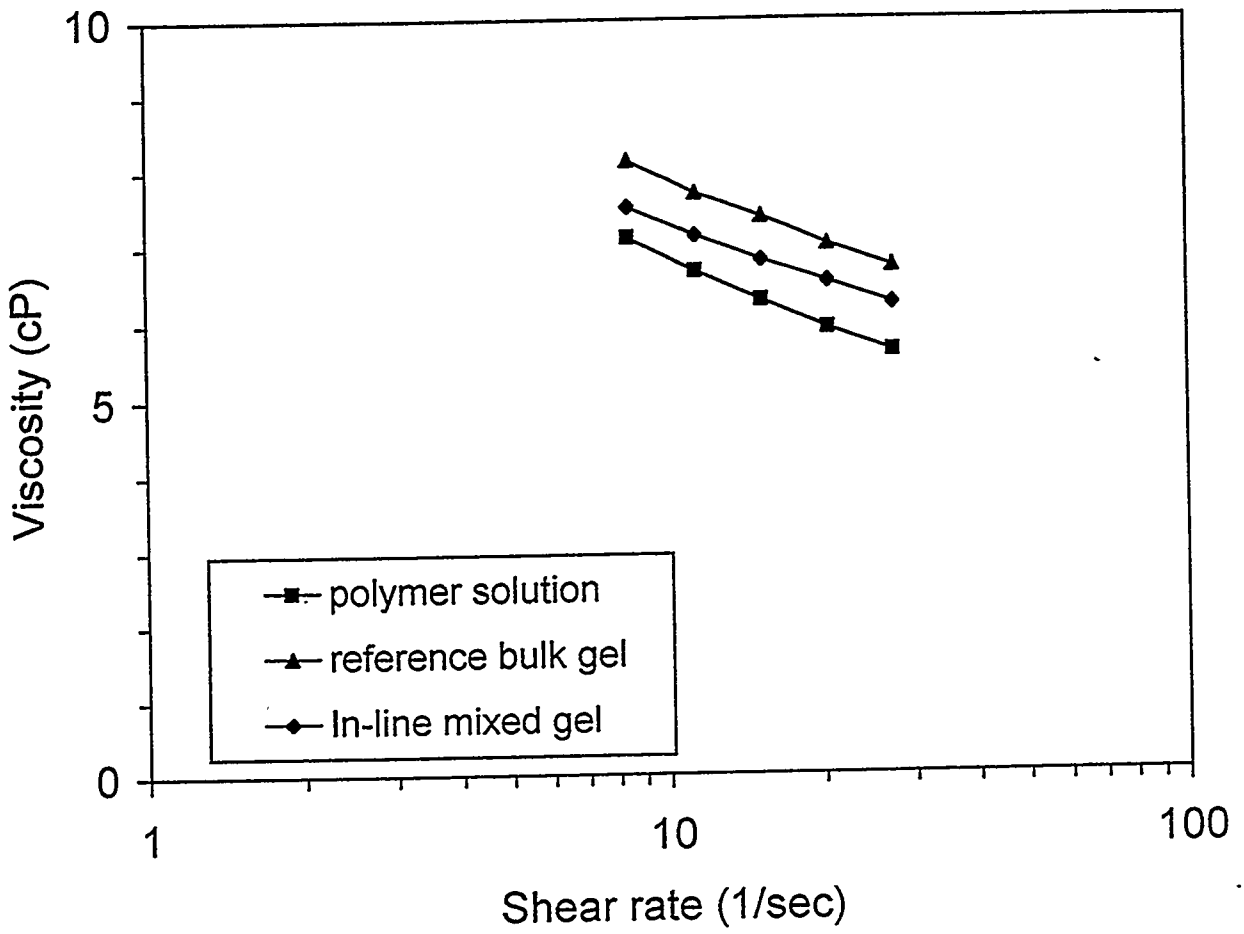

Figure 4.12 : Viscosity as a function of shear rate - SP9.

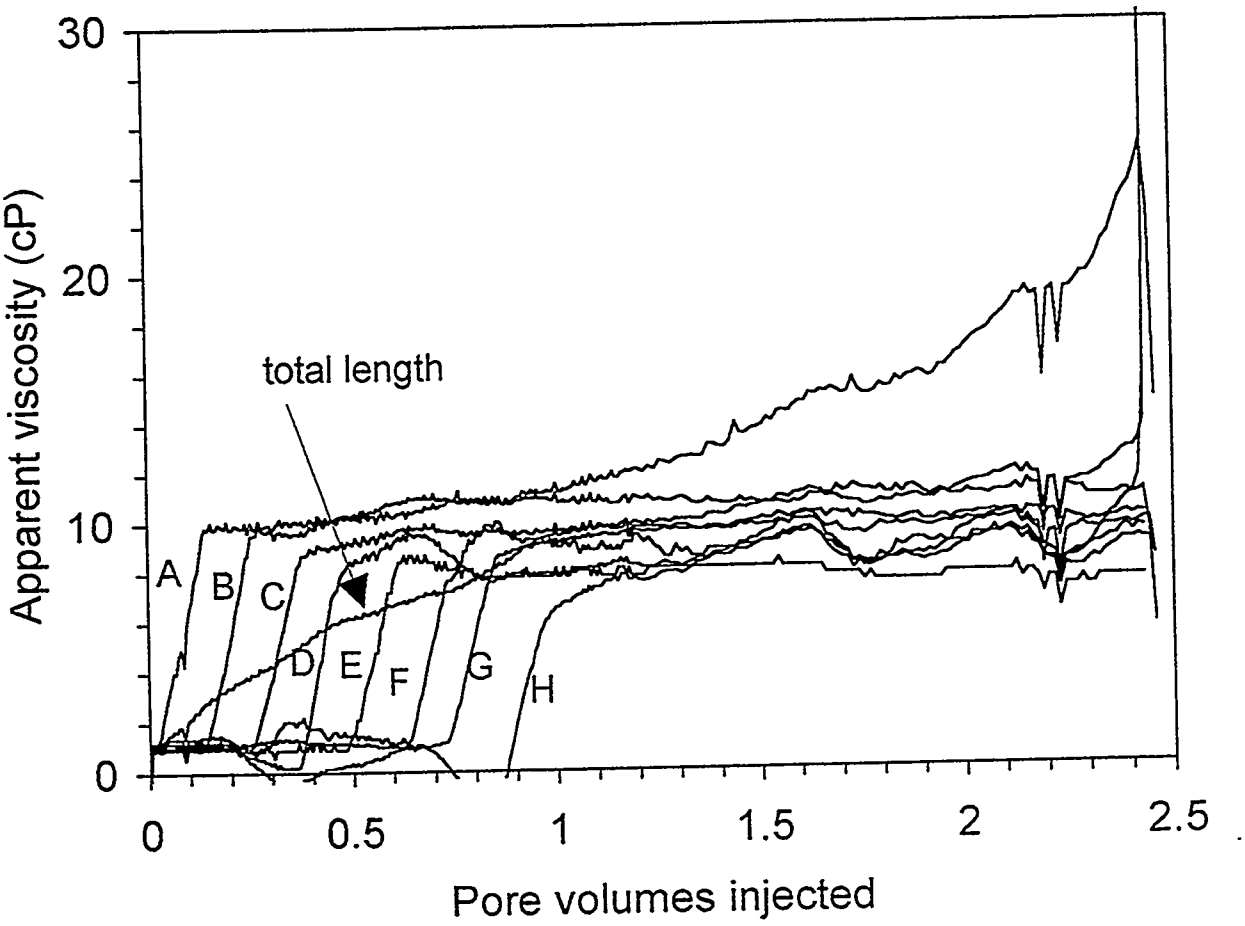

Figure 4.13 : Flow ressitance in sections and total sandpack -SP9.

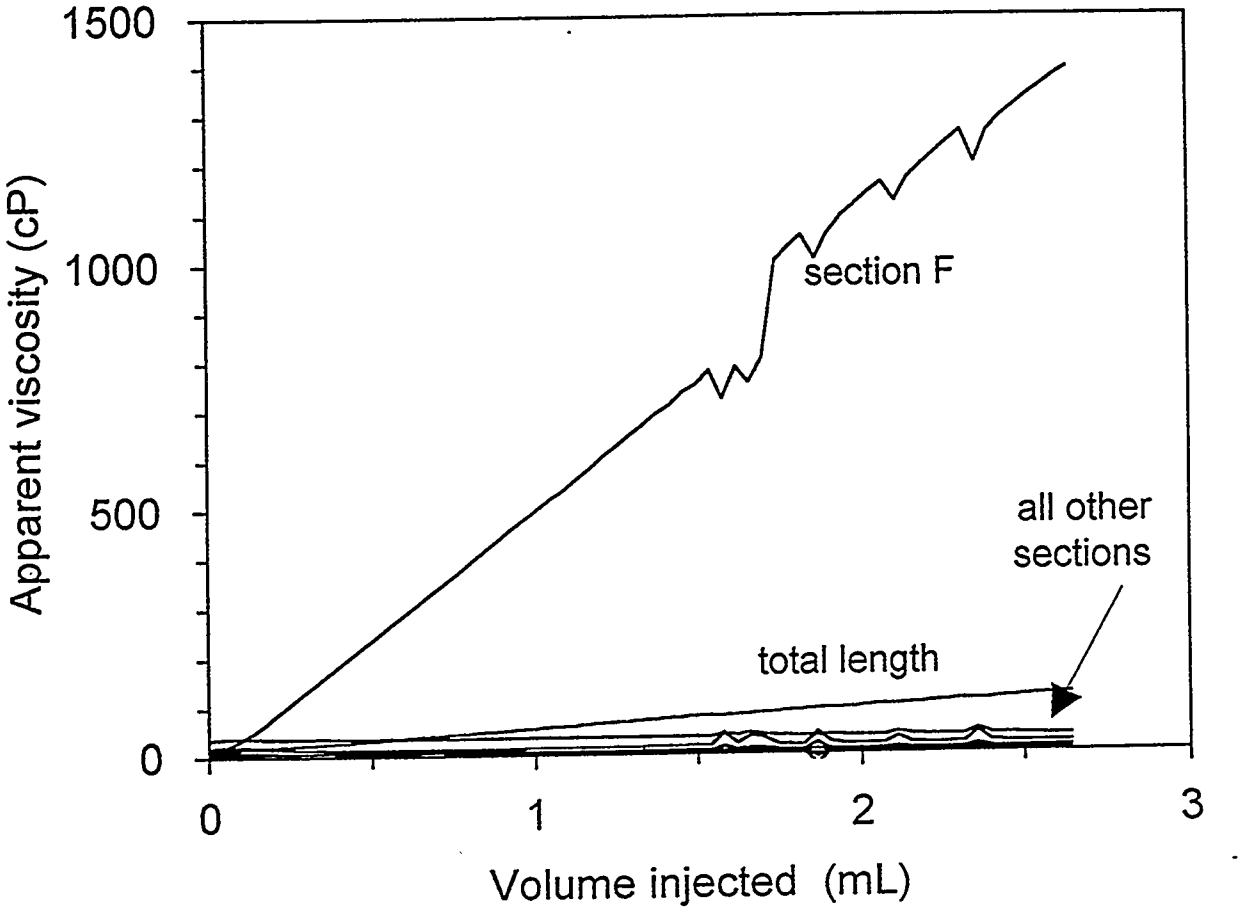

Figure 4.14 : Flow resistance of sections and total sanpack - SP9 run 2.

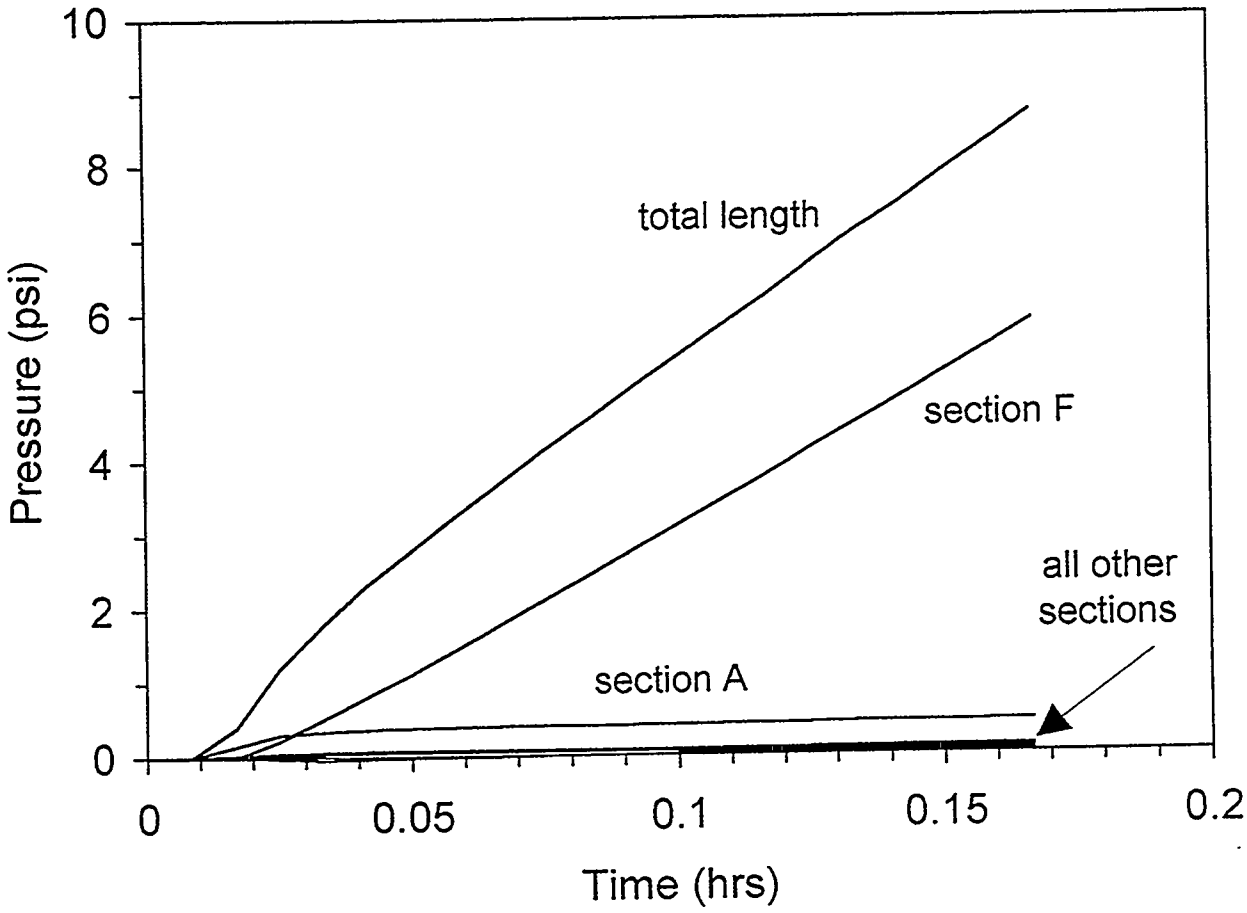

Figure 4.15 : Flow resistance in sections and total sandpack - SP9 run3.

The effluent solutions collected during the gel solution displacement were analyzed for aluminum and polymer concentrations. Viscosities of effluent samples were determined at a shear rate of 10 sec^{-1}. The results presented in Figure 4.16 are consistent with those obtained in earlier gel solution displacement experiments. The reference viscosity of the 300 ppm HPAM solution, the in-line gel solution and the bulk gel solution before the experiment began were close to each other and around 7.5-8 cP at a shear rate of 10 sec^{-1}. In contrast, the viscosities of the effluent solutions were in the range of 3-4 cP at a shear rate of 10 sec^{-1}.

Polymer concentration in the effluent solution was close to the injected concentration of 300 ppm immediately after 1 pore volume of injection and remained at the injected concentration for the remainer of the experiment. Aluminum concentration remained well below the injection concentration and was retained in larger amounts than the polymer. After 2.5 pore volumes were injected, the aluminum concentration was around 12 ppm, which was still lower than the injected aluminum concentration of 15 ppm. Measured viscosity of the reference polymer solution at the end of the experiment was 8 cP and the reference inline gel solution had a viscosity of 16 cP at a shear rate of 10 sec^{-1}.

Results from this displacement experiment can be summarized as follows.

1. The following observations from earlier experiments were confirmed.
    - The gel solution propagated through the sandpack in a manner similar to an uncrosslinked polymer solution displacement.
    - Flow resistance developed marginally across the inlet face, and is believed to be due to retention of bigger polymer molecules by filtration and adsorption of aluminum by silica and retained polymer.
    - Although polymer concentration in the effluent fractions approached the levels of the injected solution immediately after one pore-volume was injected, the physical appearance and measured viscosity of the effluent fractions was that of a thinner solution than the injected gel solution.

2. The placement of interfaces did affect the gel displacement process. Interface II developed flow resistance when the sandpack was pressured up.

3. The screen at the effluent end caused the termination of the displacement experiment due to formation of a gel blob which restricted flow. This is consistent with the observation in all the previous gel displacement experiments.

Run SP11. Run SP11 was designed to determine if the development of filter cake at the interface between high and low permeability sections when the sandpack was subjected to high pressures was due 1) the pressure forcing the gel solution to extrude through the interface resulting in the formation of filter cake similar to those in the screens, or 2) formation of a gel during shutin.

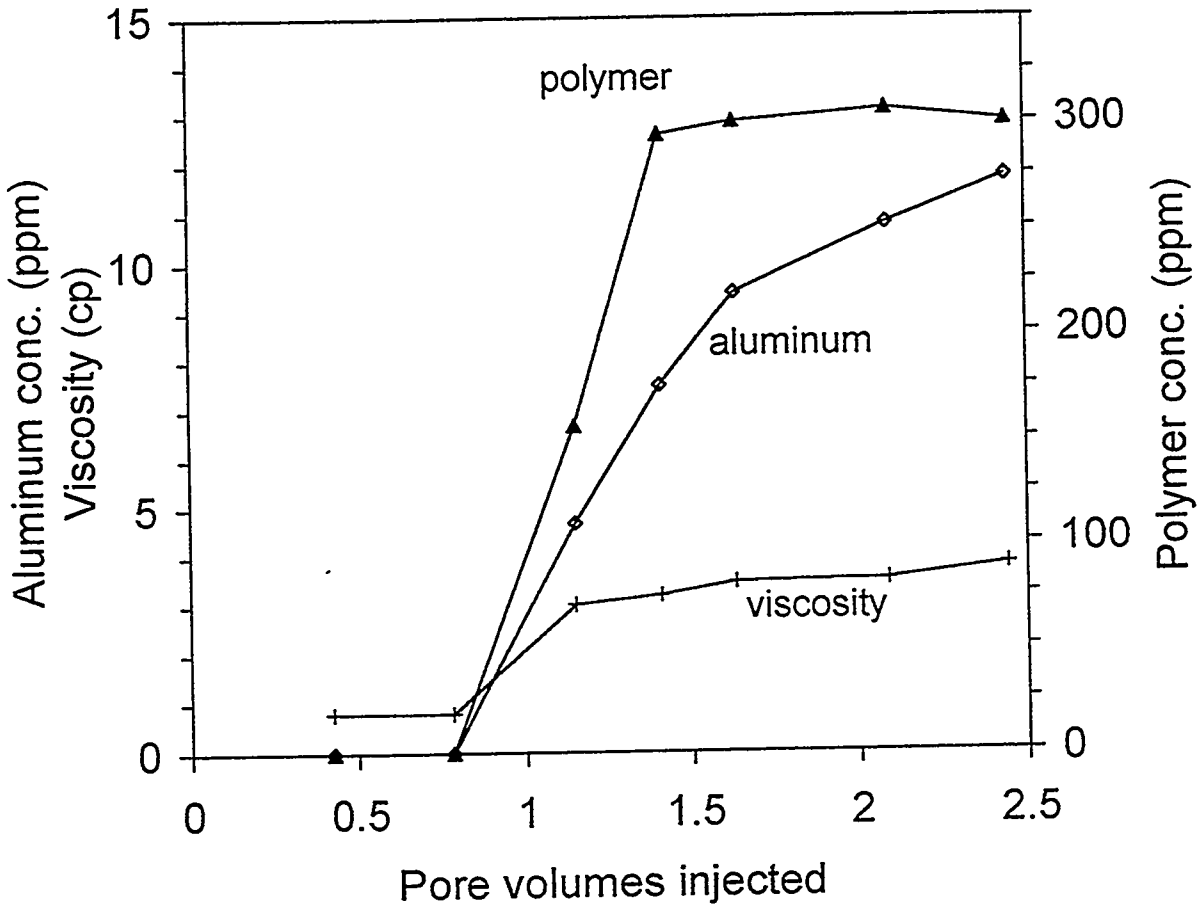

Figure 4.16 : Polymer and aluminum concetrations and viscosity of effluent from SP9.

Sandpack SP11 was prepared using the same procedure as for SP9. The permeability of the different sections and the total sandpack is presented in Table 4.3. A dispersion test was performed to determine the pore volume and the dispersion coefficient.

Table 4.3: Permeability to brine for the sections A through H and total length - SP11.

Section	Total	A	B	C	D	E	F	G	H
Permeability, md	4840	3800	4000	4250	9200	13600	5160	3800	4450

It was planned to inject about two pore volumes of the gelant into the sandpack to ensure complete saturation of the pore space with the gel solution at injected concentration. The sandpack would be shut-in for about 8-12 hours. Injection of gel solution was to be resumed and the pressure drop across the interface sections observed to determine if a filter cake developed during the shut-in period. If there was no increase in pressure drop, the sandpack would be pressurized to 100 psi over a period of about 8 hours by closing the effluent port while continuing to inject gel solution through the sandpack.

The experiment could not be carried out as planned. After about 1.3 pore volumes of gelant was injected, the experiment was stopped due to pressure build up across the inlet section. Apparent viscosity profiles for the sections A through H and the total sandpack are presented in Figure 4.17. Upon examination of the sandpack, it was observed that gel aggregates had collected out in the narrow gap at the inlet end between the sandpack endplate and sandface where they formed a filter cake. The filter cake was removed and the sandpack was left shut-in for 12 hours. Injection of gel solution resumed at the same rate for about 2 hours. No unusual pressure behavior was observed at either of the interface sections. Apparent viscosity profiles for the sections A- H and the total sandpack during injection are presented in Figure 4.18. Consequently, we concluded that in situ gelation did not occur during the shut-in period.

The sandpack was then subjected to a high pressure by closing the effluent port and injecting gel solution. After the pressure had increased to about 100 psi, the sandpack was left shut-in. After 10 hours of shut-in, the pressure in the sandpack was released gradually. Sandpack ends and pressure ports were cleaned thoroughly. Then, 5000 ppm potassium chloride brine was injected at a rate of 10 ml/h. The apparent viscosity profiles during this time are presented in Figure 4.19. Pressure drop across the interface in section F started rising almost immediately and continued to increase rapidly. The sandpack was disconnected and the sandpack was displaced from the holder to examine the interface. A filter cake formed across the interface II in section F. We conclude from this experiment that pressurizing the sandpack caused the formation of the filter cake at interface II.

Run BC1 - Berea core. A possible hypothesis for the "interface phenomena" observed in sandpacks is that gel aggregates build up resistance whenever they encounter a change in shear rate in their flow path. If so, this gel could prove useful in treating fractures in porous media. The interface between a fracture and the matrix is an abrupt change in shear.

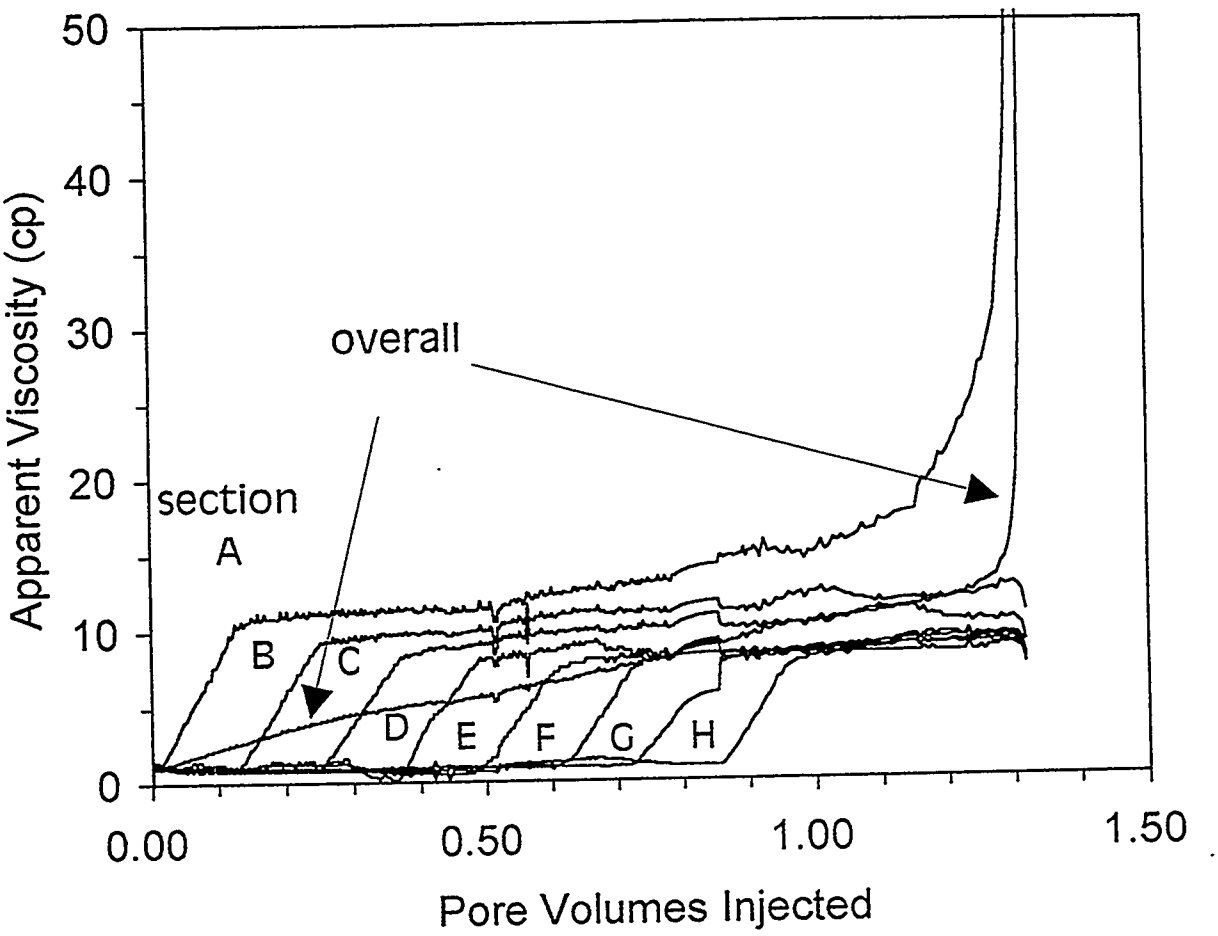

Figure 4.17 : Flow resistance in SP11 during gelant injection.

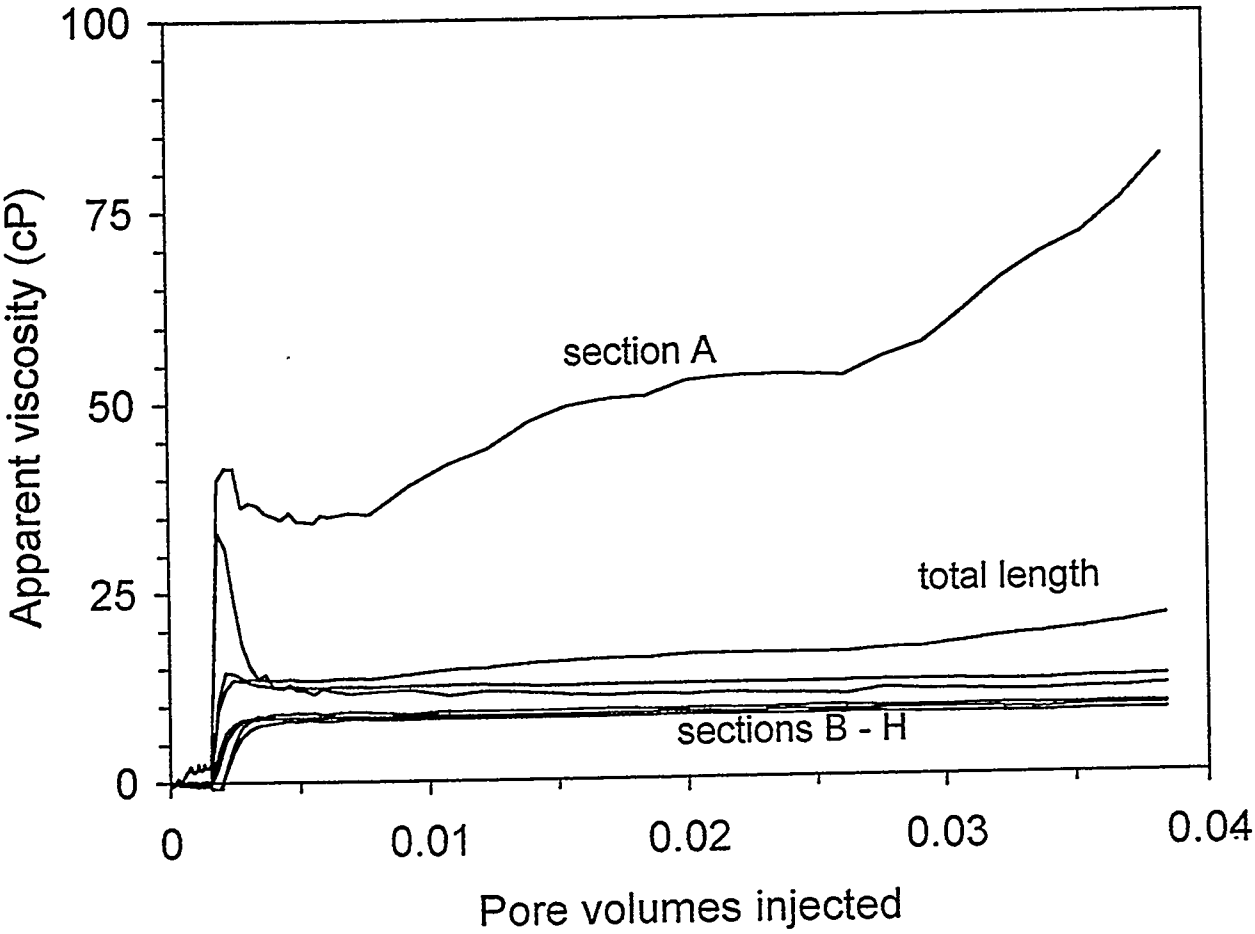

Figure 4.18 : Flow resistance during gelant injection - SP11 run 2.

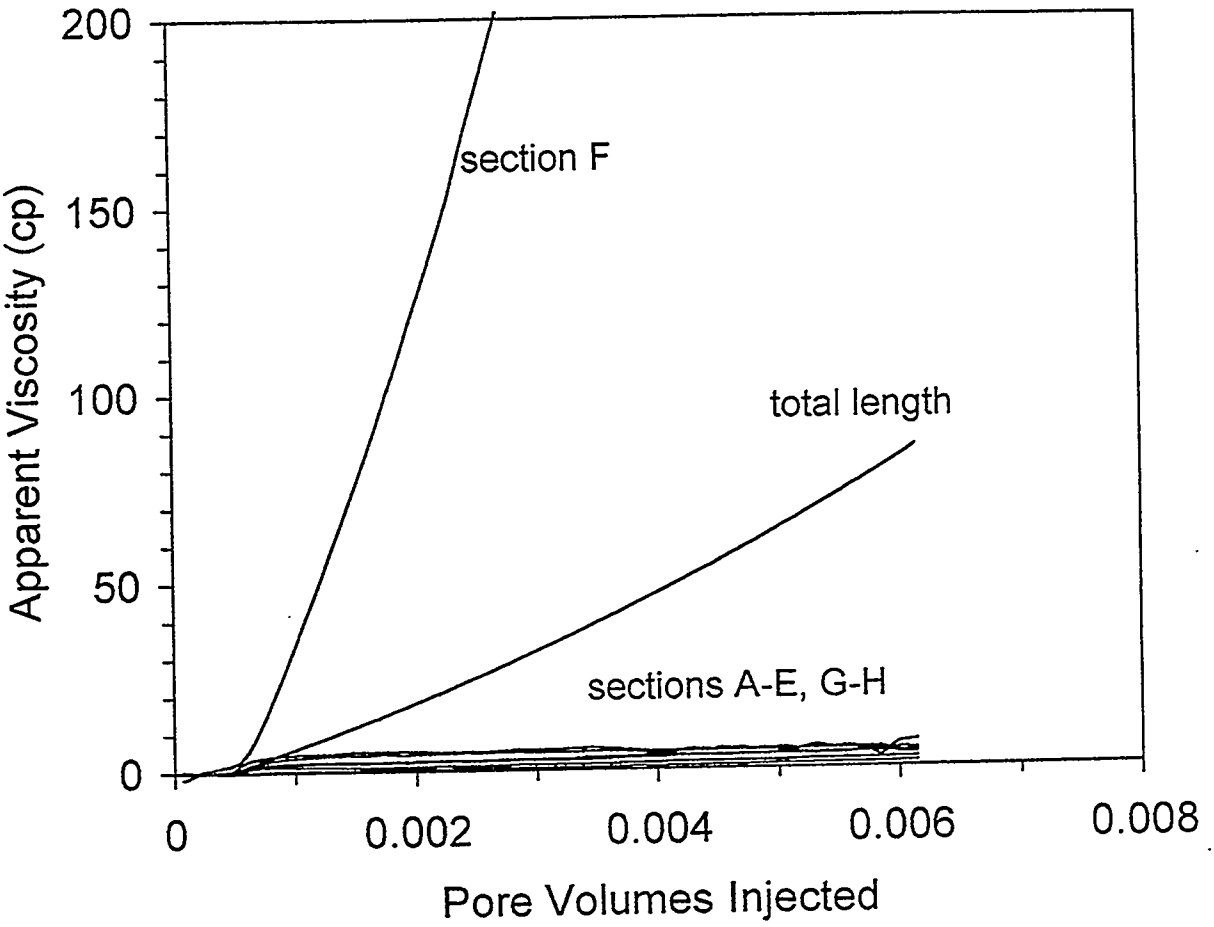

Figure 4.19 : Flow resistance during injection - SP11 run3.

A simulated fracture was created in a Berea sandstone core by cutting a slot halfway along its length. The Berea sandstone core was 5.08 cm. x 5.08 cm. cross-section and 30.48 cm. Length. The core was encapsulated with an epoxy coating and prepared for the gel displacement experiment by installing pressure ports at locations indicated in Figure 4.20. Sections A, B, C, and D are the four sections in this core and are delimited by the pressure ports along the length of the core. Three sections were also delimited along the fracture slot, sections E, F, and G, respectively. Fifty-mesh acid washed sand was placed in the slot. The core was saturated with 5000 ppm potassium chloride brine.

Pressure differentials were measured at three flow rates across all the sections in order to determine permeability of the different sections of the slotted Berea core BC1. Table 4.4 lists permeability for sections A through D.

Table 4.4 : Permeability to brine and the residual resistance factors for sections A through D and the total core length - Berea sandstone core BC1.

Section	Total	A	B	C	D
Permeability, md	826	8580	1920	444	518

No attempt was made to use the pressure data for the fracture sections to calculate permeability for these sections as there was no way to realistically allocate the portion of the overall flow that was moving through the fracture slot. The fracture permeability was estimated using Equation 4.2. Permeability of the matrix portions of sections A and B was taken to be equal to the average permeability of sections C and D.

$$k_f = \frac{k_t h_t - k_m h_m}{h_f} \qquad \text{(eq. 4.2)}$$

where, k_f = fracture permeability, h_f = fracture height,
k_m = matrix permeability, h_m = matrix height, and
k_t = section permeability, h_t = section height

The value of k_f/k_m calculated based on the above method for BC1 was found to be 183, which is well within the expected range in reservoirs.

A test was conducted to determine the response of tracer concentration as a function of injected pore volume. The tracer test was conducted by injecting 50,000 ppm potassium chloride brine through the core to displace resident 5,000 ppm potassium chloride brine. Effluent concentration was monitored using a manually operated refractive index meter. Refractive index values were converted to tracer concentration (C/C_i) and plotted as a function of pore volumes injected. Results of the tracer test are shown in Figure 4.21 and discussed later along with the results of a similar dispersion test conducted after gel injection.

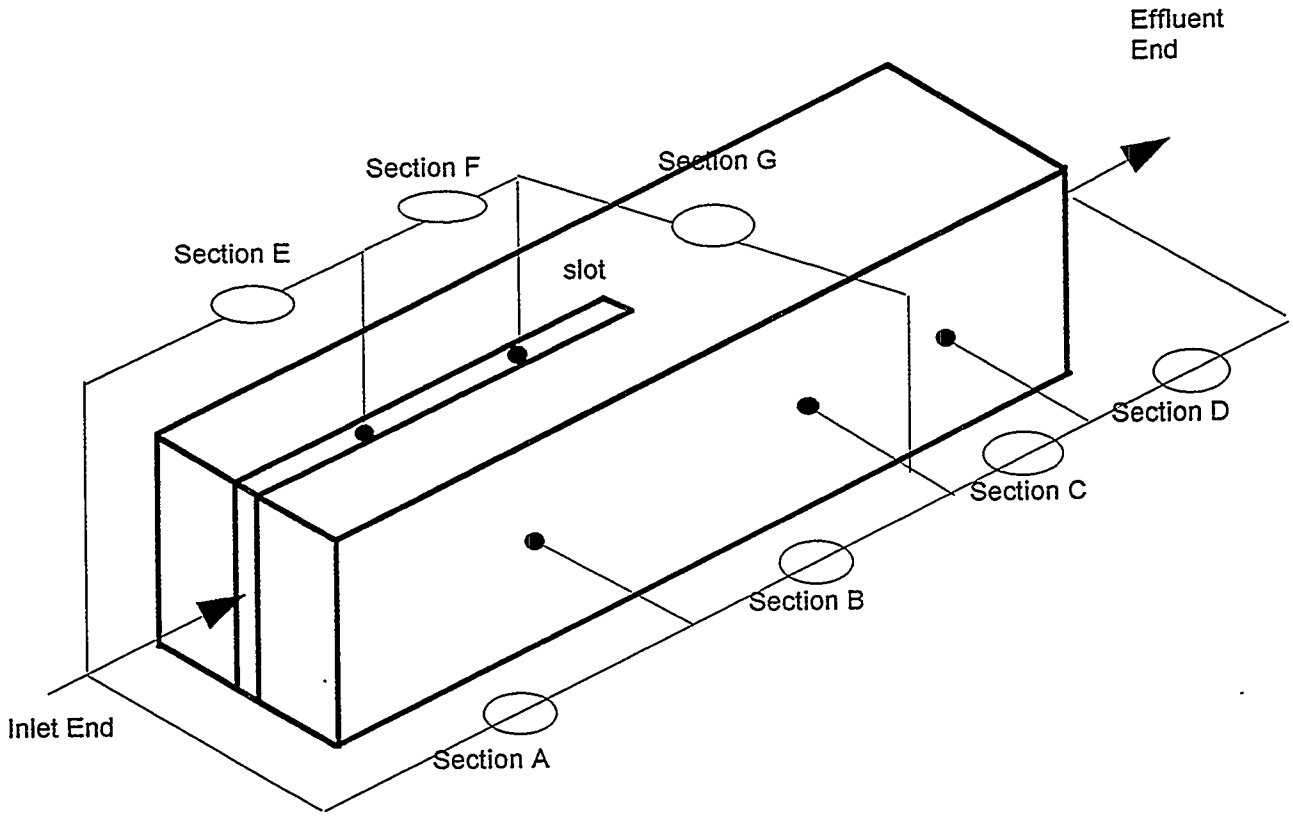

Figure 4. 20 : Diagram of slotted Berea core -BC1.

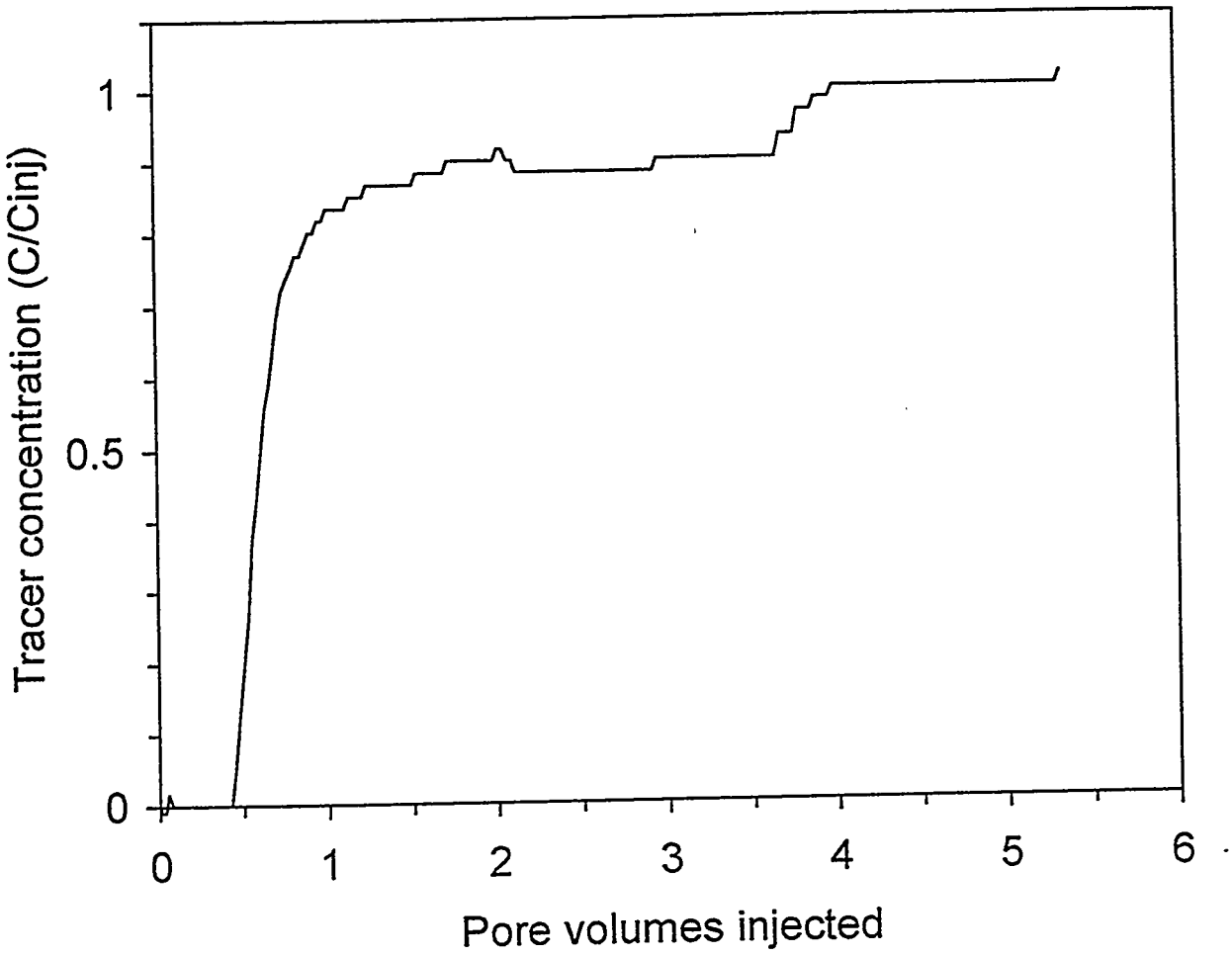

Figure 4.21 : Tracer concentration in effluent before treatment - Berea core.

The core was mounted vertically, fracture topside, to avoid settling of sand. A delay loop was introduced at the inlet of the core to delay the entry of the gelant into the core by a period of two hours after being mixed in-line. Injection of 300 ppm HiVis 350® and 15 ppm aluminum (as citrate, TIORCO 677®) gel began at a frontal velocity of 2 ft/day and a displacement rate of 16 cc/hr. Pressure differentials across all the sections were monitored and recorded during gel injection. Effluent samples were collected for monitoring rate, pH, HPAM and aluminum concentrations.

Figure 4.22 shows the apparent viscosity profiles for the sections and overall length of the core during gel displacement. Initially, section C shows the highest apparent viscosity. A sharp increase of resistance in section A began after about 3 PV of gelant were injected. Gel displacement was discontinued when the pressure drop in section A increased to 30 psi. Apparent viscosity data for fracture sections and corresponding matrix sections are furnished in Figure 4.23. Most of the pressure increase in sections A and B was the result of resistance built up inside the slot. However, as fracture section E had its pressure tap outside the core, there was possibility of face plugging across the inlet port, subsequently confirmed to be true. Inspection of the inlet port revealed a gel blob plugging it.

Effluent samples were analyzed for polymer and aluminum content and the results are presented in Figure 4.24. Polymer concentration gradually increased to the influent concentration of 300 ppm after about 5 pore volumes were injected, but decreased in the subsequent sample at 6 pore volumes. This sharp pressure increase is caused by polymer retention in the inlet section of the core. Aluminum concentration never reached then injected concentration of 15 ppm. This is consistent with other studies that aluminum is retained strongly in Berea sandstone.[9]

After the core was left sitting for two weeks, mobile polymer was displaced with 5000 ppm potassium chloride brine. Residual resistance factors were determined by measuring pressure differentials at three different flow rates. The residual resistance factors are presented in Table 4.5.

Table 4.5 : Residual resistance factors for the sections and total core length after gel treatment - slotted Berea sandstone core BC1.

Section	Total	A	B	C	D	E	F	G
RRF	7.53	4.16	13.	8.7	4.7	5.0	2.40	13.7

Although it was not possible to calculate fracture permeability based on the pressure data directly, a method similar to the one used for pre-gelation permeability determination was employed and k_f / k_m for the first two sections was determined. The matrix permeability for these two sections was assumed to be equal to the reduced matrix permeability of Section D. The value of k_f / k_m for section was calculated as 169, which is close to the initial value of 183. However, for the section B it was calculated as 3.5, which is a significant reduction in fracture conductivity. The residual resistance factor for the Section B was also found to be higher than the other sections. A similar increase in residual resistance factor occurred in fracture section G. This suggests that the gel "interface phenomena" might have contributed to this result.

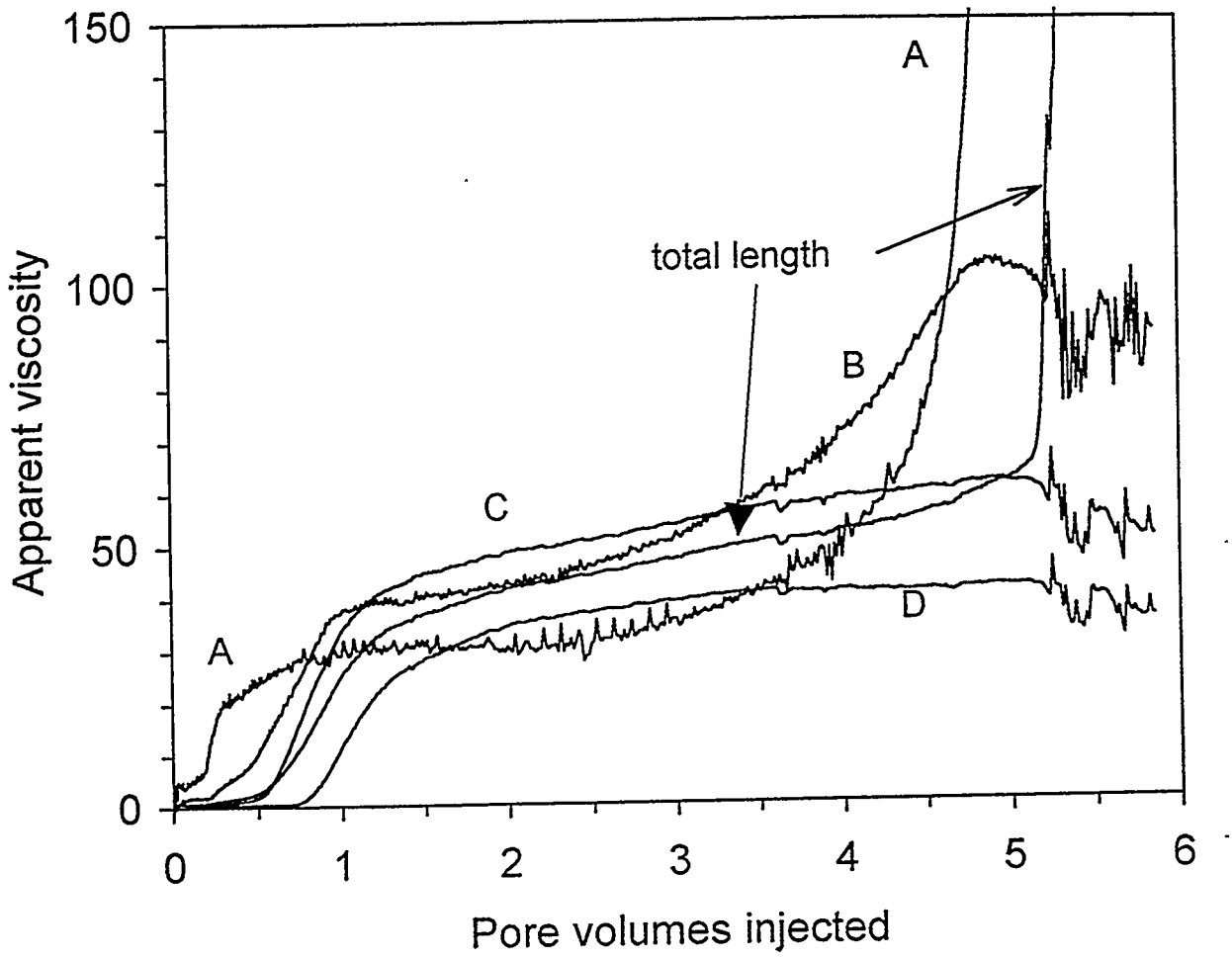

Figure 4.22 : Flow resistance during gelant injection - Berea core.

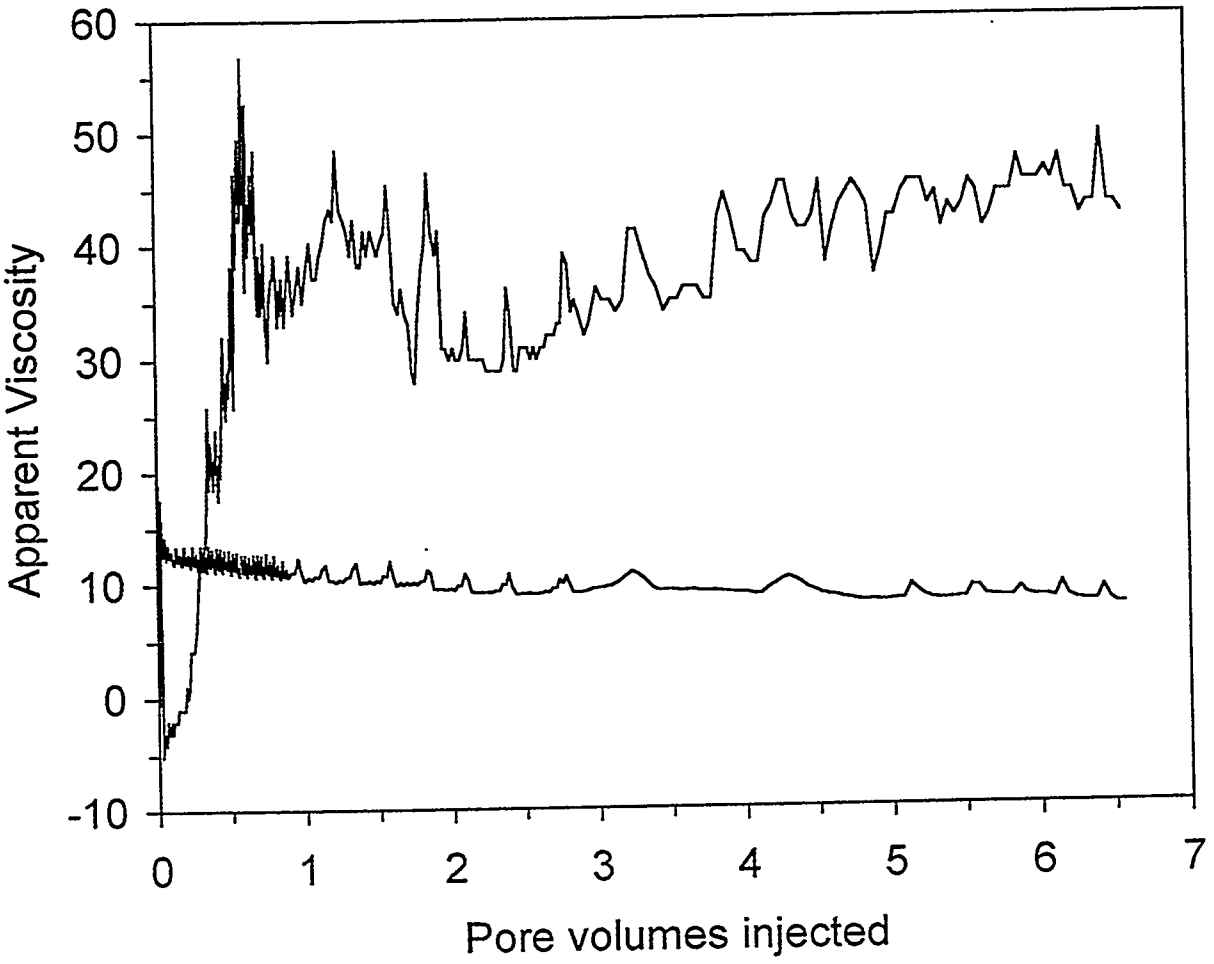

Figure 4.23 : Flow resistance during brine injection - Berea core.

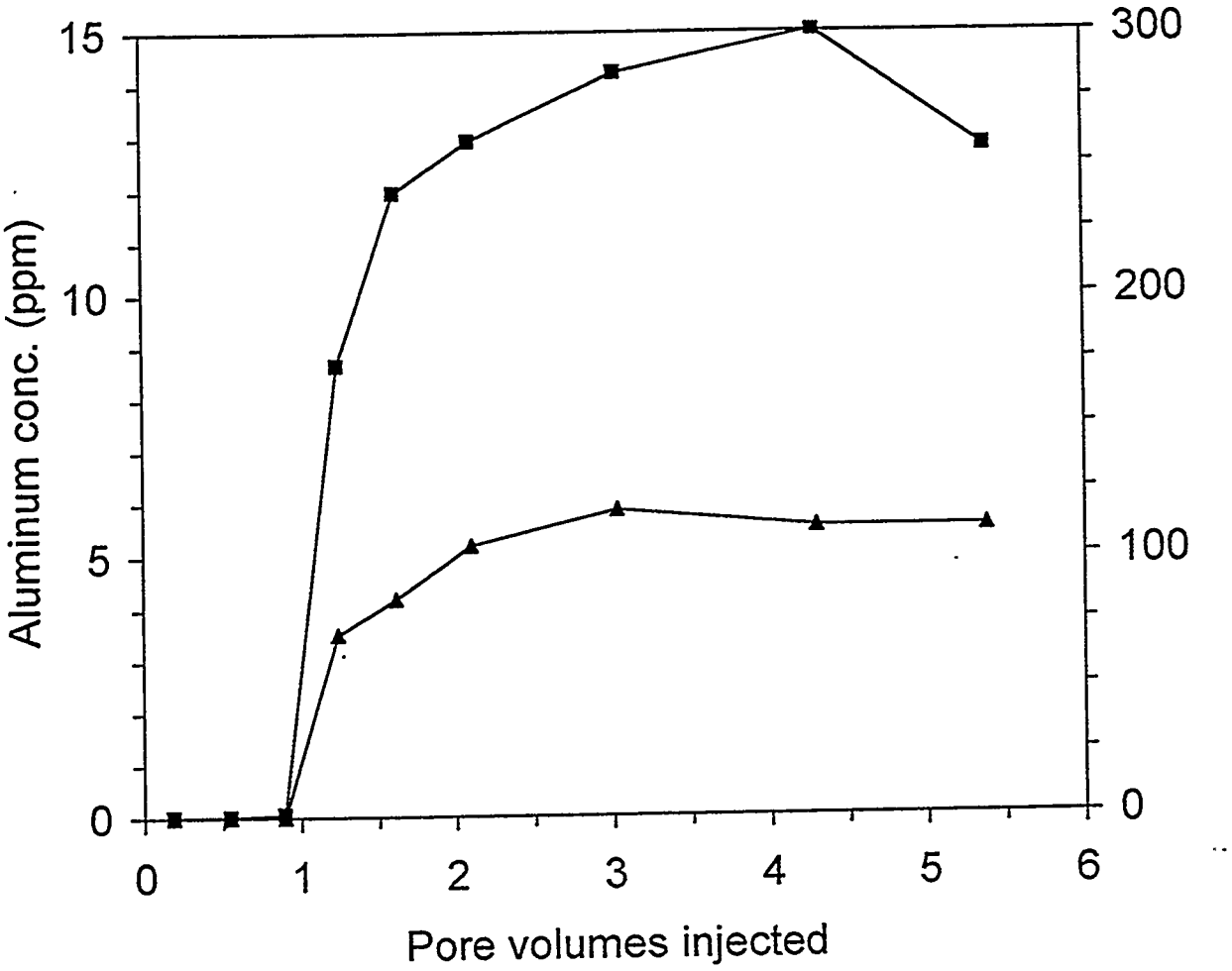

Figure 4.24 : Aluminum and poymer concentrations in effluent - Berea core.

A test was conducted using 50,000 ppm potassium chloride brine as the tracer to displace the 5000 ppm potassium chloride left in the core after gel displacement. The ratio of effluent to injected tracer concentration during this test is shown as a function of pore volumes injected in Figure 4.25 with the pre-gel injection tracer curve. Comparison of the two curves reveals certain distinctive features of the tracer profiles. The tracer front breaks through at about 0.5 pore volumes because part of the tracer moves through the slot and flows through half of the core. A portion of the incoming flow moves through the matrix part at the inlet face and forms a secondary front which appears after some time in the effluent stream. Although both the pre- and post- gel injection tracer profiles follow this trend, there are differences. In the post-gel tracer curve, the initial breakthrough is later and the secondary front arrives earlier. This indicates that the velocity of the tracer flowing through the matrix portions of sections A and B is higher in the post-gel injection dispersion thus delaying the initial breakthrough of the tracer front and causing early arrival of the secondary front. The tracer tests suggest development of flow resistance in the fracture slot.

The core was split to physically examine the slot. Although the sand inside the slot did not have any gel structure, it showed some stickiness and elasticity due to the presence of gel aggregates. The slot-matrix interface was coated with a film of gel that was thicker at the tip of the slot.

Significant results from this experiment were:

- The gel solution flowed through the core with relative ease and the development of flow resistance was not high indicating in situ gelation had not occurred.
- There was development of resistance across the tip of the fracture slot as evidenced by a combination of apparent viscosity, residual resistance factors, and dispersion test data.
- The build up of gel aggregates at the inlet port remains a problem in laboratory experiments.

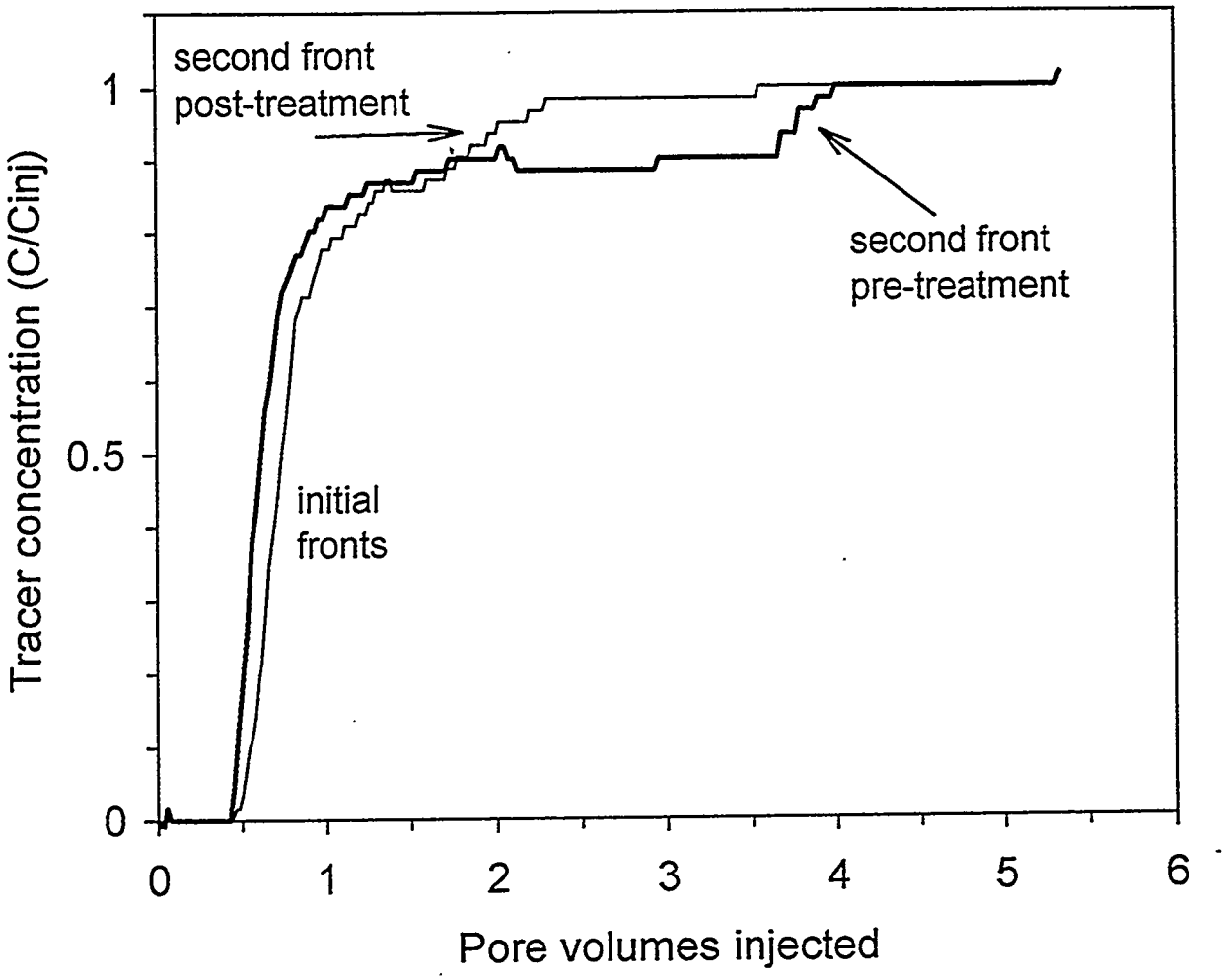

Figure 4.25 : Comparison of tracer concentration in effluent before and after treatment - Berea core.

Conclusions

The conclusions in this report are based on solutions of HiVis® polymer and aluminum citrate gelant systems in 0.5 wt% KCl brine displaced through unconsolidated sandpacks and one Berea core at 25°C.

1. Small concentrations of chlorine (<1/4 ppm) degrade the polymer solutions and gels prepared at polymer concentrations of 300 ppm. Chlorine must be eliminated from the solutions before reproducible and stable viscometry and TGU measurements can be made.
2. The viscosity was correlated as a function of shear rate and polymer concentration for a polymer solution. The viscosity of polymer solutions decreased with time over a period of three weeks.
3. Solutions containing 300 ppm of polymer lose over half of their solution viscosity when displaced through 4 foot sandpacks which have an average permeability of 3-4 darcies.
4. Growth of gel aggregates was not observed for gelant samples which reacted for 4, 8, and 12 hours.
5. The gel solution flows through the porous media in a similar manner to polymer solution. Although the polymer concentration of effluent samples was equal to the injected solution, the viscosity was significantly lower as observed for polymer solutions flowing through sandpacks.
6. Gel retention occurs at the inlet of sandpacks and is enhanced when there is a screen retaining the sand. Retention is faster when the gelant is given some time to react before it is injected. Aggregates are retained at the interface between regions of high permeability and in void spaces under certain conditions.
7. In-depth permeability reduction was not observed. Resistance developed at the porous media inlet only. When propagated through porous media, the colloidal dispersion gel loses all gel-like properties. The effluent solutions obtained during both the polymer and gel displacement experiments were found to have low viscosities and never formed a gel structure.
8. Aluminum was retained in significant amounts in the sandpacks and Berea sandstone.

References

1. Mack, J.C. and Smith, J.E., "In-Depth Colloidal Dispersion Gels Improve Recovery Efficiency," SPE/DOE 27780 presented at the SPE/DOE 9th Symposium on Improved Oil Recovery, Tulsa, OK, (Apr. 17-20, 1994).
2. Fielding, R.C. Jr., Gibbons, D.H. and Legrand, F.P., "In-Depth Fluid Diversion using an Evolution of Colloidal Dispersion Gels and New Bulk Gels : An Operational Case History of North Rainbow Ranch Unit," SPE/DOE 27772 presented at the SPE/DOE 9th Symposium on Improved Oil Recovery, Tulsa, OK, (Apr. 17-20, 1994).
3. Ranganathan, R., Lewis, R., McCool, C.S., Green, D.W. and Willhite, G.P.: "An Experimental Study of a Polyacrylamide/Aluminum Citrate "Colloidal Dispersion " Gel in a Porous Medium and its Aggregate Growth During Gelation Reaction" SPE Paper 37220 presented at the 1997 SPE International Symposium on Oilfield Chemistry, Houston TX, February 18-21, 1997.
4. Smith, J.E., "The Transition Pressure : A Quick Method for Quantifying Polyacrylamide Gel Strength," SPE 18739 presented at the 1989 SPE International Symposium on Oilfield Chemistry, Houston, TX, (Feb. 8-10, 1989).
5. Green, D.W. and Willhite, G.P., "Improving Reservoir Conformance Using Gelled Polymer Systems," Report No. DOE/BC/14881-12, Annual Report for the Period Sept. 25, 1993 to Sept. 24, 1994, for Research Program performed under DOE Contract No. DE-AC22-92BC14881 (July 1995), Chapter 8.
6. Green, D.W. and Willhite, G.P., "Improving Reservoir Conformance Using Gelled Polymer Systems," Report No. DOE/BC/14881-18, Annual Report for the Period Sept. 25, 1994 to Sept. 24, 1995, for Research Program performed under DOE Contract No. DE-AC22-92BC14881 (May 1996), Chapter 3.
7. Green, D.W. and Willhite, G.P., "Improving Reservoir Conformance Using Gelled Polymer Systems," Report No. DOE/BC/14881-18, Annual Report for the Period Sept. 25, 1994 to Sept. 24, 1995, for Research Program performed under DOE Contract No. DE-AC22-92BC14881 (May 1996), Chapter 4.
8. Parmeswar, R. and Willhite, G.P., "A Study of the Reduction of Brine Permeability in Berea Sandstone with the Aluminum Citrate Process," SPE Reservoir Engineering (Aug. 1988) pp. 959-966.
9. Rocha, C.A., Green, D.W., Willhite, G.P. and Michnick, M.J., "An Experimental Study of the Interactions of Aluminum Citrate Solutions and Silica Sand," SPE 18503 presented at the 1989 SPE International Symposium on Oilfield Chemistry, Houston, TX (Feb. 8-10, 1989).
10. Seright, R.S., "Propagation of an Aluminum Citrate - HPAM *Colloidal Dispersion* Gel through Berea Sandstone," Report No. PRRC 94-29, New Mexico Petroleum Recovery Research Center, New Mexico Institute of Mining & Technology, (Jun. 1994).

Chapter 5

Gelation and Permeability Reduction of Resorcinol-Formaldehyde Gel Systems

Principal Investigators: C.S. McCool, D.W. Green and G.P. Willhite
Research Assistants: Yingfeng Zuang, S.N. Pandey

Two phenolic-aldehyde systems were studied. One was composed of resorcinol and formaldehyde (designated the RF system) and the other composed of sulfomethylated-resorcinol and formaldehyde (designated the SMRF system). Bottle testing to characterize the RF system revealed the gelation was sensitive to pH, salinity and hardness. The performance of the SMRF system was determined to be superior to that of the RF system by bottle tests. Gelation of the SMRF was studied in several types of core material. This chapter summarizes the study. Experimental procedures and detailed results are presented in references 1 and 2.

Result and Discussion

Bottle tests of the resorcinol-formaldehyde (RF) system. Bottle tests were conducted to determine the effect of resorcinol concentration, mole ratio of formaldehyde to resorcinol, initial pH, salinity and hardness on the gel time for the RF system. The gel time was not significantly affected by the mole ratio of formaldehyde to resorcinol (F/R) above the ratio of 1.5. Gel times increased significantly as the F/R mole ratio was decreased below the 1.5 value. At these lower values of the mole ratio, the data suggest that formaldehyde was the deficient reactant and, thus, controlled the rate of gelation. The data are consistent with the statistical polymerization theory for condensation reactions which states that the raction rate would not decrease at F/R mole ratios above 1.33. Steric effects make reaction sites less accessible as molecular size increases which results in a stoichiometric mole ratio to be a value somewhat larger than 1.33.

Gelation behavior of the RF system was sensitive to the initial pH of the system and to the procedure for adjusting the initial pH. The rate of adding 0.1 N NaOH to the sample affected the amount of base required. This, in turn, affected the pH during gelation, the gelation time and sometimes the gel quality, especially at higher monomer concentrations and higher initial pH.

Gel times and precipitation times for a series of gel solutions that were adjusted initially to selected pH values are shown in Figure 5.1. Gels formed for initial pH values of 8.0 and above. Samples prepared at initial pH values of 7.35 and below did not form homogenous gels but formed precipitate or gelatinous precipitate. Stronger gels were formed at longer gel times as the initial pH was increased in the range from 8 to 10.

The effect of the concentration of salt and salt type on gel times for a series of gel samples are shown in Figures 5.2. These data show that the gelation behavior was sensitive to small changes in salinity at salt concentrations below 1.0% salt. Salt significantly increased the gelation rate and decreased the gel time. The divalent cation Ca^{2+} had an stronger influence than the monovalent ions.

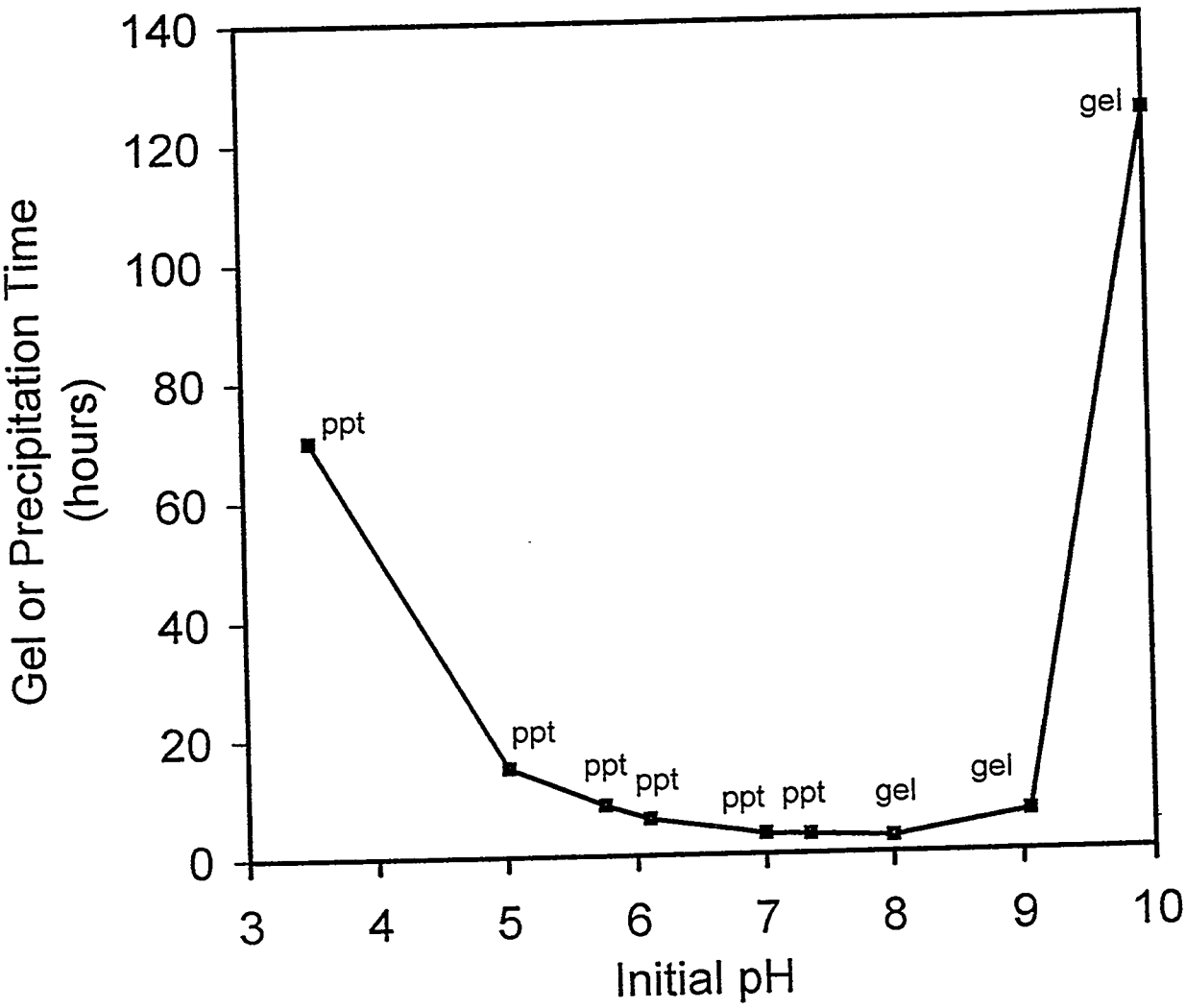

Figure 5.1 : Gel Times as a Function of Resorcinol Concentration; Gelants contained a mole ratio of formaldehyde-to-resorcinol of 1.3, initial pH= 9.0, 0.5% KCl; 41 °C.

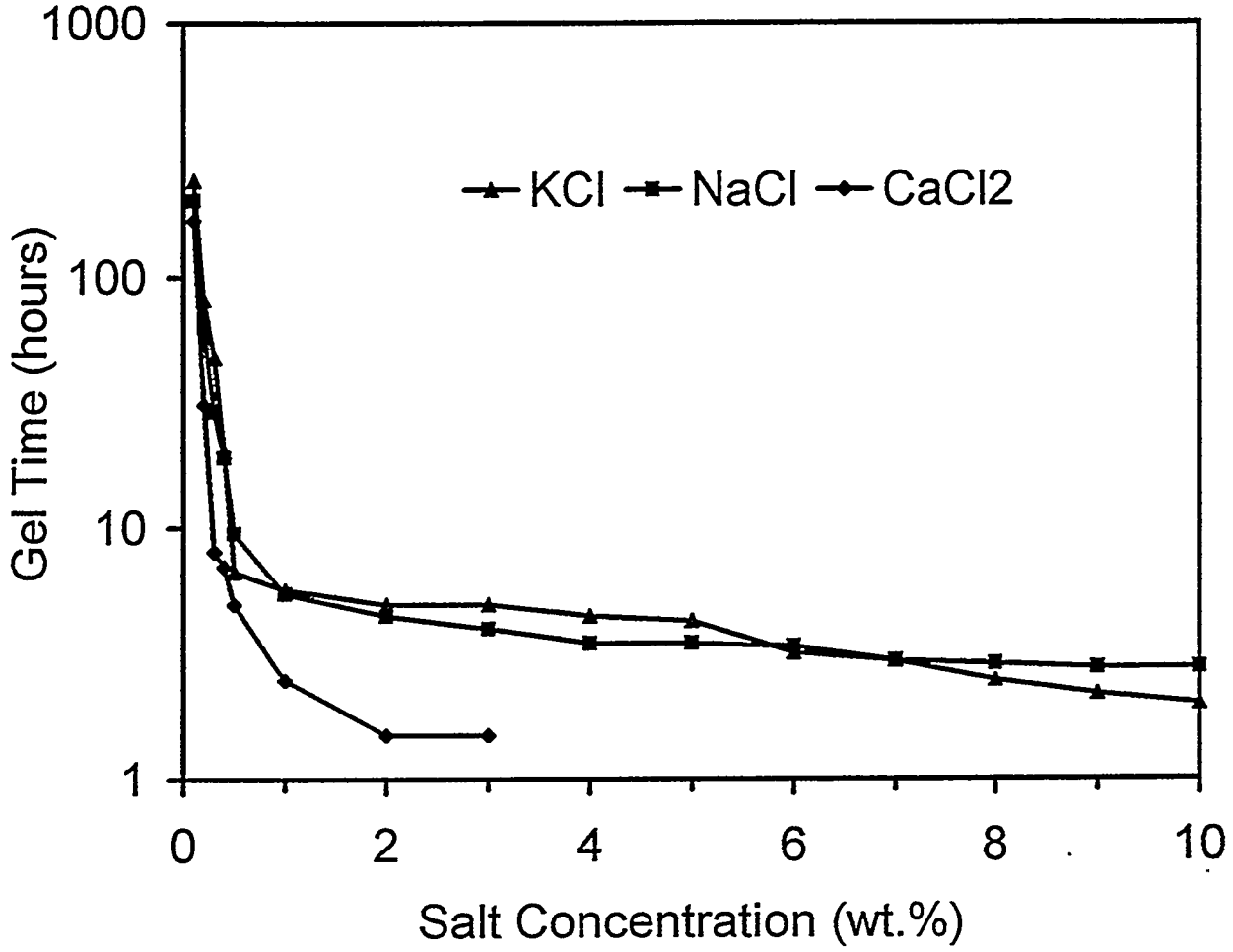

Figure 5.2 : Effect of Salt Concentrations on Gel Times for Gelants Containing 3.0 % Resorcinol for RF System; Gelants contained a mole ratio of formaldehyde-to-resorcinol of 1.5, initial pH = 9.0; 41 °C.

Gel times for the RF system were less than ten hours at component concentrations that were considered applicable for use in permeability reduction treatments. Longer gel times would be required for in-depth application. Long gel times for the RF system were only observed at low salt concentrations where the gel time was very sensitive to salt concentration. At theses conditions, field application would be difficult.

Bottle tests of the sulfomethylated resorcinol-formaldehyde (SMRF) system. Screening experiments were conducted to determine the effects of various parameters on the gelation and gel times of the SMRF system. SMRF systems were prepared in two steps. The first step was the sulfomethylation of the resorcinol. The sulfomethylated resorcinol was then used to prepare the gel mixture. Composition of SMRF samples are described by the weight percent of resorcinol and the mole ratios, F_2:F_1:S:R, where F_1, S and R are formaldehyde, sodium sulfite and resorcinol used in the preparatory sulfomethylation step, and F_2 is the formaldehyde used to prepare the gelant mixture. All values are based on the final gelant mixture.

The viscosity as a function of time for the samples prepared at initial pH of 8.0 are shown in Figure 5.3. Initial viscosity was 0.72 cp, comparable to water viscosity of 0.71 cp. The viscosity remained low for extended period of time and then increased rapidly. Visible gels formed at the time the viscosity was about 300 to 400 cp, while firm gels that did not fall upon inversion of the sample bottle formed at much higher viscosities (above 1000 cp).

The effects of initial pH and NaCl concentration on the gelation of the SMRF system using 3.0% resorcinol are shown in Figure 5.4. The data show increased salt concentration accelerated the gelation process. The initial pH also affected the gel times. SMRF gels were formed at initial pH values that ranged from 5.0 to 10, in contrast to the RF system where gels were not formed at initial pH values between 5.0 and 7.0.

A comparison of gel times for similar RF and SMRF systems is shown in Figure 5.5 as a function of NaCl concentration. These data show that sulfomethylation of the resorcinol increased the gel time. For example, under the condition of 41°C, 0.5% NaCl and an initial pH of 9.5, the gel time of RF gel solution (3%R, F:R=1.5) was about 3 days; while the gel time of SMRF gel solution (3%R, SMRF F_2:F_1:S:R=1.3:0.75:0.5:1) was more than two months.

Gel times are given in Table 5.1 for a selected SMRF system at initial pH values of 6, 7 and 8 and at several brine compositions. Inspection of these data show that gel times for the SMRF system were on the order of days and that the gel times were not as sensitive to pH and salt concentrations as for the RF system. SMRF gel systems that were prepared at pH values less than 6 or more than 9 gelled at longer times and the gel times were more sensitive to small changes in pH.

Gel times for samples at selected initial pH and temperatures are given in Table 5.2. At initial pH values of 7.0 and below, the gel time decreased with increased temperature and the gels were firm. Samples prepared at a pH of 8.0 and at 2.5% resorcinol formed weaker gels. Increasing the resorcinol concentration to 2.75% (initial pH of 8.0), decreased the gel time and produced firm gels. No gel was formed at initial pH values of 9.0.

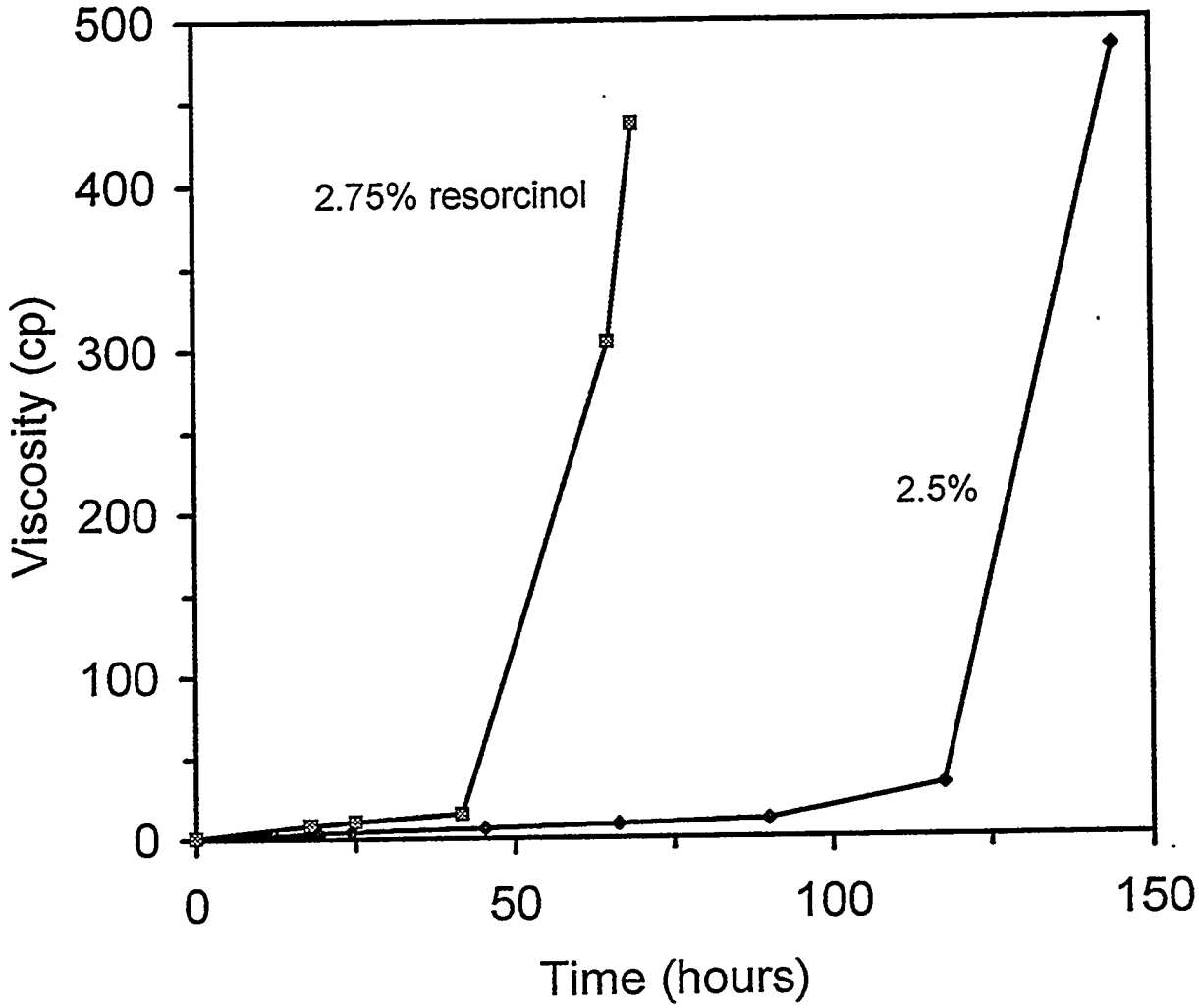

Figure 5.3 : Viscosity as a Function of Time and Resorcinol Concentration for SMRF Gel System; Gelants contained mole ratios of $F_2 : F_1 : S : R = 1.4 : 0.75 : 0.5 : 1$, 5.0% NaCl, 0.035% $CaCl_2$-$2H_2O$; 41 °C.

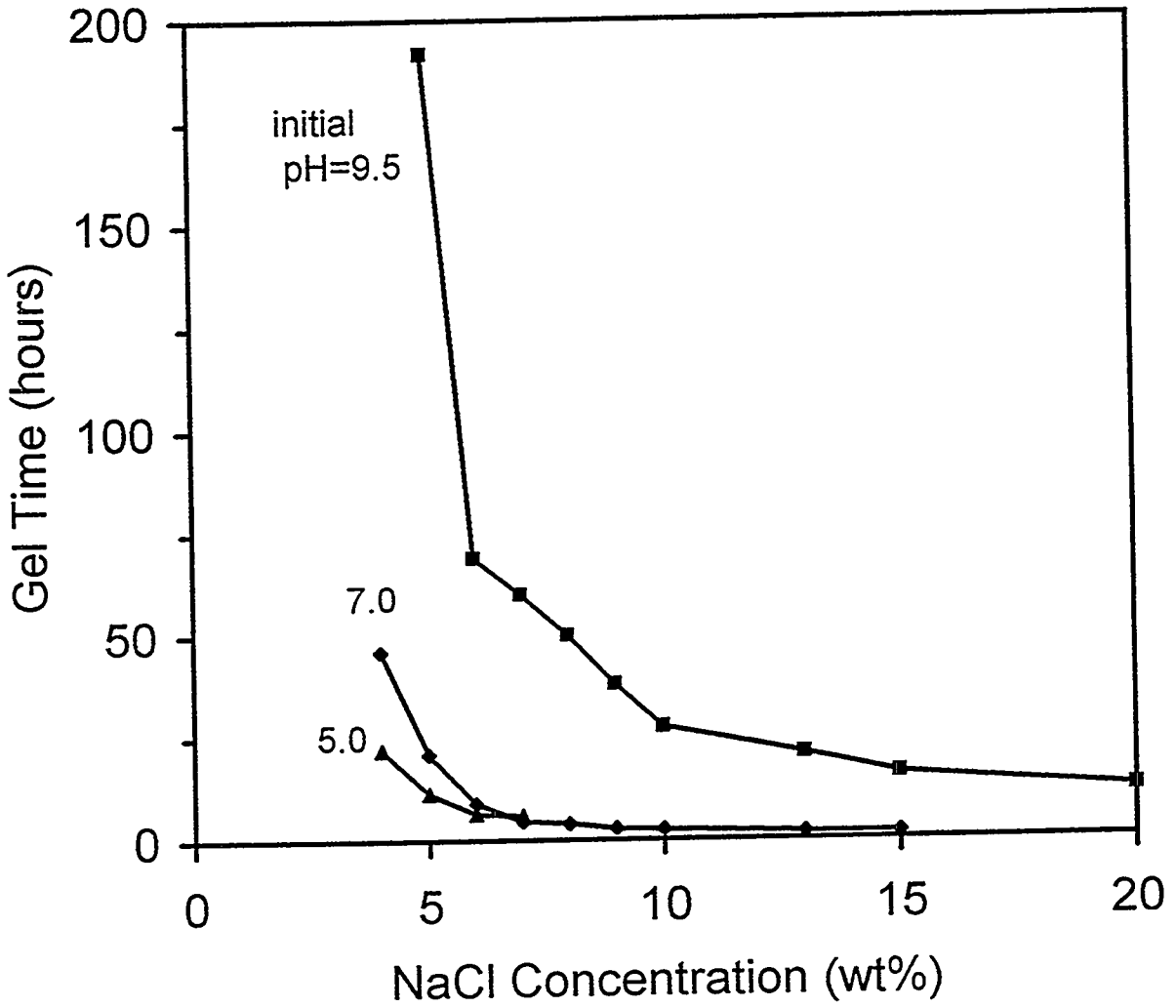

Figure 5.4 : Effect of NaCl Concentration on Gel Time for SMRF System; Gelants contained 3.0% resorcinol, mole ratios of $F_2 : F_1 : S : R = 1.3 : 0.75 : 0.5 : 1$; 41 °C.

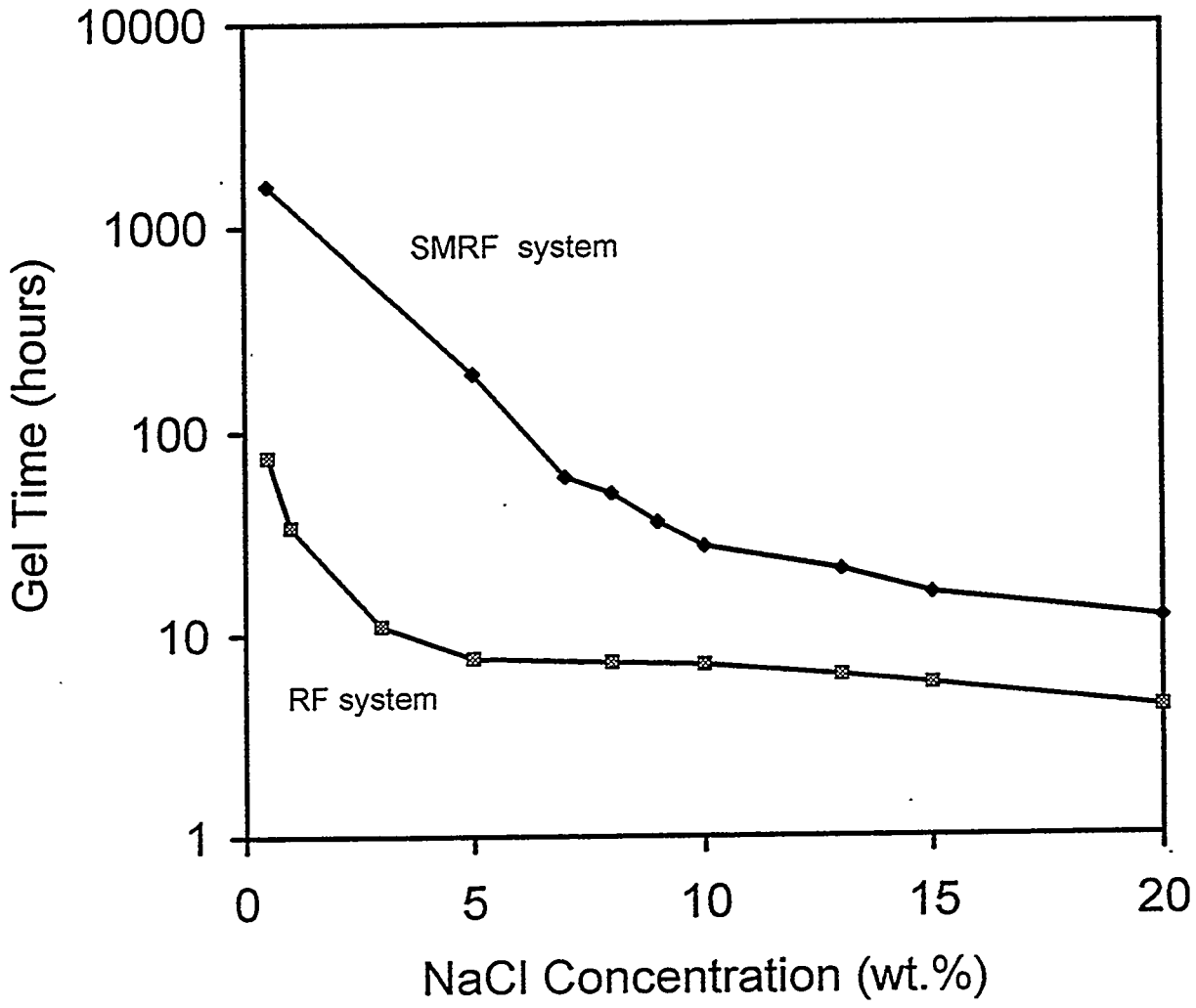

Figure 5.5 : Comparison of Gel Times Between RF and SMRF Gel Systems; Both systems contained 3.0% resorcinol, mole ratio of formaldehyde-to-resorcinol was 1.5; initial pH = 9.5; 41 °C; SMRF system - mole ratios of $F_2 : F_1 : S : R = 1.5 : 0.75 : 0.5 : 1$.

Table 5.1 : Gelation Behavior of Sulfomethylated Resorcinol-Formaldehyde System at 41 °C; Gelants contained 2.5% resorcinol, mole ratios of $F_2 : F_1 : S : R = 1.4 : 0.75 : 0.5 : 1$.

NaCl Conc. (%)	$CaCl_2 \cdot 2H_2O$ Conc. (%)	Initial pH		
		6.0	7.0	8.0
		Gel Time (hours)		
5.0	0.0	50-60	50-60	110-120
5.0	0.036	50-60	36-46	44-54
5.0	0.36	36-46	22-30	22-30
5.0	1.8	13-23	9-13	6-8
4.0	0.036	~288	~175	~202
4.0	0.36	~77	59-69	~120
4.0	1.8	18-22	10-13	6-10
3.0	0.36	312-323	275-285	
3.0	1.8	34-44	10-20	10-20

Table 5.2 : Gel Times and Final pH of Sulfomethylated Resorcinol-Formaldehyde Gels at 25, 41, and 52°C; Gelants contained mole ratios of $F_2:F_1$ S:R = 1.4:0.75:0.5:1, 5.0% NaCl, 0.035% $CaCl_2$-$2H_2O$.

Initial pH	25°C		41°C		52°C	
	Gel Time (hours)	Final pH	Gel Time (hours)	Final pH	Gel Time (hours)	Final pH
5.0	66		43			
6.0	28	5.42	25	5.21	12	5.16
7.0	30-42	5.70-5.89	26-43	5.45-5.64	17	5.46
8.0	64-72	6.48-7.19	120-200	6.30-6.69	216	6.12
8.0*	41	7.25	67	6.45		
9.0	No gel	No gel	No gel	No gel	No gel	No gel

* resorcinol concentration was 2.75% in samples.

In situ gelation in core plugs. Eight in situ gelation experiments were conducted in selected core plugs using three gel compositions. The diameter of the core plugs ranged form 2.5 to 3.8 cm and the lengths ranged form 5.6 to 10.2 cm. Composition of the gelants are given in Table 5.3. Three pore volumes of freshly-prepared gelant were injected into the core plugs over time periods between one-half and one hour. Pressure drops across the core plugs during gelant injection showed the flow resistance was slightly higher than the value that would be observed for brine flow demonstrating the high injectivity of the gelant.

pH values of the effluent from the plugs were measured at several times during the sequence of flow experiments and are presented in Table 5.3. The pH of the brine (initially between 7 and 8) was elevated to values of 8.9 and above by the flow through the plugs prior to gelant injection. The pH of the gelant displaced through the plugs at the end of gelant injection was approximately the same as the injected value indicating the capacity of the gelant to resist the pH-altering capability of the rock. pH values during post-gelation brine injection were lower than when brine was injected prior to gelant injection as shown in Table 5.2. The presence of gel in some manner prevented the pH of the injected brine to be elevated to the high pH values that were observed before gelant injection.

Samples of the injected gelant and the effluent gelled during the shut-in time for the plugs (except for DOL-3). Brine was then injected to determine post-treatment permeabilities. The reduction in permeability produced by the gel treatments are presented in Table 5.3. Residual resistance factors are a ratio of the initial permeability to the post-treatment permeability. The treatments reduced the permeabilities of the core plugs by factors greater than 9,000 (except for DOL-3). The three limestone plugs were completely sealed by the gel and no brine could be displaced. For the other plugs, the post-treatment permeabilities were determined only after the pressure drops stabilized. During brine injection, the pressure drops decreased with time (at a given flow rate) demonstrating that the permeabilities were even lower initially.

The gel system used for plug DOL-3 did not gel as predicted by the screening experiments. This resulted in no reduction in permeability of the plug by the treatment. It was determined in the screening experiments that the SMRF gel system prepared at an initial pH of 8.0 and resorcinol concentration of 2.5%, a weak gel was formed at times of 120 to 200 hours. The particular sample prepared for the DOL-3 plug formed a weak gel only after many weeks. Brine was injected after 25 days of shut-in and before gelation occurred. It is not known if this *weak* gel would reduce the permeability of core plugs if left shut-in for a longer period of time. At an initial pH of 8.0 and a resorcinol concentration of 2.75%, much stronger gels are formed and the permeabilities of core plugs are effectively reduced as shown in Table 5.3 for plugs DOL-1, DOL-4 and LST-3. (The gelant for DOL-1 was prepared at a resorcinol concentration of 2.5%, but evaporation losses during preparation resulted in a resorcinol concentration of approximately 2.75%.)

Table 5.3 : Details and Results of Gel Treatments Using the Sulfomethylated Resorcinol-Formaldehyde System.

Core No.	Gelant Composition *	pH of Effluent			Shut-In Time	Initial Permeability (md)			Post-Treatment Permeability			Residual Resistance Factor
	Initial pH Resorcinol Conc.	Pre-Treatment Brine Injection	Gelant Injection	Post-Treatment Brine Injection	(days)	Total	Section 1	Section 2	Total	Section 1	Section 2	
DOL-1	pH 8.0 2.5% resorcinol (2.75%)**	9.12	7.80	7.36	10	163	158	170	0.02	0.03	0.01	9050
DOL-2	pH 7.0 2.5% resorcinol	9.43	7.0	7.87	5	161	194	139	0.02	0.06	0.01	9450
DOL-3	pH 8.0 2.5% resorcinol	9.53	8.03		24	113	104	120				
DOL-4	pH 8.0 2.75% resorcinol	9.62	8.10	7.19	11	128	110	159	0.01	0.01	0.01	14500
LST-1	pH 7.0 2.5% resorcinol	8.98	7.17		5	11.5	10.4	12.4	0.0			∞
LST-2	pH 7.0 2.5% resorcinol	8.94	7.16		5	19.7	10.8	106	0.0			∞
LST-3	pH 8.0 2.75% resorcinol	9.09	8.04		11	35.3	49.3	33.1	0.0			∞
BR-1	pH 7.0 2.5% resorcinol	8.94	6.76	7.38	5	500	514	462	0.01	0.01	0.02	34700

* All gelants contained sodium sulfite and formaldehyde at F_2 :F_1 : S : R mole ratios of 1.4 : 0.75 : 0.5 : 1. See Experimental section for details. Gelants also contained 5.0% NaCl and 0.036% $CaCl_2$-$2H_2O$.

** Evaporation occurred in this resorcinol solution. Concentration was estimated at 2.75% resorcinol.

Conclusions

1. The sulfomethylated resorcinol-formaldehyde (SMRF) system has improved gelling characteristics and wider field applicability as compared to the RF system. Bottle tests demonstrate that the SMRF system gels over longer time periods and over wider pH ranges (5-8) than the RF system.

2. The SMRF system was effective in reducing the permeability of limestone, dolomite and sandstone core plugs. Permeabilities were reduced by factors greater than 9000.

3. The resorcinol-formaldehyde (RF) system has limited applicability for use in gelled polymer treatments in the range of compositions that were studied in bottle tests (41 °C). At salt concentrations less than approximately 1%, the gel time was very sensitive to salt concentration which presents difficulties in controlling the process in the field. At salt concentrations greater than 1%, the gel times are on the order of 10 hours or less. These relatively short gel times would only be applicable for near well-bore treatments in shallow wells. Additionally, the RF system did not gel at pH values below approximately 7.5.

References

1. Green, D.W. and Willhite, G.P., "Improving Reservoir Conformance Using Gelled Polymer Systems - Annual Report - September 25, 1994 to September 24, 1995," U.S. Department of Energy report number DOE/BC/14881-18.
2. Zhuang, Y., Pandey, S.N., McCool, C.S. and Willhite, G.P. "Permeability Modification using Sulfomethylated Resorcinol-Formaldehyde Gel System," SPE Paper No. 37245, 1997 SPE International Symposium on Oilfield Chemistry, Houston, TX (18-21 Feb 1997).

Chapter 6

Gel Systems for Application with Carbon Dioxide Miscible Displacement

Principal Investigators: S. Vossoghi, G.P. Willhite and D.W. Green
Graduate Research Assistant: Koorosh Asghari

Introduction

This chapter presents the progress to develop gel systems for application with carbon dioxide miscible displacement. Four new gel systems were developed at the University of Kansas. Three systems are based on a biopolymer termed KUSP1.[1-5] The fourth system is a modification of a previously reported organic crosslinking system. Details of the experimental procedures and findings are presented in DOE annual reports[6,7] and elsewhere.[8,9]

All systems studied revealed promising potential for the permeability modification in a supercritical CO_2 environment. KUSP1 solution produced *in situ* gelation in Berea cores upon injection of supercritical CO_2. The permeability reduction was about 85% of the original permeability. This level of reduction was observed for both the effective permeability of CO_2 and the effective permeability of brine. The advantage of this system over other conventional gel treatments is that it requires no cross linker for the application in CO_2 floods.

It was discovered[5] that KUSP1 dissolved in sodium hydroxide produces a delayed gel system with orthoboric acid. The gelation time varies depending on the concentration of the orthoboric acid, temperature, and initial pH of the solution. The gelation seems to be of cross-linking type reaction, hence kinetically controlled. The physical qualities of the boric acid gels are different than those produced from alkaline KUSP1 solution in the presence of CO_2 or ester as a pH-reducing agent. Boric acid gels are stronger and more uniform than gels formed without boric acid.

The third system uses the hydrolysis of an ester to control the rate of neutralization of KUSP1 solution. The ester slowly hydrolyses and causes pH reduction to the level for the KUSP1 alkaline solution to gel. Commercially available esters that are soluble in solution have high rates of hydrolysis and produce gelation times in the order of minutes. An ester (mono ethyl phthalate) was synthesized in our lab to produce slow rate of hydrolysis. The rate of hydrolysis is controlled by the concentration of the ester and the initial pH of the solution.

The fourth gel system developed and studied in this work for application to CO_2 flooding is the SMRF (sulfomethylated resorcinol formaldehyde) system. This is a modification to the system used commercially for a limited period of time and abandoned due to its extreme sensitivity to salinity and solution pH.[10] Tolerance for both pH and a broad range of salinity was obtained by sulfomethylating the resorcinol.[7] Gel time is controlled by the composition of the reactants (see Chapter 5). The injected solution has a low viscosity (0.72cp at 41°C) and is easily injected into porous rocks. The gel system has a nominal gel time of 23 hours. The focus of this work was to determine the effectiveness of this system in reducing the mobility of CO_2 under supercritical conditions. The SMRF system effectively shuts off the flow of brine in Berea sandstone and is equally effective in reducing the mobility of the CO_2 under supercritical conditions. The effective permeability was less than 1 md for a Berea core with an initial brine permeability of 700 md. Effectiveness of the permeability reduction did not deteriorate with the flow of supercritical CO_2 through the treated core.

Experimental

The experimental program consisted of gelling each polymer system in a one-foot long Berea core (two-inch diameter) which was mounted in a high-pressure core holder. A schematic of the experimental equipment used in this study is shown in Figure 6.1. The equipment consisted of an ISCO syringe pump used for injecting CO_2, brine, and gel solutions into the core, TEMCO high-pressure core holder equipped with pressure ports, pressure transducers and a computer-based data gathering system and a TEMCO back-pressure regulator connected to a cylinder of high pressure nitrogen. The effluent was collected by a fraction sample collector. The core assembly was placed in an air bath cubicle in which the temperature of the core and the injected fluids was kept constant.

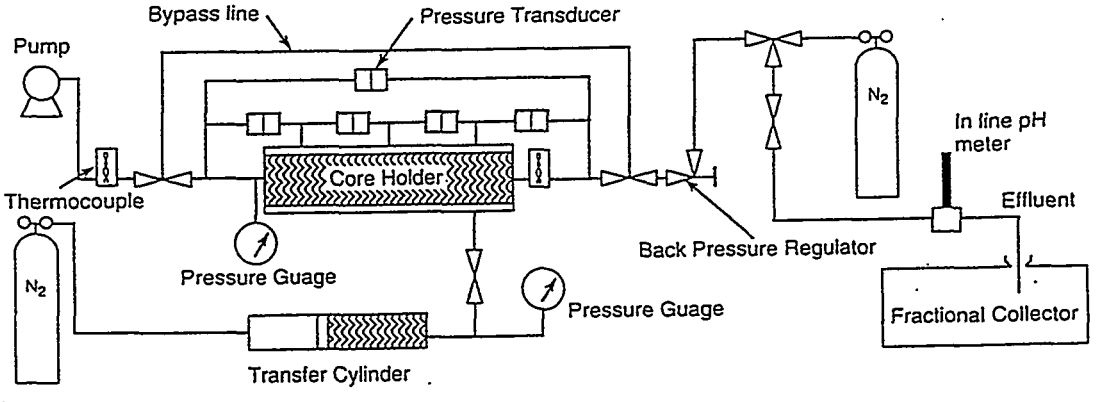

Figure 6.1 : Schematic presentation of experimental equipment

KUSP1- CO_2 System

This system is based on neutralization of the alkaline polymer solution by controlled injection of CO_2. Bubbling of CO_2 through the polymer solution in a test tube produces an opaque gel with bubbles of CO_2 trapped in the gel body. Initial experiments were conducted in sandpacks under atmospheric conditions to investigate the possibility of *in situ* gelation by CO_2 injection in porous media saturated with the KUSP1.[9] Later experiments were conducted under supercritical CO_2 conditions and in Berea cores.[9] The focus of the work was to determine the permeability reduction that could be achieved

under supercritical conditions.

Experimental Approach. The concentration of the KUSP1 polymer solution was 1 % by weight. The polymer was dissolved in 1 N NaOH solution with a 1 % by weight NaCl concentration. The polymer solution was filtered through a 5 micron nylon filter to remove impurities. The pressure and temperature of the core were maintained at 1300 psi and 90°F, respectively. The experiments were carried out under constant flow rate conditions. The complete solution preparation and experimental procedure along with a description of the experimental apparatus were reported earlier.[8,9]

Results and Discussion. Four Berea cores were used to investigate CO_2-induced gelation of KUSP1. Table 6.1 presents the overall initial permeabilities of the cores as well as the permeabilities for each individual section of each core. Permeabilities of the cores varied from 72 md to 384 md. Three CO_2 injection rates of 0.5, 0.1, and 0.005 ml/min were studied with one replication(Cores 1 and 2). Brine permeabilities after CO_2 injection are given in Table 6.2. Permeability reductions on the order of 78% to 93% were observed after CO_2 injection into the core saturated with KUSP1 in alkaline solution. The highest permeability reduction occurred for the lowest CO_2 injection rate.

The effective permeability for carbon dioxide in the presence of a trapped liquid saturation was determined in Berea Core #3 by displacing the initial alkaline solution with carbon dioxide. Effective permeabilities to CO_2 for the CO_2-NaOH system are presented in Table 6.3. Also presented in Table 6.3 are the effective permeabilities for the KUSP1-CO_2 system after the pressure stabilized. Inspection of Table 6.3 shows that *in situ* gelation of KUSP1 caused a reduction of 85% in the overall effective permeability to CO_2. A reduction of 85% in overall CO_2 effective permeability is comparable to the 88% reduction in overall brine permeability reported in Table 6.2 for Berea core No. 3.

Brine was injected to determine the brine permeability after the treatment and to investigate the gel stability under brine injection. A total of 12 pore volumes was injected into the core and the permeability was evaluated after every 2 pore volumes injected. Results for Berea core No. 1 are presented in Table 6.4. The gel was stable under the operating conditions studied in this experiment.

Conclusions. The injection of supercritical CO_2 into Berea cores saturated with an alkaline solution of KUSP1 causes in situ gelation and reduces the permeability to both brine and supercritical CO_2. The amount of permeability reduction was about 85 % of the original permeability. The reduction in effective permeability of CO_2 (86%) was close to that of brine (84%) and the permeability reduction was uniform and stable under prolonged brine injection throughout the length of the cores.

Table 6.1 : Properties of Berea sandstone cores.

Initial Brine Permeabilities (md)				
	Berea Core #			
	1	2	3	4
Overall	384	163	72	93
Section 1	331	154	68	72
Section 2	423	174	70	97
Section 3	384	163	73	106
Section 4	332	161	53	101
Porosity (%)	21.4	26.3	17.5	--

Table 6.2 : Brine permeabilities after CO_2-induced gelation.

	Brine Permeabilities (md)			
	Berea Core #			
	1	2	3	4
Overall	86	34	9	6
Section 1	88	30	7	4
Section 2	92	38	11	5
Section 3	78	41	11	10
Section 4	90	43	7	13
CO_2 Injection Rate (ml/min)	0.5	0.5	0.1	0.005
Permeability Reduction (%)	78	79	88	93

Table 6.3 : Comparison of CO_2 effective permeability for Berea Core 3.

	CO_2 Effective Permeability (md)		
	CO_2-NaOH system	CO_2-KUSP1 System	Reduction (%)
Overall	3.65	0.56	85
Section 1	4.83	1.20	75
Section 2	6.05	0.95	84
Section 3	4.84	0.32	93
Section 4	1.21	0.48	60

Table 6.4 : Gel stability study for Berea Core 1.

	Brine Permeability (md) after Injecting Indicated Pore Volumes				
	4 PV	6 PV	8 PV	10 PV	12 PV
Overall	90	90	93	85	86
Section 1	89	91	94	91	88
Section 2	89	92	93	93	92
Section 3	85	84	85	72	78
Section 4	103	103	103	98	90

KUSP1- Boric Acid System

KUSP1 is gelled by adding a small amount of orthoboric acid to an alkaline solution of KUSP1. The mechanism by which the orthoboric acid gels KUSP1 is unknown and it is different than by pH reduction. It is possible to achieve gelation times from several minutes to several days by adjusting the orthoboric acid concentration and the initial solution pH.

Experimental Approach. The preparation of the KUSP1 gelant samples is reported elsewhere[11]. During the development of the gelant procedure, it was noted that alkaline KUSP1 solutions turned yellow and then brown over a period of many days when stored at room temperature. The rate at which the solutions changed color increased at 40° C and decreased at 4° C when compared to the change in color at 25° C. Testing of the solutions revealed that the gel time was not affected by the color change for polymer solutions stored at 25° C up to 7 days. Longer storage periods resulted in the solutions developing a dark brown color and a diminished gelling ability.

It was discovered that storing 1.0% KUSP1 solutions with 0.2 M boric acid at a pH of approximately 13 resulted in no color change and no gelation for several weeks at 25°C. Samples prepared with a polymer solution stored under these conditions did not affect the gelation behavior. The shelf life of KUSP1 solutions can be extended by this technique. There was no core testing of this system during the period of this project.

Results and Discussion. The gelation behavior of the KUSP1-boric acid system was studied using bottle tests. Gel times for the KUSP1-boric acid system were determined to be a function of the boric acid concentration and the initial pH. The results of the experiment reveal that the gel time decreased with a decrease in boric acid concentration. Also, the gel time was reduced as the temperature was increased. The results from the bottle tests were used to select suitable compositions of the gel system for testing the performance of the system in porous media.[11] Syneresis of the gels increased with increase in temperature and decreased pH.

The physical characteristics of the gels as the pH dropped were different than those prepared by other means, i.e. ester hydrolysis or CO_2 contact. The gels prepared at a boric acid concentration of 0.5 mole/kg solution were transparent and rigid. Increasing the boric acid concentration reduced the pH at which KUSP1 formed a gel.

The storage modulus and dynamic viscosity were determined as functions of time for a gel system at three boric acid concentrations. The storage modulus and dynamic viscosity increased faster at lower boric acid concentrations supporting the results obtained from the bottle tests.

Conclusions. Gel times for the KUSP1-boric acid system can be controlled by selecting the boric acid concentration or the pH of the gel solution. At a given pH, a decrease in the boric acid concentration decreased the gel time. Additionally, the gel time decreased and syneresis increased with increased temperature.

The physical qualities of the boric acid gels are different than those produced using alkaline KUSP1 solution. Boric acid gels are stronger and more uniform than gels formed without boric acid.

KUSP1- Ester System

Hydrolysis of an ester can be used to reduce the pH of the alkaline polymer solution below its gelation point. This will, therefore, produce a delayed gel system. Several esters tested for this purpose are reported elsewhere.[5-7,12] By selecting proper ester, gelation time in the order of a few days can be achieved.

Experimental Approach. Experimental procedure for preparation of ester was presented in Chapter 2. Core experiments were performed under supercritical conditions of CO_2. Mono Ethyl Phthalate (MEP) was used as an ester in this part of study. The recipe was 2% by weight KUSP1 in 0.1 N NaOH with 0.06 mole MEP. This mixture provided a gelation time of 30 to 35 hours in test tube experiments. The core was first filled with KUSP1-ester solution and it was left in a controlled-temperature air bath to gel. The gelled core was then tested under several WAG (Water Alternating Gas) cycles.

Results and Discussion. Table 6.5 shows the permeability of the core at the end of each cycle. The initial permeability of the core used in this experiment was 145 md. It is clear from the table that the KUSP1-ester system is effective in reducing the permeability of the core to brine and as well as to CO_2. Its effectiveness in reducing the core permeability to water did not diminish by being exposed to supercritical CO_2.

Conclusions. The KUSP1-ester gelling system was found to be a viable gelation technique for CO_2 flood under supercritical conditions. The gel system was persistent to many pore volumes of brine and CO_2 injection.

Table 6.5 : Permeability of the core at the end of each cycle.

step	Injected Fluid	Pressure, psi	Temp., °C	Permeability, md
1	brine	atmospheric	25	1.1
2	brine	1200	25	2.8
3	CO_2	1200	25	3.6
4	brine	1200	25	2.0

SMRF System

SMRF gel system was described in Chapter 5 of this report. A permeability reduction larger than 9000 was achieved in core plugs using SMRF gelation system. Therefore, the SMRF system was tested to determine the effectiveness of SMRF gel to reduce CO_2 mobility under the supercritical condition. In this part of experimentation, the composition of the sulfomethylated resorcinol (SMR) was maintained at a mole ratio of F/S/R = 0.75/0.5/1; where, F is formaldehyde, S, is sodium sulfite, and R is resorcinol. SMRF gelling solution was prepared by adding brine (10% NaCl + 0.072% $CaCl_2$) and formaldehyde solution to the SMR solution. Solution pH was adjusted to approximately 7 by adding 20% acetic acid solution.

Experimental Approach. The core preparation procedure was identical to the KUSP1-ester experiment except the core was saturated with brine having the same composition as the gelling solution and the temperature was maintained at 41°C. Core pressure was either at atmospheric pressure or at 1200 psi.

Results and Discussion. Table 6.6 presents the initial permeability of the different sections of the core produced at two different flow rates and also permeabilities of the same sections after the SMRF gel treatment. Because of the extreme reduction in permeability the maximum flow rate of brine was limited to 0.007 ml/min to keep the pressure drop within the transducer range. The overall permeability was reduced by more than a factor of 14,000. Reduction of permeabilities in all sections is a factor of greater than or around 9000. The SMRF gelation system practically shuts off flow of water in the core.

The pressure of the core was then raised to 1200 by using high pressure nitrogen gas cylinder connected to the back pressure regulator. A leakage from the water sleeve into the core was detected. The pressure was removed and the core holder was disassembled. Leakage was corrected and the core was again pressurized to 1200 psi and the brine injection started. Brine was injected at two different rates of 0.1 ml/min and 0.2 ml/min. Permeability of the gelled core at 1200 psi and 41°C was determined to be 0.9 md. This is significantly higher than the earlier brine permeability of 0.05 md but still a permeability reduction of a factor of 800 is being maintained at this high pressure.

Injection of supercritical CO_2 at 0.2 ml/min, 1200 psi and 41°C into the core followed the brine. Pressure drop data were collected for all sections over nine pore volume of CO_2 injection. Effective permeability to CO_2 of each section was calculated from the pressure data. These are reported in Table 6.7. The pressure drop for section 1 at 0.2 ml/min was too low to produce meaningful permeability calculation. Therefore, it is not reported in Table 6.7.

The effective permeability of the treated core to the supercritical CO_2 is at the same order of magnitude as the permeability to brine at 1200 psi, i. e. 0.9 md as reported earlier. Therefore, a CO_2 permeability reduction in the order of greater than 9000 can be expected from SMRF treatment of the core.

Table 6.6 : Permeability modification for SMRF gel system.

Brine Permeability (md)			
Porosity - 0.23	Initial (2 ml/min)	Initial (5 ml/min)	After Gelation (0.007 ml/min)
Overall	705	695	0.049
Section 1	531	567	0.060
Section 2	776	744	0.085
Section 3	638	622	0.034
Section 4	716	707	0.042

Table 6.7 : CO_2 effective permeability of the treated core.

Core Section	CO_2 Effective Permeability (md)
Overall	0.557
Section 1	---
Section 2	0.642
Section 3	0.406
Section 4	0.309

Breakthrough of CO_2 was observed after 220 minutes of CO_2 injection at the rate of 0.2 ml/min. Produced brine during this period was 23.7 ml. This leaves 21.63 ml of CO_2 to be dissolved into the brine. Assuming a CO_2 solubility of 5.2% (at 1176 psi and 40°C)[13] and the core pore volume of 138 ml fully saturated by 4% SMRF, the dissolved CO_2 is calculated to be 6.89 g. This gives a dissolved volume of 22.37 ml for a CO_2 density of 0.308 g/ml[14] at 1200 psi and 41°C. This is in good agreement with the experimental data for dissolved CO_2.

The CO_2 injection rate was increased to 0.4 ml/min and an additional 12 pore volumes of CO_2 were injected. Total liquid production during this injection period was 0.42 ml which indicates that CO_2 is mainly flowing through the CO_2 channel. Doubling the CO_2 injection rate did not produce any additional channels. The CO_2 injection rate was reduced to 0.2 ml/min and an additional 3 pore volume of CO_2 was injected. The effective permeability of the treated core to CO_2 was determined at the end of each injection period which is reported in Table 6.8.

Table 6.8 : Gel stability under continuous supercritical CO_2 injection.

CO_2 Injection Rate (ml/min)	Permeability (md)	Pore Volume Injected
0.2	0.557	9
0.4	0.640	12
0.2	0.607	3

The SMRF gel system is quite stable and the effective CO_2 permeability does not increase with a prolonged CO_2 injection of 24 pore volumes. CO_2 injection was switched back to brine at an injection rate of 0.1 ml/min. The overall effective permeability to brine was 1.7 md which is 0.24% of its initial value of 705 md.

Conclusion. The SMRF gel system effectively shuts off the flow of brine and is equally effective in reducing the mobility of the CO_2 under atmospheric and under supercritical conditions. The permeability reduction due to the gel treatment of this system is significantly higher than the other systems studied. The gel is stable under prolonged injection of brine followed by supercritical CO_2.

References

1. Buller, C.S., "Water Insoluble Polysaccharide Polymer and Methods Thereof," U.S. Patent No. 4,908,310 (March 13, 1990).
2. Buller, C.S. and S. Vossoughi, "Subterranean Permeability Modification by Using Microbial Polysaccharide Polymers," U.S. Patent No. 4,941,533 (July 17, 1990).
3. Vossoughi, S., and C.S. Buller, "Permeability Modification by *In Situ* Gelation with a Newly Discovered Biopolymer," SPE Reservoir Engineering, (November 1991) 485-489.
4. Vossoughi, S., and A. Putz, "Reversible *In Situ* Gelation by the Change of pH within the Rock," SPE paper 20997 presented at the SPE International Symposium on Oilfield Chemistry held in Anaheim, CA, February 20-22, 1991.
5. Vossoughi, S., and A. Putz, "Application of a Newly Discovered Biopolymer in Enhanced Oil Recovery," SPE paper TT 93012 presented at the 11th Technical Conference and Exhibition of the Society of Petroleum Engineers (Trinidad and Tobago Section) held in Trinidad, West Indies, June 23-25,1993.
6. Green, D.W. and G.P. Willhite, "Improving Reservoir Conformance Using Gelled Polymer Systems - Annual Report - September 25, 1993 to September 24, 1994," U.S. Department of Energy report number DOE/BC/14881-12.
7. Green, D.W. and G.P. Willhite, "Improving Reservoir Conformance Using Gelled Polymer Systems - Annual Report - September 25, 1994 to September 24, 1995," U.S. Department of Energy report number DOE/BC/14881-18.
8. Raje, M., K. Asghari, S. Vossoughi, D.W. Green, and G.P. Willhite, "Gel Systems for Controlling CO_2 Mobility in Carbon Dioxide Miscible Flooding," SPE/DOE paper 35379 presented at the SPE/DOE 10th Symposium on Improved Oil Recovery held in Tulsa, OK, April 21-24, 1998.
9. Milind, R., "Study of *In Situ* Gelation Initiated by CO_2 Injection in Porous Media Saturated with KUSP1 Solution," M.Sc. Thesis, University of Kansas, Lawrence, KS, 1995.
10. Seright, R.S., and F.D. Martin, "Impact of Gelation pH, Rock Permeability, and Lithology on the performance of a Monomer-Based Gel," SPE paper 20999 presented at the International Symposium on Oilfield Chemistry, Anaheim, CA, February 20-22, 1991.
11. Green, D.W. and G.P. Willhite, "Improving Reservoir Conformance Using Gelled Polymer Systems - Annual Report - September 25, 1992 to September 24, 1993," U.S. Department of Energy report number DOE/BC/14881-5.
12. Fichadia, A., "Survey of Gelation Systems and a Study of the Gelation of KUSP1 by Hydrolysis of Monoethylphthalate," M.Sc. Thesis, University of Kansas, Lawrence, KS, 1995.
13. Perry's Chemical Engineers' Handbook, D. W. Green, editor, J. O. Maloney, assistant editor, 50th ed., R.R. Donnelley & Sons Co. (1984) 3-101.
14. Walas, S.M., "Phase Equilibria in Chemical Engineering," Butterworth Publishers (1985) 58.

Chapter 7

Simulation of Alkali-Sandstone Interactions During Flow Processes in Sandstone Media

Principal Investigators: G.P. Willhite, D.W. Green, C.S. McCool
Graduate Research Assistant: Vikas Midha

INTRODUCTION

Fluid-rock interactions play a key role in gelled polymer treatments. This modeling effort was directed at the KUSP1 gel system where alkaline solutions of KUSP1 are injected into the reservoir (see Chapter 2). The study considers the effects of fluid-rock interactions on the pH of alkaline solutions in sandstone cores. A one-dimensional flow model incorporating the kinetics of silica dissolution and sodium/hydrogen ion-exchange equilibria was developed. Detailed descriptions of the mathematical model and the results are available in References 1, 2 and 3.

A study of fluid-rock interactions was conducted with UTCHEM,[4-6] a powerful compositional simulator developed at the University of Texas at Austin for modeling displacement processes. It incorporates fluid-rock, fluid-fluid reaction chemistry with extensive physical and flow property models. A limitation in the UTCHEM model arises from the assumption of local equilibrium. This assumption forces the concentrations of all the chemical species in the fluid-phase to instantaneously attain equilibrium with the rock. Most fluid-fluid reactions and ion-exchange reactions are fast enough to justify this assumption. In the case of slow, kinetically-controlled reactions like silica dissolution, however, the assumption of local equilibrium is not warranted. Based on experimental evidence, it was concluded that the assumption of local equilibrium was not valid for cases involving short residence times like those used in laboratory displacement tests. A new model was developed that would be valid for all time frames in general. This model has important applications in scaling the effects of silica dissolution from laboratory experiments to field-scale conditions.

MATHEMATICAL MODEL

A mathematical model was derived that described the flow of alkaline solutions through porous media incorporating ion exchange and silica dissolution. Major assumptions in the model were:

1. A simple one dimensional, incompressible flow is assumed with no axial gradients.
2. The core is assumed to be homogenous with a constant porosity.
3. Change in the physical properties of the core (*i.e.* the porosity, bulk density *etc.*) due to chemical interactions have not been taken into account.
4. The core is isothermal.
5. Mass transfer limitations at the solid-fluid interface are negligible.
6. Silica dissolution was controlled by one rate-limiting reaction.
7. Ion exchange occurred for only sodium and hydrogen and was an equilibrium process.

The generalized equation of continuity for the i^{th} chemical species accounting for adsorption, convection, dispersion, and chemical reaction in the fluid phase was given by:

$$\frac{\partial C_i}{\partial \tau} + \sum_{i=1}^{i=N} \alpha_i \frac{\partial Ci}{\partial \tau} = -\frac{\partial Ci}{\partial \xi} + \frac{1}{Pe}\frac{\partial^2 C_i}{\partial \xi^2} + Da_i \; f_i(\mathrm{C}), \tag{7.1}$$

t and x are dimensionless time and distance defined by:

$$\tau = t\frac{v}{\phi L}, \tag{7.2}$$

and

$$\xi = \frac{x}{L}. \tag{7.3}$$

$f_i(\mathbf{C})$ denotes the dimensionless rate expression for the i^{th} chemical species.[1] The initial condition and boundary conditions were:

$$1)\ \tau = 0 \quad C_i = C_{initial} \quad for\ all\ \xi, \tag{7.4}$$

$$2)\ \xi = 0 \quad C_i = C_{inj} \quad for\ all\ \tau > 0, \tag{7.5}$$

$$3)\ \xi = 1 \quad \frac{\partial C_i}{\partial \xi} = 0 \quad for\ all\ \tau > 0. \tag{7.6}$$

Equation 7.1 is characterized by the following groups of parameters:
(1) The Peclet Number, Pe, which characterizes the physical dispersion in the core and is defined by:

$$Pe = \frac{Lv}{K_l \phi}. \tag{7.7}$$

(2) The Damkohloer Group, Da_i, given by:

$$Da_i = \frac{k_i a_s \rho_s (1-\phi)}{\phi}\frac{L\phi}{v}. \tag{7.8}$$

This group physically represents the ratio of the characteristic residence time to the characteristic reaction time for the silica-dissolution reaction. A high value of Da, therefore, signifies relatively more time is available for reaction with greater silica dissolution in the core.

The dimensionless retardation factors, a_{Na+} and a_{OH-} defined as:

$$\alpha_{Na^+} = \left(\frac{a_s \rho_s (1-\phi)}{\phi}\right) \frac{n_T K_I C_{OH^-}}{(1+K_I C_{Na^+} C_{OH^-})^2}, \tag{7.9}$$

$$\alpha_{OH^-} = \left(\frac{a_s \rho_s (1-\phi)}{\phi}\right) \frac{n_T K_I C_{Na^+}}{(1+K_I C_{Na^+} C_{OH^-})^2}. \tag{7.10}$$

These parameters characterize the chromatographic retardation of the Na^+ and OH^- species in the core due to sodium/hydrogen ion-exchange in the core.

The complete flow model consists of the set of continuity equations with the corresponding reaction expressions for the Na^+, OH^-, H_4SiO_4, $H_3SiO_4^-$ and $H_2SiO_4^{2-}$ species. The hydrogen-ion concentration is calculated by the following equilibrium relation :

$$C_{H^+} = \frac{K_w}{C_{OH^-}}. \tag{7.11}$$

The Cl^- concentration is found by an overall charge balance in the fluid phase :

$$C_{Cl^-} = C_{Na} + C_{H^+} - C_{OH^-} - C_{H_3SiO_4} - 2C_{H_2SiO_3^{2-}}. \tag{7.12}$$

The governing set of partial differential equations given by Equations 7.1 through 7.12 were solved numerically using finite-difference approximations.[1,2]

RESULTS AND DISCUSSION

The first step in simulating flow processes was to determine values of the parameters that are required. Rate constants for silica dissolution were obtained from kinetic studies conducted by several investigators.[7-12] A mathematical model was developed to simulate these static beaker tests in order to obtain rate constants for silica dissolution. The rate constants were then used in the flow model. Typical values of the ion-exchange parameters, n_T and K_I, were used.

Simulation of Silica dissolution in flow experiments. Neglecting all contributions of ion-exchange , the reaction term in the continuity equations is characterized by the Damkohler Group (Da). This group physically represents the ratio of the characteristic residence time to the characteristic reaction time of the system. A high value of Da signifies relatively more time is available for the reaction to occur which, in turn, implies greater dissolution of silica within the core. Rather than studying the effects of the rate of reaction, flow rate and core length individually, the Damkohler Group provides a single parameter for effectively analyzing the kinetic nature of the silica dissolution reaction in core-flood experiments.

A change in the physical conditions is also manifested in the value of the Damkohler group of the system. For example, typical field-scale applications correspond to core lengths of the order of 1000 ft and flow rates of 10 ft/day. In this case, the Damkohler Group is of the order of $100*Da_0$. Thus, by simply varying the value of Da in the model, it is possible to scale the effects of silica dissolution from laboratory-scale conditions to field-scale conditions.

A reference set of conditions (Da_0), corresponding to typical laboratory scales, has been adopted for simulation purposes. These conditions are summarized in Table 7.1. A silica core saturated with 1.7% NaCl brine solution was considered. A 0.5% NaOH brine solution is injected into the sand core and displaces the initial brine solution. The chemical compositions of the two solutions are shown in Table 7.2.

Core length :	1 ft
Porosity :	0.20
Superficial velocity :	1 ft/day
specific surface area :	2 m^2/g
solid density :	2.5 g/cm^3
Equilibrium quotient Q_1 :	1 E4 moles/liter
Equilibrium quotient Q_2 :	2 E4 $(moles/liter)^{-1}$
Equilibrium quotient Q_3 :	10 $(moles/liter)^{-1}$
Rate constant k_1 : exp(-14.55+0.361pH) ($moles/m^2.sec.$)	

Table 7.1: Summary of the reference physical parameters corresponding to typical laboratory scale conditions (Da_0).

INITIAL CONDITIONS (Concentrations in moles/liter PV)							
OH^-	3.23E-06	Na^+	0.2857	H_4SiO_4	0.1E-3	Cl^-	0.2857
H^+	3.12E-8	$H_3SiO_4^-$	5.24E-8	H_2SiO4^{2-}	4.07E-13		
INJECTION CONDITIONS (Concentrations in moles/liter PV)							
OH^-	0.079	Na^+	0.126	H_4SiO_4	0	Cl^-	0.05
H^+	0.13E-8	$H_3SiO_4^-$	0	H_2SiO4^{2-}	0		

Table 7.2: Summary of the initial concentrations and injected concentrations used in the simulations shown in Figures 7.1 and 7.2.

Figures 7.1 and 7.2 show the silica concentration profiles and the corresponding pH profiles after 0.25 PV injection as a function of the Damkohler Group. These profiles are also compared to the results from a simulation with the UTCHEM model using the same equilibrium parameters and physical conditions. The figures demonstrate the following features:

1) Under conditions of extremely short residence times (Da=0), the concentration of silica in the solution is negligibly small. The pH profile shows a very broad front similar to the pH profiles produced by the UTCHEM model and shows a transition from the injected value of the pH to the initial value.

2) At the given reference conditions ($Da=Da_0$), an appreciable amount of silica dissolution takes place and causes the formation of a peak in the silica concentration profile. The dissolution reaction causes an increase the silica concentration with time whereas the dispersive and the convective mechanisms tend to equalize the concentrations in the fluid phase. The peak, therefore, corresponds to the point at which these opposing mechanisms balance each other. In the absence of dispersion, this peak would lie exactly at the point x=0.25. The silica dissolution reaction is accompanied by a simultaneous decrease in the solution pH.

3) Although the maximum contact time at the given reference conditions is only 0.25 days, the silica concentrations observed here are much higher than the corresponding concentrations produced in the beaker tests. It may be concluded that the high S_L ratio of the porous core exposes a large surface area to the injected solution and causes a significant enhancement of the rate of reaction.

4) On increasing the Damkohler Group, more dissolution of the core takes place resulting in progressively higher silica concentrations in the injected solution and greater consumption of hydroxide. At a value of $Da=100*Da_0$, the results from the proposed model match the results predicted by the UTCHEM model. Under these conditions, the residence time of the system is long enough to ensure that the injected solution effectively attains equilibrium with the rock. The local equilibrium assumption in the UTCHEM model, therefore, is valid only for physical conditions corresponding to Da greater than $100*Da_0$.

Simulation of sodium/hydrogen ion-exchange in core floods. The effects of sodium/hydrogen ion exchange in simple core flood experiments in the absence of silica dissolution are examined. A coupled mechanism describing the sodium/hydrogen ion-exchange reaction on the surface of the rock was given in Eqn. 7.1. The flow model is based on the assumption of local equilibrium between the fluid-phase concentrations and the adsorbed-phase concentrations on the rock surface. Unlike the silica-dissolution reaction, ion-exchange reactions are typically fast enough to justify this assumption.

A sand core saturated with 1.7% NaCl is considered. A solution containing 0.1N NaOH is injected into the core and displaces the initial brine solution. Table 7.3 summarizes some of the system parameters used in the simulations.

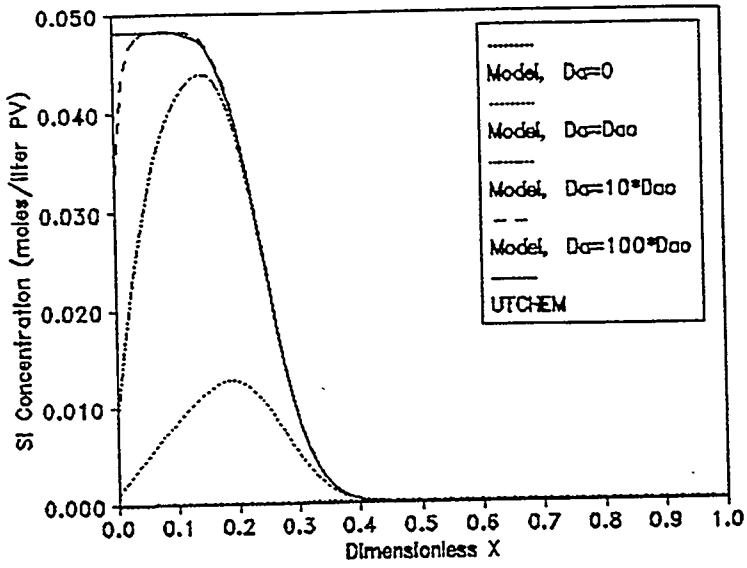

Figure 7.1 : Silica concentration profiles along the length of the core after 0.25 PV injection as a function of the Damkohler Group.

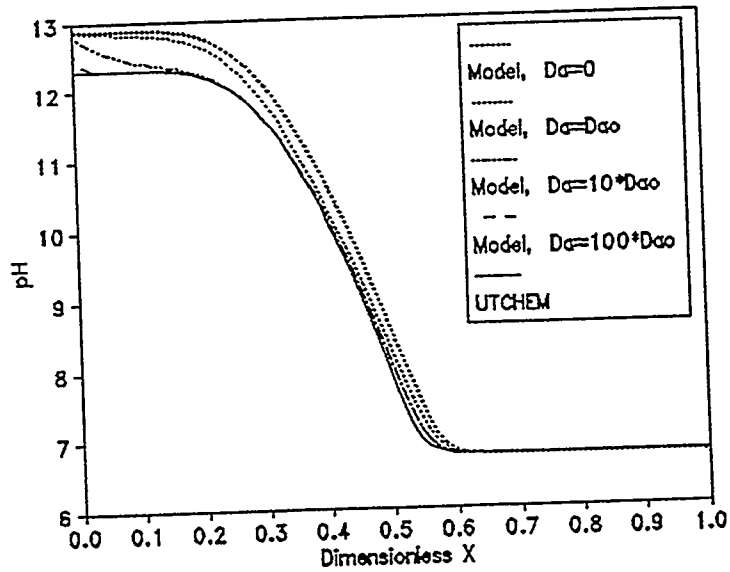

Figure 7.2: pH profiles along the length of the core after 0.25 PV injection as a function of the Damkohler Group.

CORE DATA	
Core length :	0.1 ft
Porosity :	0.20
Superficial velocity :	10 ft/day
specific surface area :	2 m^2/g
solid density :	2.5 g/cm^3
INITIAL CONDITIONS (Concentrations in moles/liter PV)	
OH^- 3.23E-06 Na^+ 0.2857 Cl^- 0.2857 H^+ 3.12E-8	
INJECTION CONDITIONS (Concentrations in moles/liter PV)	
OH^- 0.1 Na^+ 0.126 Cl^- 0.026 H^+ 0.1E-12	

Table 7.3: Summary of the initial concentrations and injected concentrations used in the simulations shown in Figures 7.3 and 7.4.

Figure 7.3 shows the concentration profiles of the Na^+ species as the injected solution advances along the length of the core for typical values of the equilibrium parameters K_I and n_T. Figure 7.4 shows the corresponding pH profiles. As expected, the ion-exchange reaction has a considerably different effect on the concentration profiles as compared to the silica dissolution reaction. The concentration profiles show the formation of two distinct fronts which move through the porous medium. For example, the profiles at 0.75 PV injection show the following features:

1) The first front is centered at x=0.75 and travels at the interstitial velocity with no retardation. This front simply entails the displacement of the initial solution and corresponds to concentration variations in the fluid phase only. These fronts are termed as *salinity waves*. The region after the salinity wave, therefore, comprises of the initial fluid-phase concentrations and solid-phase conditions.

2) The second front is centered at x=0.42 and involves a change in both the solid-phase composition and the fluid-phase concentrations. This wave front is termed the *ion-exchange wave*. Since the velocity of this wave front is slower than the interstitial velocity, the injected pH levels appear in the effluent after a delay. The region before the ion exchange wave corresponds to fluid-phase concentrations at the injected level and solid phase concentrations in equilibrium with the injected concentrations.

3) The intermediate region between the salinity wave and the ion-exchange wave has a modified fluid-phase composition in equilibrium with the initial solid-phase composition. Since the velocities of the two waves are different, the intermediate region expands as the waves progress along the core. The breakthrough of this intermediate region will result in a plateau in the effluent concentration profiles.

4) The velocities of the salinity waves and the ion-exchange waves appear to be the same for both the Na^+ species and the OH^- species. This property has also been commonly observed for other ion exchange reactions such as Na^+/Ca^{2+} ion exchange. The condition in which the concentration velocities of all the species at any given point in time and space are equal is called *coherence*.

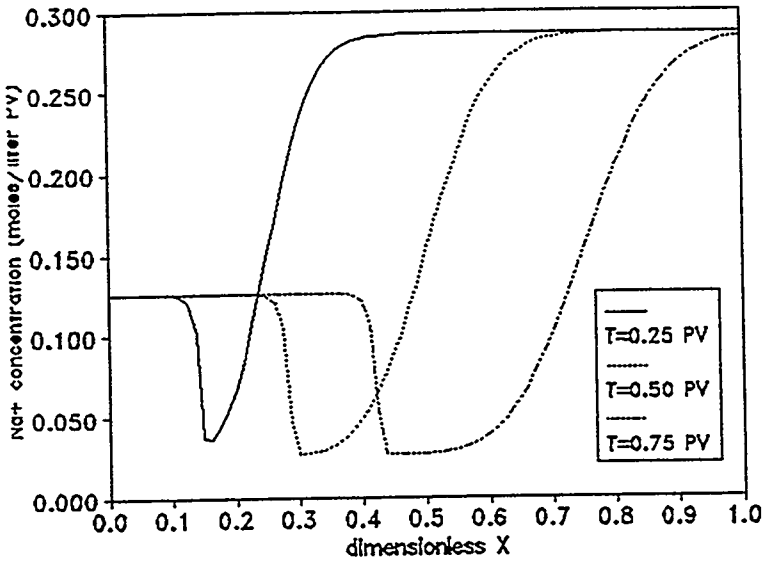

Figure 7.3: Na^+ concentration profiles along the length of the core as a function of pore volumes of injection (K_I=1E5 (moles/liter)$^{-2}$, n_T=0.85 meq/100g).

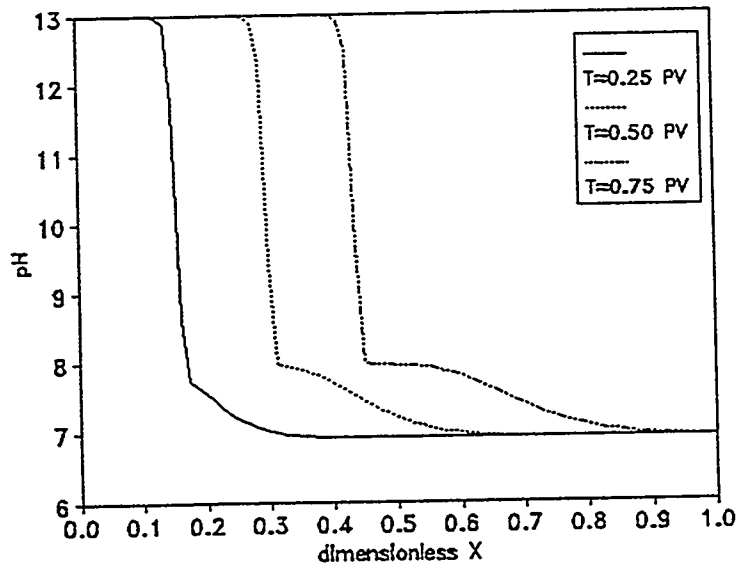

Figure 7.4: pH profiles along the length of the core as a function of pore volumes of injection (K_I=1E5 (moles/liter)$^{-2}$, n_T=0.85 meq/100g).

5) The salinity waves show a broad front governed solely by the dispersive mixing of the injected solution and the initial solution. The ion-exchange waves, however, show much sharper fronts in comparison to the salinity waves. These sharp changes in concentration are termed as *shock fronts*.

6) It is important to note that the overall shape of the shock fronts appears to be constant as the wave propagates through the core. Based exclusively on the Langmuir-like equilibrium describing the ion-exchange reactions, the ion-exchange wave is expected to continuously sharpen as it propagates through the core. These wave fronts are commonly observed in nature and are termed as *self-sharpening waves*. Lake and Helffrich have shown that physical dispersion has an important role in defining the shape of self-sharpening waves[19]. Dispersion, by nature, tends to smother all the sharp concentration gradients and therefore opposes the sharpening character of the wave fronts. These competing phenomena tend to balance each other and the resultant waves are indifferent with respect to sharpening behavior and maintain a constant shape as they progress through the core.

Simulation of actual core flood experiments. It was necessary to estimate many of the parameters required in the model for simulating experiments reported in the literature. A lumped correction factor for the Damkohler Group was used to account for the total correction in the overall rate of silica dissolution due to temperature effects and specific areas. The lumped correction factor, the ion-exchange parameters and the dispersion were estimated by matching the results from the model with experimental data.

The first experiment considered for simulation purposes consisted of a caustic flood of a Berea sandstone core at 50°C conducted by Radke and Jenson[13] to study the sodium/hydrogen ion-exchange reaction. A high flow rate was used to reduce the effects of silica dissolution on the pH profile.

Figure 7.5 shows the histories of the reduced concentrations of the Na^+ and the OH^- species (concentrations are normalized by injected values) predicted by the model compared to the experimental results. The model predicts the formation of a coherent ion-exchange wave which appears in the effluent after a delay of 2.4 PV. At the high pH values of the ion-exchange wave, hydroxide ions are consumed by the silica dissolution reaction. This consumption is small due to the short residence time of the experiment. The model also predicts the formation of the intermediate plateau in the concentration history of the Na^+ species. This plateau corresponds to breakthrough of the intermediate region between the ion-exchange wave and the salinity wave in the effluent. There appears to be some discrepancy between the predicted value of Na^+ concentration and the experimental value. The reason for this discrepancy is not completely understood.

In addition, there is a significant amount of dispersion in the experimentally determined concentration histories which are not shown by the simulated profiles. A part of this disparity is probably due to some inaccuracies in the estimation of parameters in the simulation. Radke and Jenson also propose that extraneous dispersion may be caused by internal-diffusion resistances which reduce the accessibility of the mineral exchange sites for sodium and hydrogen species. These mass-transfer limitations were not considered in the proposed model.

It is instructive to examine the parameters used in the simulations. A correction factor of 5 was applied to the reference Damkohler Group to account for the increased rate of silica dissolution at the elevated temperature. It was found that an ion-exchange capacity, n_T, of 0.125 meq/100g solid and an equilibrium constant, K_I, of 10^4 N^{-2} were required to match the experimental data. These values are well within the expected range of values for these parameters.

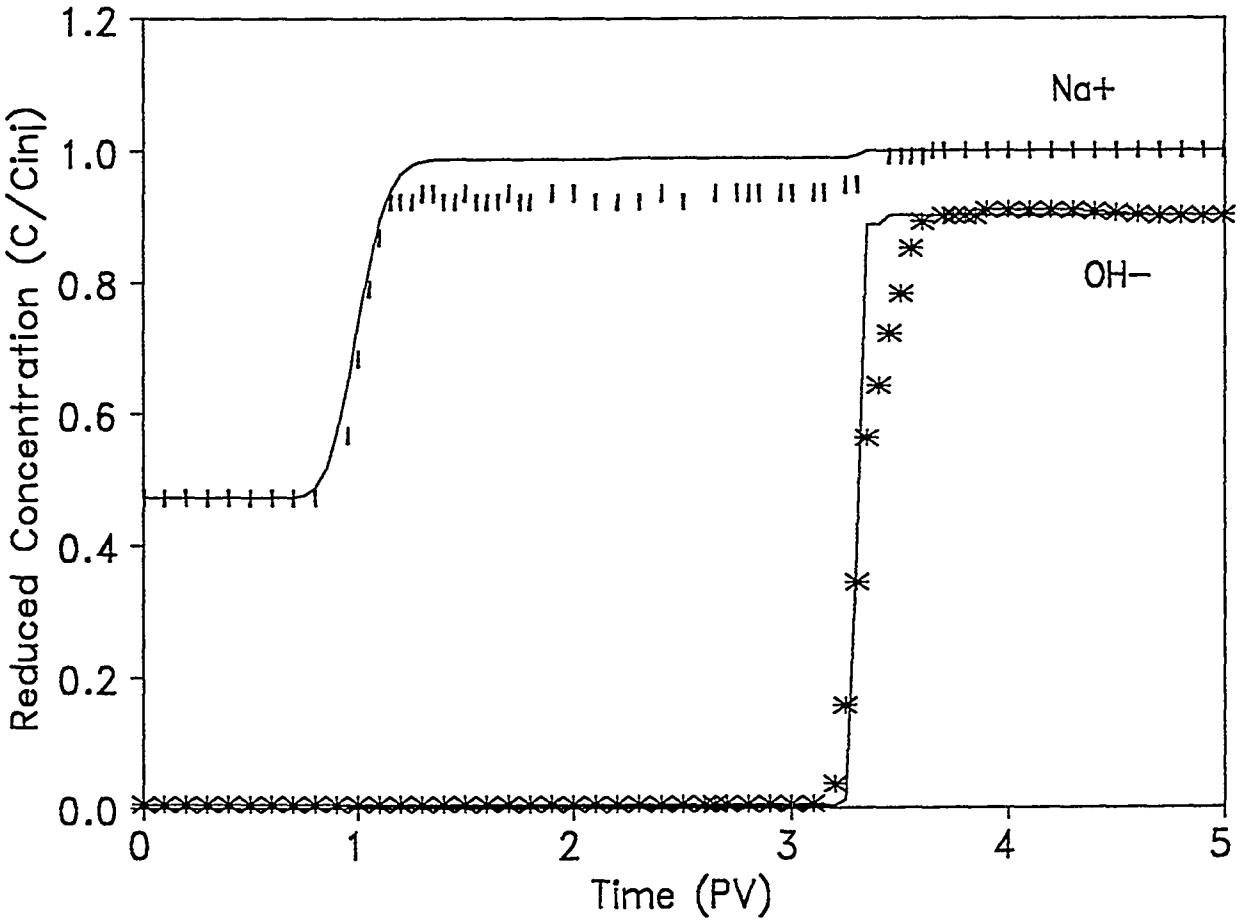

Figure 7.5 : Simulated histories of the reduced concentrations of sodium and hydroxide compared to experimental data by Radke and Jenson[13] (correction factor= 5, K_I=1E4 (moles/liter)$^{-2}$, n_T= 0.125 meq/(100g solid)).

The second case consisted of the simulation of an alkaline flood of a Berea core conducted by Novosad and Novosad[14] to study the effect of flow rate on the hydroxide- and sodium-ion concentration histories. It was necessary to estimate the ion-exchange parameters K_I, n_T and the correction factor for the Damkohler Group.

Figure 7.6 shows the experimental data compared to the profiles predicted by the model. The calculated sodium-ion history shows a good match with the experimental data. Due to the large amount of dispersion, mixing between the salinity wave and the ion-exchange wave takes place and a distinct intermediate region is not formed. Based on the theoretical considerations, the ion-exchange wave for the hydroxide species is expected to be coherent with the sodium ion-exchange wave. Thus, the model predicts a steady concentration of hydroxide in the effluent after a delay of 2 PV. The experimental values for the hydroxide-ion history, however, show considerable scatter even after the sodium-ion profile attains a constant value. Silica dissolution within the core is significant and the model predicts a steady concentration of hydroxide which is significantly less than the injected value. On halving the flow rate after 4.5 PV, the contact time for the injected solution is doubled and there is a greater consumption of hydroxide ions by the dissolution reaction. The experimental results also show a drop in the hydroxide concentration, but the decrease is greater than what is predicted by the model. As the hydroxide-ion concentration in the fluid phase decreases, the concentration of the adsorbed sodium ions (in equilibrium with the fluid-phase concentrations) also decreases. Hence, there is a slight increase in the fluid-phase concentration of the Na^+ ions when the flow rate is reduced. This increase, however, is too small to be measured in the experiment.

The final example considers the effect of flow rate on the silica dissolution reaction in greater detail. Bunge and Radke[15] reported results from alkaline floods in a Huntington Beach sand core at four different flow rates by Lieu.[16] A single set of parameters must be used to characterize all the profiles. A value of KI equal to 10^2 N^{-2} was selected in order to be consistent with the high temperature of the experiment. The cation-exchange capacity used in the simulations was 1.25 meq/(100g solid) which is relatively high but acceptable. It was also necessary to decrease the rate of the silica dissolution reaction by using a correction factor of 0.14 to fit the data.This is surprising considering the elevated temperature of the experiment, but is acceptable given the uncertainty regarding the physical characteristics of the rock.

Figure 7.7 shows that there is good agreement between the hydroxide ion history predicted by the model and the experimental data. As the flow rate is reduced, the residence time of the injected solution is increased. This results in progressively more consumption of hydroxide ions by the silica-dissolution reaction. The ion-exchange reaction results in a delay of about 2.5 PV before the breakthrough of the injected hydroxide concentrations. This delay is independent of the flow rate and suggests the validity of the assumption of local equilibrium for the sodium/hydrogen ion-exchange reaction. There are, however, some minor discrepancies between the predicted profiles and experimental data at low hydroxide concentrations. A better fit would require some adjustment of the parameters for dispersion and the ion-exchange reaction but it was not attempted due to the lack of sufficient data in this region.

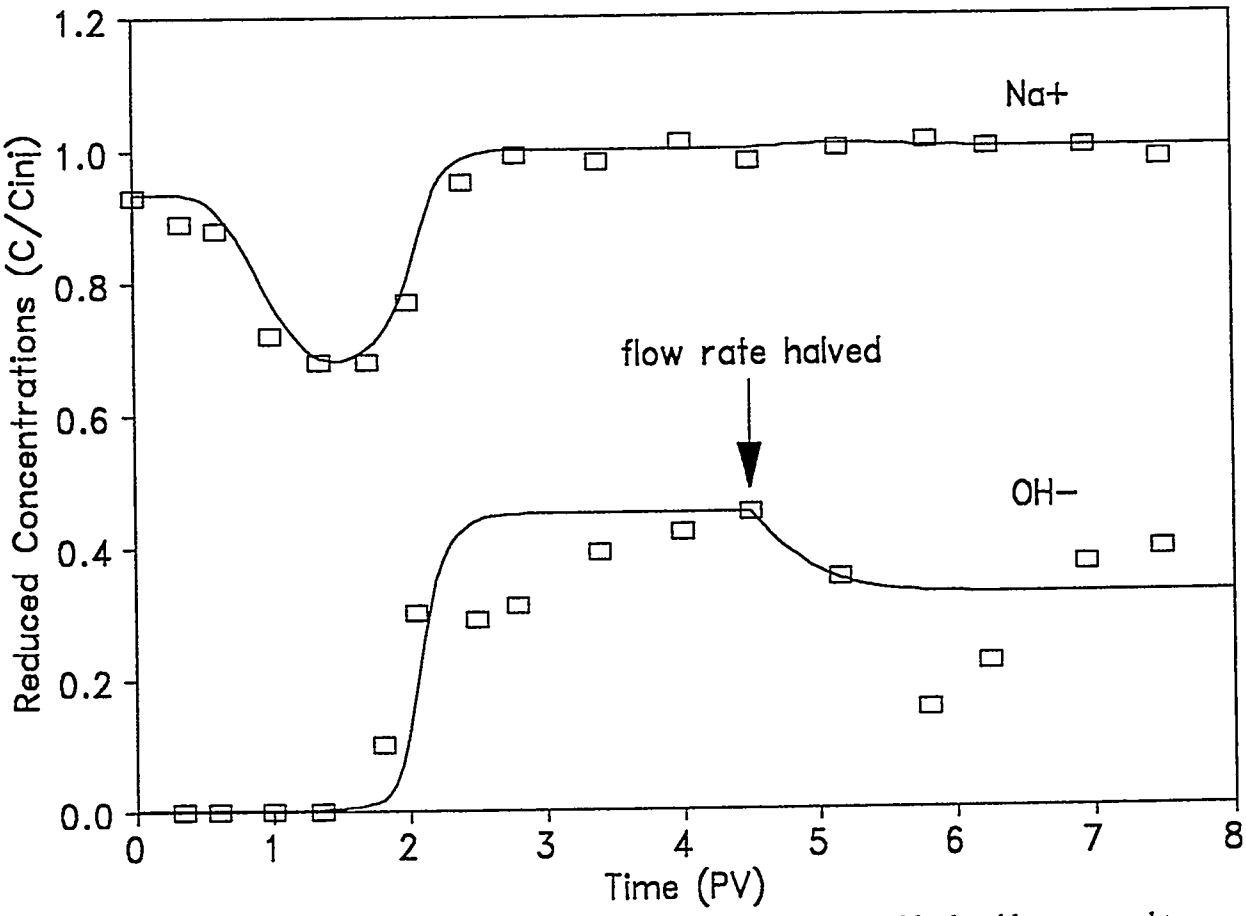

Figure 7.6 : Simulated histories of the reduced concentrations of sodium and hydroxide compared to experimental data from Novassad and Novassad[14] (correction factor=6, K_I= 1E4 (moles/liter)$^{-2}$, n_T=0.4 meq/100g solid).

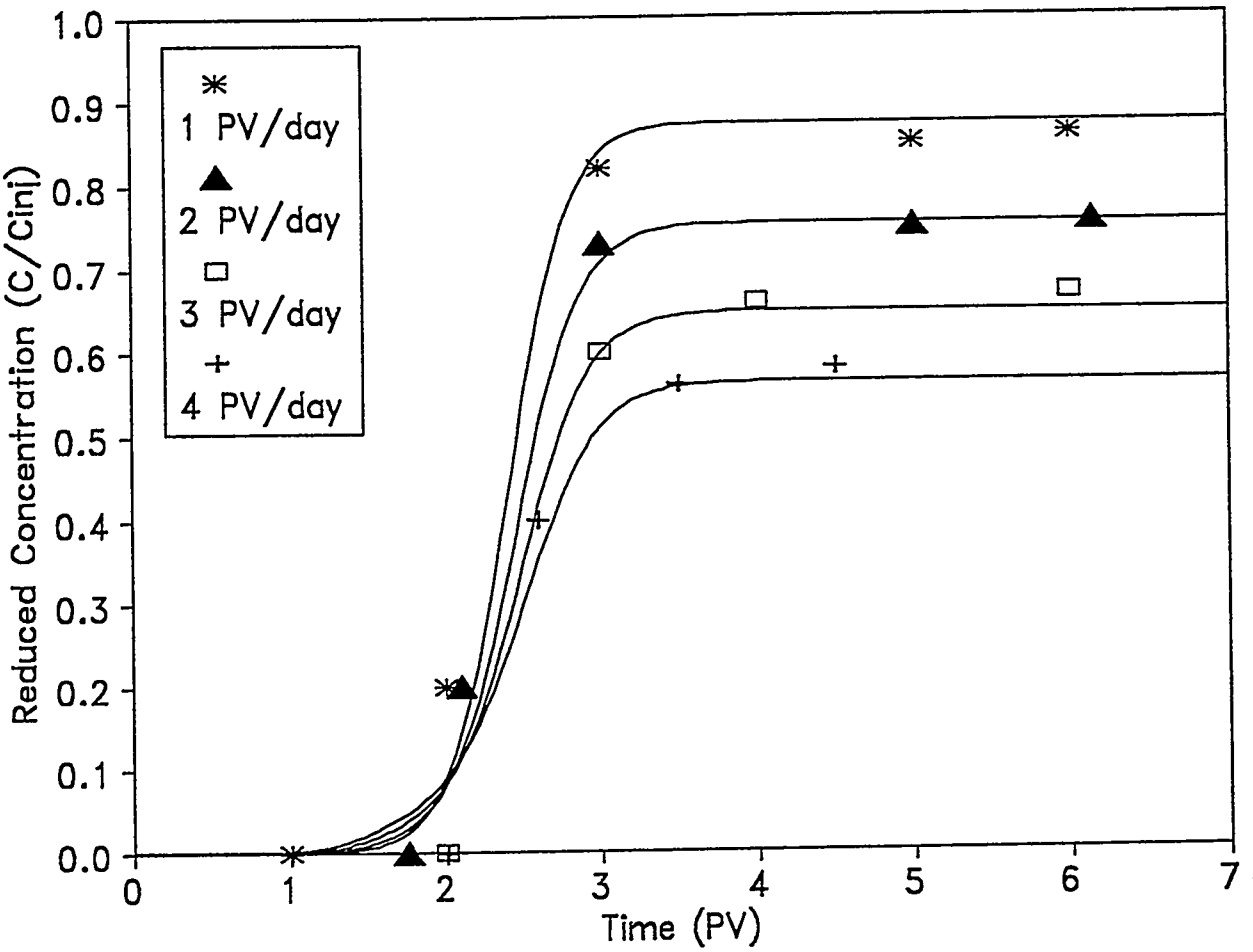

Figure 7.7 : Simulated histories of the reduced hydroxide concentrations compared to experimental data reported by Bunge and Radke[15] (correction factor = 0.14, K_I= 1E2 (moles/liter)$^{-2}$, n_T=1.25 meq/100g solid).

CONCLUSIONS

A kinetic model describing the silica dissolution reaction was developed which is generally valid for all time frames. Based on sodium/hydrogen equilibria and silica dissolution kinetics, a new mathematical model was developed for describing core flood experiments. This model describes the effects of flow rate and core length in terms of the Damkohler Group. By varying the value of the Damkohler Group it is possible to scale the effects of silica dissolution from laboratory-scale conditions to field-scale conditions. In addition, a mathematical criterion was developed for checking the validity of the local equilibrium assumption.

The proposed model was also used to study the sodium/hydrogen ion-exchange in simulated simple core floods. The model predicts a delay in the breakthrough of the injected pH levels and the formation of an intermediate plateau in the concentration profiles.

The simulation of three independent core-flood experiments shows that the proposed model describes all the essential features seen in experimental results. In each case, the estimated values of the reaction parameters correspond to typical values suggested in the literature. Furthermore, a single set of parameters was used to simultaneously describe all the concentration profiles in an experiment. These results, therefore, establish the validity of the assumptions in the model and the underlying mechanisms for silica dissolution and sodium/hydrogen ion exchange.

NOMENCLATURE

a_s specific surface area of the solid particles (m^2/g).
C vector representing the concentrations of all the transported species (moles/liter PV).
C_i concentration of i^{th} species in the fluid phase (moles/liter PV).
C_{inj} injected value of concentration (moles/liter PV).
Da Damkohler Group (moles/liter).
$f_i(C)$ reaction rate expression in terms of the species concentrations (dimensionless).
k_1 surface reaction rate constant ($moles/m^2.hr$).
K_1 dispersion coefficient (m^2/hr).
K_I equilibrium constant for sodium/hydrogen ion-exchange reaction $(moles/liter)^2$.
K_w equilibrium quotient for water $(moles/liter)^2$.
L length of the core (m).
n_{Na+} concentration of the adsorbed form of the Na^+ species on the rock (meq/m^2 solid).
n_{OH-} concentration of the adsorbed form of the OH^- species on the rock (meq/m^2 solid).
n_T total cation exchange capacity of the rock (meq/m^2 solid).
Pe Peclet Number (dimensionless).
$R_i(C)$ rate of generation of the i^{th} species per unit volume (moles/liter.hr).
t time (hr).
v superficial velocity of injected brine (m/hr).
x distance (m)

Greek symbols

α_{Na+} retardation factor for the Na^+ species (dimensionless).
α_{OH-} retardation factor for the OH^- species (dimensionless).
ξ dimensionless distance in x direction.
ρ_s bulk density of the rock (g solid/liter solid).
τ dimensionless time.
ϕ porosity of the core (dimensionless).

REFERENCES

1. Midha, V., "Mathematical Modeling of Fluid-Rock Interactions During the Flow of Alkaline Solutions Through Porous Media," M.S. Thesis, University of Kansas, 1994.
2. Green, D.W. and Willhite, G.P., "Improving Reservoir Conformance Using Gelled Polymer Systems," Annual Report, DOE Contract No. DE-AC22-92BC14881, Report No.DOE/BC/14881-5 (August 1994).
3. Green, D.W. and Willhite, G.P., "Improving Reservoir Conformance Using Gelled Polymer Systems," Annual Report, DOE Contract No. DE-AC22-92BC14881, Report No.DOE/BC/14881-12 (July 1995).
4. Bhuyan, D., "Development of an Alkaline-Surfactant-Polymer Compositional Reservoir Simulator," Ph.D. Dissertation, The University of Texas at Austin (Dec. 1988).
5. Bhuyan, D., Lake, L.W. and Pope, G.A., "Mathematical Modeling of High pH Chemical Flooding," *SPERE* (May 1990) 212-220.
6. Bryant, S.L., Schechter, R.S. and Lake, L.W., "Interactions of Precipitation/Dissolution Waves and Ion-exchange in Flow through Permeable Media," *AIChE J* (May 1986) vol. 32, no. 5, 751-764.
7. Thornton, S.D. and Radke, C.J., "Dissolution and Condensation Kinetics of Silica in Alkaline Solutions," *SPERE* (May 1988) 743-752.
8. Busey, R.H. and Mesmer, R.E., "Ionization Equilibria of Silicic Acid and Polysilicate Formation in Aqueous Sodium Chloride Solutions to 300°C," *Inorg. Chem.*, vol. 16, no. 10 (1977) 2444-50.
9. Ingri, N., "Equilibrium Studies of Polyanions, IV. Silicate Ions in NaCl Medium," *Acta Chem. Scand.*, vol. 13, no. 4 (1959) 758-75.
10. Lagerstrom, G., "Equilibrium Studies on Polyanions, III. Silicate Ions in $NaClO_4$ Medium," *Acta. Chem. Scand.*, vol. 21, no. 9 (1959) 722-36.
11. Fleming, B.A. and Crerar D.A., "Silicic Acid Ionisation and Calculation of Silica Solubility at Elevated Temperature and pH," *Geothermics*, vol. 11, no. 1 (1982) 15-29.
12. House, W.A. and Orr, D.R., "Investigation of the pH Dependance of the Kinetics of Quartz Dissolution at 25°C," *J. Chem. Soc. Faraday Trans.* (1992) vol. 88, no. 2, 233-241.
13. Radke,C.J. and Jenson J.A.,"Chromatographic Transport of Alkaline Buffers Through Reservoir Rock," *SPERE*, (Aug. 1988) 849-856.
14. Novosad, Z. and Novosad, J.,"The Effect of Hydrogen Ion Exchange on Alkalinity Loss in Alkaline Flooding," *SPEJ*, (Feb. 1984) 49-52.
15. Bunge, A.L. and Radke, C.J., "Migration of Alkaline Pulses in Reservoir Sands," *SPEJ*, (Dec. 1982) 998-1012
16. Lieu, V.T.,"Long-Term Alkaline Consumption in Reservoir Sands," Second Progress Report for the City of Long Beach, THUMS Long Beach Co., DOE Contract No. DE-AC-03-76Et-12407 (June 1980).

Chapter 8

Modeling the Effect of Filtration of Pre-Gel Aggregates on Gel Placement in Layered Reservoirs with Crossflow

Principal Investigators: Don W. Green, G. Paul Willhite, C. S. McCool
Graduate Research Assistant: Vikas Midha

INTRODUCTION

Flow experiments with the polyacrylamide/chromium system show a build-up of resistance in a localized region some distance behind the front of the gelant.[1,2] Several pore volumes of gelant flow through this region till complete plugging of the sandpack occurs. The age of solution flowing through the zone of flow resistance is significantly lower than the "gel time" of the solution in a beaker. These trends suggest that the build-up of flow resistance during in-situ gelation does not result from a simple bulk gelation at the displacement front. On increasing the flowrate, the gelant penetrates further into sandpacks, but also plugs the sandpacks at a faster rate.

Previous models simulate in-situ gelation of polyacrylamide/chromium system in porous media by relating a lumped "resistance factor" to the kinetics of the redox reaction.[3,4,5,6] These models do not predict the characteristic features of the experimental results with the polyacrylamide system. More importantly, these models do not show the effect of flow rate on the rate of build-up of flow resistance. This dependance is essential for an accurate scale-up of laboratory experiments to field-scale conditions.

Todd et al. proposed a model based on the hypothesis that build-up of resistance for the polyacrylamide/chromium system is due to the filtration of pre-gel polymer aggregates by the porous medium.[7] The crosslinking ions released by the redox reaction are attached to the polymer molecules and lead to the formation of aggregates of crosslinked polymer molecules. The attached chromium ions enhance the filtration properties of the aggregates by their ability to form crosslinks with polymer deposited on the walls of the pores. The zone of flow resistance is characterized by a rapid reduction in porosity and permeability of the porous medium well before a gel structure is formed.

Since the redox reaction is a slow, kinetically-controlled process, at high flow rates it is possible to inject the gelling solution deep into the sandpack before significant amounts of crosslinking ions are released. Once chromium-ions are attached to the polymer molecules, the rate of filtration is a function of the interstitial velocity of the aggregates through the pores. Higher interstitial velocities lead to faster rates of filtration and plugging. The model of Todd et al.[7] successfully matched experimental results over a range of flow rates suggesting the validity of the underlying filtration mechanism.

This work extends the filtration hypothesis for the polyacrylamide/chromium system to simulate permeability-modification treatments in layered reservoirs with crossflow. A description of the radial flow-geometry around the wellbore is necessary not only for an accurate prediction of the radius of penetration of the gelant, but also in determining the magnitude of the build-up of flow resistance. In addition, most reservoirs are characterized by some degree of crossflow between the high-permeability and low-permeability regions. The effects of filtration of polymer aggregates on crossflow behavior are yet to be investigated.

In this work, a two-dimensional numerical model for simulating in-situ gelation of the polyacrylamide/chromium system is developed. The model is used to study the effects of the injection pressure, which constitutes an important operating parameter, and reservoir characteristics such as the permeability contrast between the layers, the vertical permeability and height of the reservoir. Once the favorable reservoir characteristics are identified, the effects of gelant viscosity and zonal isolation for improving the performance of a permeability-modification treatment are examined.

The emphasis in the main body of the paper is on this analysis. The detailed model description is in the Appendix. The model basically consists of differential equations describing Darcy flow, mass transfer of the different chemical species, chromium and gelation reaction kinetics and filtration of gel aggregates. The equations are solved numerically using a procedure described in the Appendix.

PHYSICAL DESCRIPTION

Gel placement in an idealized, two-layered reservoir, as shown in Figure 8.1, is examined. Each layer is assumed to be homogenous in nature. Table 8.1 summarizes a base set of parameters for all the simulations. These conditions represent typical field-scale conditions for a near-wellbore, permeability-modification treatment. The concentrations and reaction parameters for the chromium/polyacrylamide gelling system correspond to those used to simulate experimental results of Marty et al., in linear sandpacks.[1] The pore structure characteristics for the two layers are scaled according to the Cozeny-Karman model.[8] Variations from the set of conditions in Table 8.1 are indicated in the description of the individual runs.

In the simulations, each layer is assumed to be at a uniform relative pressure of zero prior to gel-solution injection. Gel-solution injection occurs at a constant wellbore pressure (500 psi in base case) and for some specified time period. Crossflow between layers in the reservoir is allowed. Parameters calculated in the model are pressure, flowrate, concentrations, and localized flow resistance.

RESULTS AND DISCUSSION

A key mechanism governing gel-placement behavior in reservoirs is the build-up of the resistance to flow during in-situ gelation. The build-up of resistance may be due to two mechanisms; an increase in gelant viscosity by the formation of crosslinks between the polymer molecules, and the filtration of polymer aggregates which reduces the permeability of the porous medium. In this study, the evolution of the "apparent viscosity" in the reservoir is used to characterize both effects during gelation processes. Apparent viscosity is defined as

$$\textit{apparent viscosity} = \mu\left(\frac{k^0}{k}\right) \quad \ldots\ldots\ldots\ldots\ldots\ldots \quad (1)$$

where μ is the viscosity of the gelant, k_0 is the initial permeability and k is local value of the permeability during the treatment. In the model, both the radial and vertical permeabilities are effected equally by the filtration mechanism and either value may be used in Equation A-1.

Base Case. The base case represents a direct scale-up of the laboratory experiments by Marty [1] to field-scale conditions shown in Table 8.1. The gel-placement behavior in this set of results is representative of a typical permeability-modification treatment in heterogenous reservoirs with crossflow.

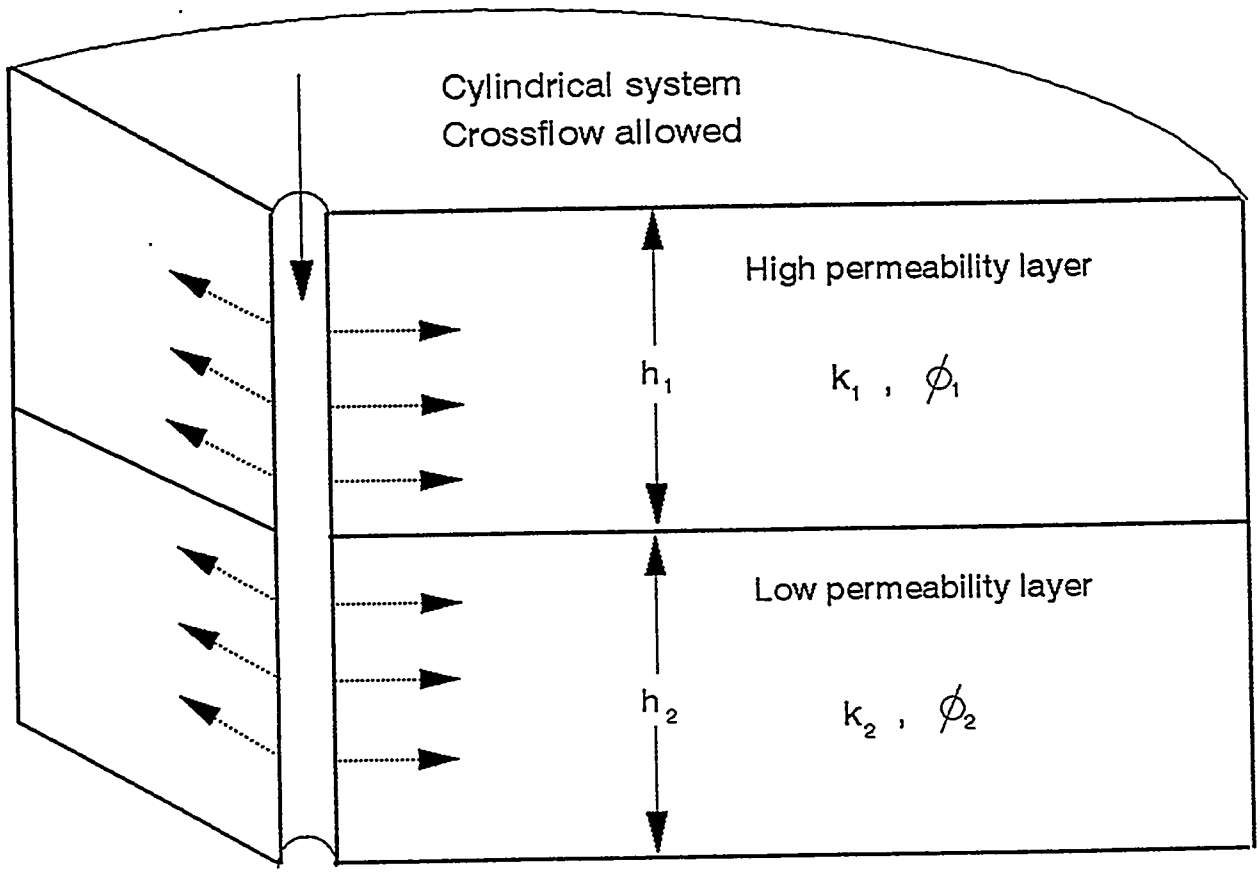

Figure 8.1: Physical system examined in simulations.

Table 8.1: Base set of parameters for the simulations.

I Reservoir Description	
wellbore pressure	500 psi
wellbore radius	0.66 ft
exterior radius	500 ft
reservoir height	32 ft
initial viscosity	1 cp
injected viscosity	10 cp
compressibility	$5*10^{-6}$ psi^{-1}
II Porous Media Characteristics	
layer 1	
height	0 - 16 ft
radial permeability	100 mD
vertical permeability	100 mD
porosity	0.24
average grain diameter	91 microns
average pore length	86 microns
median pore throat diameter	11 microns
layer 2	
height	16 - 32 ft
radial permeability	10 mD
vertical permeability	10 mD
porosity	0.16
average grain diameter	51 microns
average pore length	48 microns
median pore throat diameter	6 microns
III Reactant Concentrations	
injected polyacrylamide concentration	5000 ppm
injected dichromate concentration	400 ppm
injected thiourea concentration	1500 ppm

Figure 8.2 shows the profile of the total rate of injection of gelant as a function of time. Figure 8.3 shows the corresponding profile of the fraction of the total gelant injected into the high-permeability layer. These profiles are compared to the case where the flow behavior of the gelant is governed solely by viscous flow of the polymer solution without filtration. Comparison of the two profiles is used to differentiate the effects of viscous crossflow from the effects of filtration during the treatment. Additionally, the profiles with only viscous flow represent the behavior of the gel system under two possible conditions - when filtration is not an important characteristic of the gelling system, or, fluid-rock interactions in the reservoir inhibit the effects of filtration to insignificant levels.

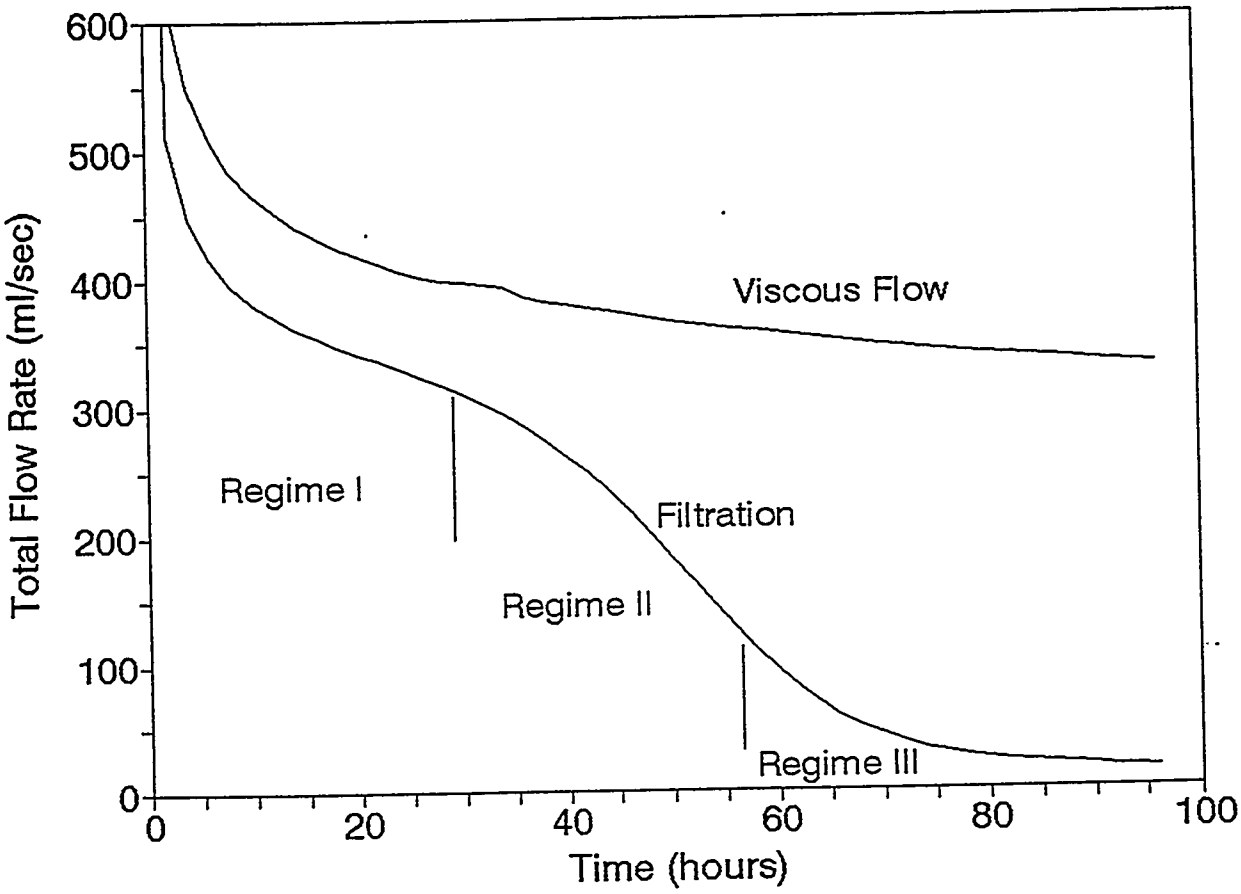

Figure 8.2: Rate of injection in the presence of filtration compared to the rate of injection with only viscous flow of gelant.

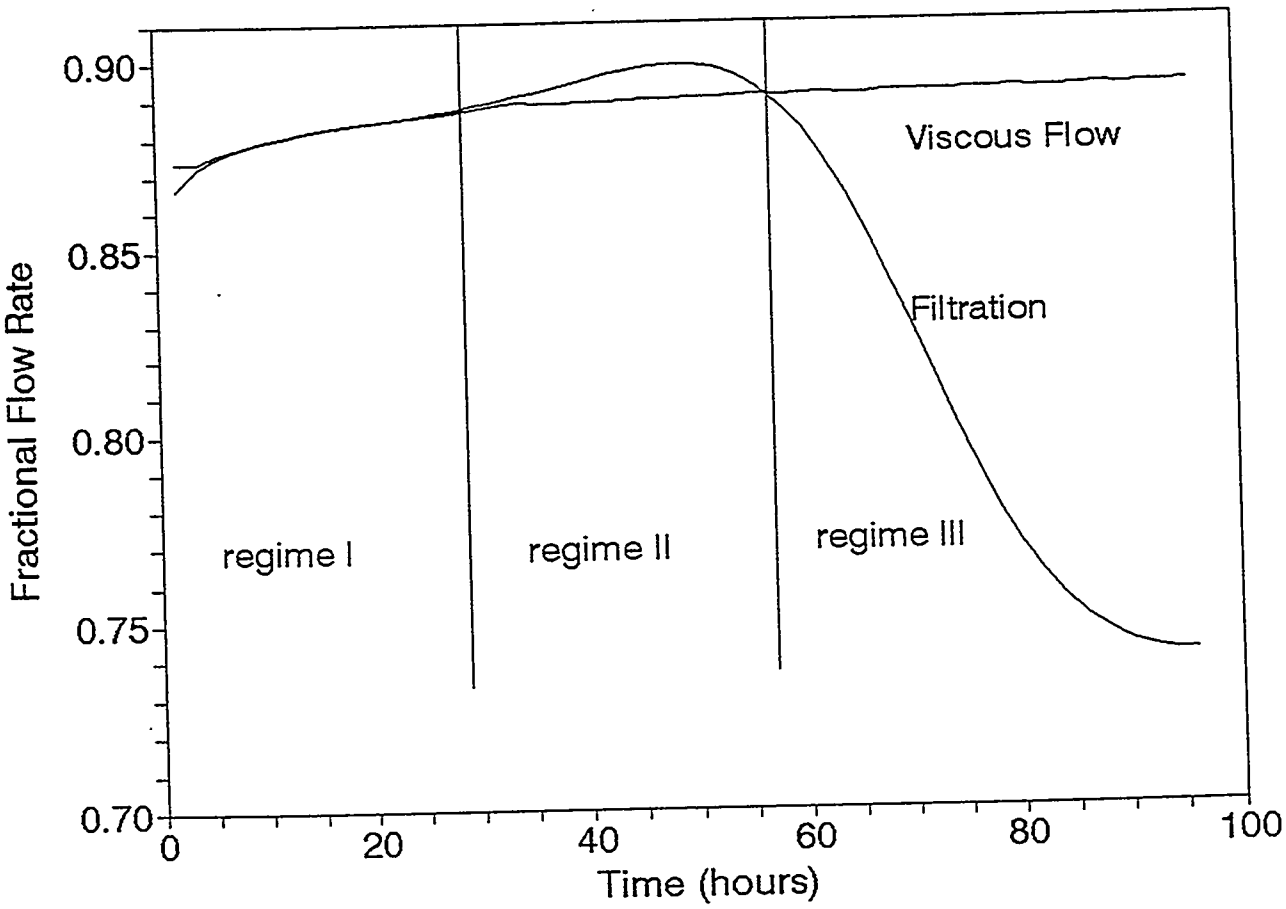

Figure 8.3: Fraction of total gelant injected into the high-permeability layer in the presence of filtration and compared to the case with only viscous flow of gelant.

In order to understand the dynamics of the placement behavior, the total injection period may be approximately divided into three regimes.

Regime I. The first regime occurs in the initial period of the treatment in which the redox reaction has not progressed significantly and little release of crosslinking ions (Cr^{3+}) occurs in the solution. Figures 8.2 and 8.3 indicate that this period lasts till approximately 30 hours of injection at the given reservoir conditions. The total flowrate in Figure 8.2 shows a rapid decline akin to that of viscous flow of the polymer under transient conditions. The fraction of the gelant injected into the high-permeability layer is also similar for the two cases.

Figure 8.4 shows the apparent viscosity contour of the gelant after 24 hours of injection and is representative of flow behavior during this regime. A small fraction of pre-gel aggregates are retained in the porous medium by interception and result in the deposition of a thin layer of polymer on the walls of the pores. This process causes a slight decrease in the permeability of the reservoir and the apparent viscosity of the advancing gelant is above the injected viscosity of 10 cp. Consequently, the total flowrate of the gelant into the reservoir with filtration is less than that for pure viscous flow of the polymer solution into the reservoir (Figure 8.2).

Crossflow behavior during this period is dominated by viscous forces. Figure 8.4 shows that the front of the gelant in the low-permeability layer is altered by crossflow from the high-permeability layer. Similarly, the front of the gelant in the high-permeability layer is modified by crossflow from the low-perm layer. Both effects reduce the effectiveness of the gel-placement in the reservoir.

Understanding the flow behavior during the first regime is critical since the bulk of the gelant is injected into the reservoir during this period. The profiles in Figures 8.3 and 8.4 show that a significant fraction of this gelant is injected into the low-permeability layer. This fraction is a function of the permeability contrast between the layers, the viscosity of the gelant and the degree of crossflow in the reservoir. Examining the effects of these parameters, therefore, constitutes an important objective of this study.

Regime II. The second regime represents the gel-placement behavior during the period from 30 to 60 hours of injection. Figure 8.2 shows that this regime is characterized by a rapid drop in the total flow-rates compared to pure viscous flow of gelant. Figure 8.3 indicates that the gelant is preferentially injected into the high-permeability layer during this regime.

The time period represented by the second regime is long enough for significant reaction between the dichromate and thiourea, but is shorter than the nominal "gel time" of 72 hours observed for the system in static beaker tests. Considerable amounts of Cr^{3+} ions are released into the solution and are subsequently attached to the polymer molecules by the uptake reaction. The attached chromium-ions enhance the efficiency of capture of the pre-gel aggregates by forming crosslinks with the polymer deposited on the walls of the pores. Thus, the dominant mechanism for the build-up of resistance during in situ gelation of the polyacrylamide/chromium system consists of the rapid reduction of permeability due to the filtration of pre-gel aggregates. Filtration of these aggregates decreases the concentration of polymer in the solution which offsets any increase in viscosity by the crosslinking reaction.

Figure 8.5 shows the apparent-viscosity contours in the two layers after 48 hours of injection. The profiles show a significant build-up of resistance in both the high-permeability and the low-permeability layers. The peaks in apparent-viscosity profiles in the two layers occurs some distance behind the front. This

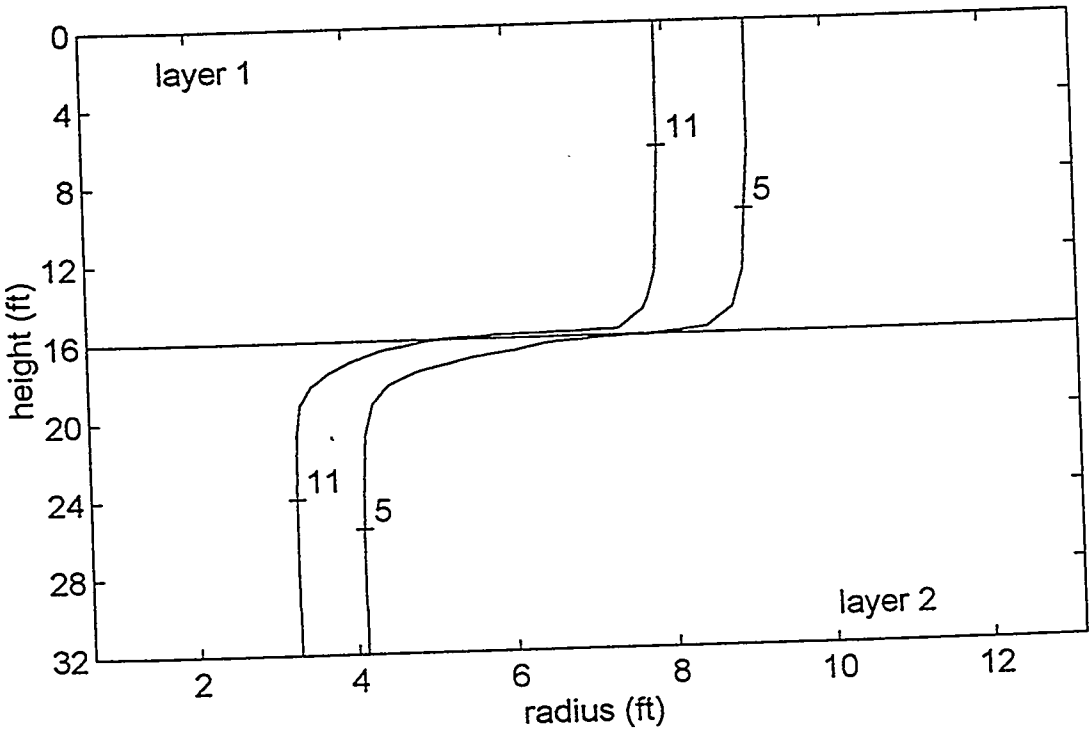

Figure 8.4: Apparent viscosity profiles after 24 hours of injection (Base Case).

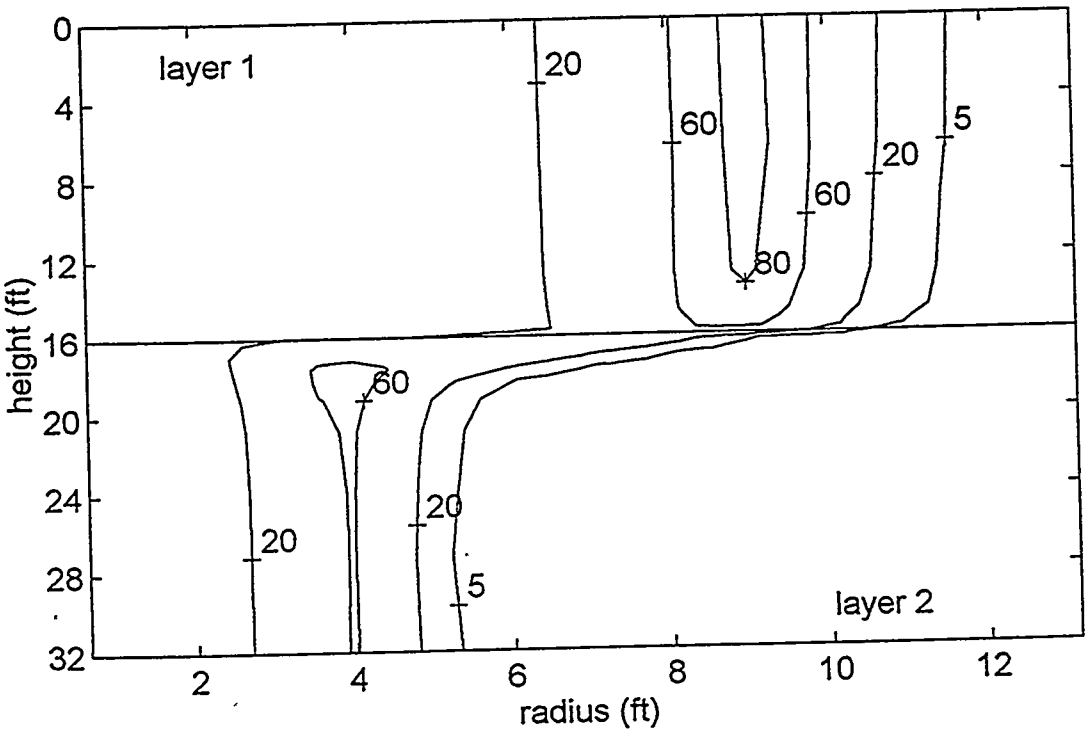

Figure 8.5: Apparent viscosity profiles after 48 hours of injection (Base Case).

behavior is characteristic of filtration processes observed in laboratory experiments with the polyacrylamide/chromium system.[1,2]

Crossflow, during this period, is due to a combination of viscous forces and the filtration mechanism. The crossflow behavior may be divided into three distinct regions.
(1) In the region between the wellbore and the peak in resistance in the low-permeability layer, crossflow is directed from the low-permeability layer towards the high-permeability layer. Since the peak in resistance in the low-permeability layer is located close to the wellbore, gelant is preferentially injected into the high-permeability layer during this period (Figure 8.3). Although the presence of gelant in the low-permeability layer will eventually reduce the injectivity of the well after the shut-in period, it is beneficial during the process of placement of the gelant.
(2) In the region intermediate to the peaks of resistance in the two layers, crossflow is directed from the high-permeability layer into the low-permeability layer. Build-up of resistance by the filtration mechanism, however, limits this front to a relatively small region near the interface of the two layers. This crossflow also results in the formation of peaks in the Cr^{3+} ion concentration and the apparent viscosity profiles in the low-permeability layer near the interface.
(3) In the vicinity of the peak in resistance in the high-permeability layer, crossflow is directed from the low-permeability layer into the high-permeability layer.

The high-permeability layer is characterized by higher interstitial velocities than the low-permeability layer. Figure 8.5 shows that the difference in velocities has two important consequences regarding the filtration behavior. First, significant concentrations of Cr^{3+} are extended over a larger region in the high-permeability layer. Filtration of polymer aggregates and ensuing build-up of resistance occurs over a larger region in the high-permeability layer than the low-permeability layer. Second, since the rate of filtration is proportional to the interstitial velocity of the pre-gel aggregates, the high-permeability layer is characterized by faster rates of filtration than the low-permeability layers.

The contrast in the rates of filtration is complicated by the following effects.
(1) The low-permeability layer is characterized by pores with smaller pore-throat diameters and pore lengths which favor the higher rates of filtration. The difference in the rates of filtration in the two layers, therefore, is reduced by the differences in the pore structure in the two layers.
(2) The radial flow-geometry around the wellbore also plays a significant role in determining the rates of filtration in the two layers. Cr^{3+} ions are released further into the reservoir in the high-permeability regions where the radial velocities decrease with increasing radius. Thus, the difference in the rates of filtration in the two layers in a radial flow-geometry is less than that expected with a linear flow-geometry.
(3) For the given system, the difference in velocities due to the permeability contrast of 10:1 between the two layers dominates over the two previously listed effects. Consequently, the high-permeability regions of the reservoir are affected by the filtration mechanism more than the low-permeability regions.

Regime III. The third regime is the period after 60 hours of injection in which the total flowrate levels off after the rapid drop in Regime II (Figure 8.2). This trend is deceptive as the levelling in flowrate does not imply a cessation in the filtration of the polymer aggregates. Figure 8.3 shows that this period is characterized by a precipitous drop in the fraction of gelant injected into the high-permeability layer.

Figures 8.6 shows the apparent viscosity profiles after 96 hours of injection. In order to understand the gel-placement behavior during this period, the fronts of the polymer solution are plotted as a function of

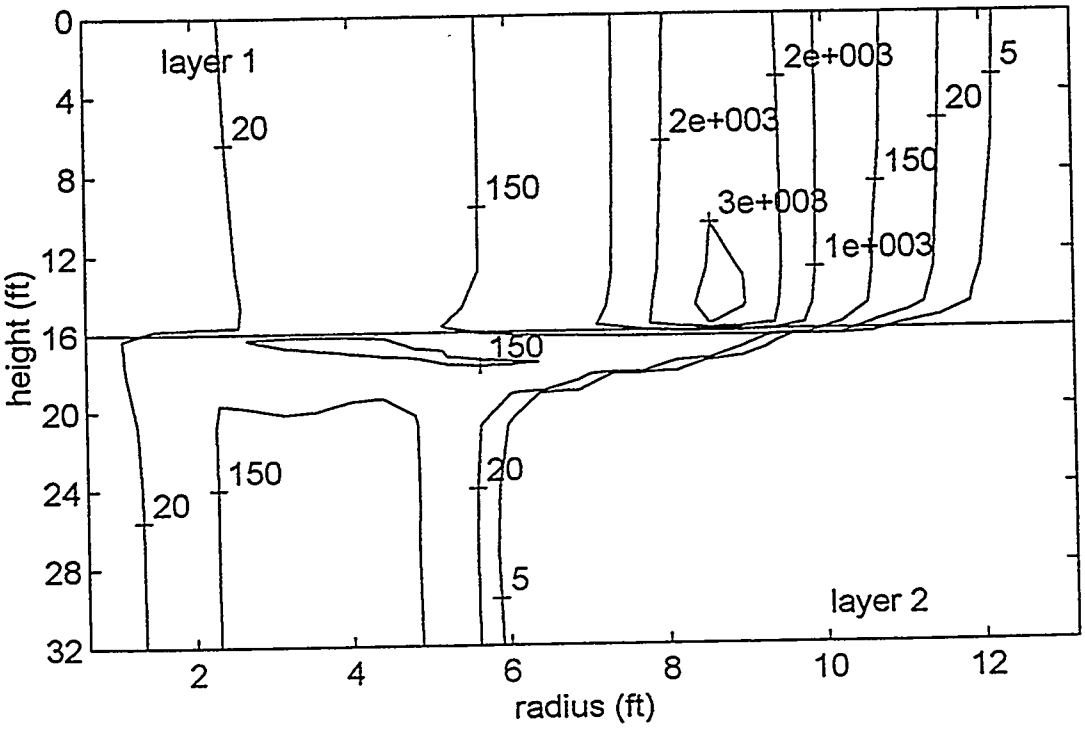

Figure 8.6: Apparent viscosity profiles after 96 hours of injection (Base Case).

time in Figure 8.7. Although the shape of the fronts is altered by filtration, these profiles demonstrate the following important features.

During the first 60 hours of injection, increasing amounts of polymer are lost from solution due to the filtration mechanism, but the polymer front still advances deeper into the reservoir. Onset of the third regime is characterized by the following behavior:
(1) In the region intermediate to the peaks of resistance in the two layers, this period is characterized by significantly more crossflow from the high-permeability layer into the low- permeability layer. This is evident from the polymer fronts at 72 and 96 hours of injection shown in Figure 8.7.
(2) As a result of the low flowrates characterizing Regime III, large amounts of Cr^{3+} ions are released near the wellbore. The rate of filtration in these regions eventually exceeds the rate of injection of the polymer and the front of the polymer in the solution recedes closer to the wellbore rather than further into the reservoir. The injected solution is rapidly stripped of polymer aggregates by filtration and the peaks in apparent viscosity in the high-permeability layer move toward the wellbore. Consequently, increasing amounts of gelant are diverted into the low-permeability region at the wellbore (Figure 8.3).

Clearly, the gel placement behavior during Regime III is detrimental for an effective permeability-modification treatment of a well. The transitional period from regime II to regime III represents the optimal time for stopping the injection of gelant. This transition is characterized by a levelling off in the flowrate profile. For the given set of conditions, this time is approximately 60 hours in Figure 8.2. Injection of gelant beyond this period results in more diversion of gelant into the low-permeability layer without increasing the penetration of the gelant in the high-permeability layer.

Effect of Injection Pressure or Flow rate. The experiments of Marty et al.[1] with the polyacrylamide/chromium system showed that higher flow rates resulted in deeper penetration of gelant into sandpacks but also caused a faster build-up of resistance. Both trends may be explained by the filtration mechanism which couples the rate of build-up of resistance to the kinetics of the redox reaction and the velocity of the polymer aggregates through the porous medium. Extension of the filtration mechanism to field-scale conditions indicates that the flow rate, or the injection pressure, is an important operating variable in a permeability-modification treatment.

Figure 8.8 compares the total flow-rate profiles for injection pressures of 1000 psi and 250 psi to the base case of 500 psi. Figure 8.9 shows the corresponding profiles of the fraction of gelant injected into the high-permeability layer. The gel-placement behavior at the three different injection pressures is similar and may be divided into the three regimes discussed earlier.

During the first regime, the filtration mechanism is insignificant and the flow behavior of the gelant is governed by viscous forces. During this period, higher injection pressures result in the injection of greater volumes of gelant into the reservoir. Figure 8.9 shows that the distribution of this gelant between the two layers is similar for the range of injection pressures investigated. For higher flow rates, a minor increase in the fraction of gelant injected into the high-permeability layer under transient conditions is observed.

Figures 8.10 and 8.11 show the apparent viscosity profiles after 48 hours of injection at 1000 psi and 250 psi respectively. The corresponding profiles for the base case were shown earlier in Figure 8.4 and show trends intermediate to the results in Figure 8.10 and 8.11. These profiles are representative of the behavior during Regime II.

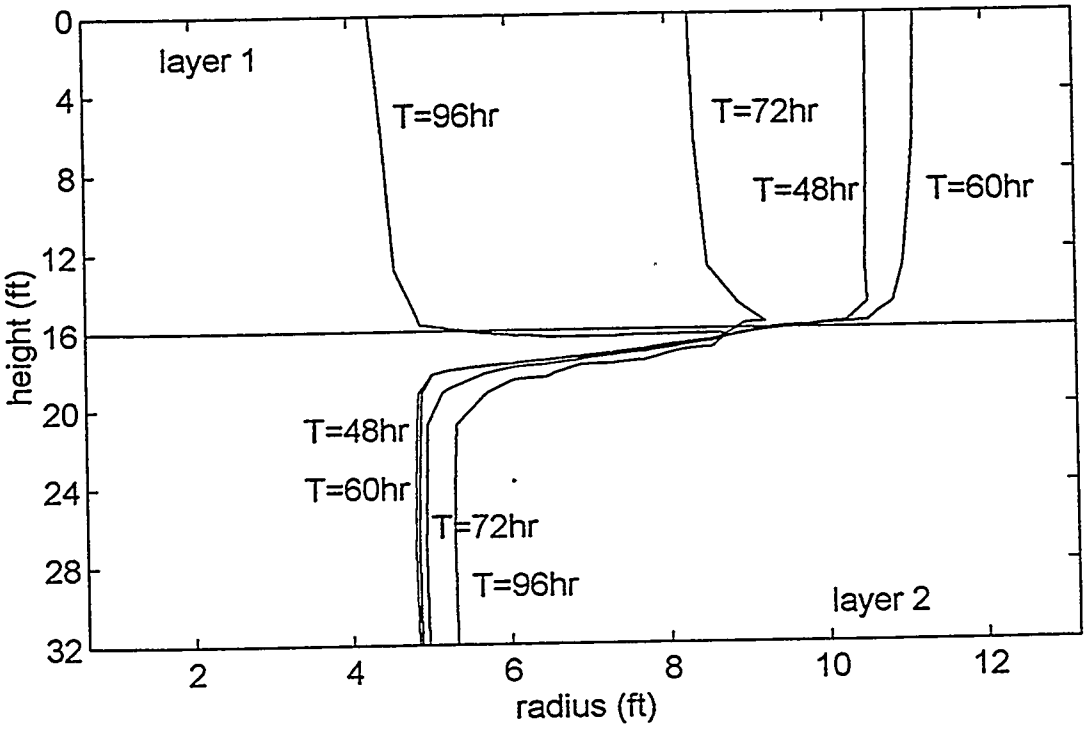

Figure 8.7: Profiles of the polymer front in the solution during gelation (Base Case).

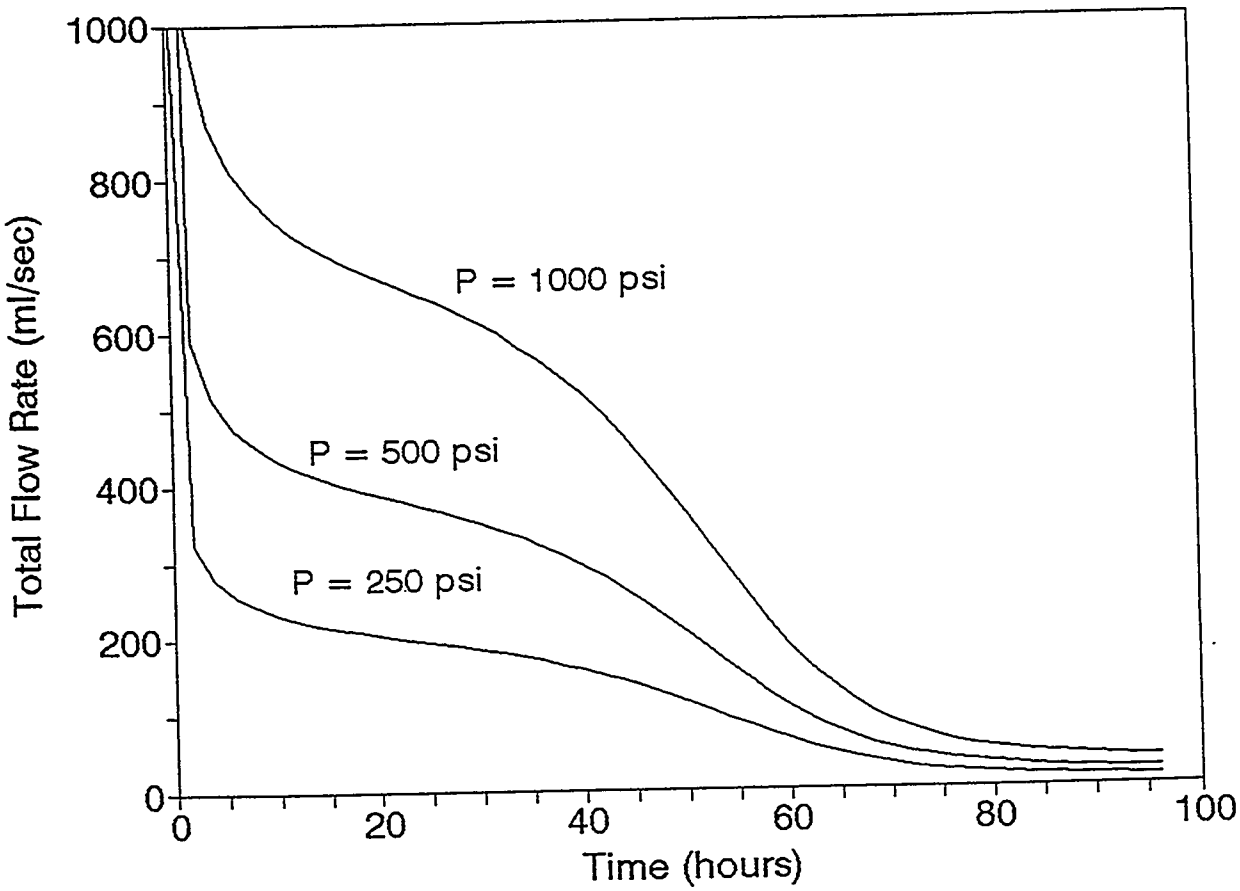

Figure 8.8: Rate of injection in the presence of filtration for different injection pressures.

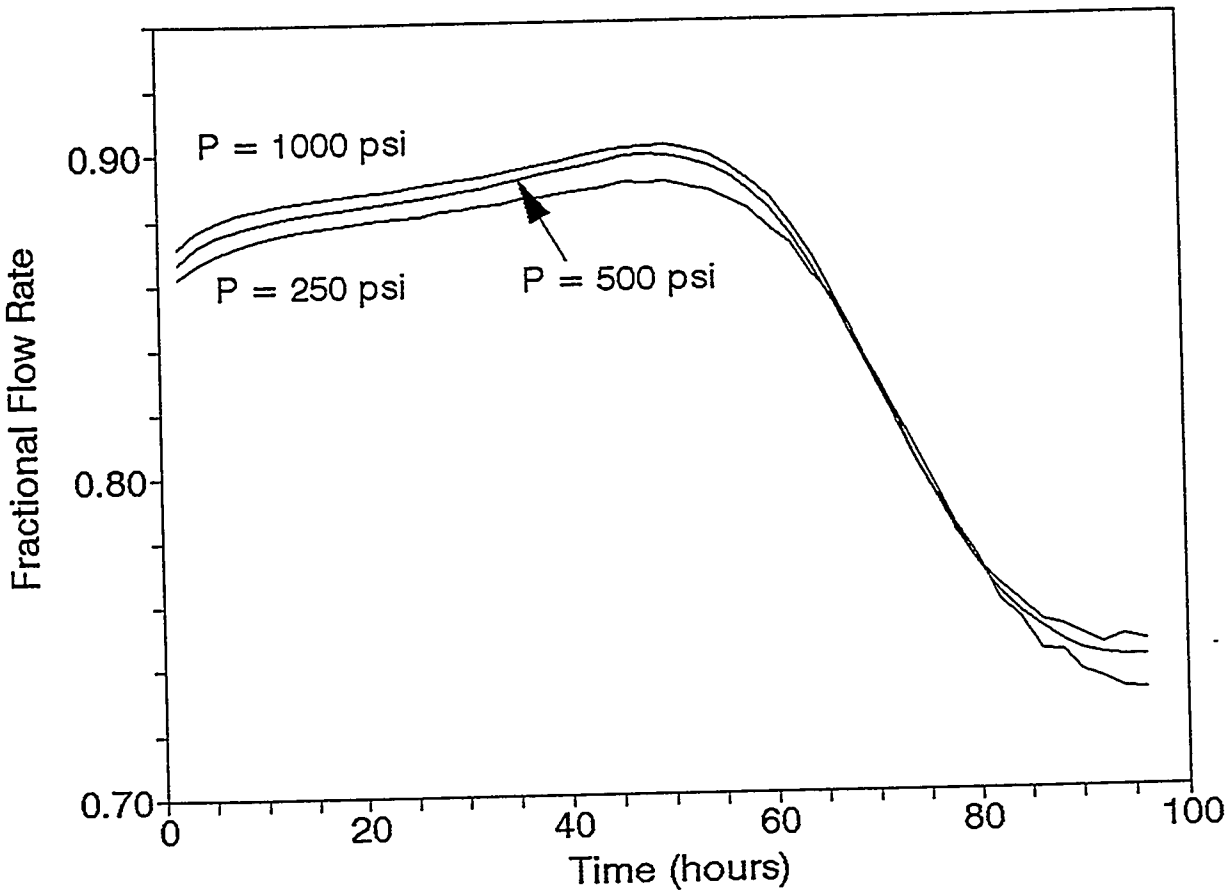

Figure 8.9: Fraction of gelant injected into the high-permeability layer for different injection pressures.

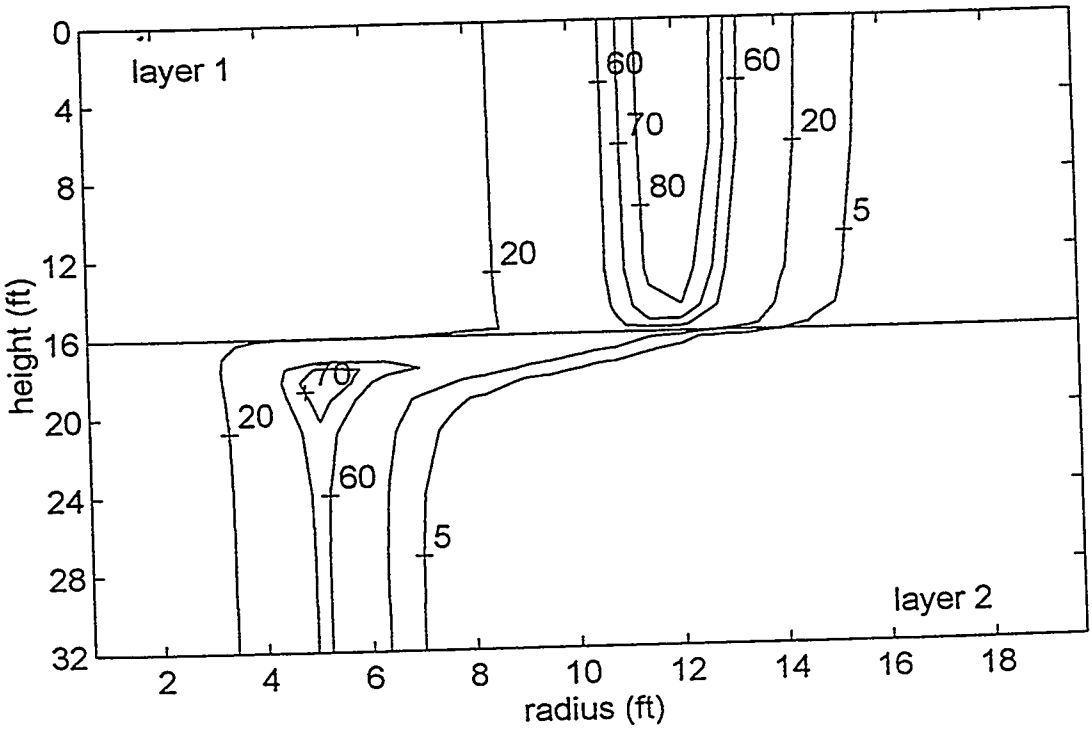

Figure 8.10: Apparent viscosity profiles after 48 hours of injection at 1000 psi.

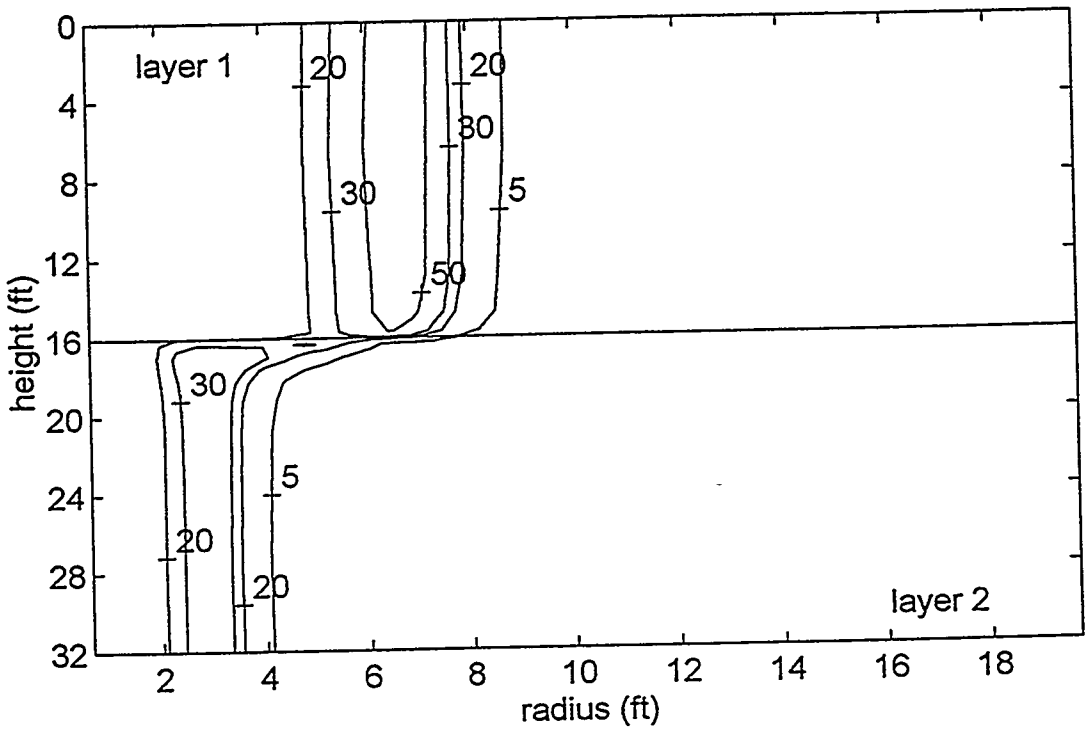

Figure 8.11: Apparent viscosity profiles after 48 hours of injection at 250 psi.

The values of the apparent viscosities at 48 hours indicate faster rates of filtration at higher flow rates. The increase in the rate of filtration is a consequence of the higher interstitial velocities of the pre-gel aggregates in the reservoir at higher injection pressures. The difference in the rates of filtration, however, is less than that expected with a linear flow-geometry. The build-up of resistance occurs further into the reservoir at higher injection pressures with the radial velocities decreasing with increasing radius. As a result, the onset of the behavior in Regime III occurs at approximately the same time of 60 hours despite the difference in the injection pressures. Therefore, in the presence of radial flow-geometry, the kinetics of the redox reaction is the critical mechanism in determining the amount of gelant which can be injected into the reservoir.

In conclusion, it is possible to inject greater volumes of gelant into the reservoir by increasing the injection pressure. The rates of filtration increase with increasing flowrate, but this effect is mitigated by the radial flow behavior around the wellbore. Unfortunately, increasing the injection pressure does not alter the injectivity pattern significantly, i.e. more polymer is injected into both layers with increasing injection pressure. The advantages of injecting large volumes of gelant into the reservoir, therefore, may be offset by the loss in injectivity of the well after the shut-in period.

Effect of Permeability Contrast. Previous results show that a significant amount of gelant is injected into the low-permeability region. After shut-in of the well, this gelant lowers the injectivity of the well and the overall effectiveness of the treatment. The ratio of radial permeabilities is an important parameter in determining the distribution of gelant in the two layers. A case in which the permeability of the high-perm layer is changed from 0.1 D to 1.0 D is examined. The resulting permeability ratio of 100:1 represents a reasonable upper limit of the contrast in absolute permeabilities expected in unfractured reservoirs. The ratio of the effective permeabilities of the layers, however, may be enhanced by the presence of unswept oil in the low-permeability regions of the reservoir. Therefore, a permeability ratio of 100:1 is representative of cases characterized by severe channeling problems during waterflooding.

Figures 8.12 and 8.13 show profiles of the total flowrate and the fraction of gelant injected into the high-permeability layer as a function of time. The initial period essentially consists of viscous flow of gelant into the reservoir. Due to the higher permeability contrast, the flowrate of the gelant into the high-permeability layer in Figure 8.12 is considerably greater than the base case (Figure 8.2) at the same injection pressure. More importantly, the fraction of the total gelant injected into the high-permeability layer is considerably higher in Figure 8.13 than that in Figure 8.3. Thus, it is possible to inject gelant into the reservoir with a more favorable distribution as the permeability contrast between the layers increases.

Regime II represents the period in which the filtration processes become significant. Figure 8.14 shows the apparent-viscosity profiles after 48 hours of injection. Due to the higher injection rates, the penetration of gelant into the high-permeability layer region is significantly deeper than for the corresponding profile in Figure 8.5. The difference in the rates of filtration in the two layers increases as the permeability contrast increases. For the permeability contrast of 100:1, the build-up of resistance near the wellbore in the low-permeability layer is not sufficient to diverting significant amounts of gelant into the high-permeability layer. Consequently, for a higher permeability contrast, preferential flow into the high-permeability layer during Regime II is reduced.

Build-up of resistance limits the crossflow of gelant from the high-permeability layer into the low-permeability layer to a relatively small distance near the interface. This result is significant since considerably more gelant is injected into the reservoir than for the base case.

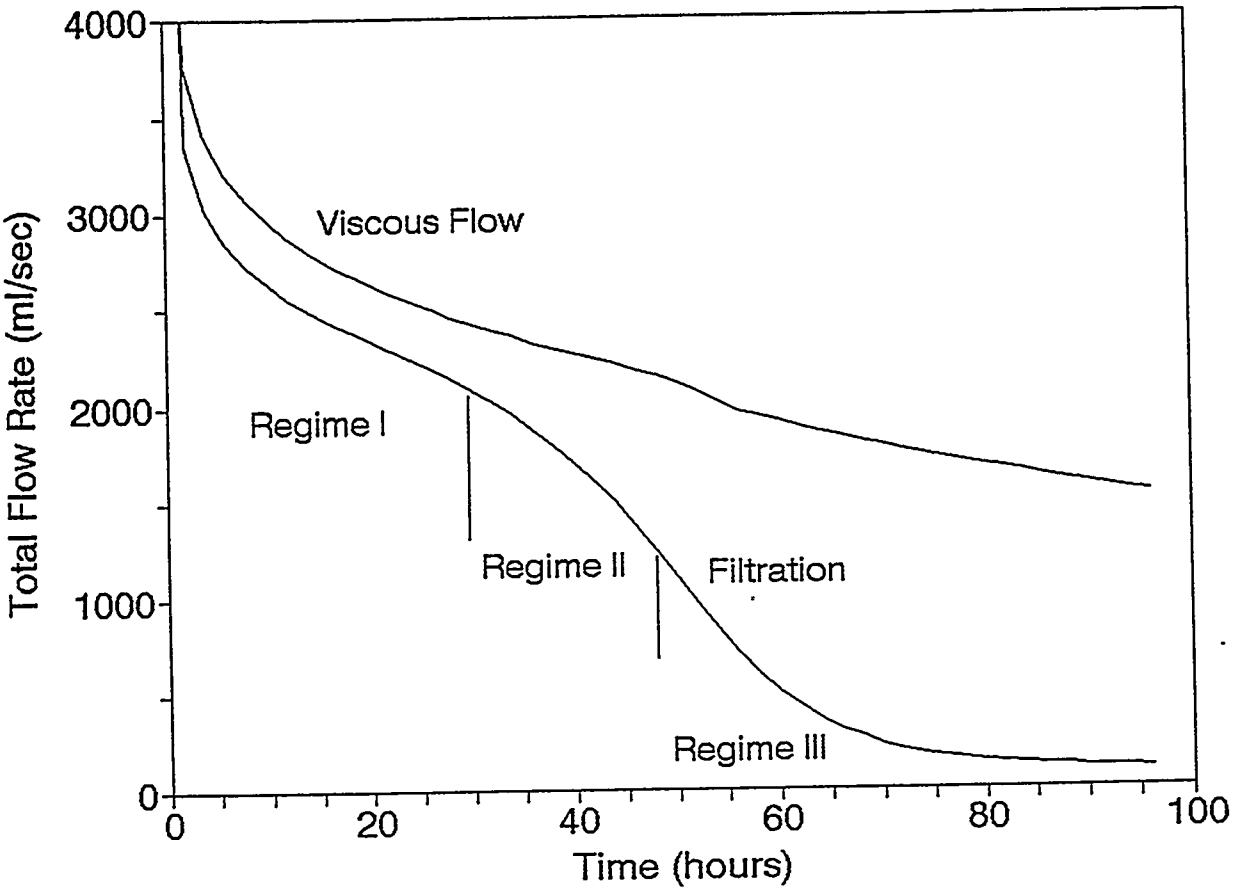

Figure 8.12: Rate of injection in the presence of filtration for a permeability contrast of 100:1.

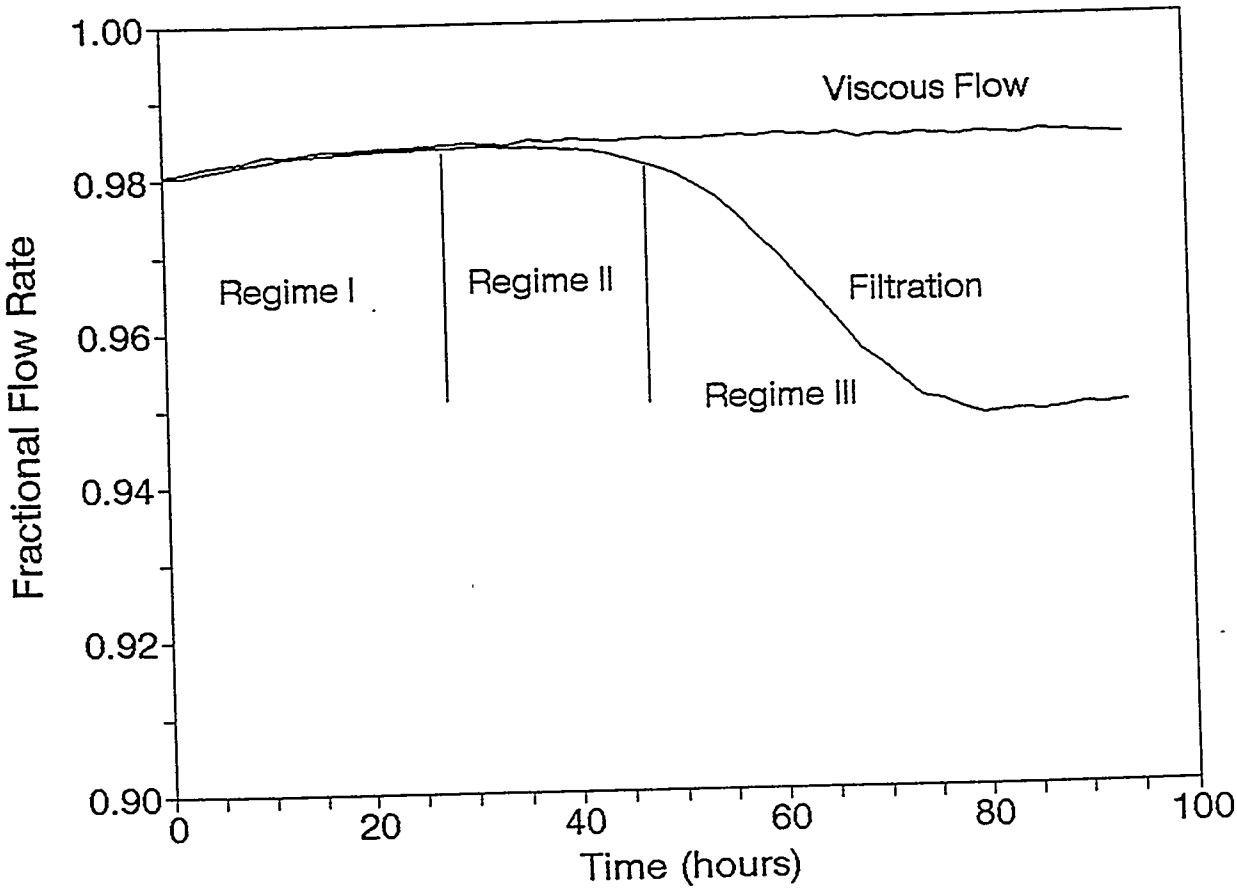

Figure 8.13: Fraction of gelant injected into the high-permeability layer for a permeability contrast of 100:1.

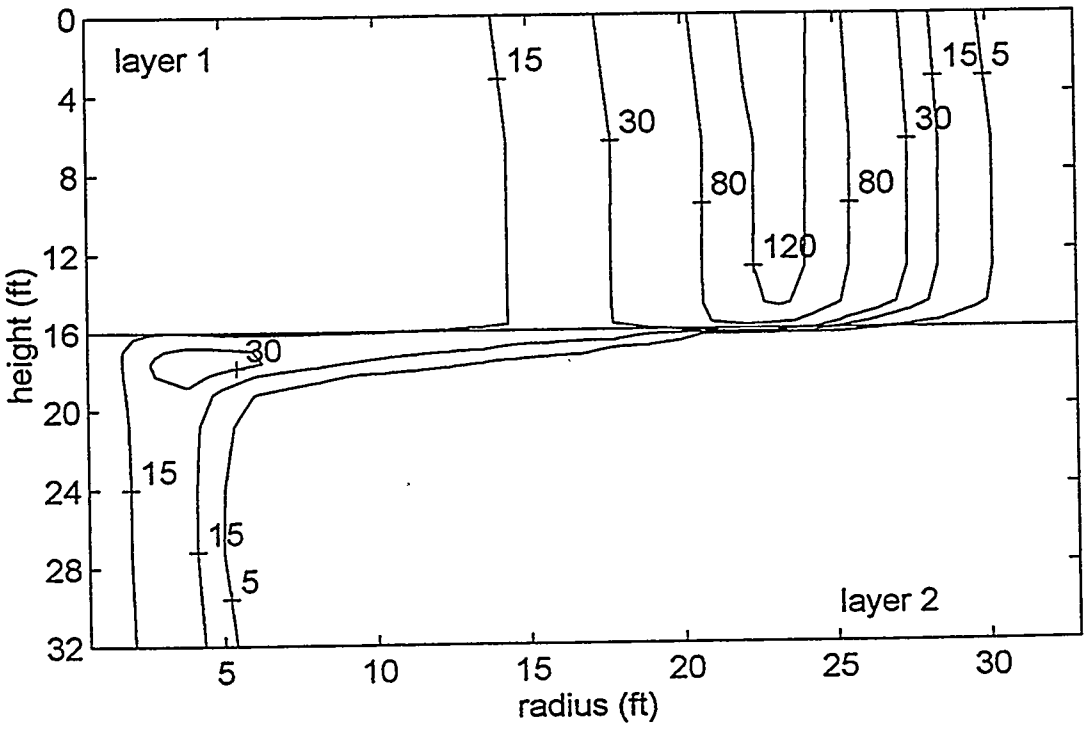

Figure 8.14: Apparent viscosity profiles after 48 hours of injection for a permeability contrast of 100:1.

During Regime III, higher flow-rates hasten the plugging of the high-permeability layer by filtration. The drop in the fractional flow profile shown in Figure 8.13 occurs about 10 hours earlier than for the base case. Clearly, the radial-flow geometry around the wellbore plays a major role in reducing this time differential. For the given conditions, therefore, injection of gelant should be stopped after approximately 50 hours.

In conclusion, a more effective treatment is possible in reservoirs with high-permeability contrast. Permeability-modification treatments, therefore, are expected to be more effective in severe cases of water channeling as opposed to mild cases of water channeling during the waterflooding stage.

Vertical Permeability and Aspect Ratio. Previous results show that the bulk of the total gelant is injected into the reservoir during Regime I. During this period, crossflow is due to viscous forces only. After the onset of filtration in Regime II, further crossflow of gelant from the high-permeability layer into the low-permeability layer is retarded by the filtration mechanism. Hence, crossflow due to viscous forces is a critical mechanism determining the effectiveness of gel placement in a reservoir.

The degree of crossflow during gel placement is determined by the aspect ratio of the treatment and the ratio of the vertical permeability to the radial permeability. The aspect ratio is defined as the ratio of a characteristic radius of penetration defining the region of treatment (R) around the wellbore to the height of the layers (H). The degree of crossflow, G, is defined as [9,10]

$$G = \frac{R}{H}\sqrt{\frac{k_z}{k_r}}\,. \qquad (2)$$

Thus, crossflow is significant in relatively thin reservoirs characterized by high vertical permeabilities. The degree of crossflow in layered reservoirs is bounded by two limiting cases. A zero value of G indicates a reservoir without crossflow representing a layered system with each layer separated by an impermeable shale layer. As G approaches infinity, the crossflow between the layers increases and approaches vertical equilibrium.

Previous results indicate that the radius of penetration for the polyacrylamide/chromium system, is confined to within 10 to 30 ft of the wellbore for typical reservoir and operating conditions. In all the simulations shown earlier, the value of the ratio of the vertical permeability to the horizontal permeability of a reservoir is unity which represents the maximum amount of crossflow expected for that particular geometry. Therefore, the typical value of the degree of crossflow for near-wellbore treatment with this system is expected to be of the order of unity. The simulated apparent viscosity profiles show that crossflow of gelant is confined to a relatively small region near the interface of the layers.

In order to study the effect that filtration has in the presence of significant amounts of crossflow, injection of gelant into a reservoir with thickness (H) of 3 ft is examined. Although this case has little practical importance for the polyacrylamide/chromium system, the degree of crossflow in this case is representative of a system in which a deeper treatment of reservoir is possible. It may also be noted that the aspect ratio of the treatment in this example is closer to some laboratory experiments used to simulate of flow in layered reservoirs.[9]

Figure 8.15 shows the apparent viscosity profiles after 24 hours of injection. The movement of the front of the solution in the low-permeability layer is accelerated by crossflow from the high-permeability layer.

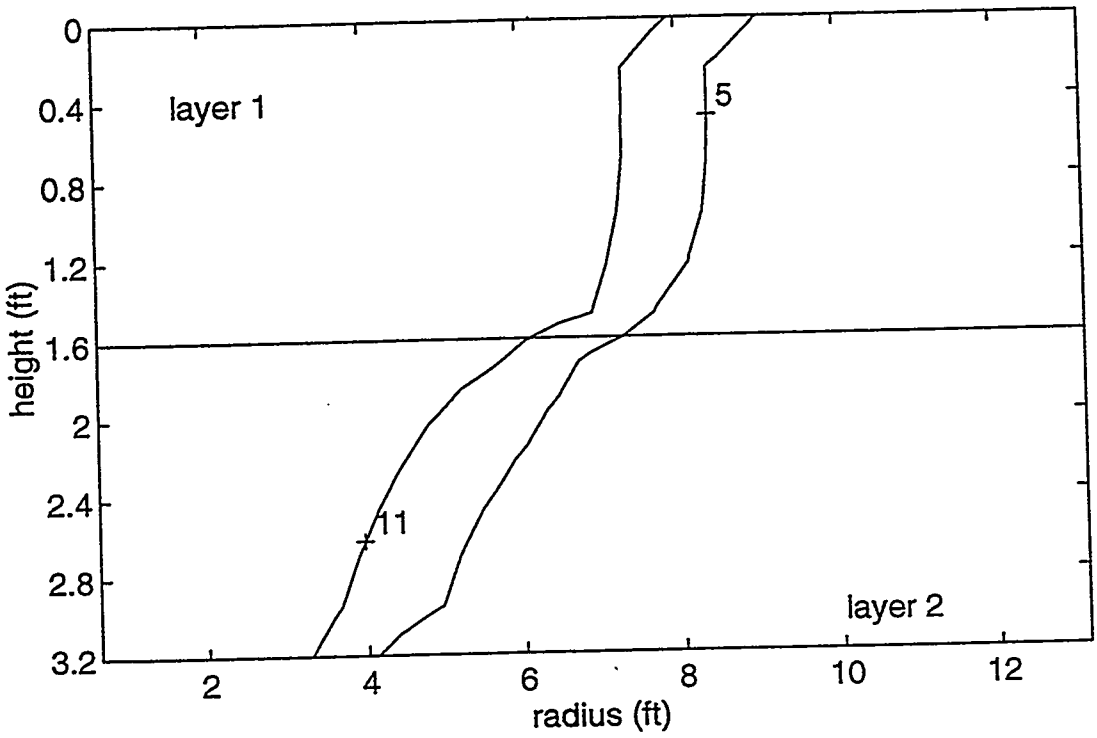

Figure 8.15: Apparent viscosity profiles after 24 hours of injection into a reservoir with height of 3.2 ft.

The movement of the front of the gelant in the high-permeability layer is retarded by crossflow from the low-permeability layer. The net effect of viscous crossflow, therefore, is to bring the fronts in the two layers closer together.

Figure 8.16 shows the apparent viscosity profiles after 48 hours of injection. Filtration of pre-gel aggregates results in a build-up of resistance in both layers. In addition, there is a build up of resistance intermediate to the peaks in the layers by crossflow. This front penetrates a significant distance into the low-permeability region.

Although viscous crossflow has a relatively small effect during typical near-wellbore treatments, the effects of viscous crossflow may become significant in deeper treatments by gelants with long gel times. In these cases, the bulk of the crossflow occurs before the onset of filtration and the filtration mechanism does not help to keep gelant from penetrating into the low-permeability regions.

Clearly, gel-placement is most effective in reservoirs characterized by low crossflow. It may be noted that reservoirs with significant amounts of crossflow may not exhibit severe problems of channeling during waterflooding. Based on crossflow behavior, therefore, it may be concluded that gel placement will be more effective in cases characterized by severe water channeling problems.

Effect of Gel Solution Viscosity. The initial viscosity of the polyacrylamide/chromium system in all the previous results was a relatively high value of 10 cp. Simulations were conducted by decreasing the gelant viscosity to 1 cp and maintaining the same reaction parameters. Although this reduction in viscosity is not physically possible for the polyacrylamide/chromium system, the results provide insight into the role of gelant viscosity on the flow behavior and filtration mechanism. These results also lead to general conclusions regarding the design of gelant systems.

Figures 8.17 and 8.18 show the total flowrate and fractional flowrate into the high-permeability layer as a function of time. During the first regime, the injection rate of the gelant shown in Figure 8.17 is considerably higher than for the base case (Figure 8.2) at the same injection pressure. Comparison of Figures 8.18 and 8.3 indicates that the fraction of the total gelant injected into the high-permeability layer is higher for low-viscosity gelants. The ratio of volume flowing in the two layers is equal to the ratio of the permeabilities for a unit-viscosity gelant and approaches the square root of the permeability ratio as the viscosity of the gelant increases.[9]

The apparent viscosity contours after 48 hours of injection are shown in Figure 8.19. The values of the apparent viscosity in this figure reflect significantly more filtration for the unit viscosity gelant than for the base case. This behavior is due to the following effects.
(1) The low-viscosity gelant is injected at a considerably higher flowrate than for the base case. These higher flowrates result in faster rates of filtration in the two layers.
(2) A characteristic of the filtration mechanism in the model is that Brownian motion of the pre-gel aggregates is more pronounced at lower viscosities. This Brownian motion results in more collisions of the pre-gel aggregates with the walls of the pores. Thus, when the Cr^{3+} ions are attached to the polymer aggregates, filtration is more rapid for low-viscosity gelants. It may be noted that Brownian motion is the dominant mechanism for the typical aggregate size of the injected polyacrylamide solution (0.1 microns). As the aggregate size increases, streamline interception begins to dominate. Streamline interception is a function of the ratio of the aggregate size to the pore diameter and is independent of the viscosity of the gelant. Thus, for gelants characterized by large molecules, the effect of viscosity on the rate of filtration may not be significant.

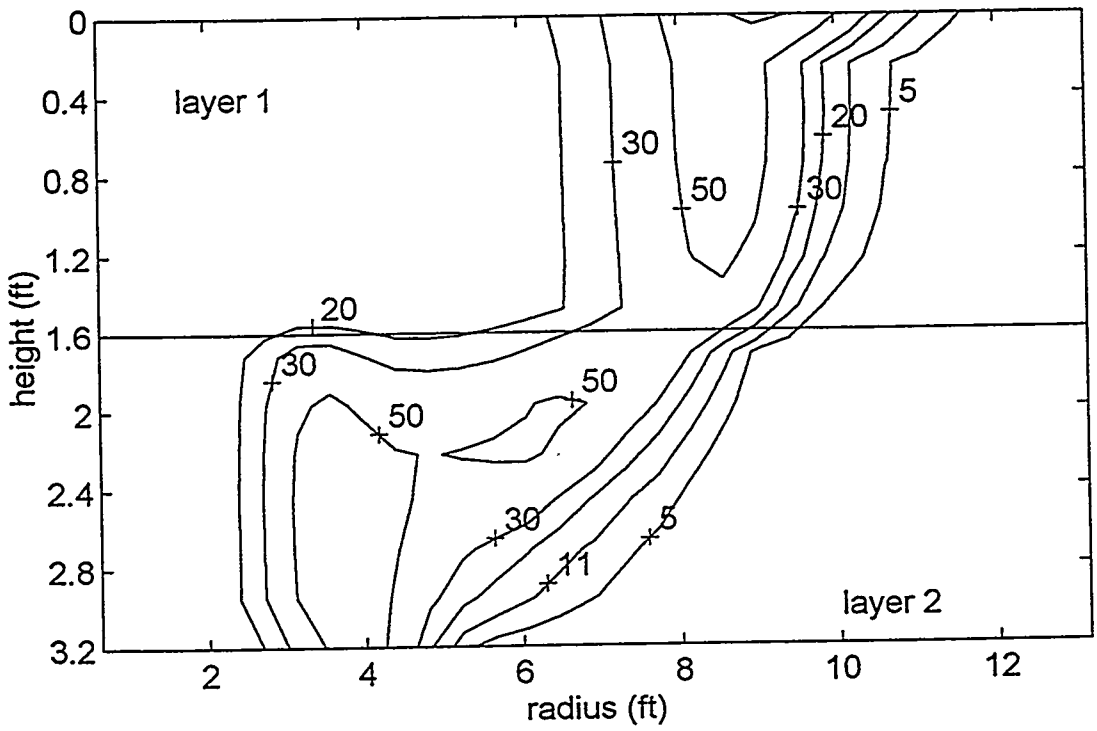

Figure 8.16: Apparent viscosity profiles after 48 hours of injection into a reservoir with height of 3.2 ft.

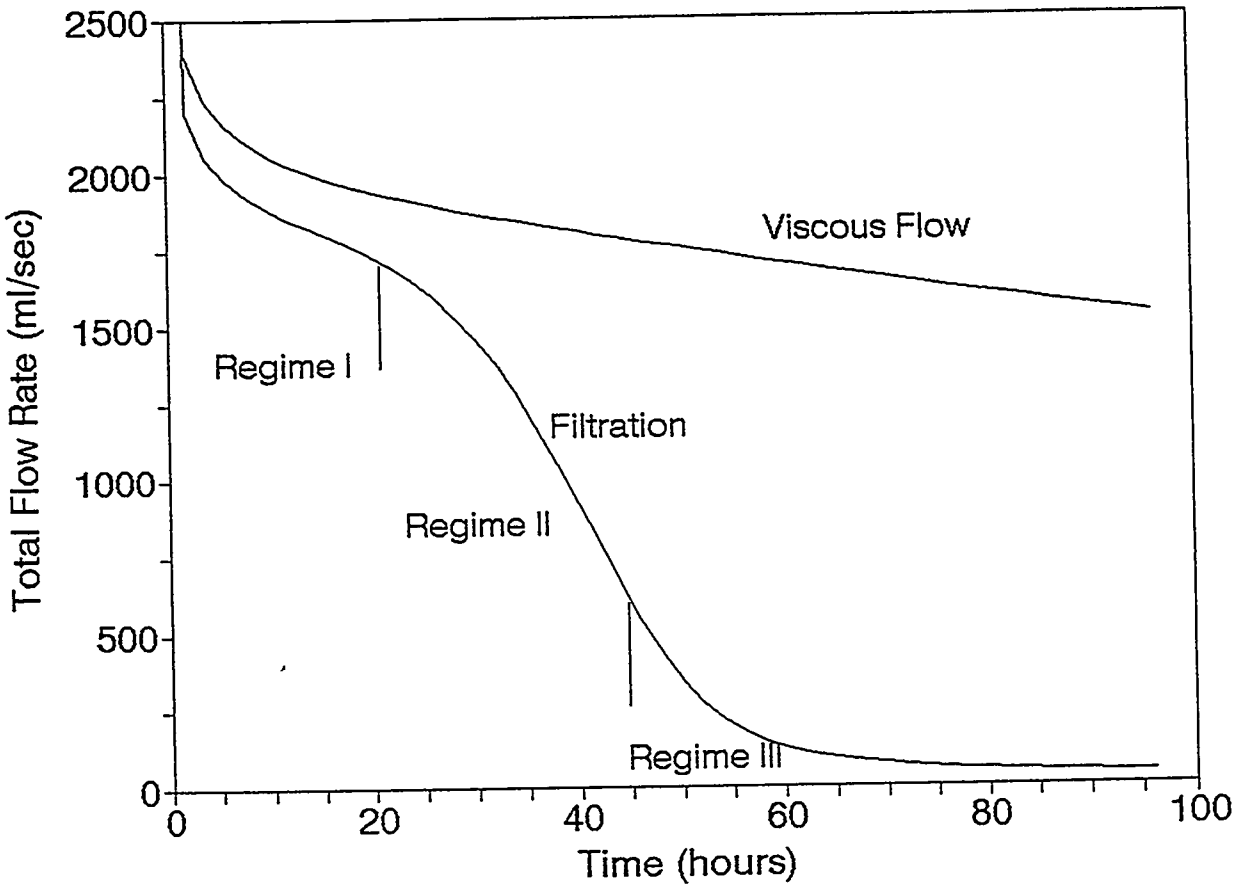

Figure 8.17: Rate of injection in the presence of filtration for a unit-viscosity gelant.

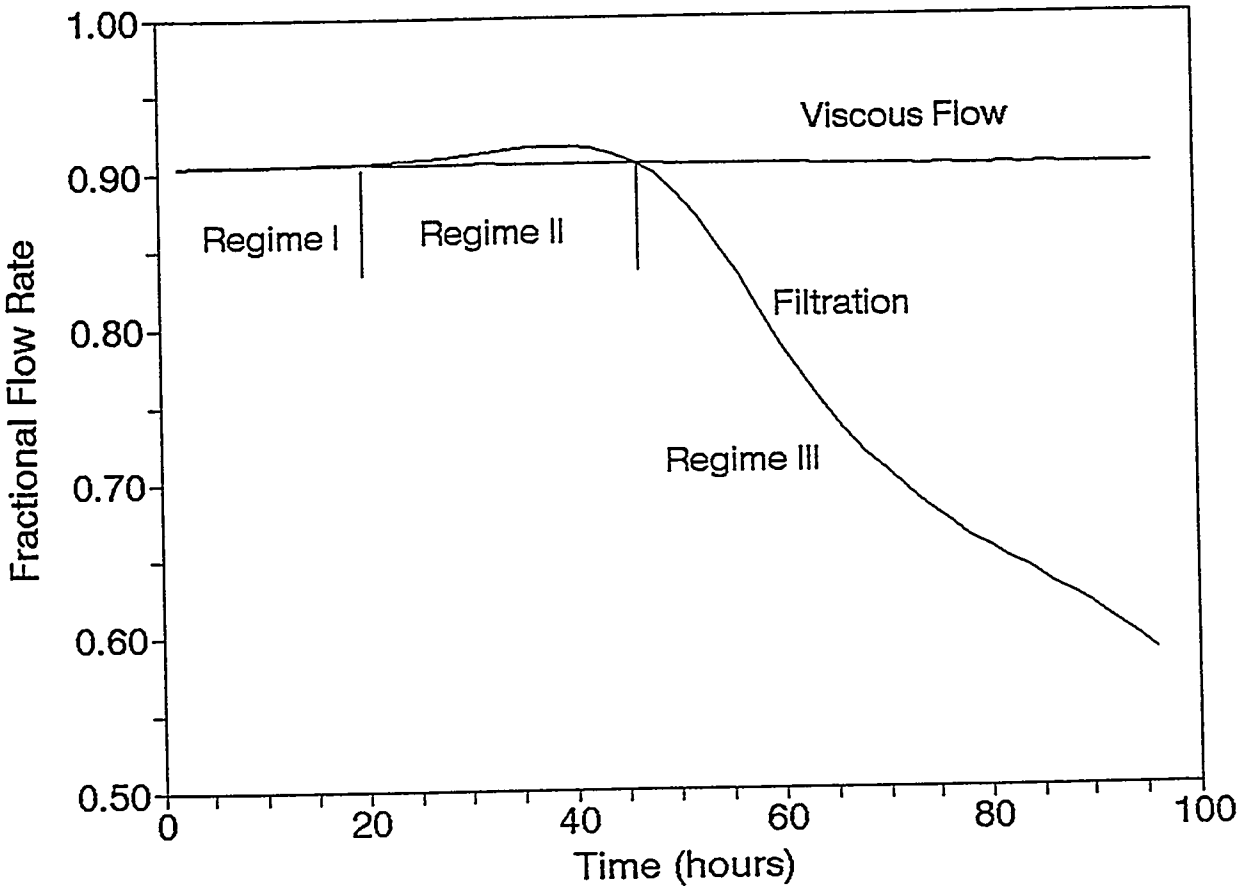

Figure 8.18: Fraction of gelant injected into the high-permeability layer for a unit-viscosity gelant.

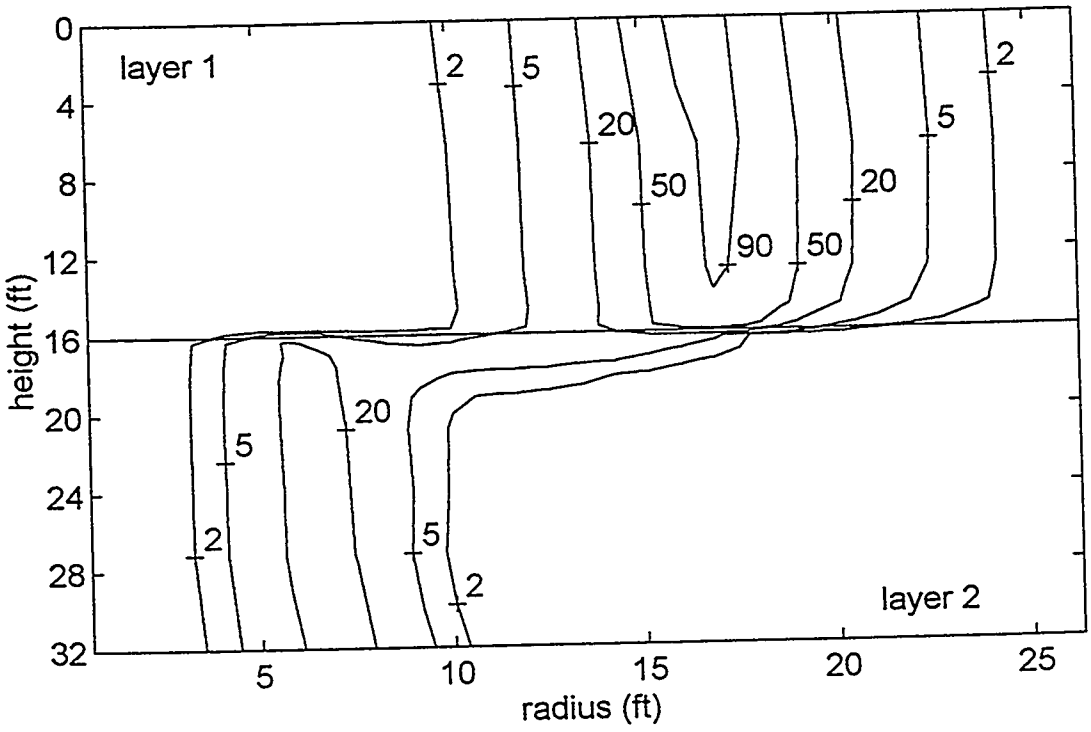

Figure 8.19: Apparent viscosity profiles after 48 hours of injection of a unit-viscosity gelant.

As a consequence of the higher rates of filtration, Figures 8.17 and 8.18 show that the onset of Regime III is hastened. The optimal time of injection of the gelant is about 45 hours which is less than the corresponding time for the base case. However, since the bulk of the gelant is injected during the first regime, it is possible to inject larger volumes of gelant into the reservoir with low-viscosity gelants.

In the case of a unit-viscosity gelant, viscous forces are absent and crossflow is due to the filtration mechanism alone. Crossflow is directed from the low-permeability to the high-permeability layer in the region before the front in the low-permeability layer. In the region intermediate to the fronts in the two layers, crossflow is directed from the high-permeability layer towards the low-permeability layer. This crossflow causes plugging at the interface of the two layers. In the vicinity of the front in the high-permeability layer, crossflow is directed from the low-permeability layer into the high-permeability layer.

In conclusion, as the viscosity of the gelant is lowered, it is possible to inject larger amounts of gelant into the reservoir with a more favorable distribution between the two layers. Although viscous crossflow is reduced as the viscosity of the gelant is reduced, crossflow of gelant may occur due to build-up of resistance by the filtration mechanism.

Zonal Isolation. Previous results show that significant amounts of gelant are injected into the low-permeability regions during conventional permeability-modification treatments. This gelant reduces both the overall effectiveness of the gel placement in the high-permeability layer and the injectivity of the low-permeability regions after the shut-in period. Simulations were conducted to study permeability-modification treatments in reservoirs where it is possible to mechanically isolate the layers and inject gelant into the high-permeability layer alone. Base case conditions were used.

Figure 8.20 shows the apparent viscosity profiles after 24 hours of injection into the high-permeability layer only. In addition to viscous crossflow, there is a considerable amount of crossflow into the low-permeability layer close to the wellbore. This crossflow is due to the significant amount of time required for the pressure transient to equilibrate across the height of the low-permeability layer. Note that this crossflow is not due to viscous forces and is present even in case of injection of a unit-viscosity gelant.

Figure 8.21 shows the apparent viscosity profiles after 48 hours of injection into the high permeability layer only. The values of the apparent viscosity and the volume of gelant injected into the high-permeability layer are similar to the case with injection in both layers (Figure 8.5). Injection of gelant into the low-permeability layer, however, is avoided by zonal isolation and results in a more effective gel placement than conventional treatments. There is some penetration of the gelant into the low-permeability layer by crossflow. Filtration of polymer aggregates at the front, however, confines this gelant to a small region near the interface of the layers.
The effects of viscous crossflow and filtration on gel placement with zonal isolation are similar to the case with injection into both layers. In the case of zonal isolation, however, crossflow near the wellbore is an additional mechanism limiting the volume of gelant which can be injected into the reservoir. As the injection pressure is increased, it is possible to inject larger volumes of gelant into the high-permeability layer before the onset of Regime III (Figures 8.22 and 8.23). Since most of the crossflow occurs before the onset of the filtration mechanism, increase in injection pressure also increases crossflow near the wellbore.

As in the case of conventional treatments, favorable gel-placement behavior is achieved when the permeability contrast between the layers is large. This is seen by comparison of Figures 8.24 and 8.21 (Figure 8.21 is for the base-case parameters). The significance of crossflow increases as the aspect ratio

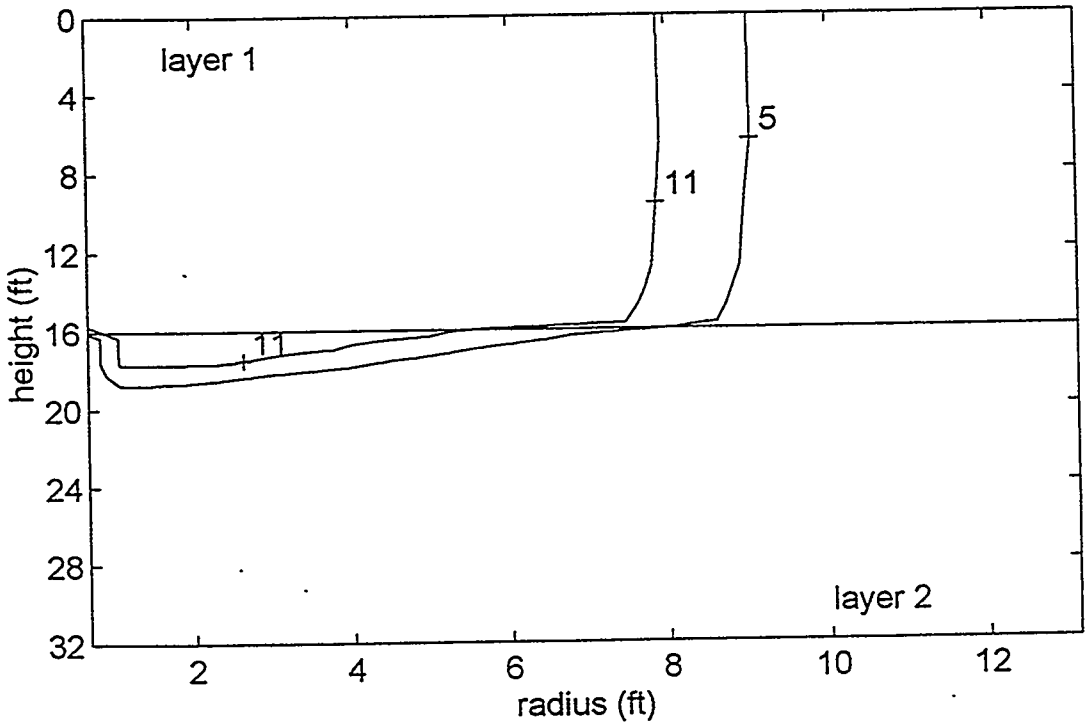

Figure 8.20: Apparent viscosity profiles after 24 hours of injection into the high-permeability layer only.

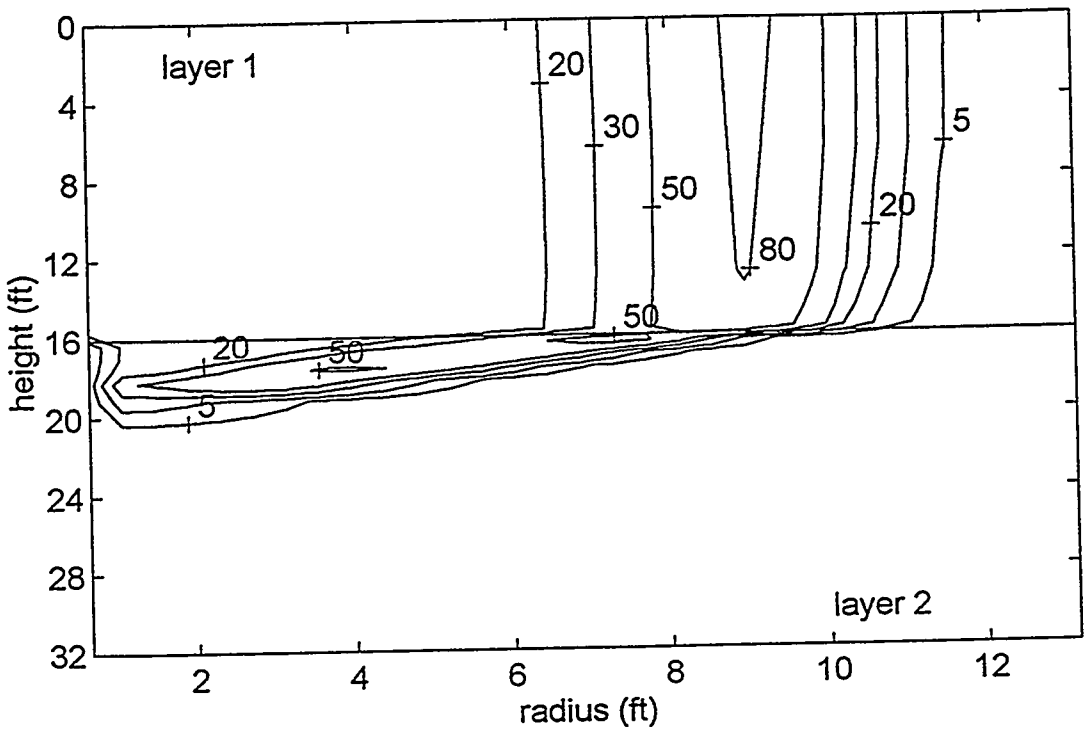

Figure 8.21: Apparent viscosity profiles after 48 hours of injection into the high-permeability layer only.

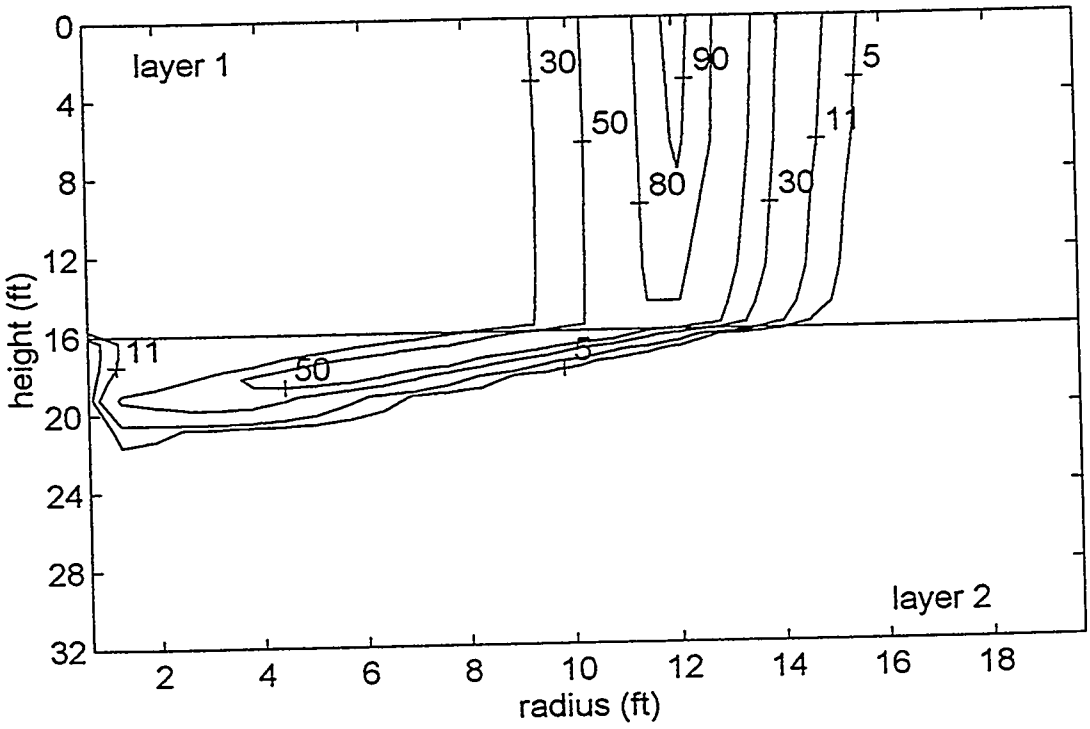

Figure 8.22: Apparent viscosity profiles after 48 hours of injection at 1000 psi only into the high-permeability layer.

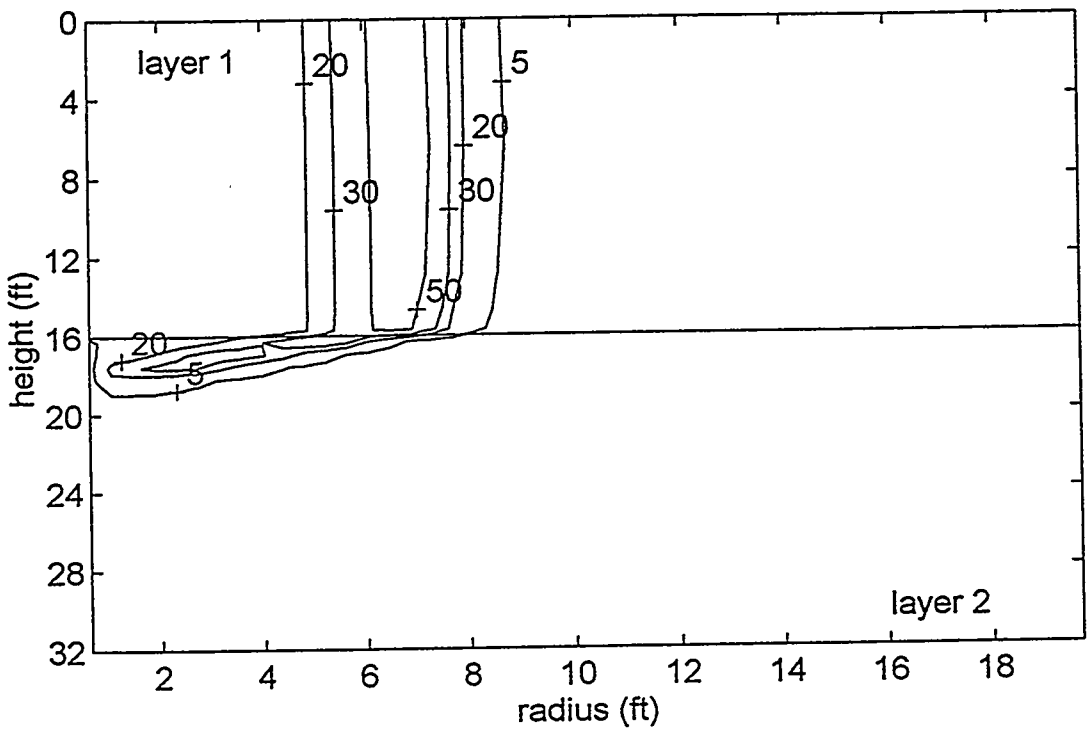

Figure 8.23: Apparent viscosity profiles after 48 hours of injection at 250 psi only into the high-permeability layer.

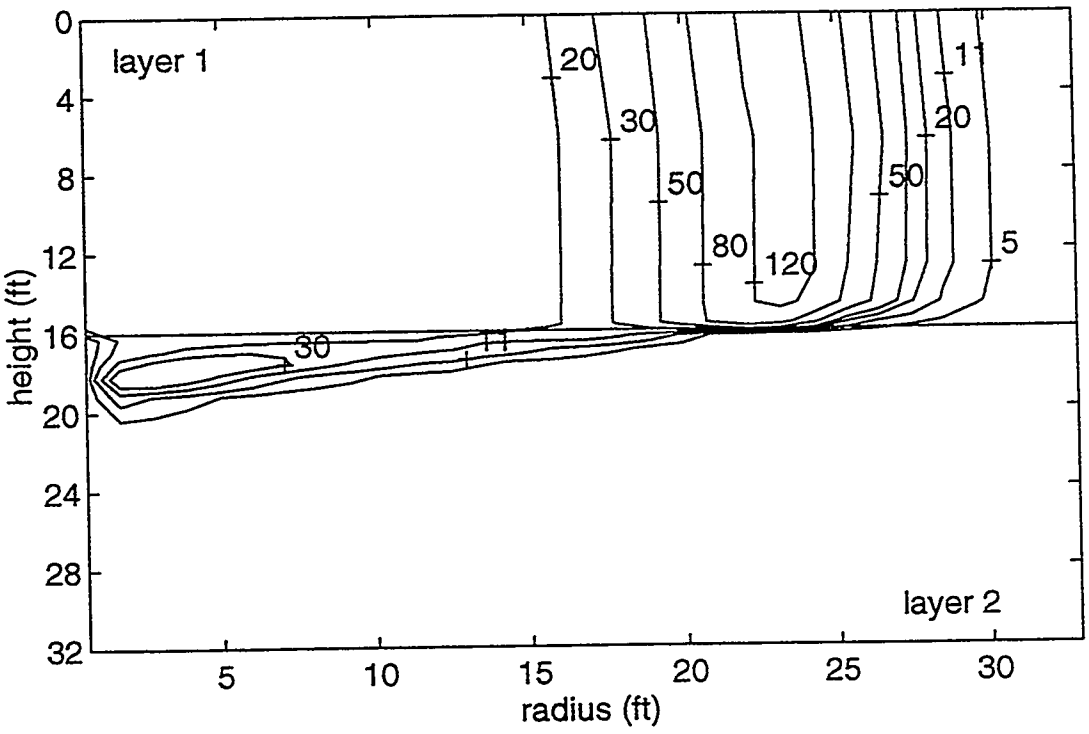

Figure 8.24: Apparent viscosity profiles after 48 hours of injection into the high-permeability layer of a reservoir with a permeability contrast of 100:1.

and vertical permeability increase. Figure 8.25 shows apparent viscosity profiles in a system with a height of 3.2 ft where crossflow near the wellbore renders the treatment ineffective. Low-viscosity gelants minimize the effects of viscous crossflow, but, as a result of the higher flow rates, tend to penetrate more into the low-permeability layers before filtration becomes dominant. This is shown by a comparison of the behavior for injection of a unit-viscosity gelant (Figure 8.26) and the base-case gelant (Figure 8.21).

CONCLUSIONS

The gel-placement behavior of the polyacrylamide/chromium system in layered reservoirs was examined. The following points summarize the major conclusions from this study:

(1) For a given set of reservoir conditions, there exists an optimal time for stopping the injection of gelant. This period is characterized by a levelling off in the flowrate profile. Injection of gelant beyond this period results in more diversion of gelant into the low-permeability layer without increasing the penetration of the gelant in the high-permeability layer.

(2) It is possible to inject more volume of gelant into the reservoir by increasing the injection pressure. The rates of filtration increase with increasing flowrate, but this effect is mitigated by the radial flow behavior around the wellbore. Unfortunately, increasing the injection pressure results in injection of more gelant into both the high-permeability and the low-permeability layers.

(3) Although viscous crossflow has a relatively small effect during typical near-wellbore treatments, its effects may become significant in deeper treatments with gelants characterized by long gel times. In these cases, the bulk of the crossflow occurs before the onset of filtration.

(4) Gel-placement is most effective in reservoirs characterized with high-permeability contrast and low crossflow between layers. Permeability-modification treatments, therefore, are expected to be more effective in severe cases of water channeling as opposed to mild cases of water channeling during the waterflooding stage.

(5) As the viscosity of the gelant is lowered, it is possible to inject large amounts of gelant into the reservoir with a more favorable distribution between the two layers. Although viscous crossflow is reduced as the viscosity of the gelant is reduced, crossflow of gelant may occur due to build-up of resistance by the filtration mechanism.

(6) Isolation of the low-permeability layer results in a considerably more effective gel placement compared to conventional treatment. Filtration may aid in minimizing crossflow of gelant from the high-permeability regions into the low-permeability regions of the reservoir.

NOMENCLATURE

C_i	:	concentration of component "i", moles/cm^3.
C_{id}	:	concentration of component "i" after it is deposited by filtration in the porous medium, moles/cm^3.
C_t	:	compressibility, psi^{-1}.
D_r	:	radial dispersion coefficient, cm^2/sec.
D_z	:	vertical dispersion coefficient, cm^2/sec.
F	:	fraction of hydrolyzed repeat units on a polyacrylamide chain
g	:	matching parameter in the G' equation, dimensionless.

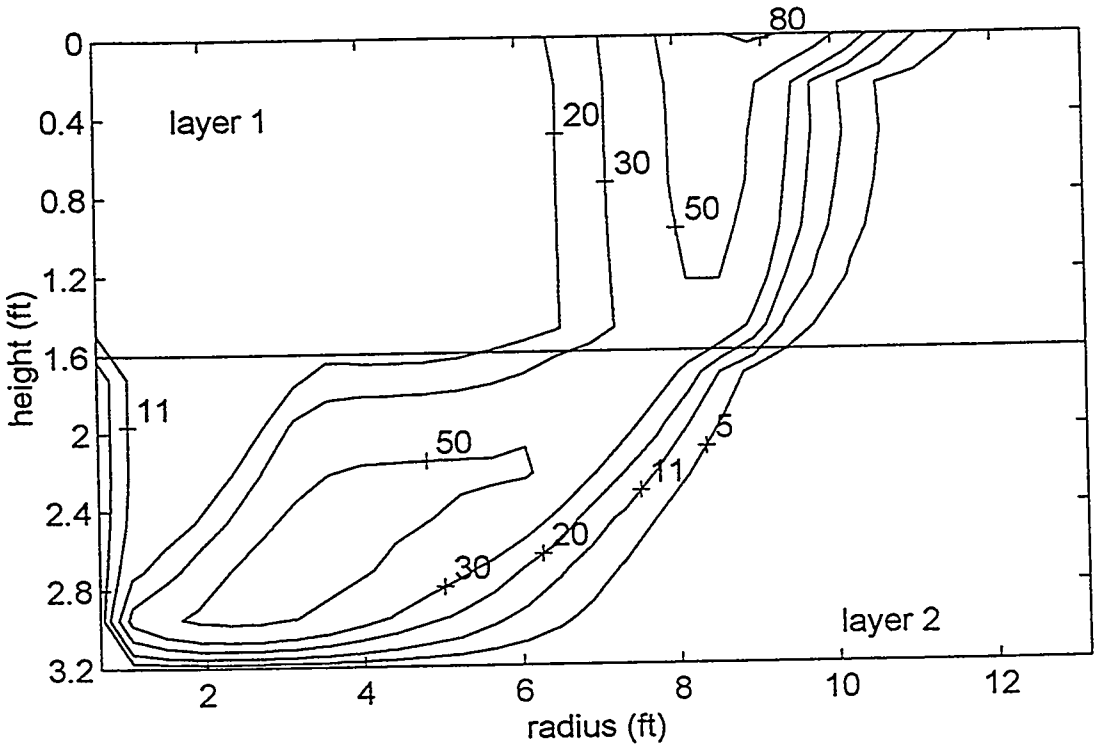

Figure 8.25: Apparent viscosity profiles after 48 hours of injection into the high-permeability layer of a reservoir with a height of 3.2 ft.

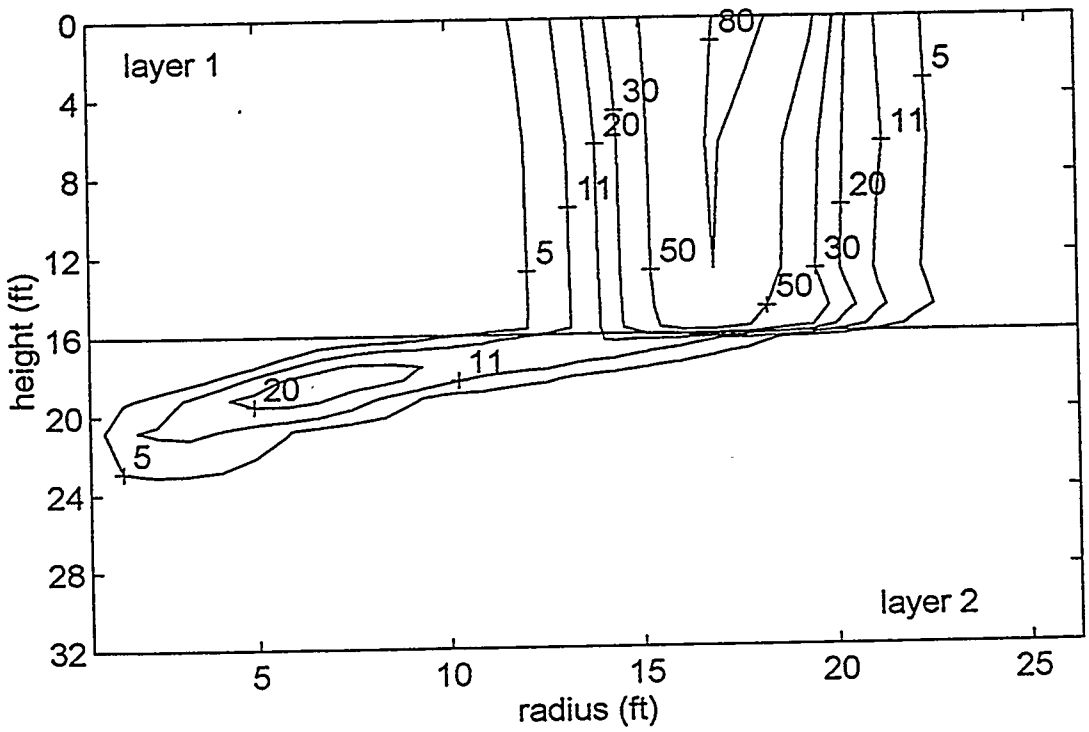

Figure 8.26: Apparent viscosity profiles after 48 hours of injection of a unit-viscosity gelant into the high-permeability layer only.

G' : shear modulus of a gelling fluid, dynes/cm^2.
G'_{en} : initial shear modulus due to polymer entanglements, dynes/cm^2.
G'_{max} : maximum shear modulus of a gelling fluid, dynes/cm^2.
K : Boltzmann's constant.
K_1, K_2: reaction rate constants for the reduction reaction.
K_{upt} : reaction rate constant for chromium uptake.
k_r : radial permeability of the reservoir, darcy.
k_z : vertical permeability of the reservoir, darcy.
l_p : average length of pore, °A.
p : pressure, psi.
MW_p : molecular weight of polymer
MW_{ru}: molecular weight of a polymer repeat unit
n : crosslink density, crosslinks/cm^3.
PSR : matching parameter for the interception efficiency equation.
r : radius, cm.
R_i : kinetic reaction term, moles/cm^3.s
R_k : rate constant for the shear modulus equation
T : temperature, K.
t : time, sec.
v_r : radial velocity, cm/sec.
v_z : vertical velocity, cm/sec.
v_{tot} : magnitude of total velocity, cm/sec.
z : height, cm.

Greek Characters

α : probability that a particle will collide with the pore walls, dimensionless.
ϵ : the fraction of collisions that result in the deposition of the particle, dimensionless.
Γ^i : interception rate coefficient
Γ^s : straining rate coefficient
ϕ^0 : initial porosity
ϕ : current value of porosity
σ : total fraction of initial porosity occupied by deposited polymer.
μ : viscosity, cp.

References

1. Marty, L., Willhite, G. P., Green, D. W., "The Effect of Flow Rate on the In Situ Gelation of a Chrome/Redox/Polyacrylamide System," *SPE Reservoir Engineering, 6* (May 1991), pp. 219-224.
2. McCool, C.S., Green, D. W., Willhite, G. P., "Permeability Reduction Mechanisms Involved in In situ Gelation of a Polyacrylamide/Chromium(VI)/Thiourea System in Porous Media," *SPE Reservoir Engineering, 6* (February 1991), pp. 77-83.
3. Sorbie, K.S., Roberts, L.J. and Clifford, P.J.,"Calculations on the Behavior of Time Setting Polymer Gels in Porous Media," presented at the AIChE National Spring Meeting, Houston, Texas, 1985.
4. Hortes, E.,"Development of a Reservoir Model for Polymer/Gel Treatments," Report 87-3, University of Texas at Austin, 1986.

5. Gao, H.W., and Chang, M.M.,"A Three-Dimensional, Three-Phase Simulator for Permeability Modification Treatments Using Gelled Polymers," Report No. NIPER-388, NTIS Order No. DE9000227, U.S.DOE (March 1990).
6. Scott, T., Roberts, L.J., Sharpe, S.R., Clifford P.J. and Sorbie K.S.,"In-Situ Gel Calculations in Complex Reservoir Systems Using a New Chemical Flood Simulator," *SPERE,* (November 1987), pp. 634-646.
7. Todd, B.T., Willhite, G. P., and Green, D. W., "A Mathematical Model of In-Situ Gelation of Polyacrylamide by a Redox Process," *SPE Reservoir Engineering, 8* (February 1993), pp. 51-58.
8. Dullien, F.A.L.,"Fluid Transport and Pore Structure", New York: Academic Press, 1979.
9. Sorbie, K.S. and Seright, R.S.,"Gel Placement in Heterogenous Systems With Crossflow," SPE/DOE 24192, Presented at SPE/DOE Eight Symposium on Enhanced Oil Recovery, Tulsa, Oklahoma, April 22-24, 1992.
10. Zapata, V.J. and Lake, L.W.,"A Theoretical Analysis of Viscous Crossflow," paper SPE 10111 presented at the 1981 SPE Annual Technical Conference and Exhibition, San Antonio, Oct. 5-7.
11. Maxcy, T.A.,"A Kinetic Study of the Reduction of Chromium(VI) by Thiourea," PhD dissertation, University of Kansas, 1991.
12. Hunt, J.A., Young, T. S., Green, D. W., and Willhite, G. P., "A Kinetic Study of the Cr(III)-Polyacrylamide Crosslinking Reaction by Equilibrium Dialysis," *AIChE Journal, 35*, (February 1989), pp. 250-258.
13. Bhasker, R.K. "Transient Rheological Properties of Chromium/Polyacrylamide Solutions Under Superposed Steady and Oscillatory Shear Strains," PhD dissertation, University of Kansas, 1988.
14. Graessley, W.W.,"The Entanglement Concept in Polymer Rheology," *Advances in Polymer Science*, Spring-Verlag, New York, 1974.
15. Flory, P.J., *Principles of Polymer Chemistry*, Cornell University Press, Ithaca, New York, 1953.
16. Herzig, J.P., LeClerc, D.M. and LeGoff, P.,"Flow of Suspensions Through Porous Media - Application to Deep Filtration," *Ind. Eng. Chem., 62*, (1970).
17. Soo, H. and Radke, C. ," A Filtration Model for the Flow of Dilute Stable Emulsions in Porous Media - I. Theory," *Chem. Eng. Sc.,* Vol. 41, No. 2, (1986) pp. 263-272.
18. Blair, P. M. and Weinaug, C.F.,"Solution of Two-Phase Flow Problems Using Implicit Difference Equations," *SPEJ* (1960), pp. 417-424.
19. MacDonald, R.C. and Coats, K.H.,"Methods for Numerical Simulation of Water and Gas Coning," *SPEJ* (1970), pp. 425-436.
20. Scheisser, W.E.,"The Numerical Method of Lines," *Academic Press*, San Diego, 1991.
21. Aziz, K. and Settari, A., *Petroleum Reservoir Simulation*, Applied Science Publishers Ltd., London, 1979.
22. Hindmarsh, A.C.," ODEPACK, A Systemized Collection of ODE Solvers," 10th IMACS World Congress on Systems Simulation and Scientific Computation, Montreal, Canada, 8-13, August 1982.

APPENDIX - Governing Equations

In order to simplify the formulation of the mathematical model, the following set of assumptions are adopted in the continuity equations.

(1) Flow is assumed to be symmetric around the wellbore. Two-dimensional Darcy flow of the gelant is considered in the radial and vertical directions.

(2) Only single-phase flow is considered during the process of gel placement. Oil is assumed to be immobile and its effects on the gelation processes are neglected.

(3) A single-well model is developed in which the well is isolated from all effects of surrounding wells.

Pressure Equation. Based on the above assumptions, the overall equation of continuity for a fluid with a small and constant compressibility is given by

$$\frac{1}{r}\frac{\partial}{\partial r}\left(r\frac{k_r}{\mu}\frac{\partial p}{\partial r}\right) + \frac{\partial}{\partial z}\left(\frac{k_z}{\mu}\frac{\partial p}{\partial z}\right) = \phi_0 c_t \frac{\partial p}{\partial t} \quad \text{..... (A-1)}$$

The radial and vertical components of the fluid velocity are given by

$$v_r = -\frac{k_r}{\mu}\frac{\partial p}{\partial r}, \quad \text{..... (A-2)}$$

$$v_z = -\frac{k_z}{\mu}\frac{\partial p}{\partial z}. \quad \text{..... (A-3)}$$

The mobility terms in Equation A-1 are a function of the gelation process of the polyacrylamide/redox system. Both the radial and vertical permeabilities of the reservoir vary as the pre-gel aggregates of polymer are filtered by the porous medium. Similarly, the viscosity of the gelant is usually greater than the viscosity of the initial fluid and the fluid viscosity in Equation 1 undergoes a rapid drop at the front of the injected solution. The gelant viscosity increases as crosslinks between the polymer molecules are formed.

Initial and Boundary Conditions. The selection of boundary and initial conditions for Equation A-1 deserves some discussion. Well operation may be modelled for two conditions- injection of gelant at a constant flow-rate, or, injection of gelant at a constant injection pressure. At constant flow-rate conditions, the flow rate of gelant into the individual layers with constant permeabilities may be obtained by simply dividing the total flow-rate in proportion to the radial permeabilities of the layers. However, in the presence of the filtration mechanism, the radial permeability of the reservoir varies as a function of both position and time. In order to avoid iterative calculations of the varying flow rates across the height of the wellbore, this study is restricted to the relatively straightforward case of well operation at constant-pressure conditions alone. The boundary condition for Equation 1 at the wellbore, therefore, is given by

$$p = p_{inj} \qquad at\ r = r_w \quad \text{..... (A-4)}$$

Since the model is restricted to near-wellbore treatments only, the boundary condition at the exterior radius is developed by assuming that the well is isolated from the surrounding wells. The exterior radius is typically far enough from the wellbore that the exterior boundary-condition does not significantly effect flow behavior near the wellbore. The exact form of the boundary condition for the pressure equation is developed in conjunction with the initial condition for Equation A-1.

The initial condition must be selected so as to represent the pressure distribution around the wellbore after an extended period of waterflooding. Two sets of initial and boundary conditions may be envisioned. The first set of conditions physically represents steady-state operation of the well in which pressure has equilibrated across the height of reservoir:

$$p = \frac{p_{inj} \ln(\frac{r}{r_{ext}})}{\ln(\frac{r_w}{r_{ext}})} \qquad at\ t = 0 \quad \ldots\ldots\ldots\ldots\ldots \quad (A\text{-}5)$$

$$p = 0 \qquad at\ r = r_{ext} \quad \ldots\ldots\ldots\ldots\ldots \quad (A\text{-}6)$$

This boundary condition is representative of the pressure distribution in laboratory experiments simulating flow through layered reservoirs. For field-scale conditions, however, this set of conditions is oversimplified since it neglects the presence of unswept oil in the low-permeability regions of the reservoir. Simulated pressure contours after an extended period of waterflooding by Scott et al.[6] show that pressures in the high-permeability layer are greater than the corresponding pressures in the low-permeability layer. An additional complication arises in practical cases as permeability-modification treatments usually require some period of shut-in of the well before injection of the gelant is initiated.

In this study, pressure behavior is described by a second set of conditions which represent the transient operation of the well after a shut-in period.

$$p = 0 \qquad at\ t = 0 \quad \ldots\ldots\ldots\ldots\ldots \quad (A\text{-}7)$$

$$\frac{\partial p}{\partial r} = 0 \qquad at\ r = r_{ext} \quad \ldots\ldots\ldots\ldots\ldots \quad (A\text{-}8)$$

Pressure transients are propagated faster in the high-permeability regions than the low-permeability regions of the reservoir. After a relatively short period, the pressure distribution in the reservoir becomes similar in nature to that shown by Scott et al.[6] This set of initial conditions also enables a direct comparison between conventional treatments with injection of gelant into both layers and treatments with zonal isolation where gelant is injected into the high-permeability layer alone.

Numerical results for the two sets of conditions show that the choice of initial conditions effects the flow behavior near the wellbore only for a short period (typically less than 10 hours) during the early stages of the treatment. During this period, the transient initial conditions produce considerably higher flow-rates than the steady-state conditions and result in a greater cumulative volume of gelant being injected into the reservoir. The overall gel placement behavior and the effects of parameters, however, are quite similar for the two sets of conditions.

Mass Transport. Based on the velocity field given by Equation A-1, in-situ gelation of the polyacrylamide/chromium system is described by the transport of the following chemical species:

1. sodium dichromate
2. thiourea (reducing agent)

3. ionic chromium (III)
4. chromium attached to polymer
5. cross-links between polymer chains
6.-10. five size categories of polyacrylamide aggregates

Mass transport of the "ith" chemical species is given by

$$\frac{1}{r}\frac{\partial}{\partial r}[r\,(-v_r C_i + D_r\frac{\partial C_i}{\partial r})] + \frac{\partial}{\partial z}[-v_z C_i + D_z\frac{\partial C_i}{\partial z}] - \phi_0 C_{i(d)}\frac{\partial \sigma}{\partial t} + R_i\phi = \frac{\partial(\phi C_i)}{\partial t}, \quad \text{(A-9)}$$

which accounts for transport of mass by convection, dispersion, filtration and chemical reaction. $C_{i(d)}$ is the concentration of the "ith" species deposited on the walls of the pores by filtration and is related to the local concentration of "i" in the solution. The dispersion coefficients in Equation 1 are linear functions of the velocity vectors. The reaction and filtration terms for the different chemical species are described below.

Reaction Kinetics. The kinetics of the chromium reactions are assumed to be independent of the flow geometry. Hence, both the form of the kinetic expressions and the reaction parameters used in this model are identical to those used by Todd et al. to match linear core-flood experiments. A detailed description of the reaction kinetics is available in Reference 7 and only a brief summary is presented here.

The gelation kinetics of the polyacrylamide/chromium system is described as a three step process:

1. The reduction of dichromate by thiourea to liberate free Cr^{3+} ions into the solution. This reaction is modeled by the following rate equation proposed by ([11])

$$\frac{d[Cr_2O_7^{2-}]}{dt} = -\frac{1}{2}[k_1[HCrO_4^-][H_4N_2CS][H^+] + k_2[HCrO_4^-][H_4N_2CS][H^+][COOH]_{PAAm}. \quad \text{(A-10)}$$

The concentration of the bichromate ion in Equation 10 is calculated from the dichromate-ion concentration using equilibrium relationships.

2. The free Cr^{3+} ions in the solution are attached to the reactive sites on the polymer molecules. The rate of Cr^{3+} uptake by the pclymer is given by Hunt et al., as [12]

$$\frac{d[Cr^{3+}]_{upt}}{dt} = k_{upt}\frac{[Cr^{3+}]^{1.32}}{F^{0.8}[H^+]}[F[PAAm] - [Cr^{3+}]_{upt}]^{0.8}. \quad \text{(A-11)}$$

3. As a result of the attached chromium ions, the polymer molecules crosslink to form large chains or aggregates of polymer molecules. This step is characterized by the evolution shear modulus (G') of the gelling solution by the following empirical relation [13]

$$\frac{dG'}{dt} = R_k[Cr^{3+}]_{upt}G'[1-\frac{G'}{G_{max}}]. \quad \text{(A-12)}$$

Based on the value of the shear modulus, the crosslink density of the gelling solution is estimated using Graessley's equation [14]

$$G' = gnkT + G'_{en} \quad \text{(A-13)}$$

where n is crosslink density in crosslinks per unit volume. The crosslink density increases as the crosslinking reaction proceeds in time and causes an increase in gelant viscosity and the formation of aggregates of polymer molecules.

The size distribution of the polymer aggregates in the solution is estimated by Flory's equation [15]. This relation provides the weight distribution of aggregate sizes in gelling solutions based on the crosslink density. For computational purposes, the overall size distribution is divided into five discrete categories according to size [7].

Deep Filtration. The pore structure of reservoir rock is typically characterized by pore lengths of the order of 100 microns and pore-throat diameters ranging from 0-20 microns .[8] The gelling solution flowing through these pores consists of aggregates of polyacrylamide molecules ranging from 0.1-2.5 microns in diameter. Under these conditions, two mechanisms for the filtration of polymer aggregates predominate.[16,17] Straining of particles occurs in the smaller pores when the particle diameter exceeds the diameter of the pore throats. In the larger pores, the aggregates may be intercepted by the walls of the pores due to the nature of the streamlines of flow, or, by the Brownian motion of the particles. The trapped particles by both filtration mechanisms reduce the porosity and the permeability of the porous medium and result in a build-up of flow resistance in the regions of high deposition.

The filtration model in this work is an extension of existing one-dimensional filtration models. [7,17] In order to incorporate the effects of crossflow on filtration, the rate of filtration of the polymer aggregates is assumed to be proportional to the magnitude of the flux of particles through the pores. The rate of filtration of the polymer in the straining and interception pores is given by

$$\frac{d\sigma_i}{dt} = [\Gamma_s(\phi_s-\phi_0\sigma_s) + \Gamma_i(\phi_i-\phi_0\sigma_i)]\frac{v_{tot}C_i}{\phi_0(1-\sigma)} \quad \text{(A-14)}$$

where σ is the fraction of initial porosity occupied by deposited polymer. v_{tot} is defined as the magnitude of the total velocity of the particles through the porous medium

$$v_{tot} = \sqrt{v_r^2+v_z^2} \quad \text{(A-15)}$$

The filtration coefficients Γs and Γi in Equation 14 are of the form

$$\Gamma = \frac{\alpha \epsilon}{l_p} \quad \text{(A-16)}$$

where α is the probability that a particle will collide with the walls of pore, ϵ is the fraction of the collisions by which the particle sticks to the pore walls and l_p is the average pore length of the pore throat. The quantities α and ϵ incorporate the effects of the straining and interception mechanisms of filtration.

The collision probability and the collision efficiency for the small straining pores are assumed to be unity. In the large interception pores, collisions with the pore walls may be due to the constriction of the streamlines of flow, or, by the Brownian motion of the particles. The collision probability due to streamline interception is dependant only on the ratio of the particle diameter to the grain diameter of the porous medium. The collision probability due to Brownian motion, however, is a function of various parameters including the particle diameter, temperature and the solution viscosity. The total collision probability is the sum of the contributions due to the two mechanisms and is calculated using the sphere-in-cell models.[7]

The polymer intercepted by the pores is retained by two mechanisms. Initially, the injected polymer is deposited into a thin dense layer which has little effect on the permeability. The efficiency of these collisions is given by the expression

$$\epsilon_i = \epsilon_0 \left(1 - \frac{\sigma_i}{\sigma_{max}}\right) \quad \text{(A-17)}$$

As the chromium/redox reaction progresses, polymer aggregates are retained in the pores by virtue of their ability to form crosslinks with previously deposited polymer

$$\epsilon_i = \left(PSR \frac{MW_{polymer}}{MW_{ru}} \frac{[Cr^{3+}]_{upt}}{[PAAm]} \right)^2 \quad \text{(A-18)}$$

where *PSR* is a matching parameter estimated from laboratory core-flood experiments at different flow-rates.

The total rate of filtration is computed as the sum of the rates of filtration of all the size fractions of the polymer aggregates. The decrease in porosity due to the filtration of polymer aggregates is related to the decrease in the permeability of the porous medium by the simplified relation

$$\frac{k_r}{k_r^0} = \frac{k_z}{k_z^0} = \left(\frac{\phi}{\phi^0}\right)^3 \quad \text{(A-19)}$$

Thus, the model allows for porous medium to be anisotropic in nature, but, both the radial permeability and the vertical permeability are assumed to be effected equally by the decrease in porosity.

In summary, the filtration model differs from other models for in-situ gelation since it couples the effects of flow rate and reaction kinetics to the build-up of flow resistance. In addition, the rate of filtration of

the polymer aggregates is a function of the aggregate size and the pore structure of the porous medium. Since the low-permeability regions are characterized by smaller pores than the high-permeability regions, the rate of filtration of polymer aggregates under similar conditions is greater in low-permeability regions of the reservoir.

Numerical Model. Single-well models are particularly subject to instability due to the sharp diverging/converging nature of flow near the wellbore. Numerical models for coning type problems show that implicit treatment of mobility terms in the pressure equation for implicit-pressure explicit-saturation (IMPES) type algorithms is more efficient than explicit treatment of the mobility terms. [18,19] Similarly, fully implicit numerical models with simultaneous solution of all variables perform better than IMPES type algorithms. Although implicit techniques require more work for each time-step, they become computationally efficient by allowing substantially larger time steps than explicit techniques thereby reducing the total number of required time-steps.

In this study, the governing set of equations are solved numerically using the Method of Lines.[20] The spatial derivatives of the partial differential equations (PDEs) are substituted by corresponding finite-difference approximations. This step converts each PDE into a set of ordinary differential equations (ODEs). The resulting set of ODEs for the model are solved simultaneously using an implicit ODE integrator, LSODES.

Evaluation of the spatial derivatives is performed using first-order finite-difference approximations based on non-uniform spacing of grid points.[21] One-point upstream weighting is employed for the non-linear component of the mobility terms in the pressure equation. Similarly, the convection terms in the mass-transfer equations are evaluated using one-point upstream finite-difference approximations. Since the direction of flow is not known a priori, the upstream direction in the radial and vertical directions is dictated by the direction of the corresponding pressure gradients.

Non-uniform spacing of the spatial grid is essential for maintaining the accuracy of the finite-difference approximations and minimizing the overall size of the model. In the radial direction, 31 grid points are used to capture the flow behavior and gelation process near the wellbore. An additional 10 grid points are then logarithmically spaced to the exterior radius to evaluate the progress of the pressure transients into the reservoir. In the vertical direction, a total of 14 grid points are used with 9 grid points in the low-permeability layer and 6 grid points in the high-permeability layer. For each layer, the mesh is refined near the interface of the two layers. Convergence studies confirm that this grid is sufficiently accurate for studying the gel-placement and crossflow behavior in the two-layered reservoir.

The temporal derivatives of the ODEs are evaluated in LSODES by variable time-step, variable order, backward-difference formulas.[20,22] The time-stepping procedure is adaptive in nature with the maximum time-step size selected to meet stability requirements and specified error tolerances. At each time-step, the resulting set of non-linear algebraic equations are solved iteratively by Newton's method. Since the non-linear nature of the original equations remains undisturbed, Newton's method avoids linearizations or lagging of the non-linear terms in the governing equations. Simulations showed that incorporation of Newton's method typically increased the size of the permissible time steps by a factor of 1000.

The LSODES integrator incorporates the Yale sparse-matrix solver for evaluating the Jacobian matrix required for Newton's method. Since the Jacobian matrix for the problem is more than 99% sparse, the sparse-matrix solver minimized the storage requirements for the model considerably and enabled efficient solution of the Jacobian matrix. Further details about LSODES are available in References 20 and 22.

The MOL technique, therefore, results in a fully implicit numerical scheme for solving the governing equations. Numerical simulations were performed on a Digital Alpha 7000-610 computer and typically required 3-8 CPU hours depending on the flow rate and degree of crossflow.